Calorimetry
in High energy Physics

G.Y.Lim
IPNS/KEK

Nuclear Physics School 2017: 21th, June@POSTECH,Phhang

Great amount of data on-line and powerful search ability enable me to make slides easier.
However, I should taken care of copyright to use the image, contents, etc…
I don’t believe my slides to be public - sorry

Observable

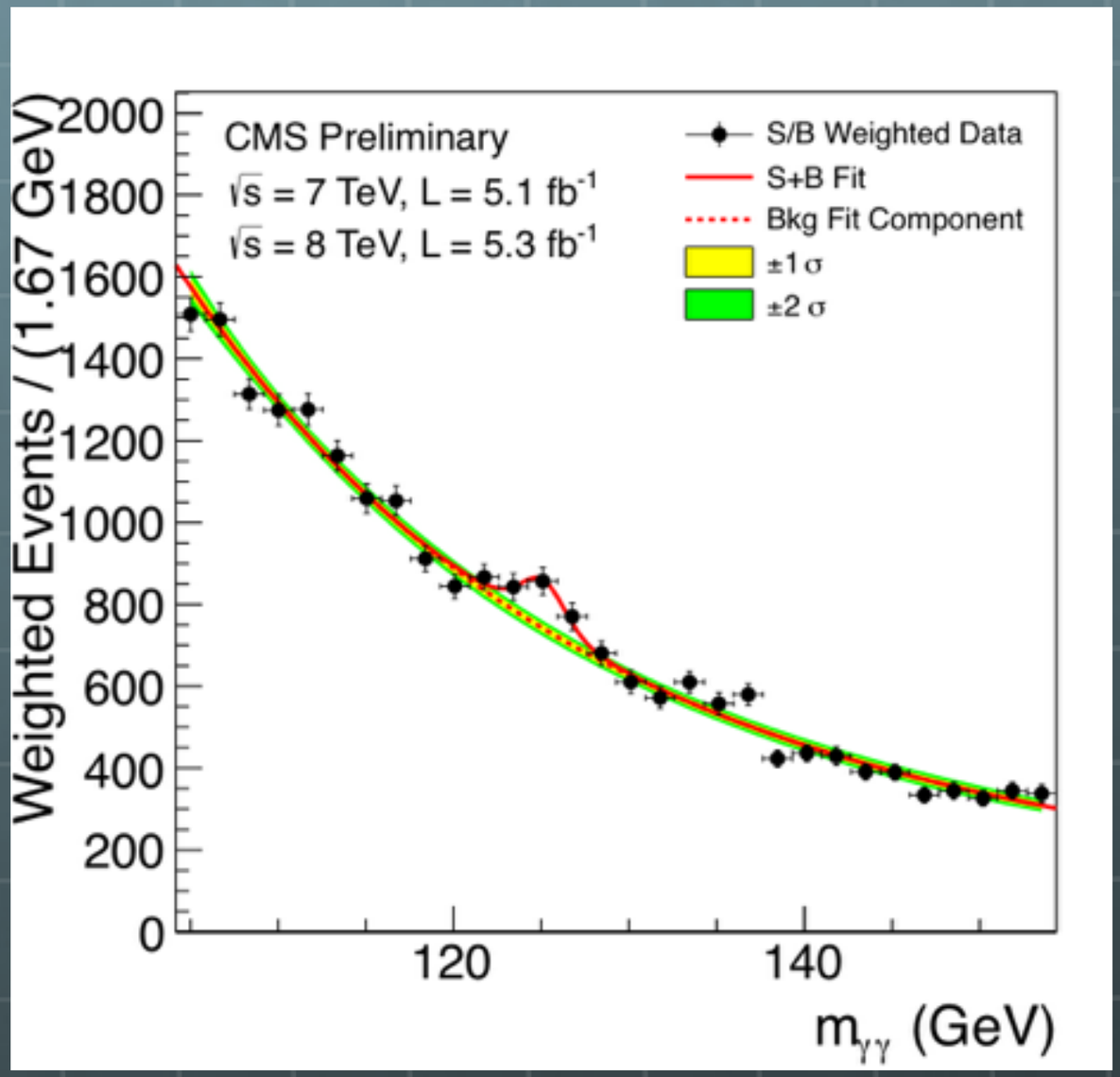
CMS Preliminary
√s = 7 TeV, L = 5.1 fb-1
√s = 8 TeV, L = 5.3 fb-1
S/B Weighted Data
S+B Fit
Bkg Fit Component
±1 σ
±2 σ
Weighted Events / (1.67 GeV)
2000
1800
1600
1400
1200
1000
800
600
400
200
0
120
140
mγγ (GeV)

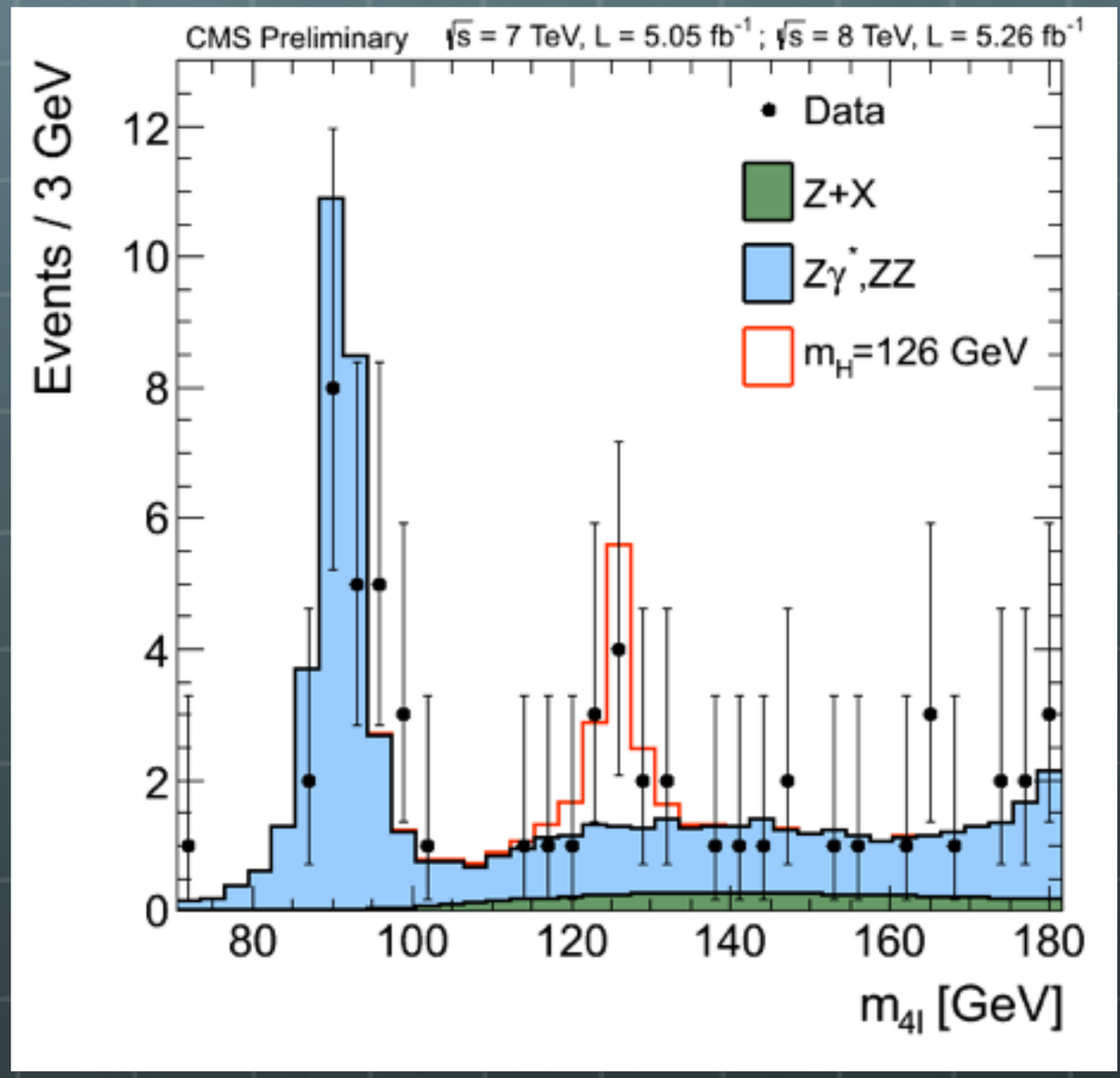
CMS Preliminary
√s = 7 TeV, L = 5.05 fb-1 ; √s = 8 TeV, L = 5.26 fb-1
Data
Z+X
Zγ*,ZZ
mH=126 GeV
Events / 3 GeV
12
10
8
6
4
2
0
80
100
120
140
160
180
m4l [GeV]

perhaps new world(s) of SM replicas

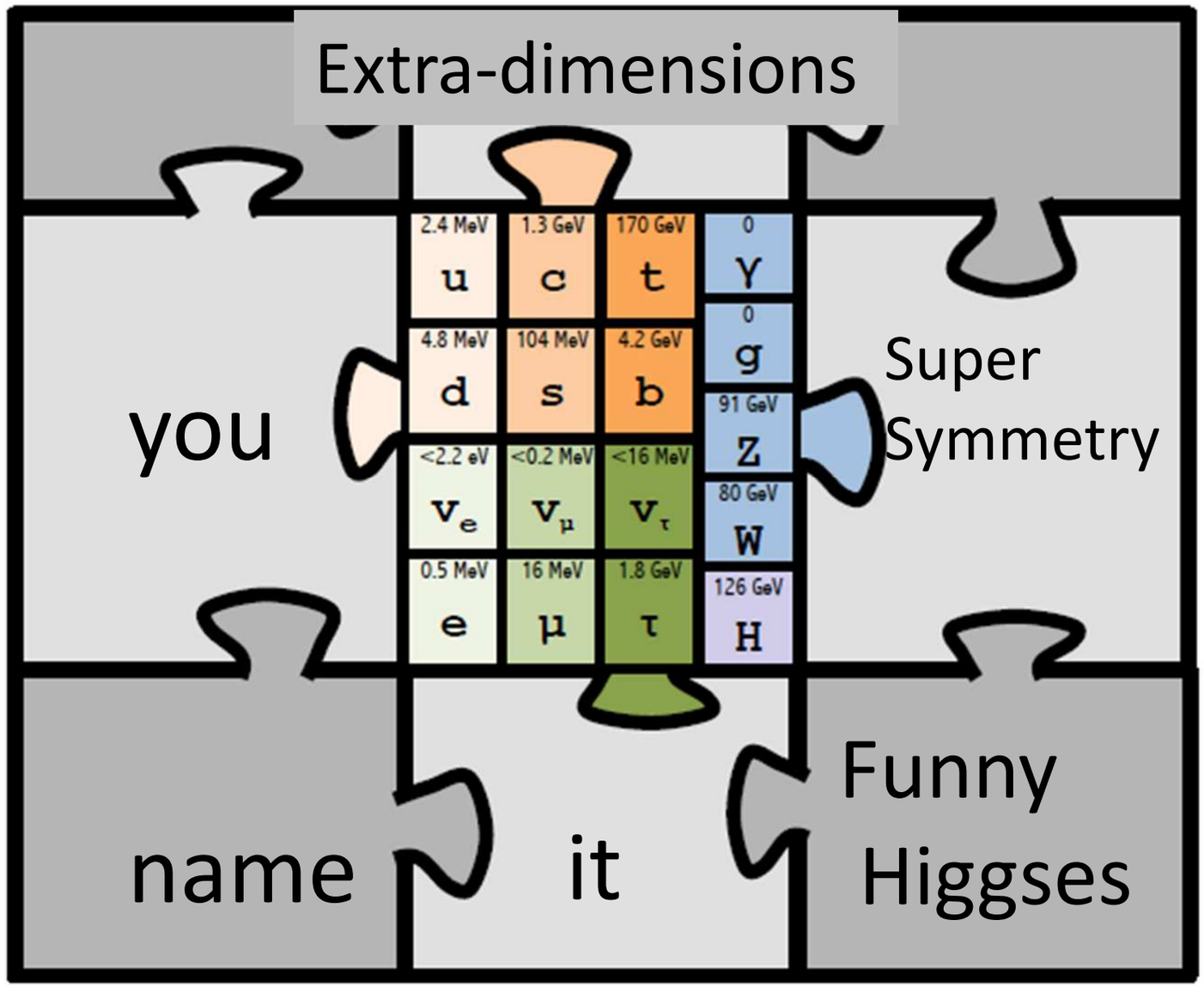

Typically supersymmetry, same couplings as the Standard Model

Can generate $\mu \rightarrow e\gamma$ $Z \rightarrow \mu\tau$ anomalies in CKM measurements, etc. etc…

Dark Matter and BAU. High intensity and luminosity:

Many parameters but must be protected otherwise Higgs mass goes to infinity

CMS DETECTOR

Total weight : 14,000 tonnes
Overall diameter : 15.0 m
Overall length : 28.7 m
Magnetic field : 3.8 T

STEEL RETURN YOKE
12,500 tonnes

SILICON TRACKERS
Pixel (100x150 µm) ~16m² ~66M channels
Microstrips (80x180 µm) ~200m² ~9.6M channels

SUPERCONDUCTING SOLENOID
Niobium titanium coil carrying ~18,000A

MUON CHAMBERS
Barrel: 250 Drift Tube, 480 Resistive Plate Chambers
Endcaps: 468 Cathode Strip, 432 Resistive Plate Chambers

PRESHOWER
Silicon strips ~16m² ~137,000 channels

FORWARD CALORIMETER
Steel + Quartz fibres ~2,000 Channels

CRYSTAL ELECTROMAGNETIC CALORIMETER (ECAL)
~76,000 scintillating $PbWO_4$ crystals

HADRON CALORIMETER (HCAL)
Brass + Plastic scintillator ~7,000 channels

https://cms.cern/detector

Detector

- We detector elementary particles
  - gamma, electron, muon, pion, proton, neutron, ions
  - We measure kinematical variables
    - time, position, velocity, momentum, mass, energy
- We reconstruct
  - invariant mass, trajectory

$$E^2 = m^2c^4 + p^2c^2$$

$$(E, P)_{in} = (E, P)_{out}$$

- Ionization, Scintillation, Semiconductor, Cherenkov, …

We measure physical variables as a result of interaction between particle and material.

- inelastic collisions with the atomic electrons
- elastic scattering from nuclei
- emission of Cherenkov radiation
- bremsstrahlung
- pair production
- nuclear reaction (strong interaction)
- Particle decay (weak interaction)

Contents

- Passage of charged particles
- Scintillator
- Calorimeter
- KOTO experiment

Energy Loss of (heavy) charged particles by atomic collision

Energy Loss

- Charge ze, velocity v, mass M, Impact parameter b
- Momentum Transfer

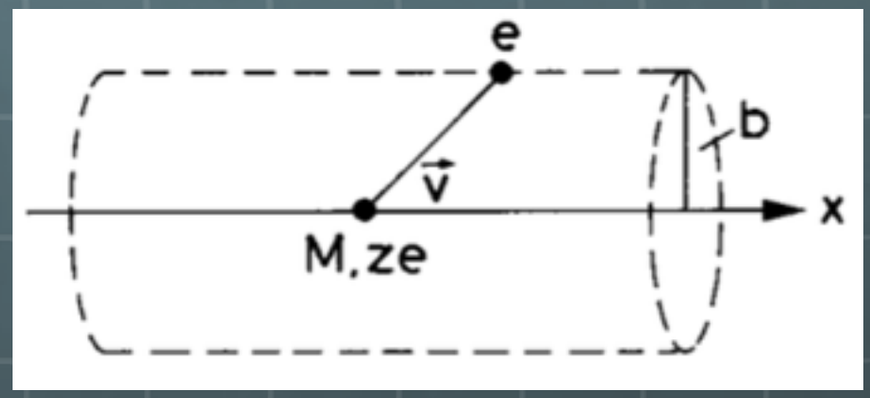

$$\Delta P_T = \int F dt = \int F_T dt = \int F_T \frac{dx}{v}$$

$$= \int \frac{ze^2}{(x^2+b^2)} \cdot \frac{b}{\sqrt{x^2+b^2}} \cdot \frac{1}{v} dx$$

$$= \frac{2ze^2}{bv}$$

- Electron obtains energy as $\Delta E(b) = \frac{\Delta P_T^2}{2m_e} = \frac{2z^2e^4}{m_e v^2 b^2}$

Energy Loss (cont.)

- Consider a bulk of electrons
  - Number of electrons

$$N_e = \rho \cdot 2\pi b \cdot db\ dx$$

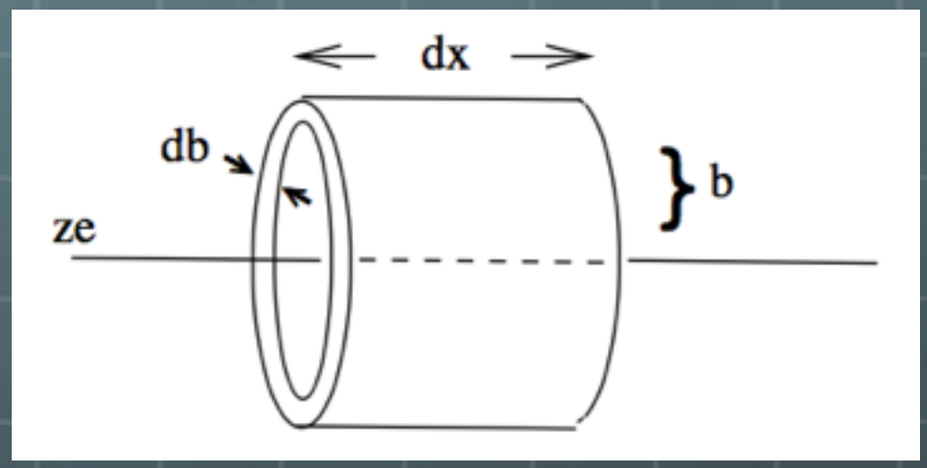

  - Energy loss becomes

$$dE(b) = N_e \cdot \Delta E(b) = \frac{4\pi z^2 e^4}{m_e v^2} \rho \frac{db}{b} dx$$

$$\frac{dE}{dx} = \frac{4\pi z^2 e^4}{m_e v^2} \rho \int \frac{db}{b} \quad \rightarrow \frac{4\pi z^2 e^4}{m_e v^2} \rho \cdot \mathbf{ln}(\frac{b_{max}}{b_{min}})$$

Bohr's Formula

b_{min} : head-on collision

$$2m_e v^2 = \frac{ze^2}{b_{min}} \quad \Rightarrow \quad b_{min} = \frac{ze^2}{2m_e v^2}$$

b_{max} : adiabatic invariance

$$F \cdot \tau = \Delta P$$

τ : Period of bound electron's orbital motion

$$\frac{ze^2\tau}{b_{max}^2} = \frac{2ze^2}{b_{max} v} \quad \Rightarrow \quad b_{max} = \frac{v\tau}{2} = \frac{v}{2\nu}$$

$$< -\frac{dE}{dx} >= \frac{4\pi z^2 e^4}{m_e v^2} N_A \frac{Z}{A} \ln\left(\frac{mv^3}{\nu z e^2}\right)$$

PDG particle data group 1957 2017

About PDG | PDG Authors | PDG Citation | Contact Us

The Review of Particle Physics (2017)

C. Patrignani *et al.* (Particle Data Group), Chin. Phys. C, **40**, 100001 (2016) and 2017 update.

pdgLive - Interactive Listings

Summary Tables

Reviews, Tables, Plots (2016)

Particle Listings

Search

Order: Book & Booklet

Download or Print: Book, Booklet, Website, Figures & more

Previous Editions (& Errata) 1957-2016	Physical Constants
Errata in current edition	Astrophysical Constants
Figures in reviews	Atomic & Nuclear Properties
Mirror Sites	Astrophysics & Cosmology

PDG Outreach

Particle Adventure & Apps	CPEP Charts	History book

Non-PDG Resources

HEP Papers	Databases & Info	Institutions & People

Funded by:

US DOE, CERN, MEXT (Japan), IHEP-CAS (China), INFN (Italy), MINECO (Spain), IHEP (Russia)

http://pdg.lbl.gov

33. PASSAGE OF PARTICLES THROUGH MATTER

Revised August 2015 by H. Bichsel (University of Washington), D.E. Groom (LBNL), and S.R. Klein (LBNL).

Bethe Equation

$$\left\langle -\frac{dE}{dx} \right\rangle = Kz^2 \frac{Z}{A} \frac{1}{\beta^2} \left[\frac{1}{2} \ln \frac{2m_e c^2 \beta^2 \gamma^2 W_{\max}}{I^2} - \beta^2 - \frac{\delta(\beta\gamma)}{2} \right]$$

$$K = 4\pi N_A r_e^2 m_e c^2 = 0.307075 \ \mathbf{MeV} \ mol^{-1} \ cm^2$$

$$r_e = e^2/(4\pi\epsilon_0 m_e c^2) = 2.81794032 67(27) fm$$

$$W_{\max} = \frac{2m_e c^2 \beta^2 \gamma^2}{1 + 2\gamma m_e/M + (m_e/M)^2}$$

$$< -\frac{dE}{dx} >= \frac{4\pi z^2 e^4}{m_e v^2} N_A \frac{Z}{A} \ln\left(\frac{mv^3}{4\nu z e^2}\right)$$

Mean Excitation Energy

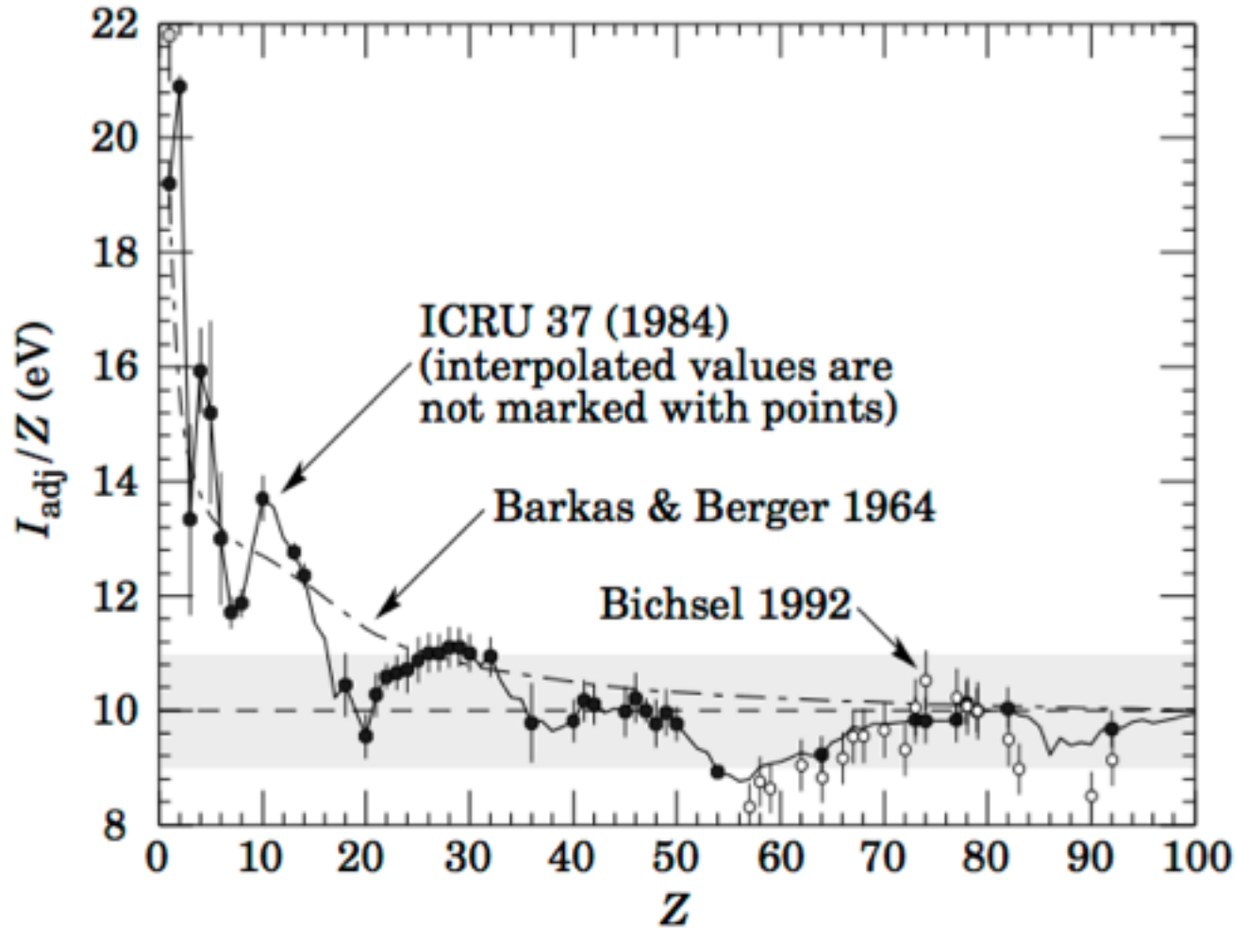

Figure 33.5: Mean excitation energies (divided by Z) as adopted by the ICRU [11]. Those based on experimental measurements are shown by symbols with error flags; the interpolated values are simply joined. The grey point is for liquid H_2; the black point at 19.2 eV is for H_2 gas. The open circles show more recent determinations by Bichsel [13]. The dash-dotted curve is from the approximate formula of Barkas [14] used in early editions of this *Review*.

Atomic and nuclear properties of copper (Cu)

Quantity	Value	Units	Value	Units
Atomic number	29			
Atomic mass	63.546(3)	g mole^{-1}		
Specific gravity	8.960	g cm^{-3}		
Mean excitation energy	322.0	eV		
Minimum ionization	1.403	MeV g^{-1}cm^2	12.57	MeV cm^{-1}
Nuclear collision length	84.2	g cm^{-2}	9.393	cm
Nuclear interaction length	137.3	g cm^{-2}	15.32	cm
Pion collision length	109.3	g cm^{-2}	12.20	cm
Pion interaction length	165.9	g cm^{-2}	18.51	cm
Radiation length	12.86	g cm^{-2}	1.436	cm
Critical energy	19.42	MeV (for e^-)	18.79	MeV (for e^+)
Molière radius	14.05	g cm^{-2}	1.568	cm
Plasma energy $\hbar\omega_p$	58.27	eV		
Muon critical energy	317.	GeV		
Melting point	1358.	K	1085.	C
Boiling point @ 1 atm	2835.	K	2562.	C

For muons, $dE/dx = a(E) + b(E)\,E$. Tables of $b(E)$: PDF TEXT
Table of muon dE/dx and Range: PDF TEXT
Explanation of some entries
Table of isotopes Warning: may not be current
x ray mass attenuation coefficients

aterials

>) tables including radiative losses for muons, nuclear and pion
ius, plasma energy, and links to isotope and x-ray mass atteunation

naterials.

					$_{2}$He
$_{5}$B	$_{6}$C	$_{7}$N	$_{8}$O	$_{9}$F	$_{10}$Ne
$_{13}$Al	$_{14}$Si	$_{15}$P	$_{16}$S	$_{17}$Cl	$_{18}$Ar
$_{31}$Ga	$_{32}$Ge	$_{33}$As	$_{34}$Se	$_{35}$Br	$_{36}$Kr
$_{49}$In	$_{50}$Sn	$_{51}$Sb	$_{52}$Te	$_{53}$I	$_{54}$Xe
$_{81}$Tl	$_{82}$Pb	$_{83}$Bi	$_{84}$Po	$_{85}$At	$_{86}$Rn
$_{113}$Nh	$_{114}$Fl	$_{115}$Mc	$_{116}$Lv	$_{117}$Ts	$_{118}$Og
$_{68}$Er	$_{69}$Tm	$_{70}$Yb	$_{71}$Lu		
$_{100}$Fm	$_{101}$Md	$_{102}$No	$_{103}$Lr		

2016/AtomicNuclearProperties/

33. PASSAGE OF PARTICLES THROUGH MATTER

Revised August 2015 by H. Bichsel (University of Washington), D.E. Groom (LBNL), and S.R. Klein (LBNL).

Bethe Equation

$$\left\langle -\frac{dE}{dx} \right\rangle = Kz^2 \frac{Z}{A} \frac{1}{\beta^2} \left[\frac{1}{2} \ln \frac{2m_e c^2 \beta^2 \gamma^2 W_{\max}}{I^2} - \beta^2 - \frac{\delta(\beta\gamma)}{2} \right]$$

- charge square of incident particle (z^2)
- charge of matter (Z)
- Inverse of mass of matter (1/A)
  - Unit of MeV · cm^2/g

33. PASSAGE OF PARTICLES THROUGH MATTER

Revised August 2015 by H. Bichsel (University of Washington), D.E. Groom (LBNL), and S.R. Klein (LBNL).

Bethe Equation

$$\left\langle -\frac{dE}{dx} \right\rangle = Kz^2 \frac{Z}{A} \frac{1}{\beta^2} \left[\frac{1}{2} \ln \frac{2m_e c^2 \beta^2 \gamma^2 W_{\max}}{I^2} - \beta^2 - \frac{\delta(\beta\gamma)}{2} \right]$$

- charge square of incident particle (z^2)
- charge of matter (Z)
- Inverse of mass of matter (1/A)
- Mixture of different dependence on the velocity (β)
- Maximum energy transfer in a single collision

$$W_{\max} = \frac{2m_e c^2 \, \beta^2 \gamma^2}{1 + 2\gamma m_e/M + (m_e/M)^2}$$

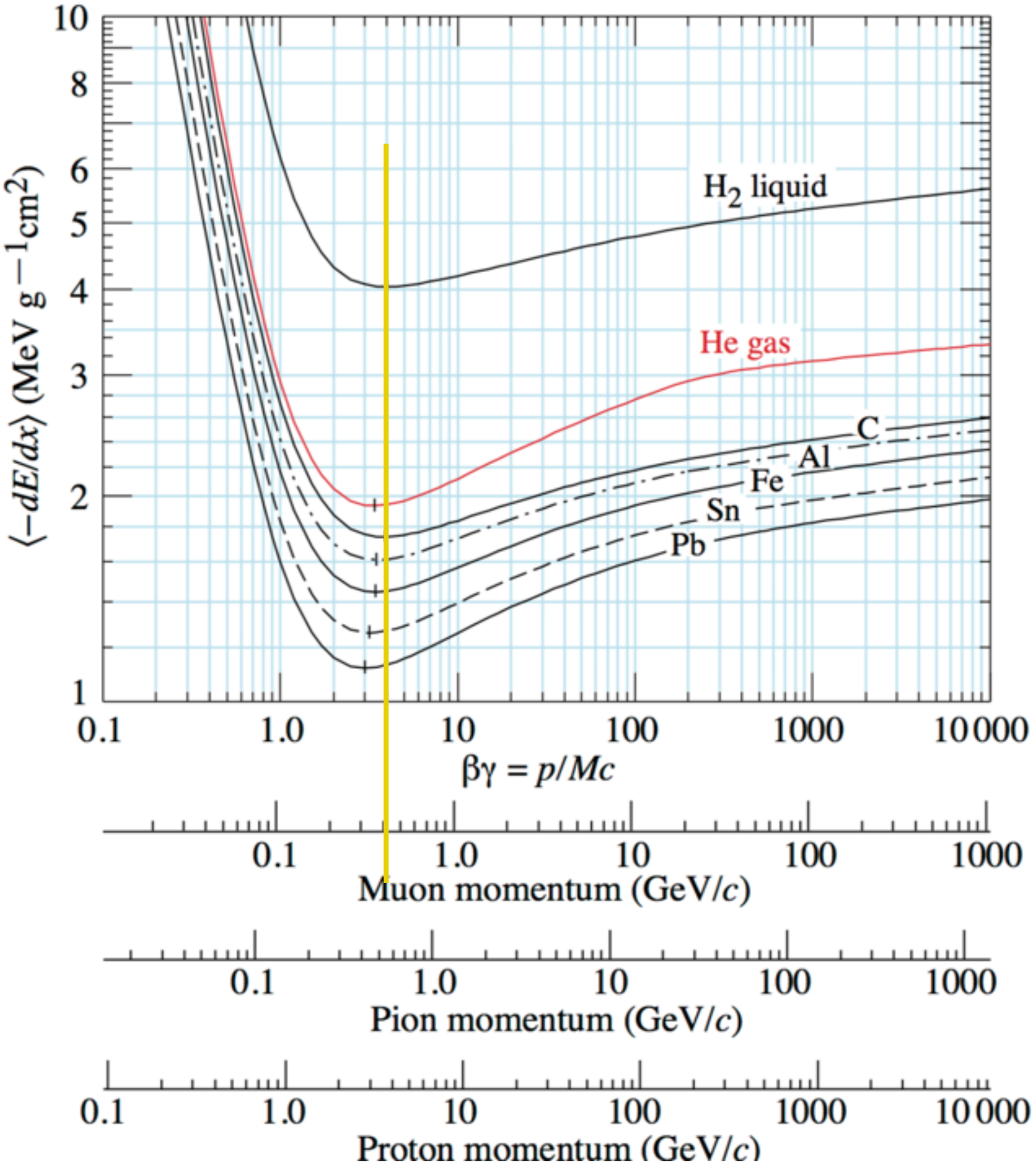
10
8
6
5
4
3
2
1
⟨−dE/dx⟩ (MeV g−1cm2)
H2 liquid
He gas
C
Al
Fe
Sn
Pb
0.1
1.0
10
100
1000
10 000
βγ = p/Mc
0.1
1.0
10
100
1000
Muon momentum (GeV/c)
0.1
1.0
10
100
1000
Pion momentum (GeV/c)
0.1
1.0
10
100
1000
10 000
Proton momentum (GeV/c)

MIP energy deposit

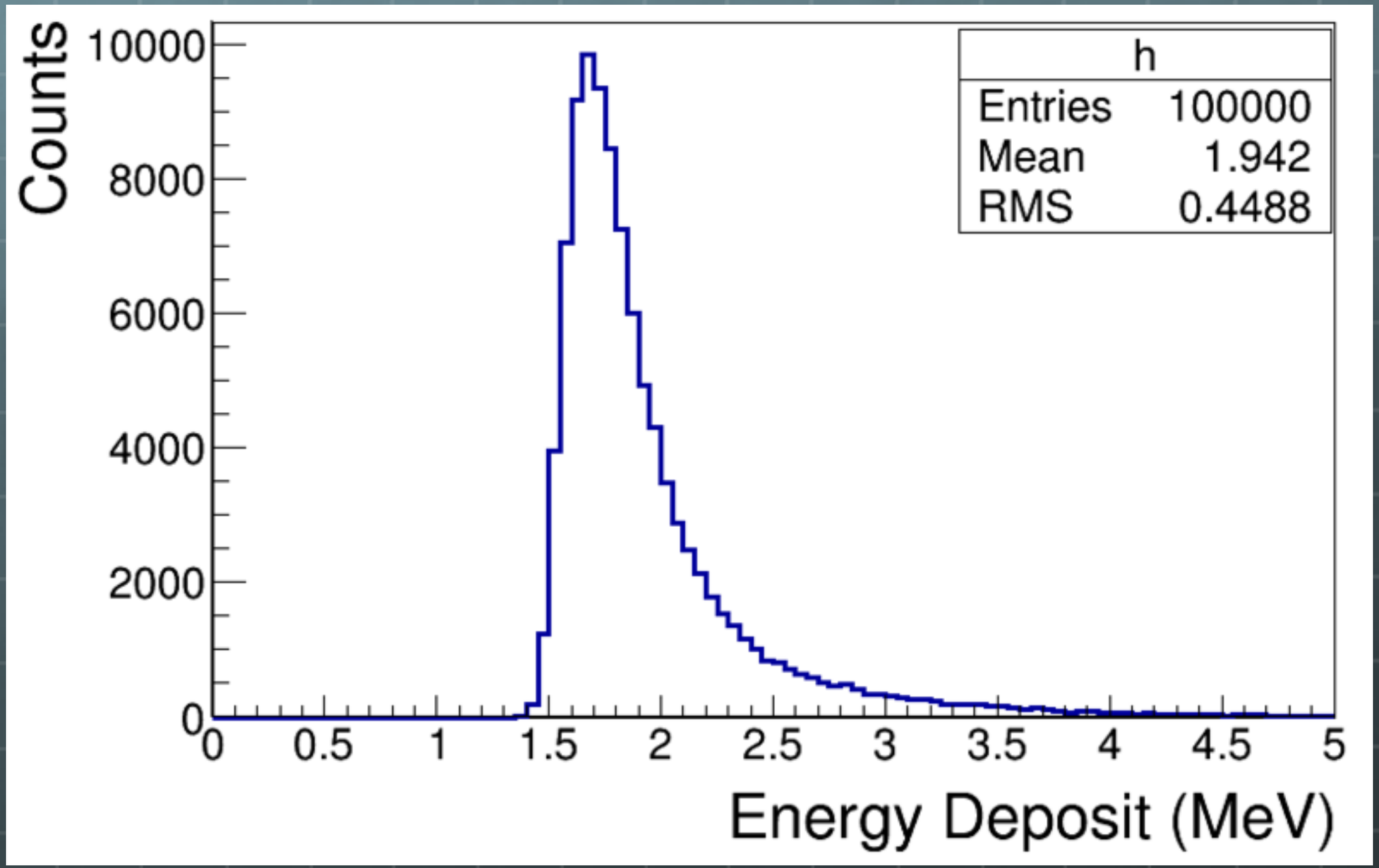

6. ATOMIC AND NUCLEAR PROPERTIES OF MATERIALS

Table 6.1 Abridged from `pdg.lbl.gov/AtomicNuclearProperties` by D.E. Groom (2015). See web pages for more detail about entries in this table and for several hundred other substances. Parentheses in the dE/dx and density columns indicate gases at 20° C and 1 atm. Boiling points are at 1 atm. Refractive indices n are evaluated at the sodium D line blend (589.2 nm); values ⩾1 in brackets indicate $(n-1)\times 10^6$ for gases at 0° C and 1 atm.

Material	Z	A	$\langle Z/A\rangle$	Nucl.coll. length λ_T {g cm^{-2}}	Nucl.inter. length λ_I {g cm^{-2}}	Rad.len. X_0 {g cm^{-2}}	$dE/dx\|_{\rm min}$ { MeV g^{-1}cm^2}	Density {g cm^{-3}} ({gℓ^{-1}})	Melting point (K)	Boiling point (K)	Refract. index @ Na D
H_2	1	1.008(7)	0.99212	42.8	52.0	63.04	(4.103)	0.071(0.084)	13.81	20.28	1.11[132.]
D_2	1	2.01410177803(8)	0.49650	51.3	71.8	125.97	(2.053)	0.169(0.168)	18.7	23.65	1.11[138.]
He	2	4.002602(2)	0.49967	51.8	71.0	94.32	(1.937)	0.125(0.166)		4.220	1.02[35.0]
Li	3	6.94(2)	0.43221	52.2	71.3	82.78	1.639	0.534	453.6	1615.	
Be	4	9.0121831(5)	0.44384	55.3	77.8	65.19	1.595	1.848	1560.	2744.	
C diamond	6	12.0107(8)	0.49955	59.2	85.8	42.70	1.725	3.520			2.42
C graphite	6	12.0107(8)	0.49955	59.2	85.8	42.70	1.742	2.210			
N_2	7	14.007(2)	0.49976	61.1	89.7	37.99	(1.825)	0.807(1.165)	63.15	77.29	1.20[298.]
O_2	8	15.999(3)	0.50002	61.3	90.2	34.24	(1.801)	1.141(1.332)	54.36	90.20	1.22[271.]
F_2	9	18.998403163(6)	0.47372	65.0	97.4	32.93	(1.676)	1.507(1.580)	53.53	85.03	[195.]
Ne	10	20.1797(6)	0.49555	65.7	99.0	28.93	(1.724)	1.204(0.839)	24.56	27.07	1.09[67.1]
Al	13	26.9815385(7)	0.48181	69.7	107.2	24.01	1.615	2.699	933.5	2792.	
Si	14	28.0855(3)	0.49848	70.2	108.4	21.82	1.664	2.329	1687.	3538.	3.95
Cl_2	17	35.453(2)	0.47951	73.8	115.7	19.28	(1.630)	1.574(2.980)	171.6	239.1	[773.]
Ar	18	39.948(1)	0.45059	75.7	119.7	19.55	(1.519)	1.396(1.662)	83.81	87.26	1.23[281.]
Ti	22	47.867(1)	0.45961	78.8	126.2	16.16	1.477	4.540	1941.	3560.	
Fe	26	55.845(2)	0.46557	81.7	132.1	13.84	1.451	7.874	1811.	3134.	
Cu	29	63.546(3)	0.45636	84.2	137.3	12.86	1.403	8.960	1358.	2835.	
Ge	32	72.630(1)	0.44053	86.9	143.0	12.25	1.370	5.323	1211.	3106.	
Sn	50	118.710(7)	0.42119	98.2	166.7	8.82	1.263	7.310	505.1	2875.	
Xe	54	131.293(6)	0.41129	100.8	172.1	8.48	(1.255)	2.953(5.483)	161.4	165.1	1.39[701.]
W	74	183.84(1)	0.40252	110.4	191.9	6.76	1.145	19.300	3695.	5828.	
Pt	78	195.084(9)	0.39983	112.2	195.7	6.54	1.128	21.450	2042.	4098.	
Au	79	196.966569(5)	0.40108	112.5	196.3	6.46	1.134	19.320	1337.	3129.	
Pb	82	207.2(1)	0.39575	114.1	199.6	6.37	1.122	11.350	600.6	2022.	
U	92	[238.02891(3)]	0.38651	118.6	209.0	6.00	1.081	18.950	1408.	4404.	
Air (dry, 1 atm)			0.49919	61.3	90.1	36.62	(1.815)	(1.205)		78.80	[289]
Shielding concrete			0.50274	65.1	97.5	26.57	1.711	2.300			
Borosilicate glass (Pyrex)			0.49707	64.6	96.5	28.17	1.696	2.230			
Lead glass			0.42101	95.9	158.0	7.87	1.255	6.220			
Standard rock			0.50000	66.8	101.3	26.54	1.688	2.650			
Methane (CH_4)			0.62334	54.0	73.8	46.47	(2.417)	(0.667)	90.68	111.7	[444.]
Ethane (C_2H_6)			0.59861	55.0	75.9	45.66	(2.304)	(1.263)	90.36	184.5	
Propane (C_3H_8)			0.58962	55.3	76.7	45.37	(2.262)	0.493(1.868)	85.52	231.0	
Butane (C_4H_{10})			0.59497	55.5	77.1	45.23	(2.278)	(2.489)	134.9	272.6	
Octane (C_8H_{18})			0.57778	55.8	77.8	45.00	2.123	0.703	214.4	398.8	
Paraffin ($CH_3(CH_2)_{n\approx 23}CH_3$)			0.57275	56.0	78.3	44.85	2.088	0.930			
Nylon (type 6, 6/6)			0.54790	57.5	81.6	41.92	1.973	1.18			
Polycarbonate (Lexan)			0.52697	58.3	83.6	41.50	1.886	1.20			
Polyethylene ($[CH_2CH_2]_n$)			0.57034	56.1	78.5	44.77	2.079	0.89			
Polyethylene terephthalate (Mylar)			0.52037	58.9	84.9	39.95	1.848	1.40			
Polyimide film (Kapton)			0.51264	59.2	85.5	40.58	1.820	1.42			
Polymethylmethacrylate (acrylic)			0.53937	58.1	82.8	40.55	1.929	1.19			1.49
Polypropylene			0.55998	56.1	78.5	44.77	2.041	0.90			
Polystyrene ($[C_6H_5CHCH_2]_n$)			0.53768	57.5	81.7	43.79	1.936	1.06			1.59
Polytetrafluoroethylene (Teflon)			0.47992	63.5	94.4	34.84	1.671	2.20			
Polyvinyltoluene			0.54141	57.3	81.3	43.90	1.956	1.03			1.58
Aluminum oxide (sapphire)			0.49038	65.5	98.4	27.94	1.647	3.970	2327.	3273.	1.77
Barium flouride (BaF_2)			0.42207	90.8	149.0	9.91	1.303	4.893	1641.	2533.	1.47
Bismuth germanate (BGO)			0.42065	96.2	159.1	7.97	1.251	7.130	1317.		2.15
Carbon dioxide gas (CO_2)			0.49989	60.7	88.9	36.20	1.819	(1.842)			[449.]
Solid carbon dioxide (dry ice)			0.49989	60.7	88.9	36.20	1.787	1.563	Sublimes at 194.7 K		
Cesium iodide (CsI)			0.41569	100.6	171.5	8.39	1.243	4.510	894.2	1553.	1.79
Lithium fluoride (LiF)			0.46262	61.0	88.7	39.26	1.614	2.635	1121.	1946.	1.39
Lithium hydride (LiH)			0.50321	50.8	68.1	79.62	1.897	0.820	965.		
Lead tungstate ($PbWO_4$)			0.41315	100.6	168.3	7.39	1.229	8.300	1403.		2.20
Silicon dioxide (SiO_2, fused quartz)			0.49930	65.2	97.8	27.05	1.699	2.200	1986.	3223.	1.46
Sodium chloride (NaCl)			0.47910	71.2	110.1	21.91	1.847	2.170	1075.	1738.	1.54
Sodium iodide (NaI)			0.42697	93.1	154.6	9.49	1.305	3.667	933.2	1577.	1.77
Water (H_2O)			0.55509	58.5	83.3	36.08	1.992	1.000	273.1	373.1	1.33
Silica aerogel			0.50093	65.0	97.3	27.25	1.740	0.200	(0.03 H_2O, 0.97 SiO_2)		

- Polyvinyltoluene
- <Z/A> =0.54141
- λ_T = 57.3 g/cm^2
- λ_I = 81.3 g/cm^2
- Xo = 43.9 g/cm^2
- dE/dx = 1.965

MeV · cm^2/g

- ρ = 1.03 g/cm^3

In case of 400 MeV/c muon entering the plastic scintillator

$$\left\langle -\frac{dE}{dx} \right\rangle = Kz^2 \frac{Z}{A} \frac{1}{\beta^2} \left[\frac{1}{2} \ln \frac{2m_e c^2 \beta^2 \gamma^2 W_{\max}}{I^2} - \beta^2 - \frac{\delta(\beta\gamma)}{2} \right]$$

- $K = 0.307075\ \mathbf{MeV} \cdot cm^2/mol$
- <Z/A> =0.54141
- $\beta = 0.9668,\ \beta\gamma = 3.7858$
- I = 64.7 eV
- $m_e c^2$ = 0.511 MeV
- W_{max} = 14.109 MeV

Quantity	Value	Units	Value	Units
<Z/A>	0.54141			
Specific gravity	1.032	g cm^{-3}		
Mean excitation energy	64.7	eV		
Minimum ionization	1.956	MeV g^{-1}cm^2	2.019	MeV cm^{-1}
Nuclear collision length	57.3	g cm^{-2}	55.56	cm
Nuclear interaction length	81.3	g cm^{-2}	78.80	cm
Pion collision length	84.8	g cm^{-2}	82.19	cm
Pion interaction length	113.3	g cm^{-2}	109.8	cm
Radiation length	43.90	g cm^{-2}	42.54	cm
Critical energy	94.11	MeV (for e^-)	91.62	MeV (for e^+)
Molière radius	9.89	g cm^{-2}	9.586	cm
Plasma energy $\hbar\omega_p$	21.54	eV		
Muon critical energy	1195.	GeV		
Index of refraction (Na D)	1.580			

Cosmic ray momentum spectrum @ KEK

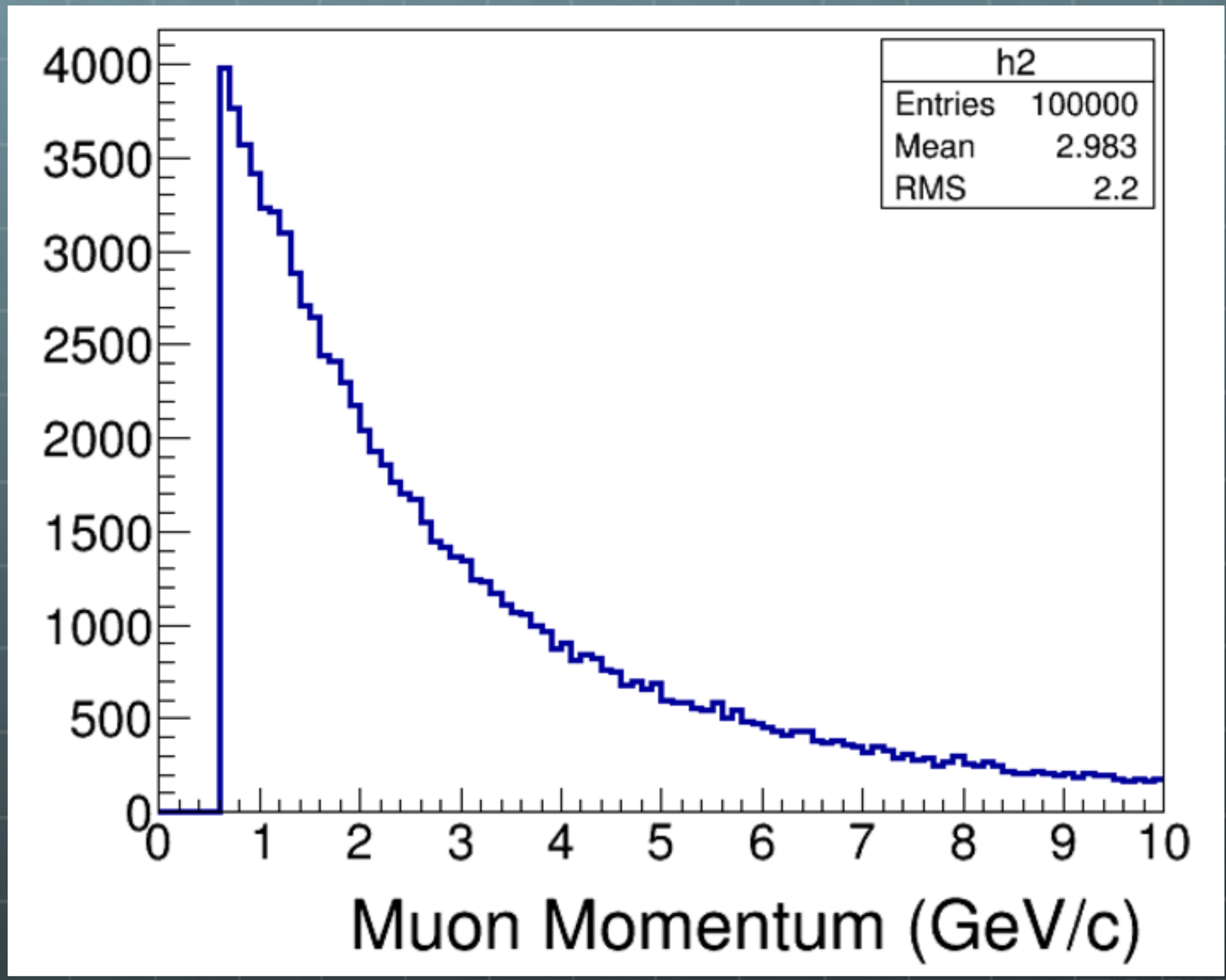

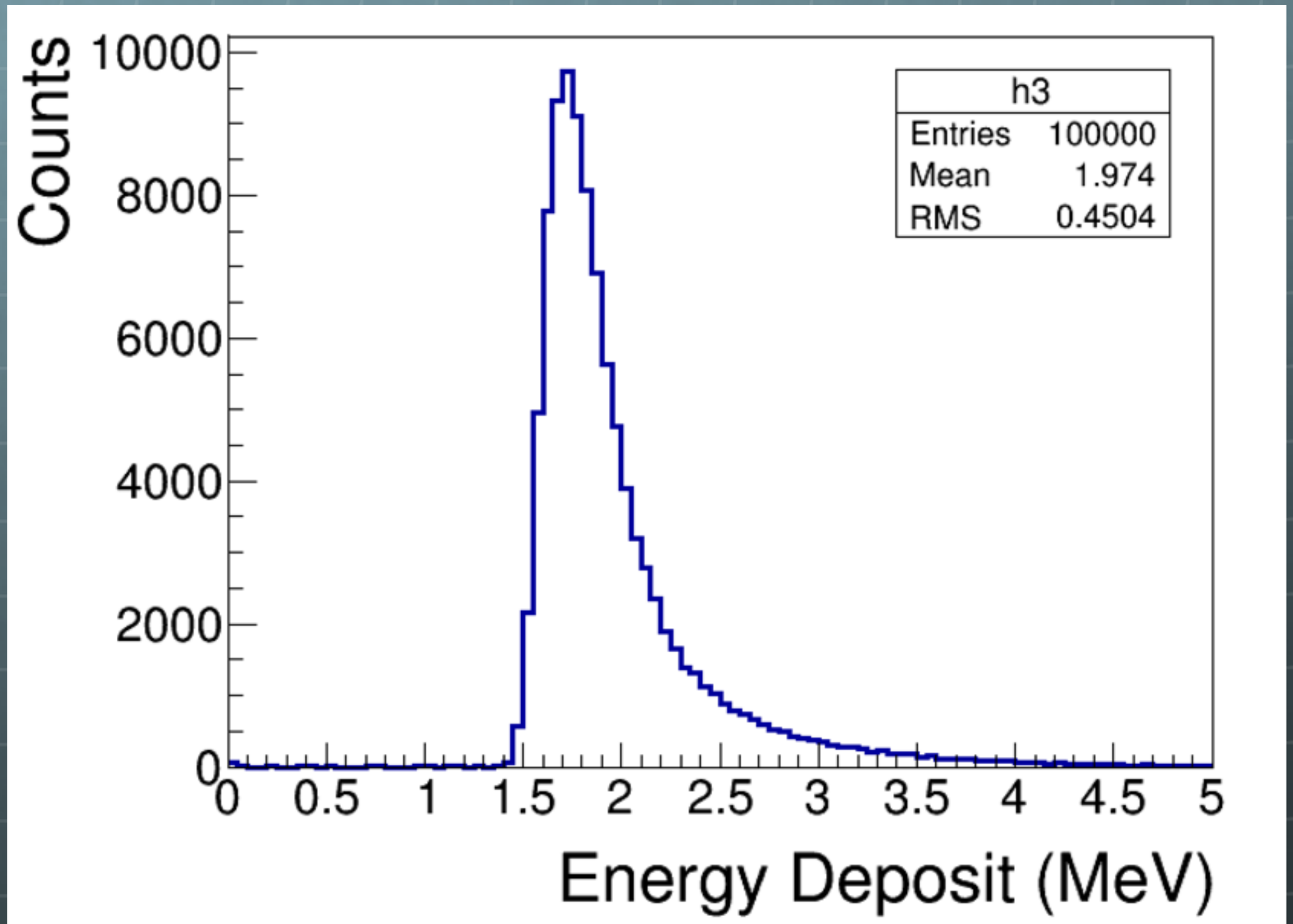
Counts
10000
8000
6000
4000
2000
0
0
0.5
1
1.5
2
2.5
3
3.5
4
4.5
5
Energy Deposit (MeV)
h3
Entries 100000
Mean 1.974
RMS 0.4504

$$\left\langle -\frac{dE}{dx} \right\rangle = Kz^2 \frac{Z}{A} \frac{1}{\beta^2} \left[\frac{1}{2} \ln \frac{2m_e c^2 \beta^2 \gamma^2 W_{\max}}{I^2} - \beta^2 - \frac{\delta(\beta\gamma)}{2} \right]$$

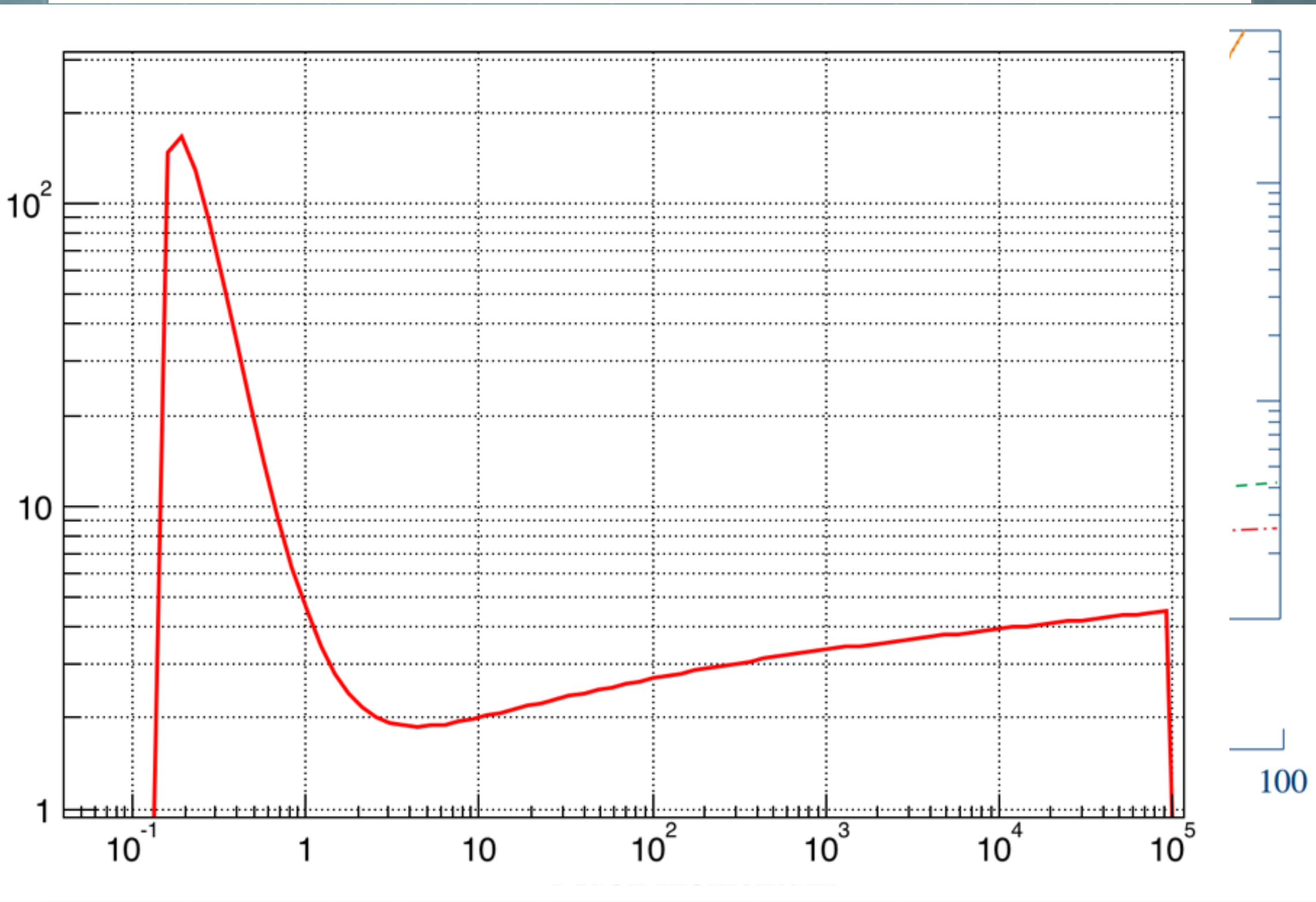

Particle Energy Deposit

$\beta\gamma > 3.5$:

$$\left\langle \frac{dE}{dx} \right\rangle \approx \left. \frac{dE}{dx} \right|_{\min}$$

$\beta\gamma < 3.5$:

$$\left\langle \frac{dE}{dx} \right\rangle \gg \left. \frac{dE}{dx} \right|_{\min}$$

Applications:

Tumor therapy

Possibility to precisely deposit dose at well defined depth by E_{beam} variation

[see Journal Club]

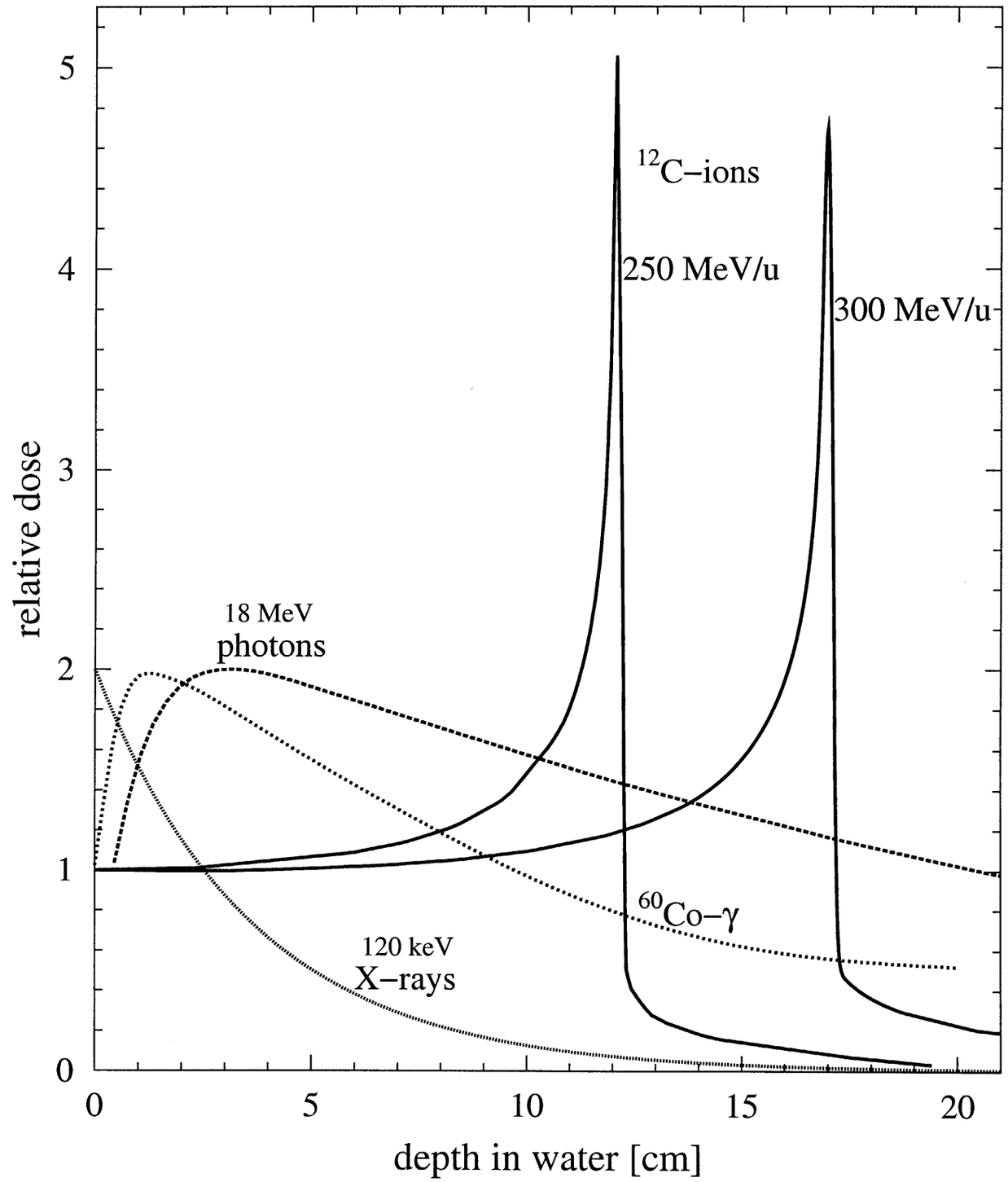

Straggling -Landau Distribution-

- For a small energy loss, prob. of fluctuations
- Let unknown function f(x,Δ)

$$\frac{\partial f}{\partial x} = \int_0^\infty \omega(\varepsilon)[f(x,\Delta-\varepsilon) - f(x,\Delta)]d\varepsilon$$

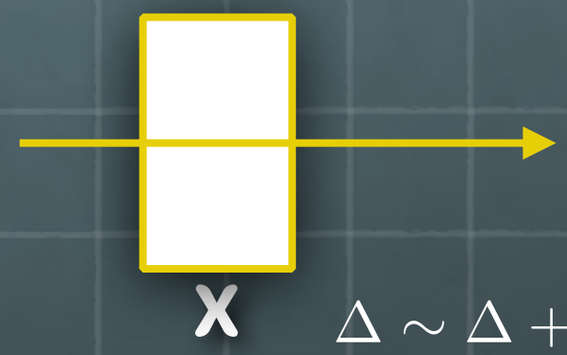

Energy Loss

$$f(x,\Delta) = \frac{1}{2\pi i}\int_{i\infty+\sigma}^{+i\infty+\sigma} e^{p\Delta}\phi(p,x)dp$$

$$f(x,\Delta) = \frac{1}{2\pi i}\int_{-i\infty+\sigma}^{+i\infty+\sigma} e^{p\Delta - x\int_0^\infty \omega(\varepsilon)(1-e^{-p\varepsilon})d\varepsilon} dp$$

$$\omega(\varepsilon) = \frac{2\pi N e^2 \rho \sum Z}{mv^2 \sum A}\frac{1}{\varepsilon^2} \quad \textbf{for} \quad \varepsilon_0 \ll \varepsilon \ll \varepsilon_{max}$$

Straggling
-Landau Distribution-

With a variable $\xi = x\dfrac{2\pi N e^2 \rho \sum Z}{mv^2 \sum A}$

$$f(x,\Delta) = \frac{1}{\xi}\phi(\lambda)$$

$$\phi(\lambda) = \frac{1}{2\pi i}\int_{-i\infty+\sigma}^{+i\infty+\sigma} e^{u\ln u+\lambda u}du$$

$$\lambda = \frac{\Delta - \xi(\ln\frac{\xi}{\varepsilon'} + 1 - C)}{\xi}$$

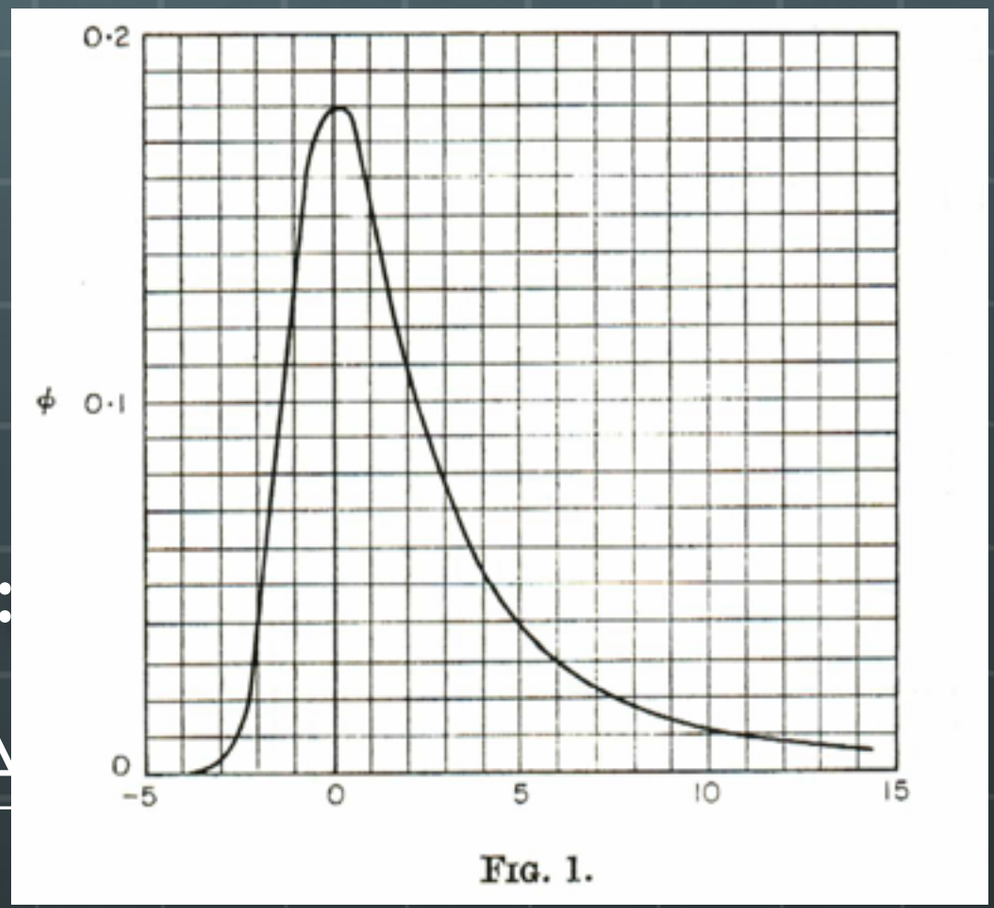

FIG. 1.

Most probable value of energy loss :

$$f(x,\Delta)d\Delta = \phi(\frac{\Delta - \Delta_0}{\xi})d(\frac{\Delta}{}$$

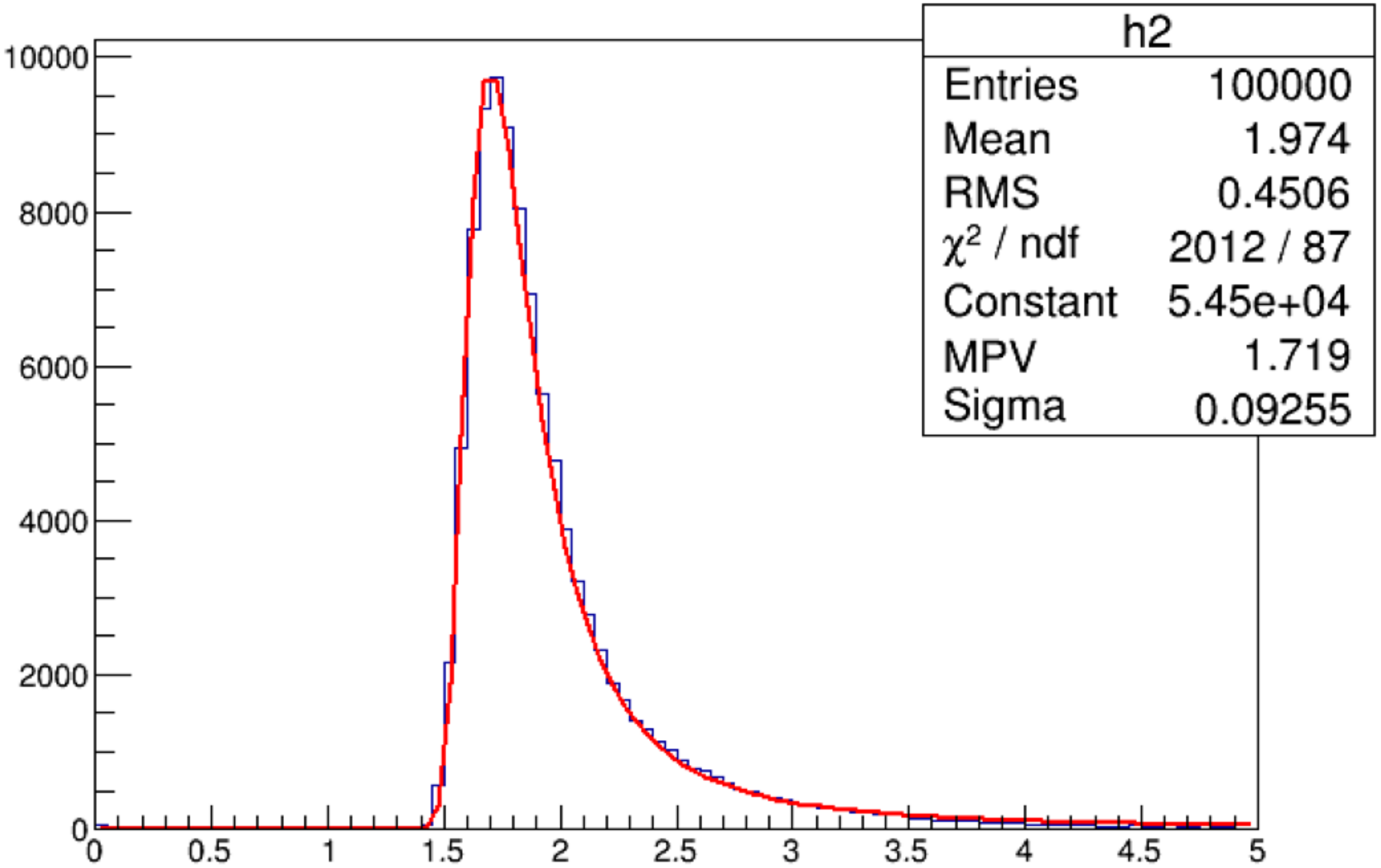
h2
Entries 100000
Mean 1.974
RMS 0.4506
χ² / ndf 2012 / 87
Constant 5.45e+04
MPV 1.719
Sigma 0.09255
10000
8000
6000
4000
2000
0
0
0.5
1
1.5
2
2.5
3
3.5
4
4.5
5

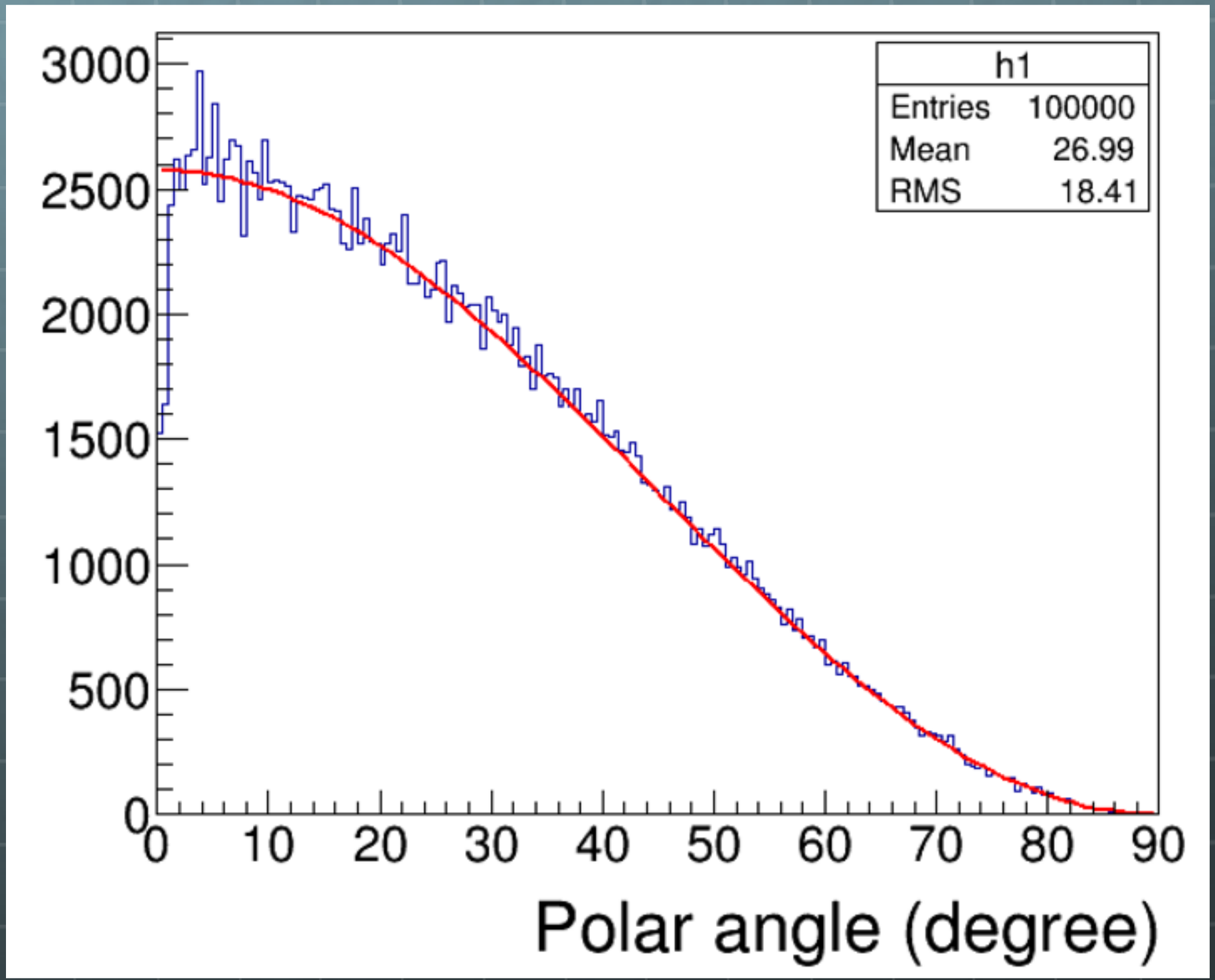
h1
Entries 100000
Mean 26.99
RMS 18.41
3000
2500
2000
1500
1000
500
0
0 10 20 30 40 50 60 70 80 90
Polar angle (degree)

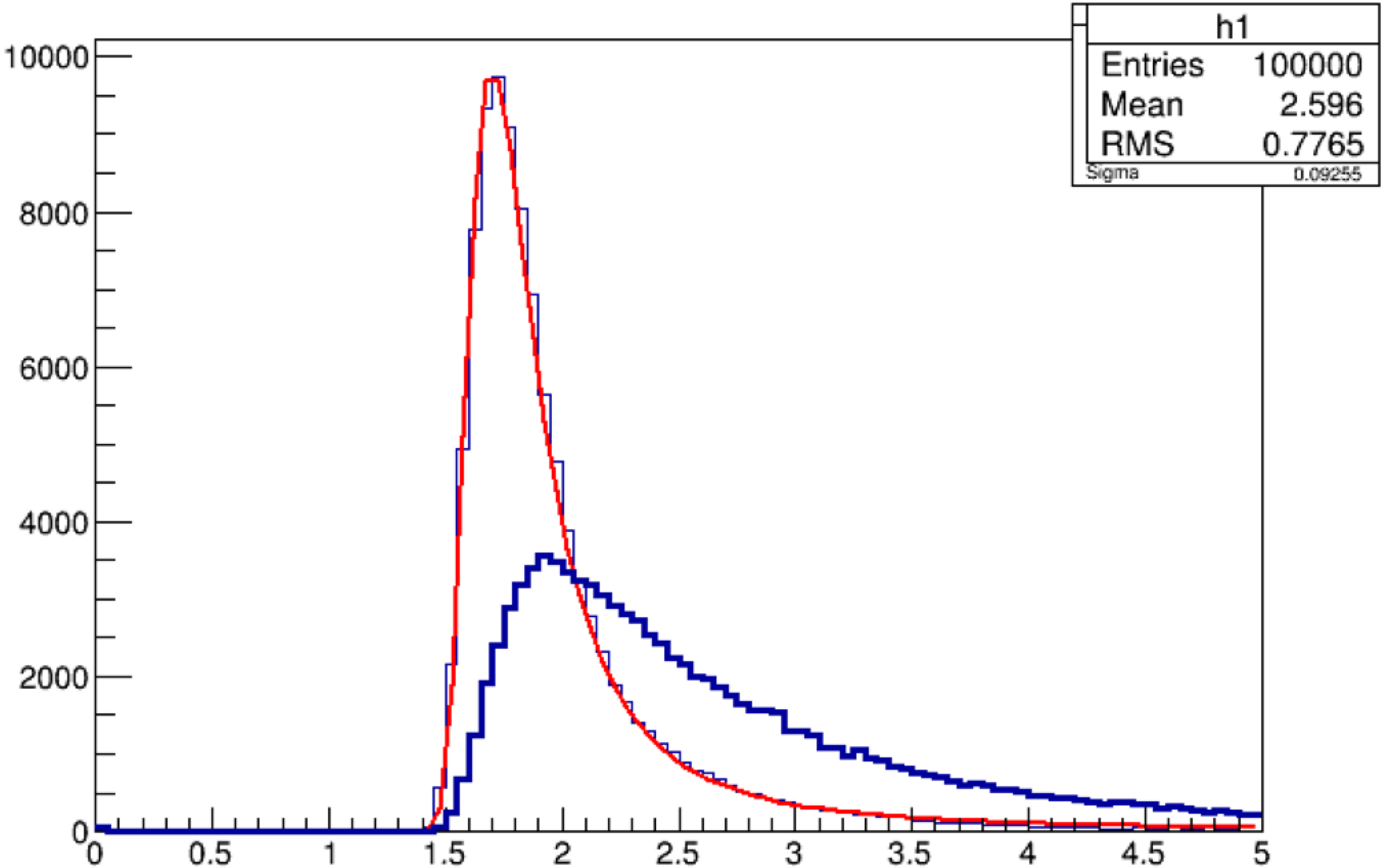
h1
Entries 100000
Mean 2.596
RMS 0.7765
Sigma 0.09255
10000
8000
6000
4000
2000
0
0
0.5
1
1.5
2
2.5
3
3.5
4
4.5
5

Energy Loss of $e^{\pm}$

Energy loss of $e^{\pm}$

$$\left\langle -\frac{dE}{dx} \right\rangle = Kz^2 \frac{Z}{A} \frac{1}{\beta^2} \left[\frac{1}{2} \ln \frac{2m_e c^2 \beta^2 \gamma^2 W_{\max}}{I^2} - \beta^2 - \frac{\delta(\beta\gamma)}{2} \right]$$

$$W_{\max} = \frac{2m_e c^2 \beta^2 \gamma^2}{1 + 2\gamma m_e/M + (m_e/M)^2}$$

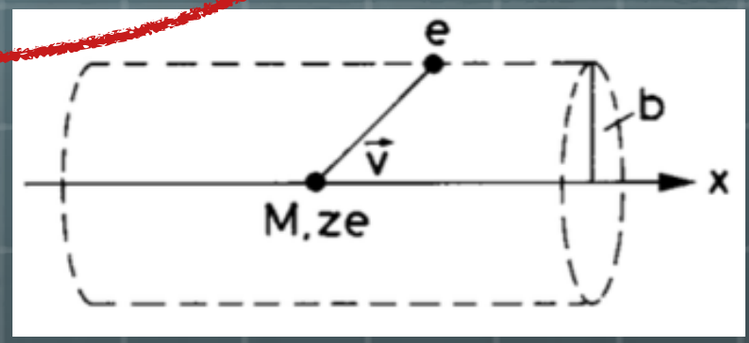

$$\frac{1}{2}\ln\left(\frac{\tau^2(\tau+2)}{2(I/m_e c^2)^2}\right) + F(\tau)$$

for e^-

$$F(\tau) = 1 - \beta^2 + \frac{(\tau^2/8) - (2r+1)\ln 2}{(\tau+1)^2}$$

for e^+

$$F(\tau) = 2\ln 2 - \frac{\beta^2}{12}\left(23 + \frac{14}{\tau+2} + \frac{10}{(\tau+2)^2} + \frac{4}{(\tau+2)^3}\right)$$

$W_{max} = T/2$

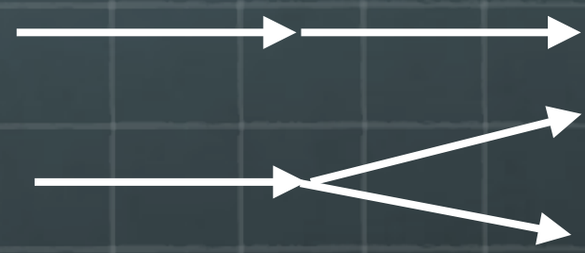

$W_{max} = T$

Energy loss of $e^{\pm}$

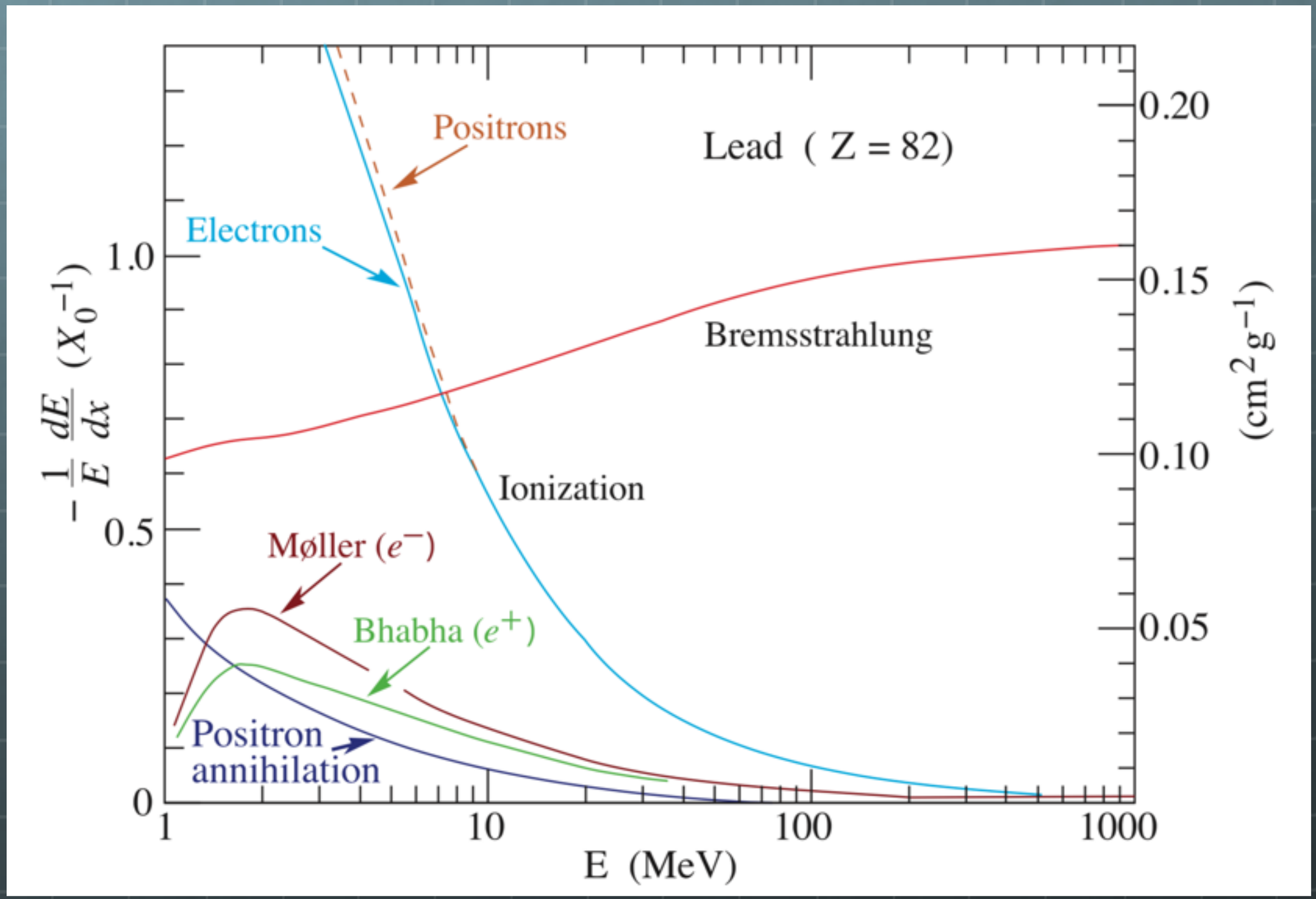

Bremsstrahlung

$$\frac{dE}{dx} = 4\alpha N_A z^2 \frac{Z^2}{A}(\frac{e^2}{mc^2})^2 E \cdot \ln\frac{183}{Z^{1/3}}$$

$$= K z^2 \frac{Z}{A}(\frac{Z}{m_e c^2})\frac{\alpha}{\pi} E \cdot \ln\frac{183}{Z^{1/3}}$$

$$= X_0 E$$

$$E(x) = E_0 e^{-x/X_0}$$

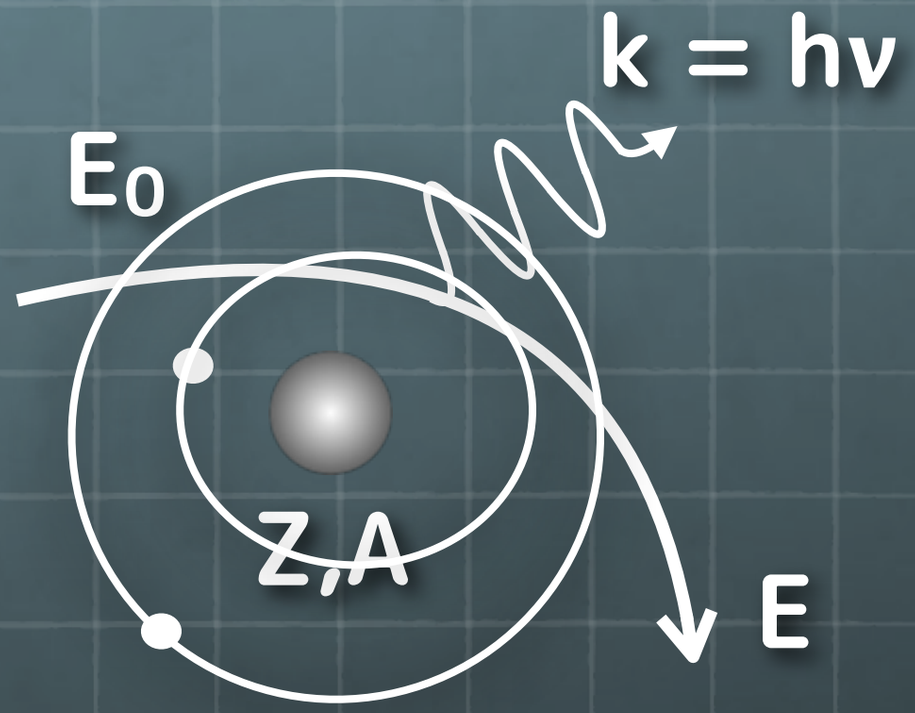

Radiation Length Xo

$$X_0 = \frac{A}{4\alpha N_A Z^2 r_e^2 \ln\frac{183}{Z^{1/3}}}$$

Energy loss of $e^{\pm}$

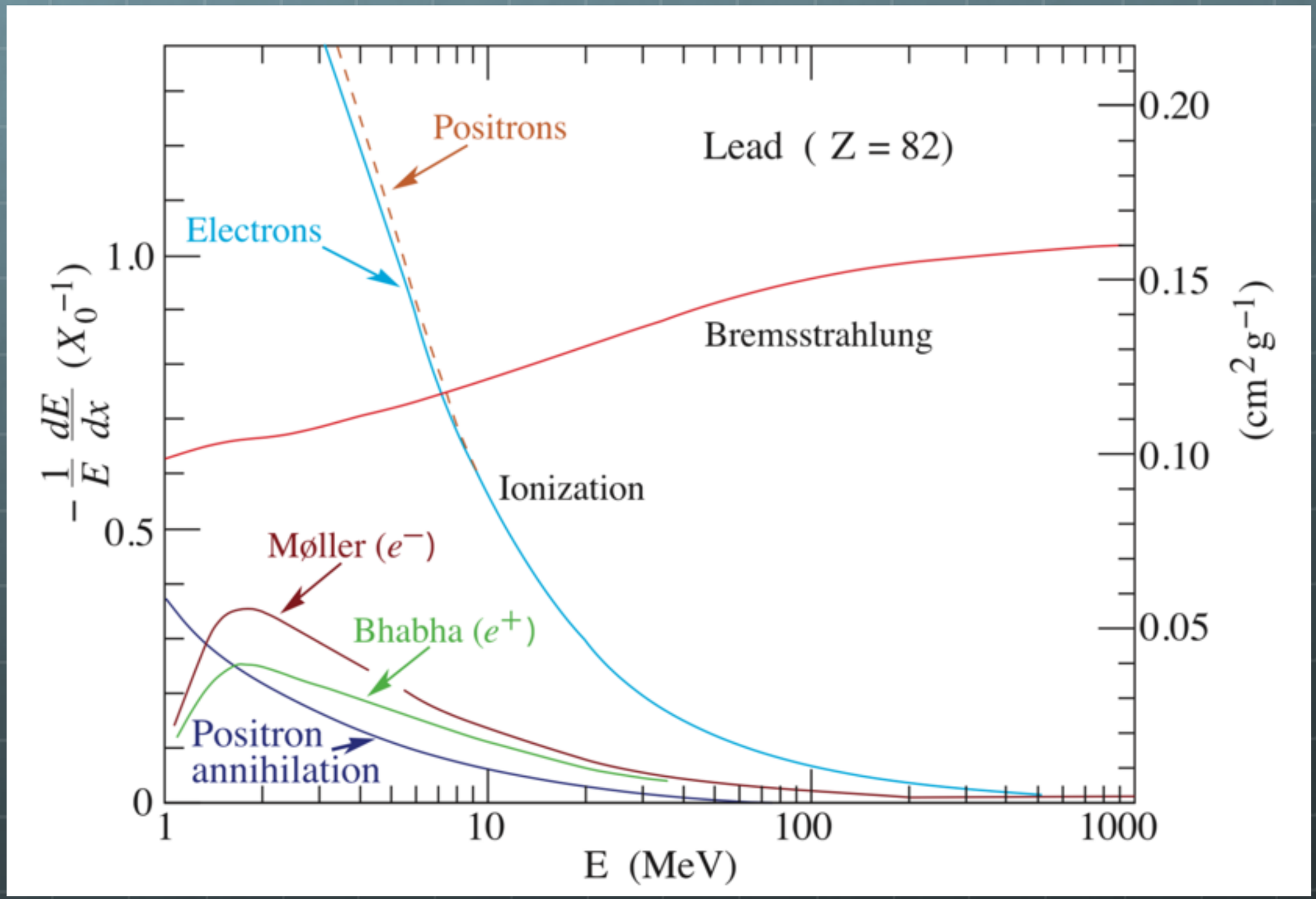

Critical energy (Ec)

- Energy at which a electron losses its energy as same amount by bremsstrahlung and ionization.
- Energy at which the ionization loss per Xo is equal to the electron energy.

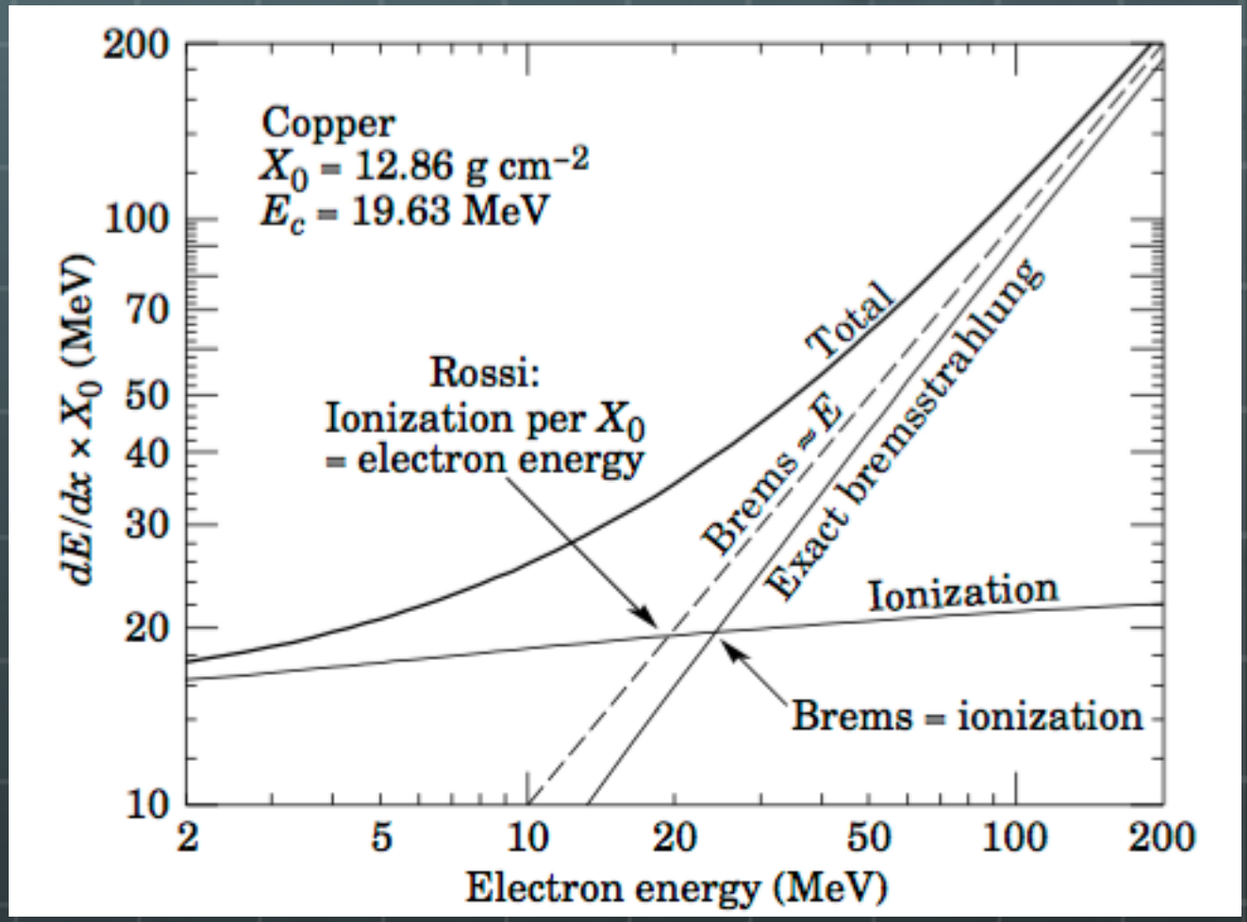

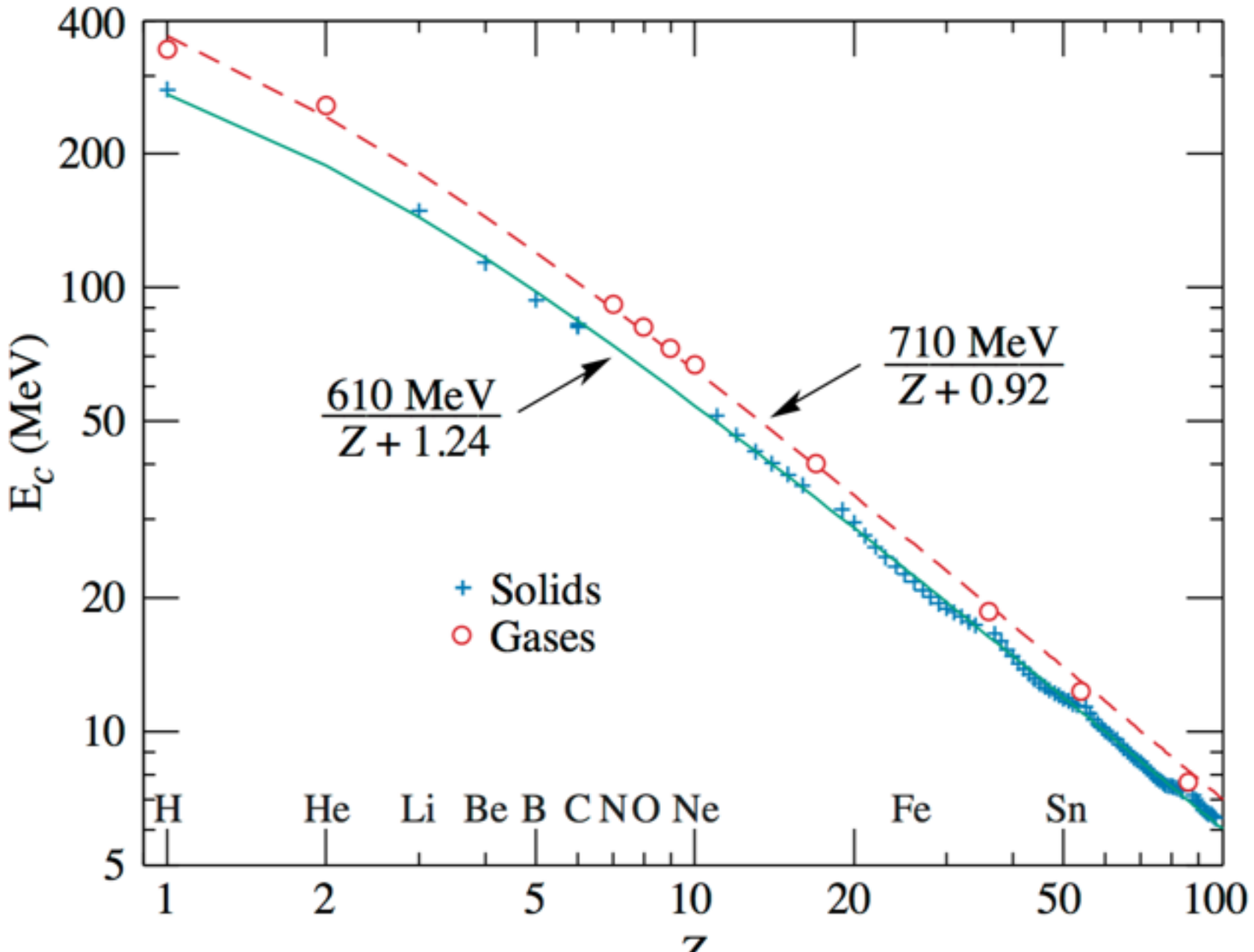

Figure 33.14: Electron critical energy for the chemical elements, using Rossi's definition [2]. The fits shown are for solids and liquids (solid line) and gases (dashed line). The rms deviation is 2.2% for the solids and 4.0% for the gases. (Computed with code supplied by A. Fassó.)

Cherenkov radiation

- In 1934, P.A. Cherenkov observe new type of luminescence irradiating gamma rays into uranyl salt.
  - Originated by charged particle
  - Not to be radiative origin
  - Observed at a certain angle along particle direction

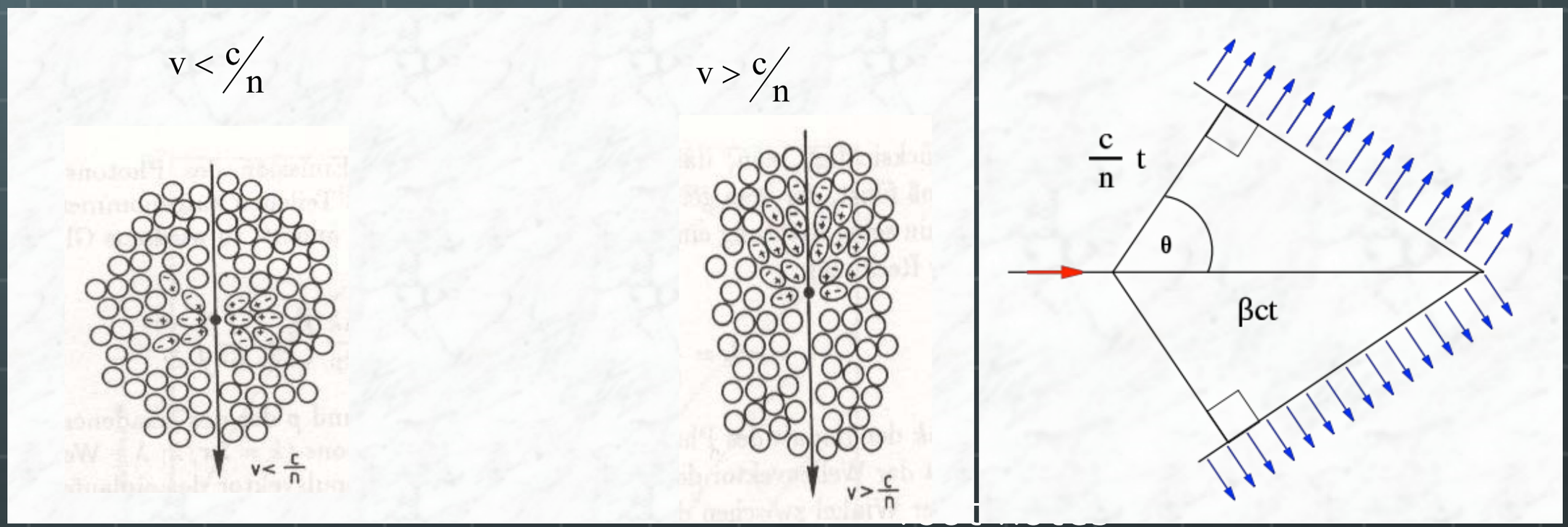

Refractive indices, Cherenkov threshold values

Material	$n-1$	β-Schwelle	γ-Schwelle
festes Natrium	3.22	0.24	1.029
Bleisulfit	2.91	0.26	1.034
Diamant	1.42	0.41	1.10
Zinksulfid ($ZnS(Ag)$)	1.37	0.42	1.10
Silberchlorid	1.07	0.48	1.14
Flintglas (SFS1)	0.92	0.52	1.17
Bleifluorid	0.80	0.55	1.20
Clerici-Lösung	0.69	0.59	1.24
Bleiglas	0.67	0.60	1.25
Thalliumformiat-Lösung	0.59	0.63	1.29
Szintillator	0.58	0.63	1.29
Plexiglas	0.48	0.66	1.33
Borsilikatglas	0.47	0.68	1.36
Wasser	0.33	0.75	1.52
Aerogel	0.025 - 0.075	0.93 - 0.976	4.5 - 2.7
Pentan (STP)	$1.7 \cdot 10^{-3}$	0.9983	17.2
CO_2 (STP)	$4.3 \cdot 10^{-4}$	0.9996	34.1
Luft (STP)	$2.93 \cdot 10^{-4}$	0.9997	41.2
H_2 (STP)	$1.4 \cdot 10^{-4}$	0.99986	59.8
He (STP)	$3.3 \cdot 10^{-5}$	0.99997	123

Tabelle 6.2: Cherenkov-Radiatoren [94, 32, 313]. Der Brechungsindex für Gase bezieht sich auf $0°C$ und $1\,atm$ (STP). Festes Natrium ist für Wellenlängen unterhalb von 2000 Å transparent [373, 209].

problematic: region between liquids and gases

Aerogel: mixture of
m (SiO_2) + 2m (H_2O)

light structure with inclusions of air, bubbles with diameter < λ_{Licht}

→ n: average from n_{air}, n_{SiO2}, n_{H2O}

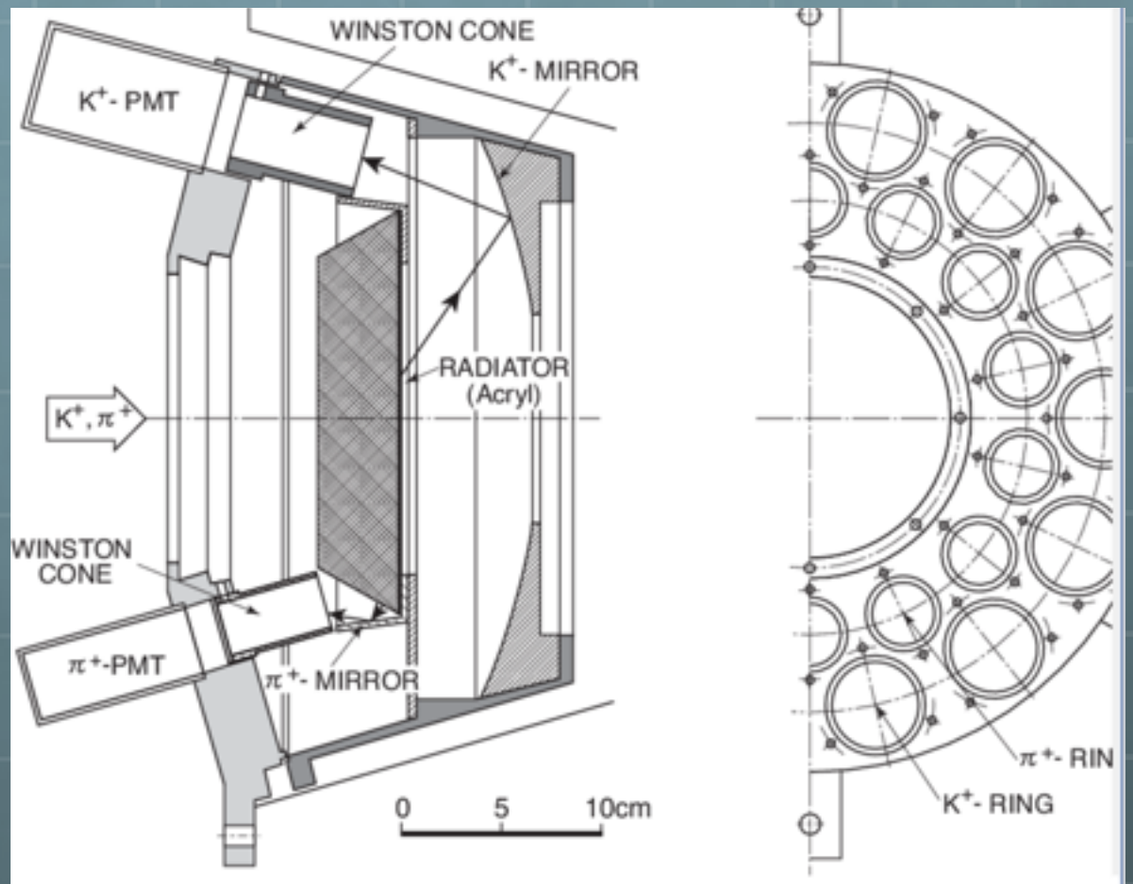
WINSTON CONE
K+- MIRROR
K+- PMT
RADIATOR
(Acryl)
K+, π+
WINSTON
CONE
π+-PMT
π+- MIRROR
0
5
10cm
π+- RIN
K+- RING

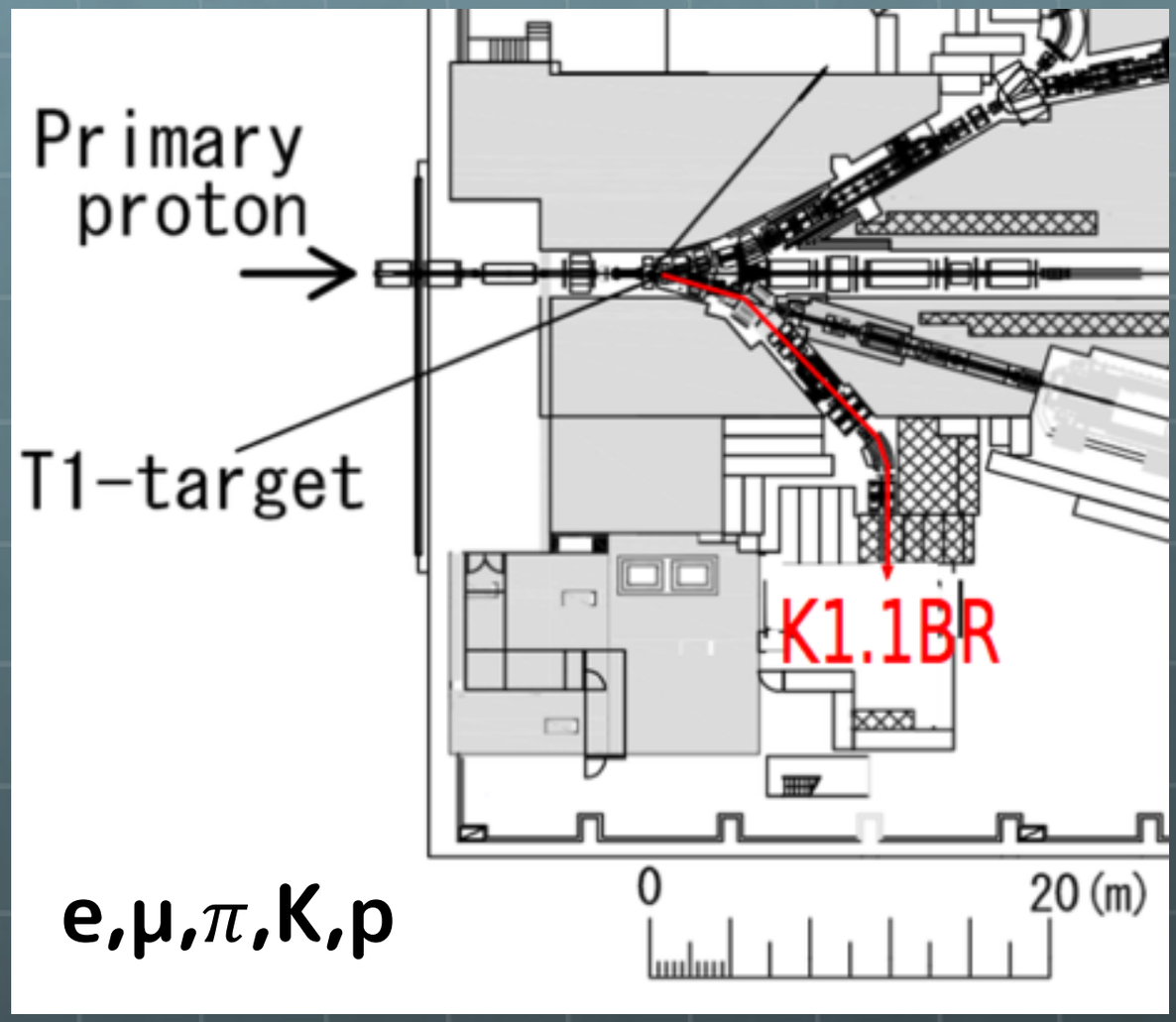
Primary
proton
T1-target
K1.1BR
e,μ,π,K,p
0
20 (m)

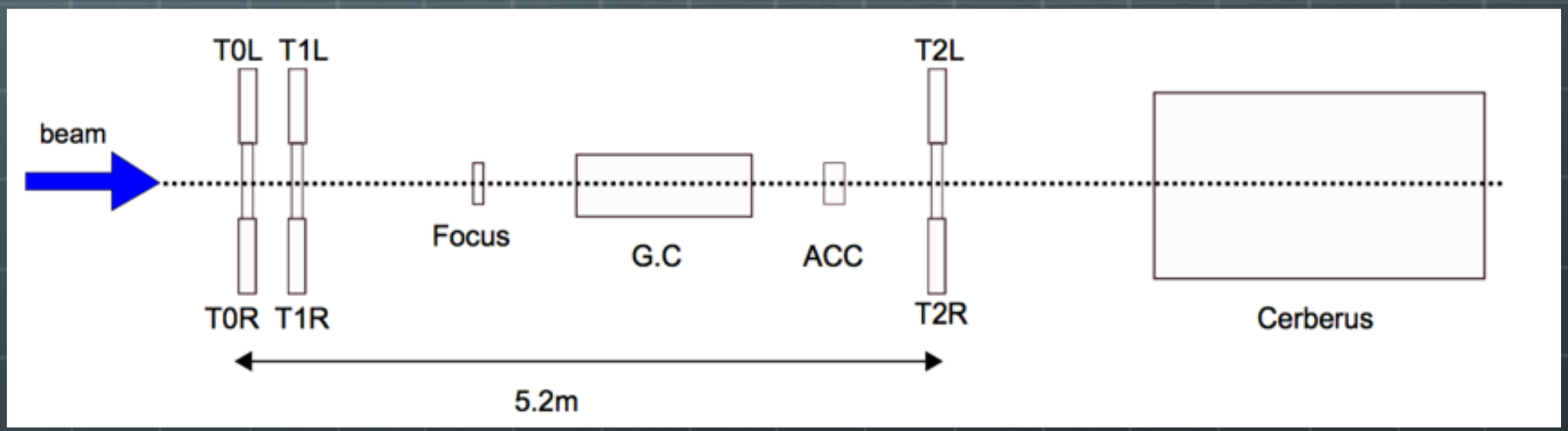
T0L
T1L
T2L
beam
Focus
G.C
ACC
Cerberus
T0R
T1R
T2R
5.2m

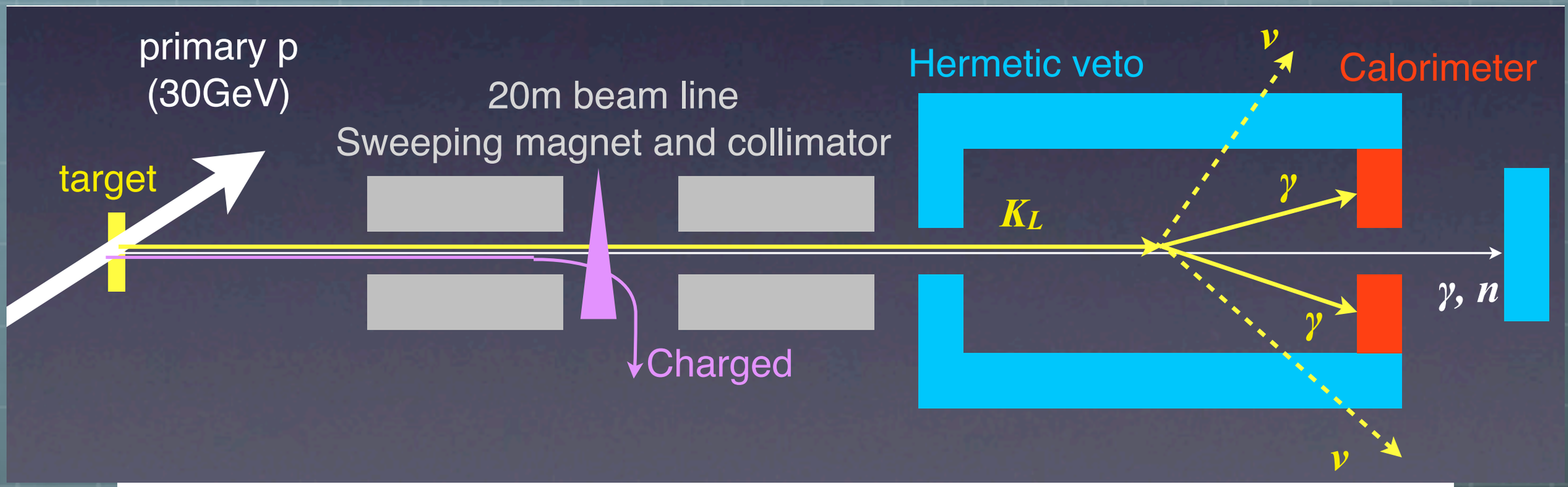

Trigger scintillator for calibration

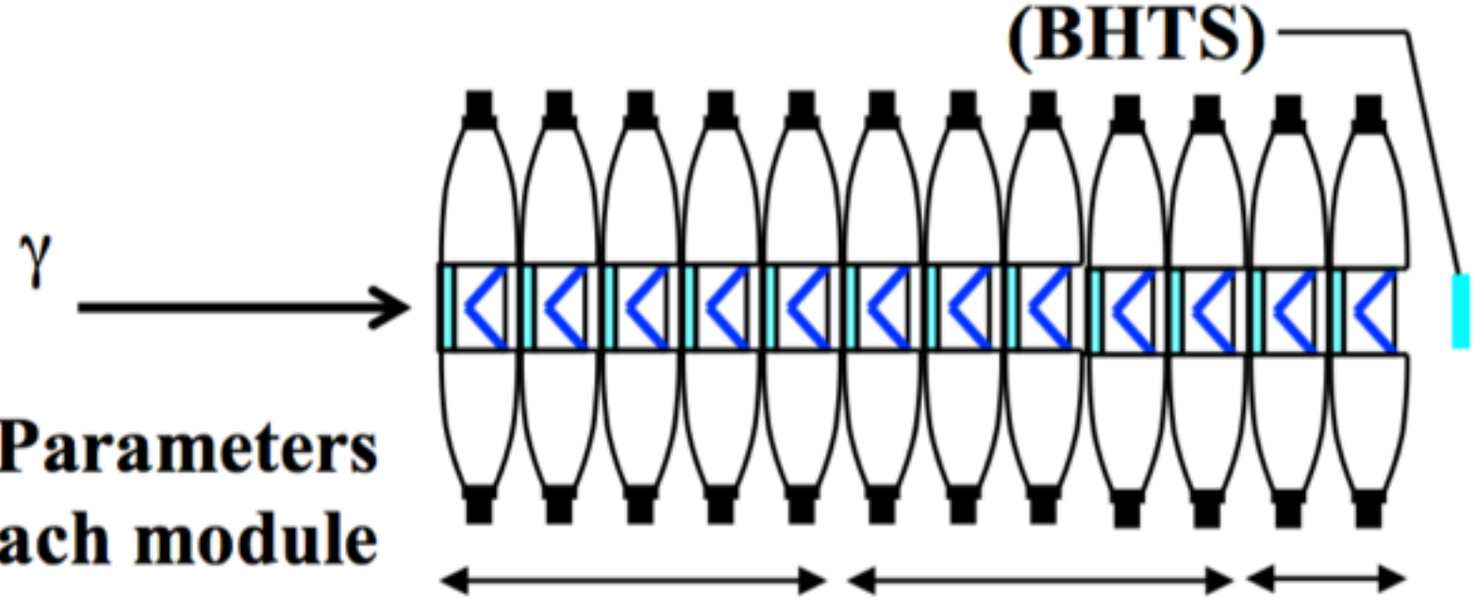

Parameters for each module			
Module No.:	1-5	6-10	11-12
Thickness of lead sheets:	1.5 mm	3.0 mm	-
Thickness of aerogel:	5.8 cm	5.8 cm	5.8 cm

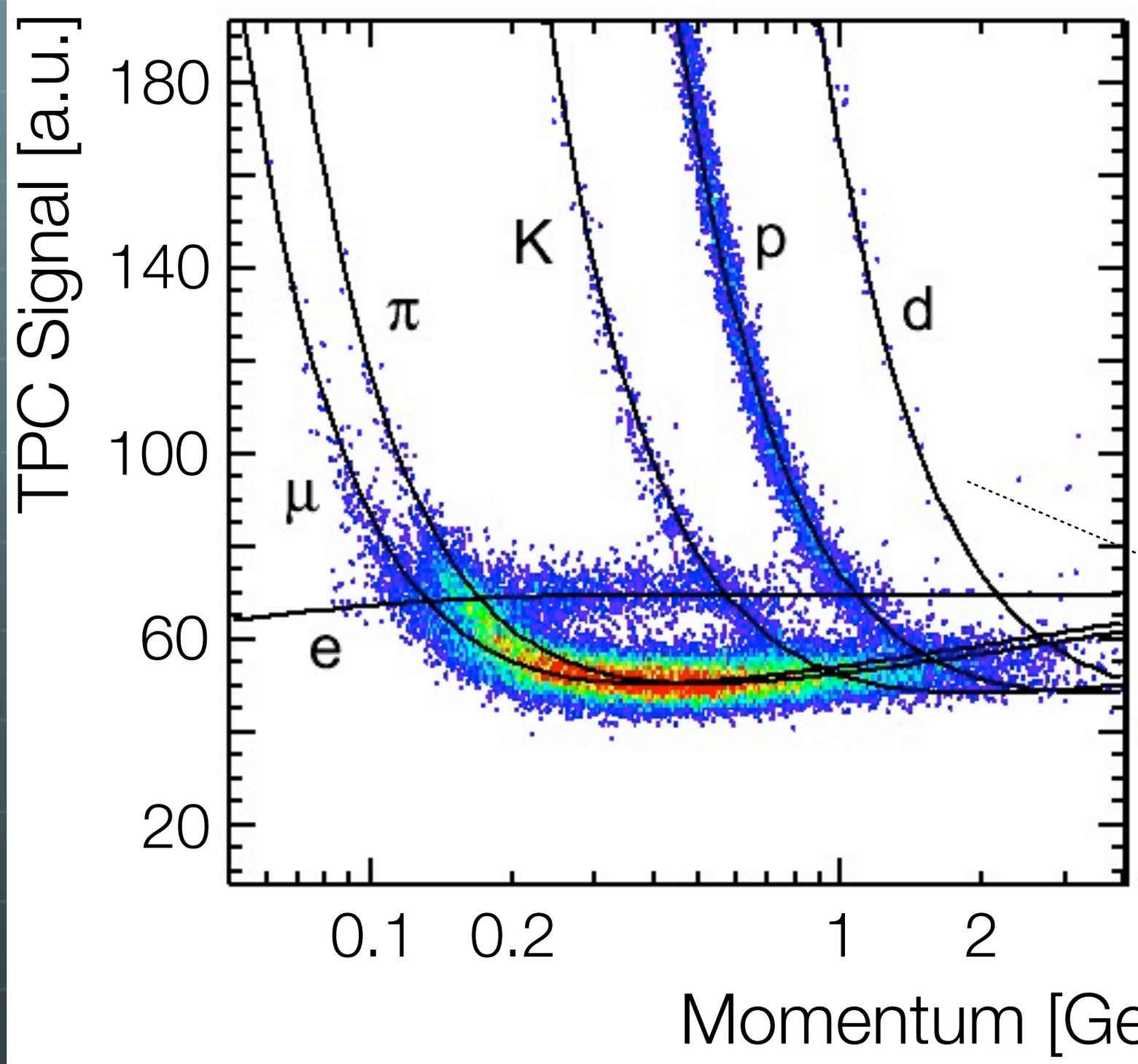

Measured
energy loss

[ALICE TPC, 2009]

Bethe-Bloch

Remember:
dE/dx depends on β!

Transition radiation (TRD)

Charged particle passes through materials with different dielectric properties
→ particle forms dipole with the mirror charge
→ dipole changes with time
→ radiation

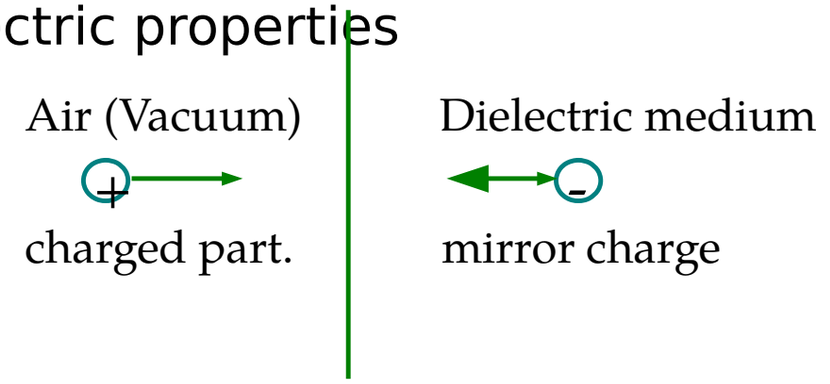

- radiated energy W proportional to the energy of particle!

$$W = \frac{1}{3}\alpha \hbar \omega_p \gamma$$

- with ω_p Plasma frequency

$$\omega_p = \sqrt{\frac{N_e e^2}{\epsilon_0 m_e}} \qquad \hbar\omega_p = 20\,eV$$

- only important for highly relativistic particles

Energy spectrum for CH_2 foil

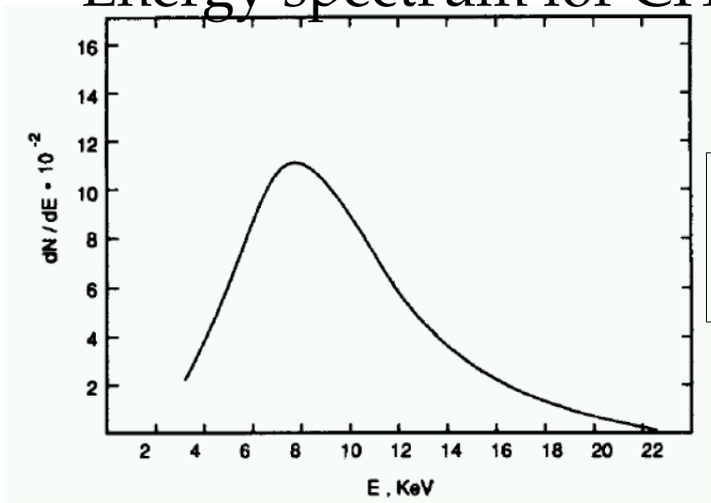

keV!

- energy: keV (x-rays)

- $\theta \propto 1/\gamma$: emission in very forward direction

- probability for photon emission very small → many transitions (foils with gaps)
- # photons <N> ~ W / hν ~ O (α)=1/137 α fine structure constant
- energy loss due to TRD negligible for single transition
- important for particle ID at high energies, other effects used for PID ∝ β (β≃1)
  Review article: B. Dolgoshein; NIM A 326 (1993) 434

Interaction of photons

Interaction of photons

Photoelectric effect

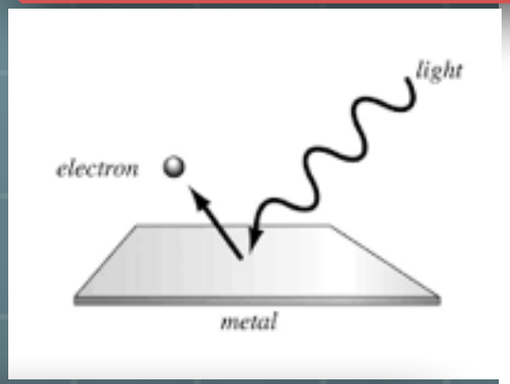

Rayleigh scattering

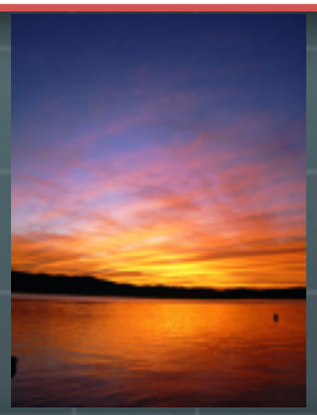

Compton scattering

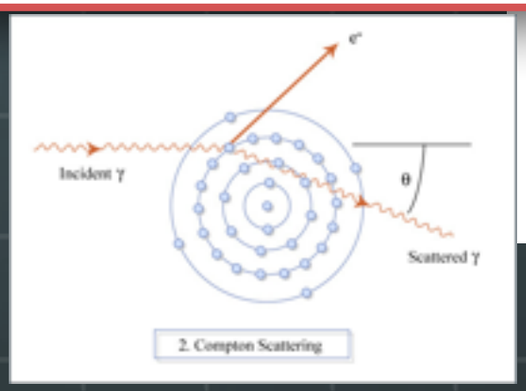

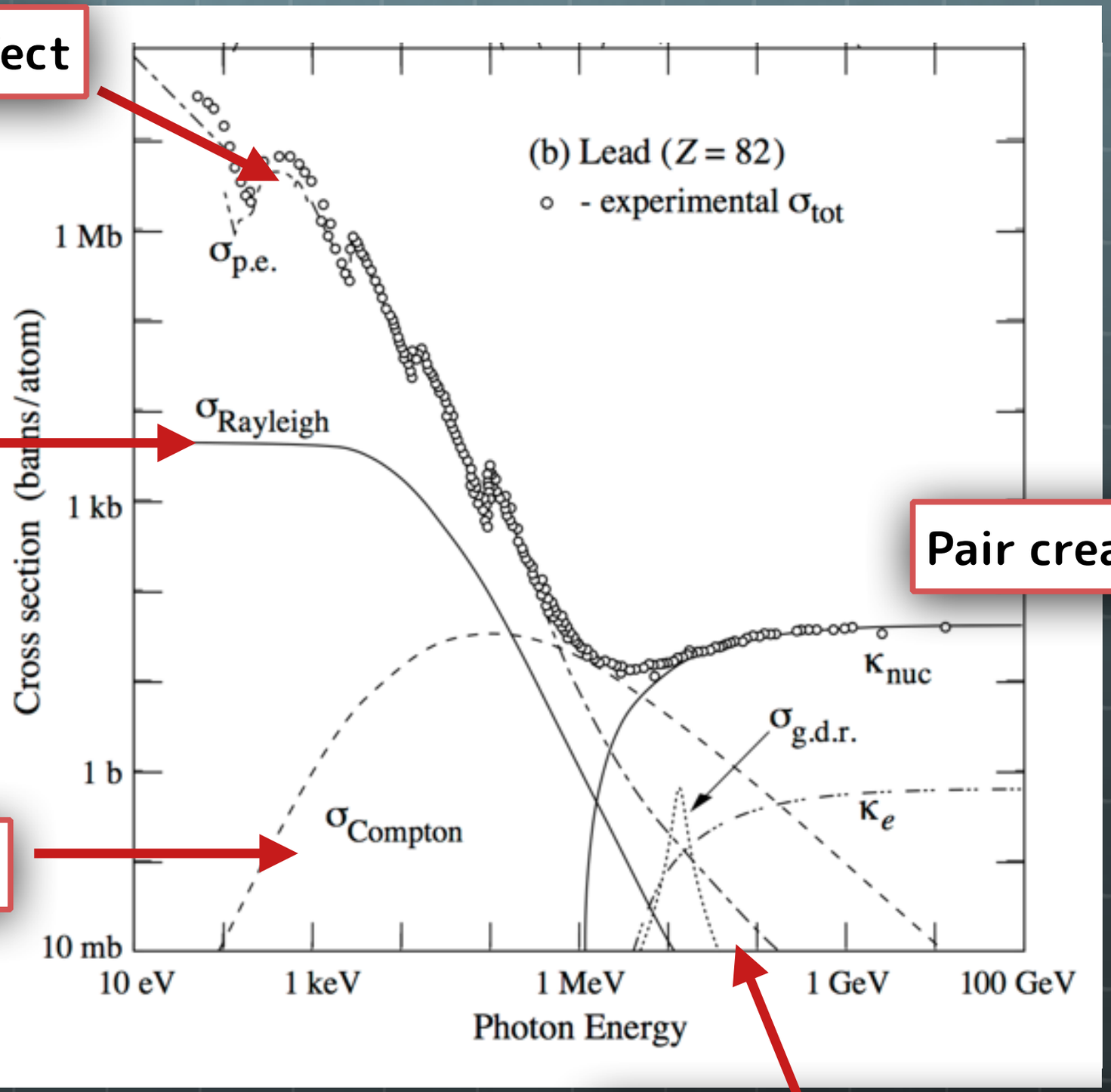

Pair creation

Photonucleear interaction

PMT

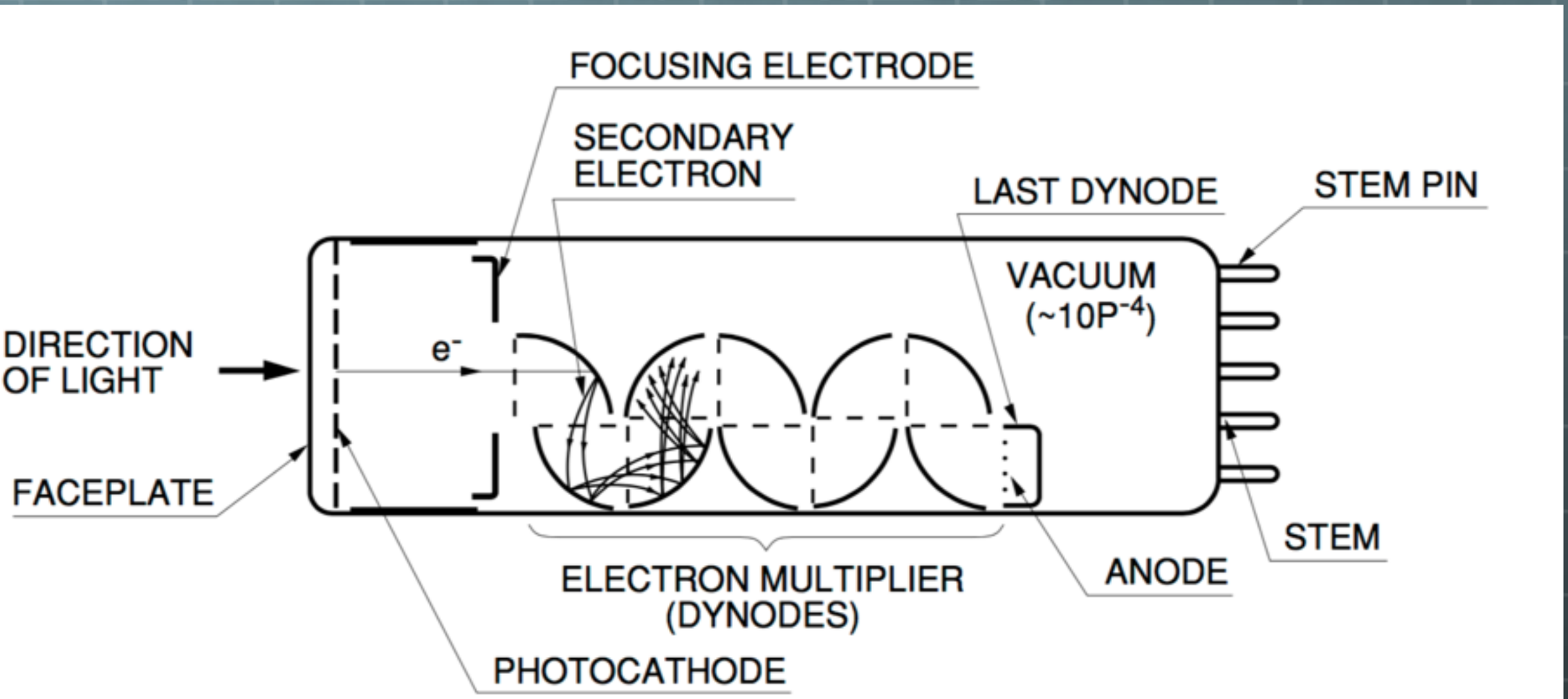
FOCUSING ELECTRODE
SECONDARY ELECTRON
LAST DYNODE
STEM PIN
VACUUM (~10P-4)
DIRECTION OF LIGHT
e-
FACEPLATE
STEM
ANODE
ELECTRON MULTIPLIER (DYNODES)
PHOTOCATHODE

Transmission Mode Photocathodes

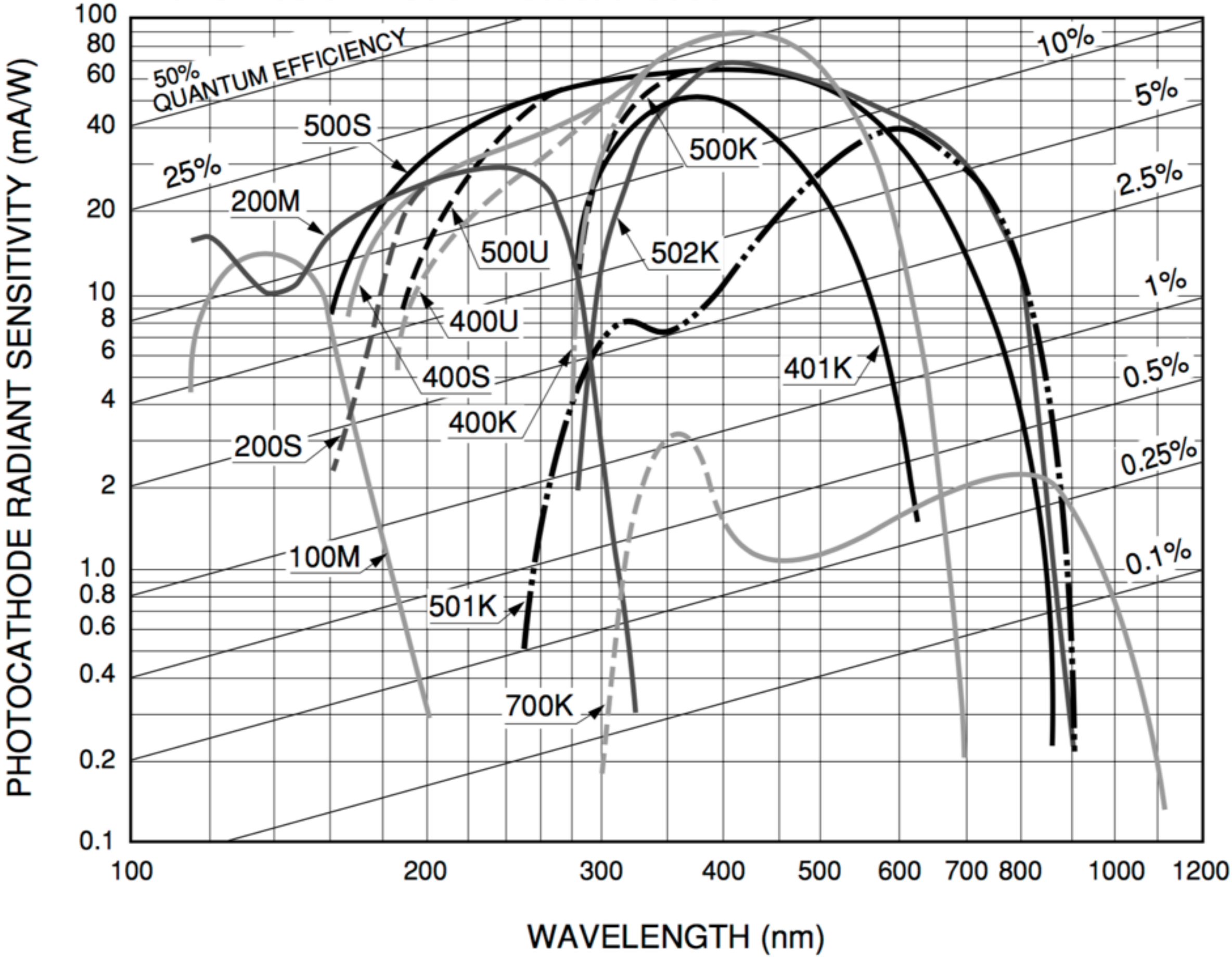

Transmission mode photocathodes

Curve Code (S number)	Photocathode Material	Window Material	Luminous Sensitivity (Typ.) (μA/lm)	Spectral Response				
				Spectral Range (nm)	Peak Wavelength			
					Radiant Sensitivity		Quantum Efficiency	
					(mA/W)	(nm)	(%)	(nm)
100M	Cs-I	MgF_2	—	115 to 200	14	140	13	130
200S	Cs-Te	Quartz	—	160 to 320	29	240	14	210
200M	Cs-Te	MgF_2	—	115 to 320	29	240	14	200
400K	Bialkali	Borosilicate	95	300 to 650	88	420	27	390
400U	Bialkali	UV	95	185 to 650	88	420	27	390
400S	Bialkali	Quartz	95	160 to 650	88	420	27	390
401K	High temp. bialkali	Borosilicate	40	300 to 650	51	375	17	375
500K (S-20)	Multialkali	Borosilicate	150	300 to 850	64	420	20	375
500U	Multialkali	UV	150	185 to 850	64	420	25	280
500S	Multialkali	Quartz	150	160 to 850	64	420	25	280
501K (S-25)	Multialkali	Borosilicate	200	300 to 900	40	600	8	580
502K	Multialkali	Borosilicate (prism)	230	300 to 900	69	420	20	390
700K (S-1)	Ag-O-Cs	Borosilicate	20	400 to 1200	2.2	800	0.36	740
—	GaAsP(Cs)	—	—	300 to 720	180	580	40	540
—	GaAs(Cs)	—	—	380 to 890	85	800	14	760
—	InP/InGaAsP(Cs)	—	—	950 to 1400	21	1300	2.0	1000 to 1300
—	InP/InGaAs(Cs)	—	—	950 to 1700	24	1500	2.0	1000 to 1550

Compton Scattering

$$h\nu = \frac{h\nu_0}{1 + \left(\frac{h\nu_0}{m_e c^2}\right)(1 - \cos\theta)},$$

$$E = h\nu_0 - h\nu = m_e c^2 \frac{2(h\nu_0)^2 \cos^2\phi}{(h\nu_0 + m_e c^2)^2 - (h\nu_0)^2 \cos^2\phi},$$

$$\tan\phi = \frac{1}{1 + \left(\frac{h\nu_0}{m_e c^2}\right)} \cot\frac{\theta}{2},$$

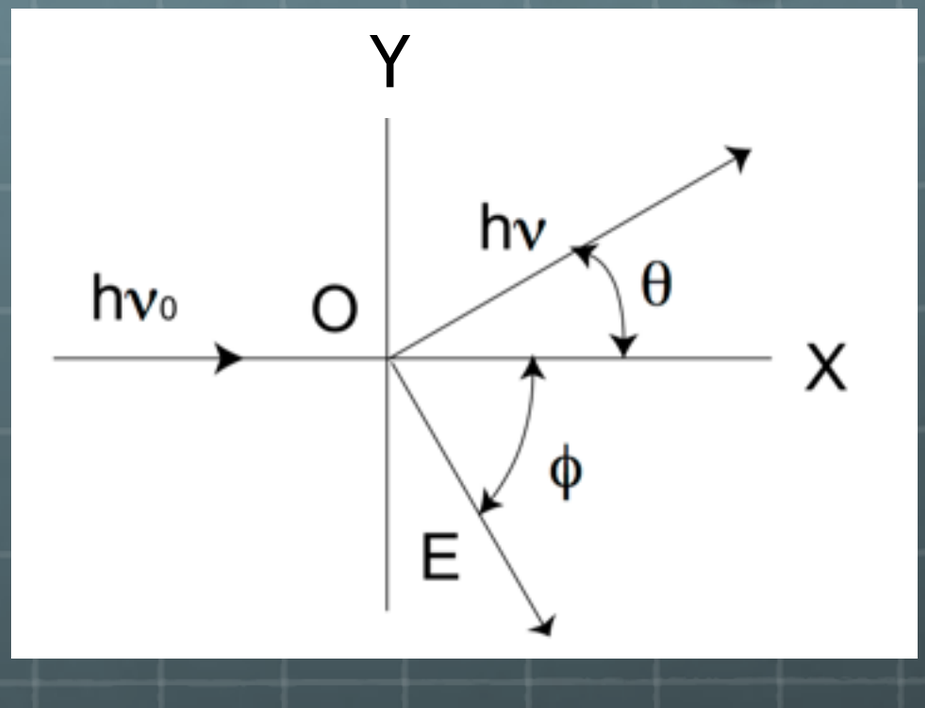

We can also calculate the recoil kinetic energy (T) spectrum of the electron:

$$\frac{d\sigma}{dT} = \frac{\pi r_e^2}{m_e c^2 \gamma^2}\left(2 + \frac{s^2}{\gamma^2(1-s)^2} + \frac{s}{(1-s)}\left(s - \frac{2}{\gamma}\right)\right) \quad \text{with } s = T / E_{\gamma,in}$$

This cross section is strongly peaked around T_{max}:

$$T_{max} = E_{\gamma,in}\frac{2\gamma}{1+2\gamma}$$

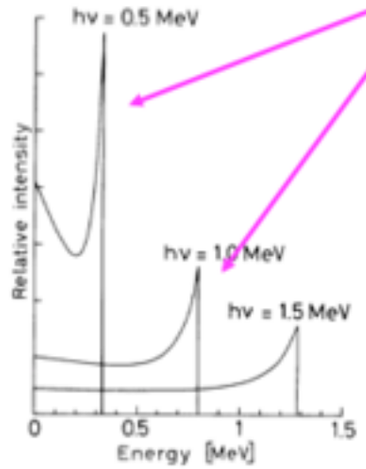

T_{max} is known as the Compton Edge

Kinetic energy distribution of Compton recoil electrons

Pair Production

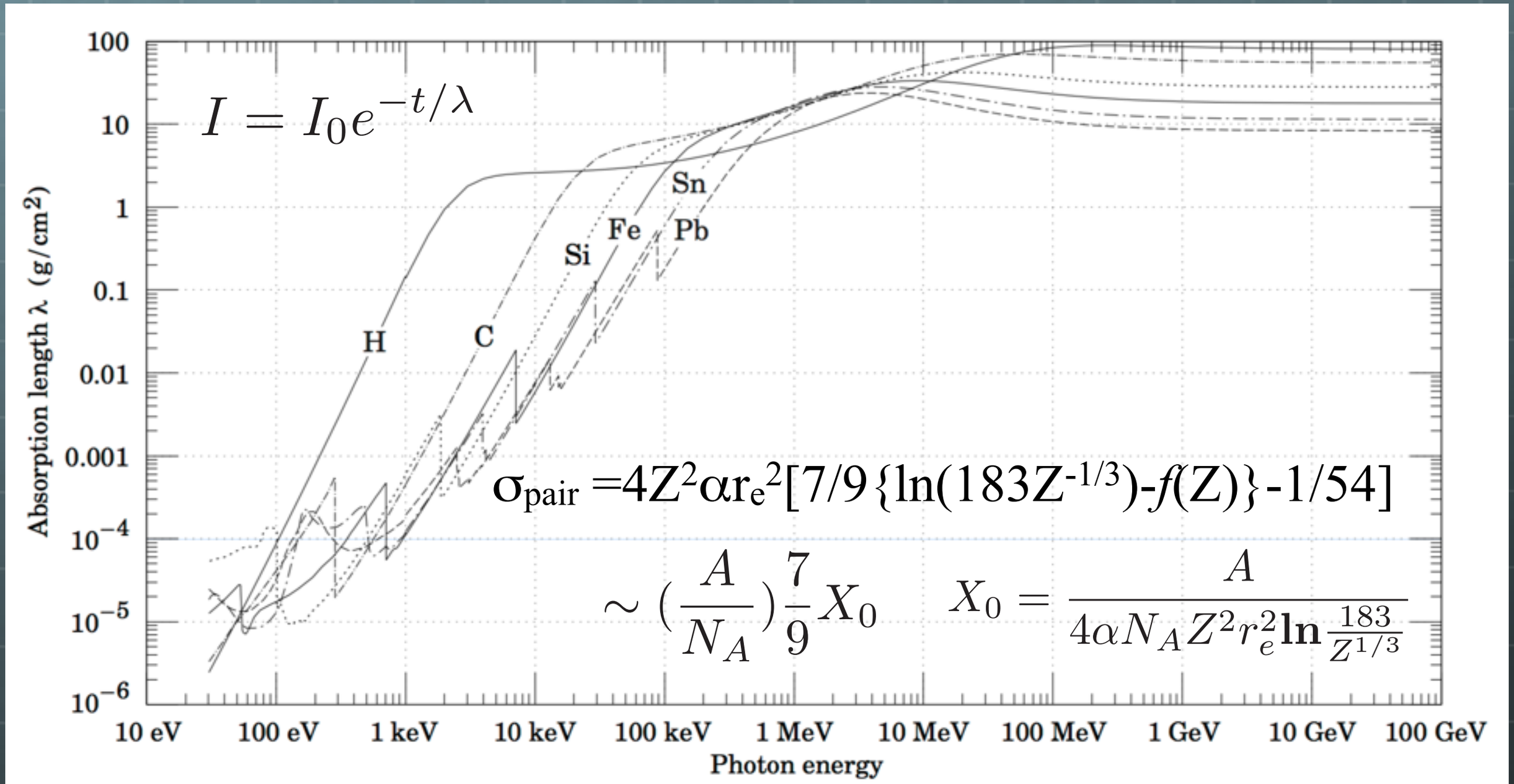

Detector

To convert energy loss into observable signal

Scintillation counter

- The energy loss produce scintillation light
- Conversion should be linear
- Light collection; Self-Transparency
- Response time
- Size to use in experiments

Organic scintillator

- Aromatic hydro-carbons, Bensen ring
- P

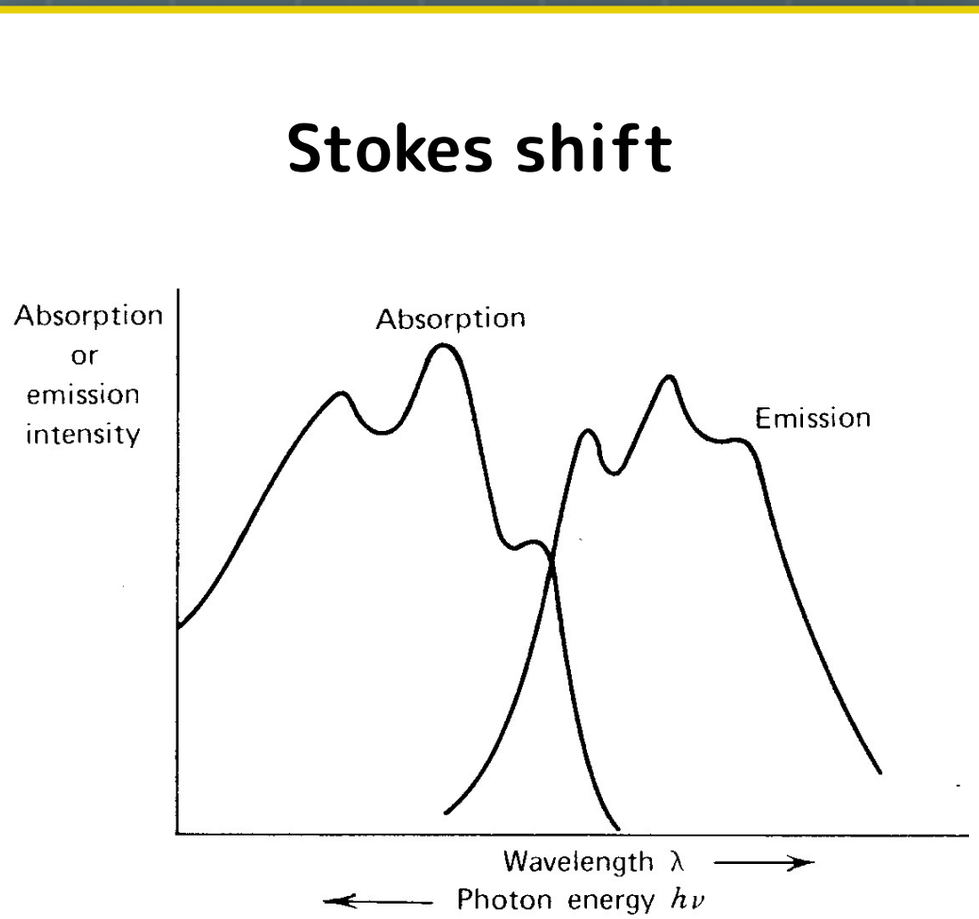

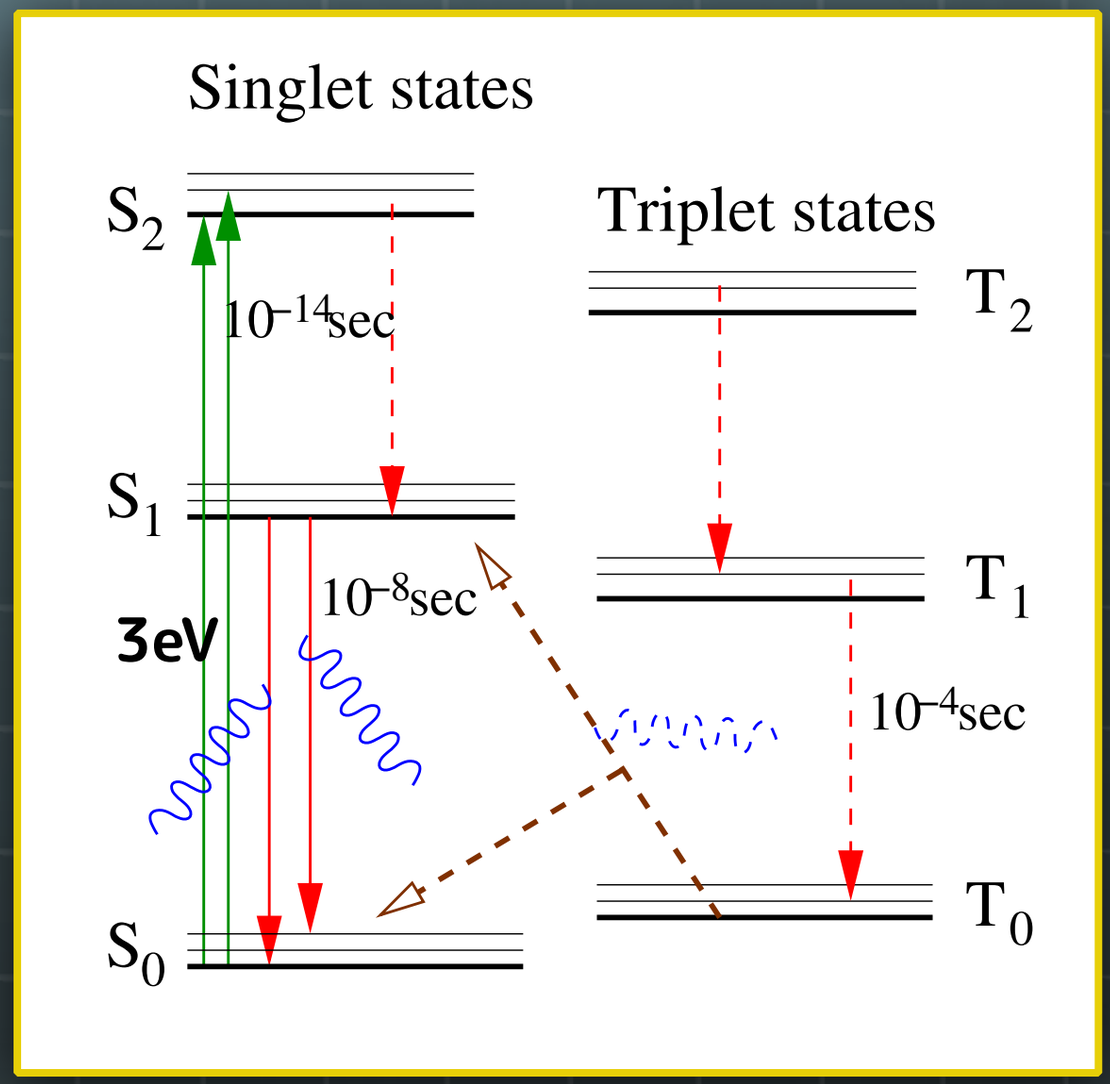

Organic scintillator

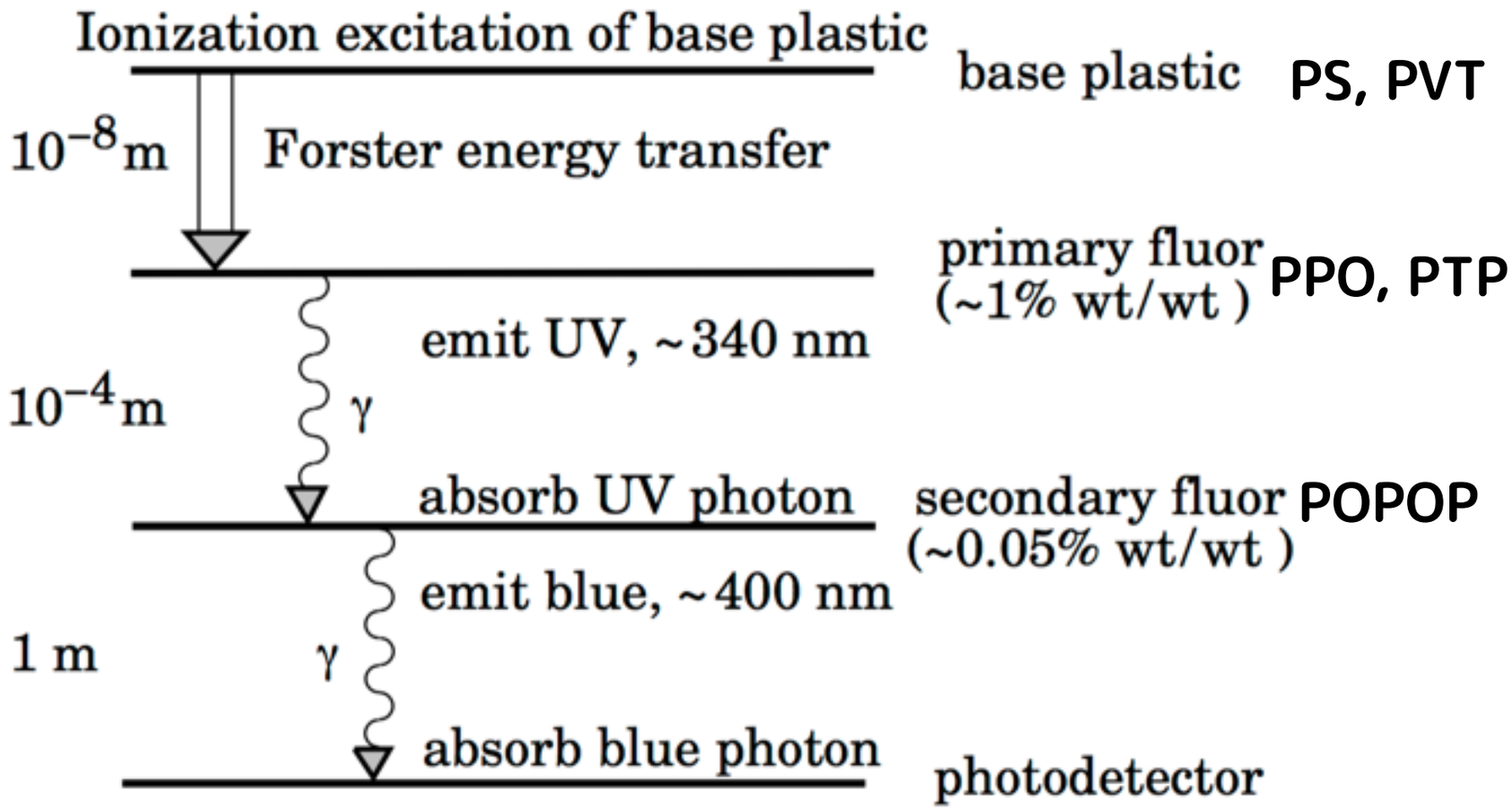

Figure 34.1: Cartoon of scintillation "ladder" depicting the operating mechanism of organic scintillator. Approximate fluor concentrations and energy transfer distances for the separate sub-processes are shown.

		Commercial
EJ-299-33A	PSD plastic, Fast neutron-	
EJ-299-34	PSD plastic, Fast neutron-gamma discrimination, Small bar arrays	-

PROPERTIES	EJ-200	EJ-204	EJ-208	EJ-212
Light Output (% Anthracene)	64	68	60	65
Scintillation Efficiency (photons/1 MeV e^-)	10,000	10,400	9,200	10,000
Wavelength of Maximum Emission (nm)	425	408	435	423
Light Attenuation Length (cm)	380	160	400	250
Rise Time (ns)	0.9	0.7	1.0	0.9
Decay Time (ns)	2.1	1.8	3.3	2.4
Pulse Width, FWHM (ns)	2.5	2.2	4.2	2.7
No. of H Atoms per cm^3 ($x10^{22}$)	5.17	5.15	5.17	5.17
No. of C Atoms per cm^3 ($x10^{22}$)				
No. of Electrons per cm^3 ($x10^{23}$)				
Density (g/cm^3)				
Polymer Base				
Refractive Index				
Softening Point				
Vapor Pressure				
Coefficient of Linear Expansion				
Light Output vs. Temperature				
Temperature Range				

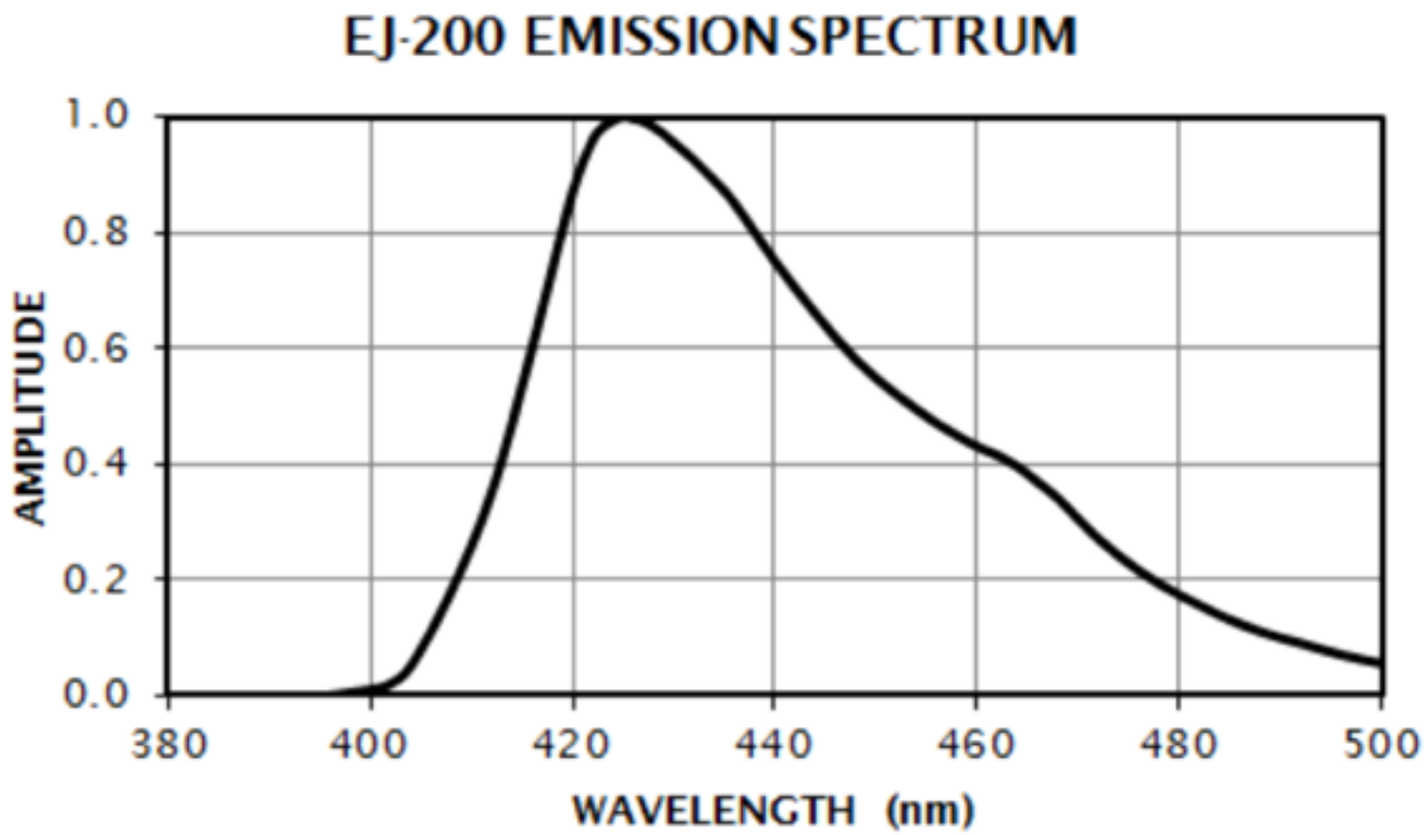

http://www.eljentechnology.com/products/plastic-scintillators

Saturated light output

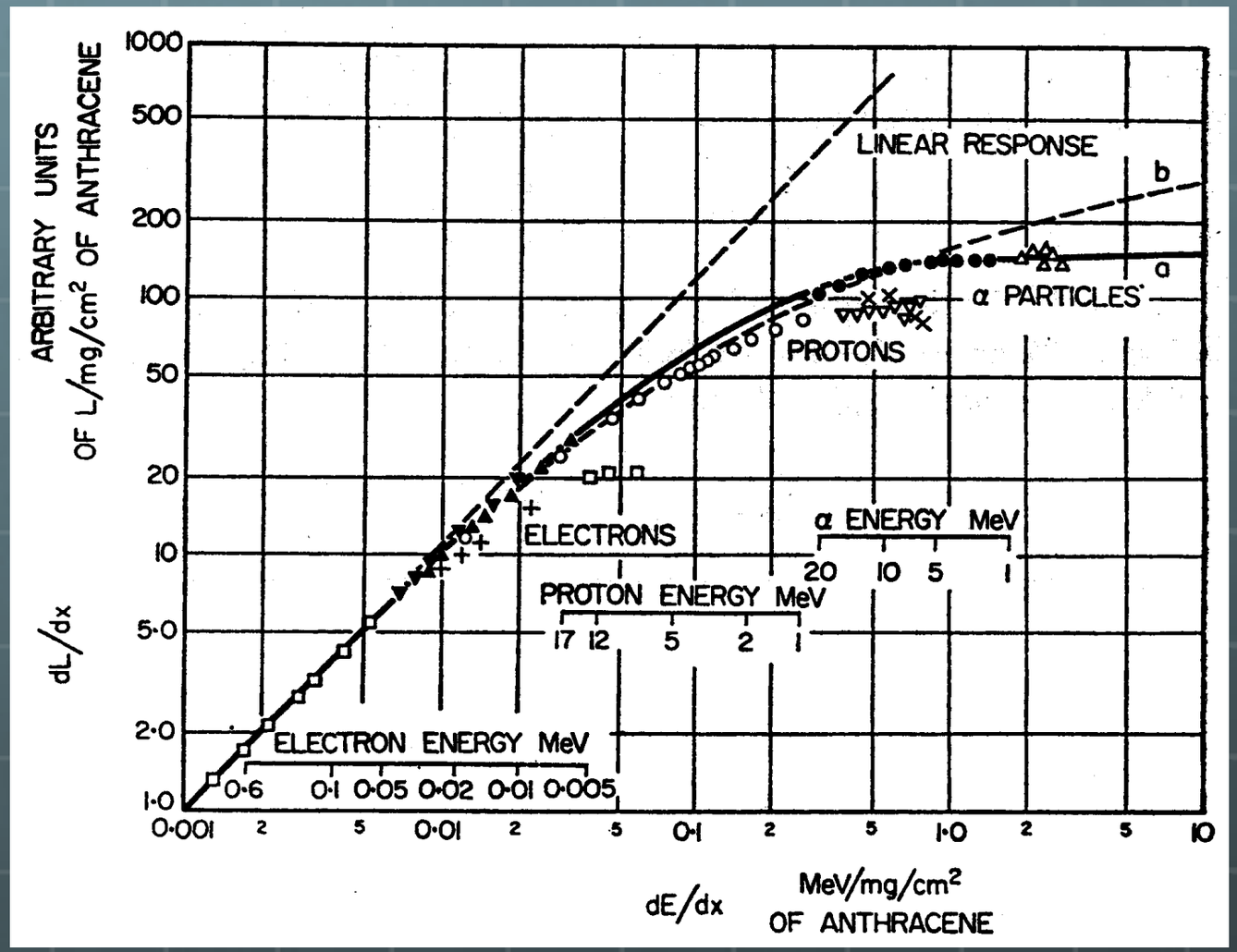

- Light yield

$$L = AE$$

$$\frac{dL}{dx} = A\frac{dE}{dx}$$

- Damaged molecules for large dE(ionization)

$$B\frac{dE}{dx}$$

- Birks' law

$$\frac{dL}{dx} = \frac{A\frac{dE}{dx}}{1 + kB\frac{dE}{dx}}$$

Example of Quench

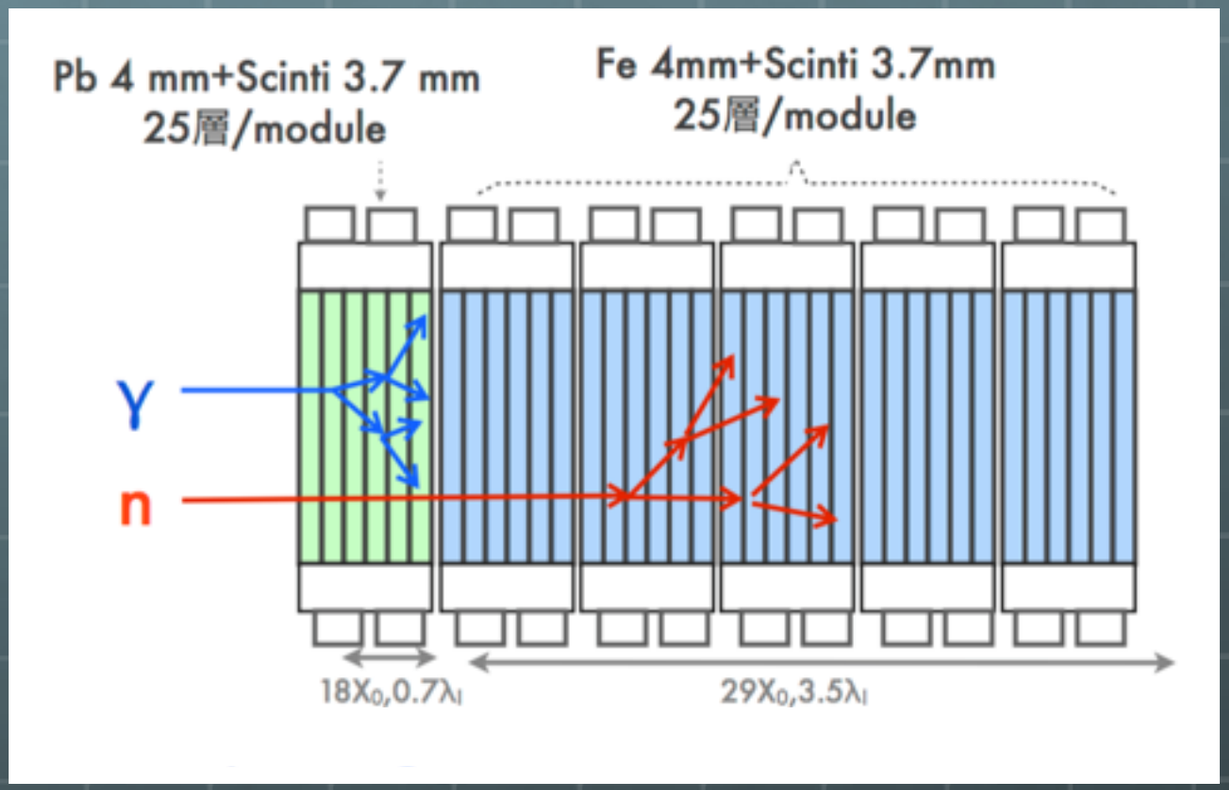

1 GeV/c pion incident

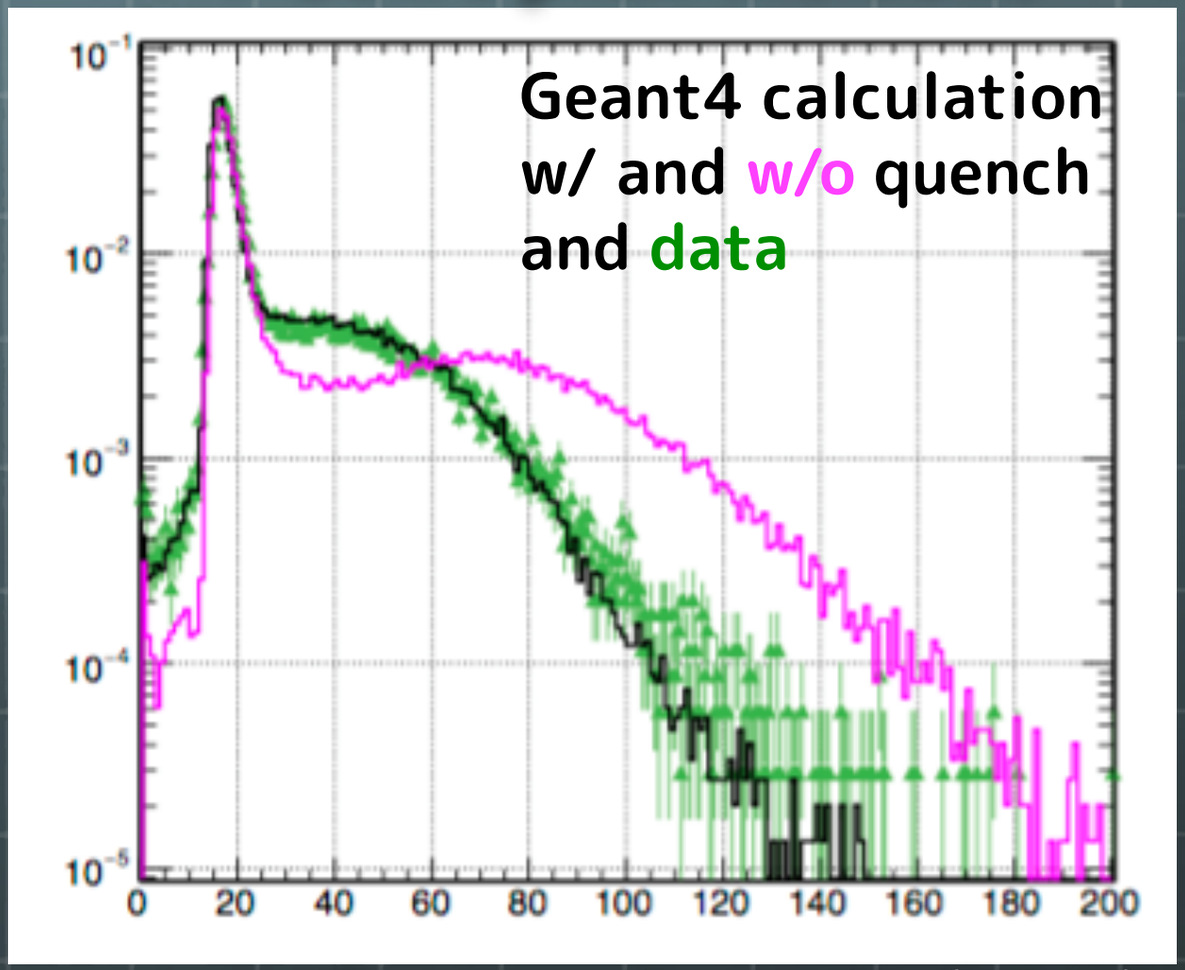

Pulse shape discrimination

- Two components of scin.
- slow component
  - nature of the exciting particle
- Large dE/dx
  - Large Triplet excit.
- Bimolecule interaction
  - T_0 ->S_0 or S_1

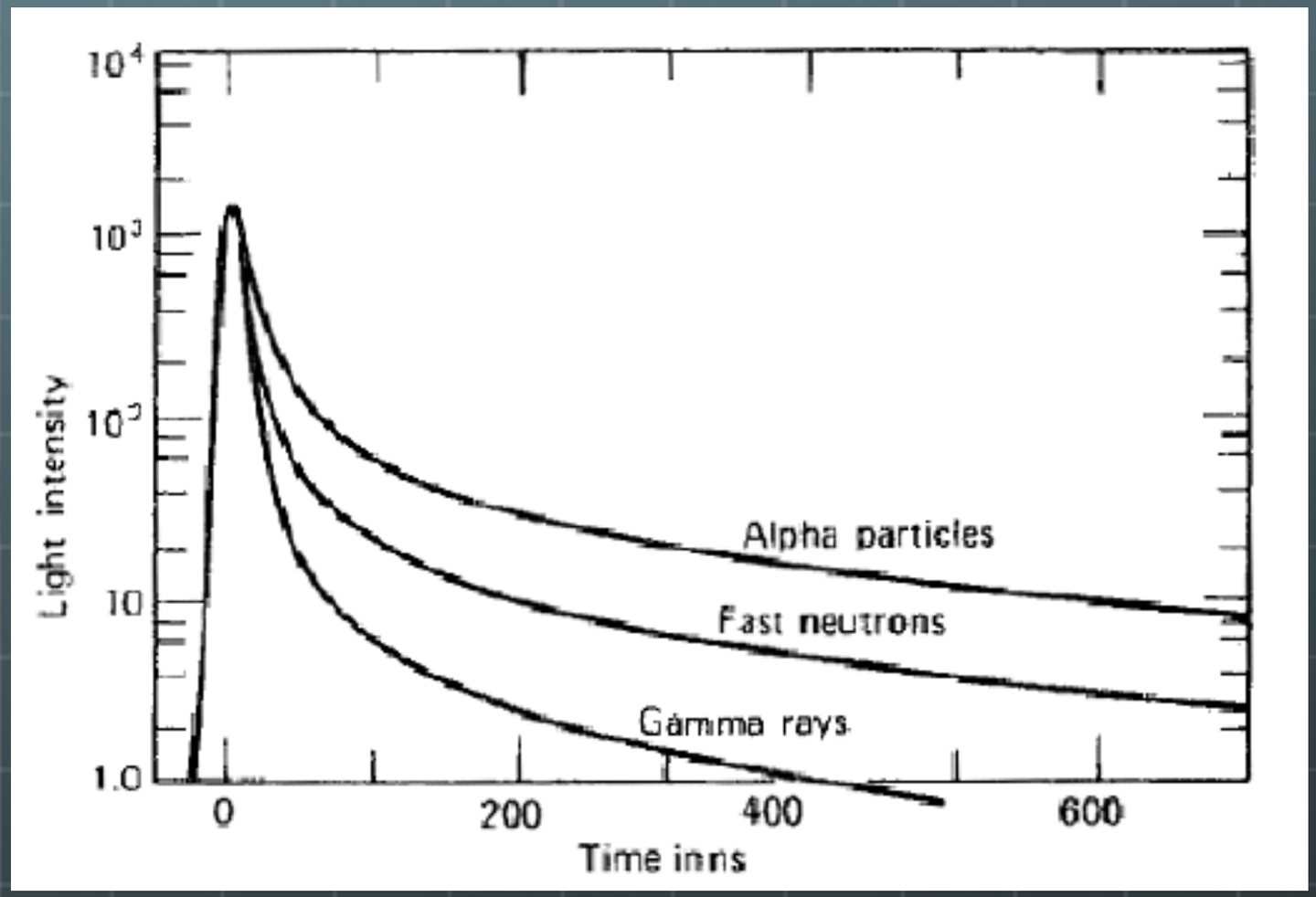

In organic scintillator

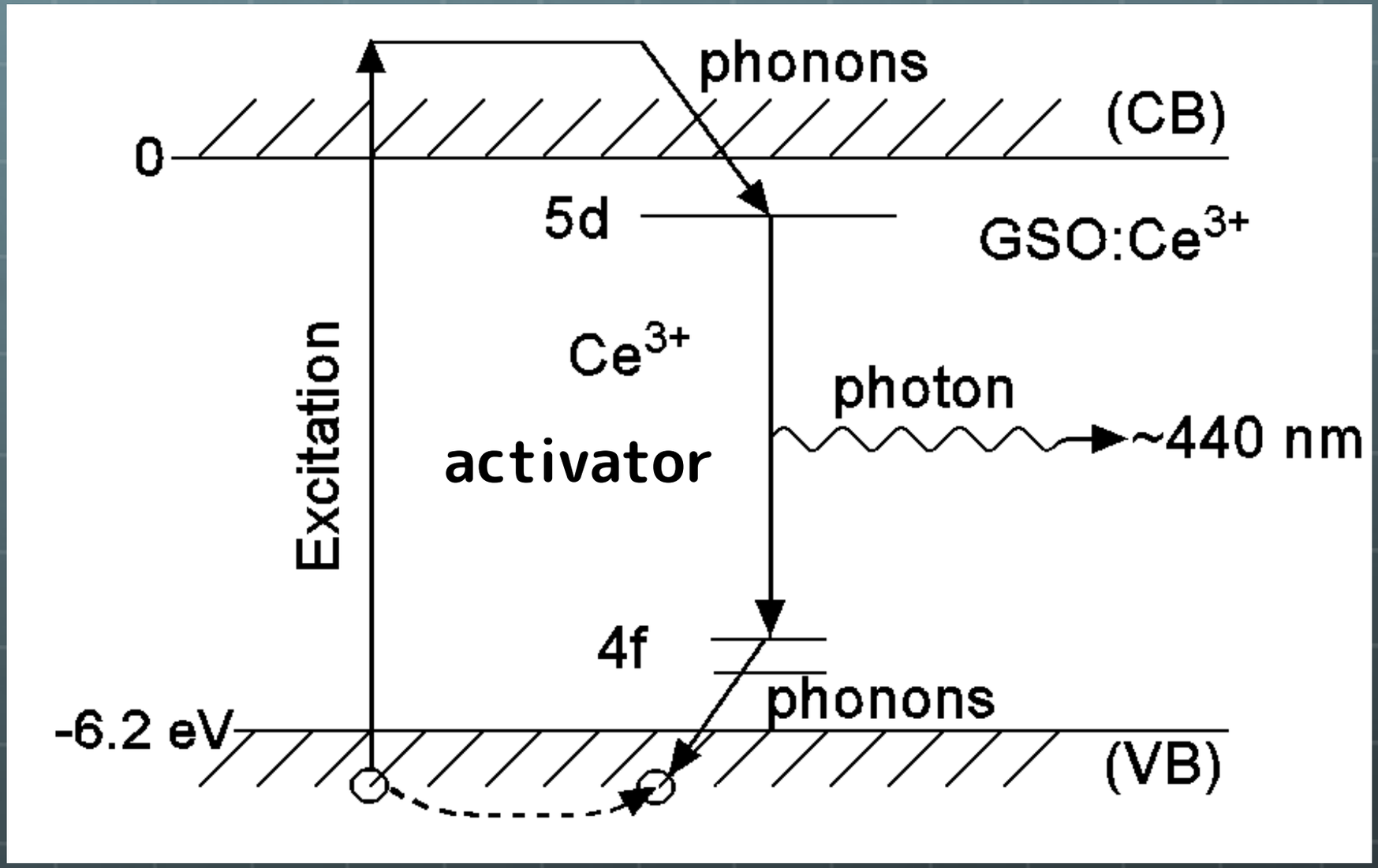

Temperature dependency

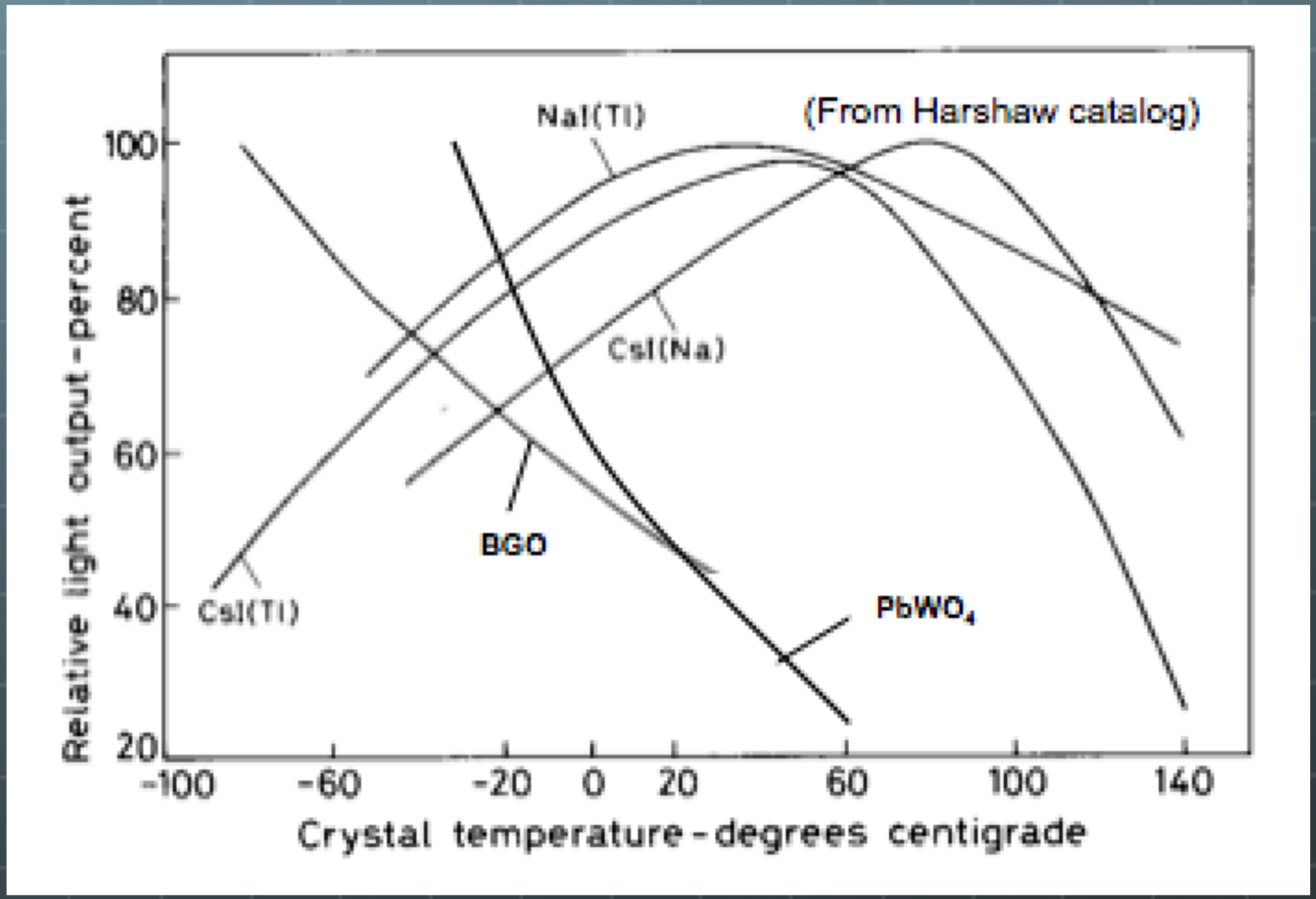

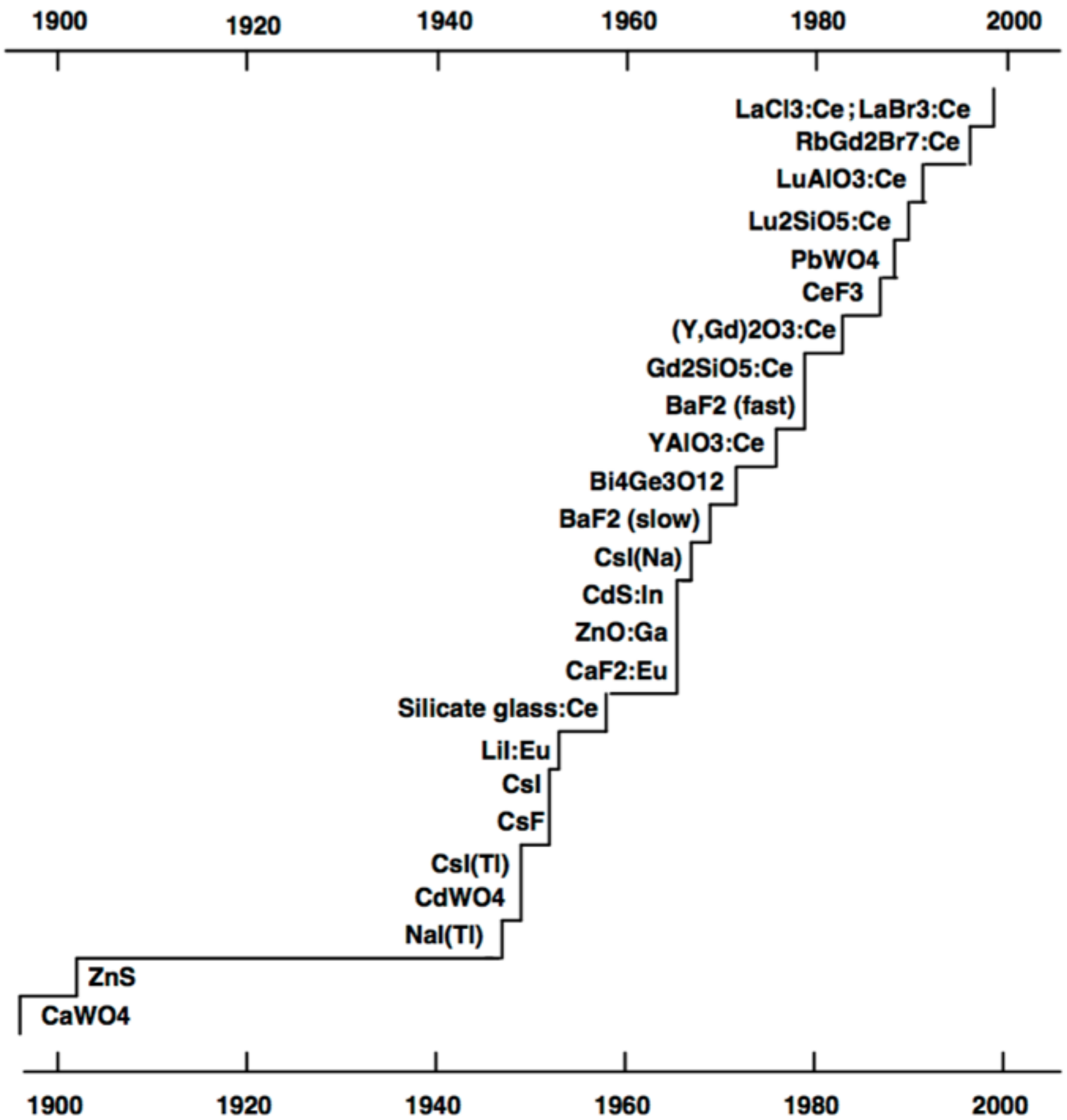

Fig. 1. History of the discovery of major inorganic scintillator materials.

Table 34.4: Properties of several inorganic crystals. Most of the notation is defined in Sec. 6 of this *Review*.

Parameter:	ρ	MP	X_0^*	R_M^*	dE^*/dx	λ_I^*	τ_{decay}	λ_{max}	$n^\natural$	Relative output†	Hygro-scopic?	$d(\text{LY})/dT$
Units:	g/cm^3	°C	cm	cm	MeV/cm	cm	ns	nm				%/°C‡
NaI(Tl)	3.67	651	2.59	4.13	4.8	42.9	245	410	1.85	100	yes	−0.2
BGO	7.13	1050	1.12	2.23	9.0	22.8	300	480	2.15	21	no	−0.9
BaF_2	4.89	1280	2.03	3.10	6.5	30.7	650^s	300^s	1.50	36^s	no	−1.9^s
							0.9^f	220^f		4.1^f		0.1^f
CsI(Tl)	4.51	621	1.86	3.57	5.6	39.3	1220	550	1.79	165	slight	0.4
CsI(Na)	4.51	621	1.86	3.57	5.6	39.3	690	420	1.84	88	yes	0.4
CsI(pure)	4.51	621	1.86	3.57	5.6	39.3	30^s	310	1.95	3.6^s	slight	−1.4
							6^f			1.1^f		
$PbWO_4$	8.30	1123	0.89	2.00	10.1	20.7	30^s	425^s	2.20	0.3^s	no	−2.5
							10^f	420^f		0.077^f		
LSO(Ce)	7.40	2050	1.14	2.07	9.6	20.9	40	402	1.82	85	no	−0.2
PbF_2	7.77	824	0.93	2.21	9.4	21.0	-	-	-	Cherenkov	no	-
CeF_3	6.16	1460	1.70	2.41	8.42	23.2	30	340	1.62	7.3	no	0
$LaBr_3$(Ce)	5.29	783	1.88	2.85	6.90	30.4	20	356	1.9	180	yes	0.2
$CeBr_3$	5.23	722	1.96	2.97	6.65	31.5	17	371	1.9	165	yes	−0.1

Liquid noble gases light generation

- Energy deposition leads to
  - ▷ scintillation: time scale ≈ 10 ns and $130 < \lambda < 180$ nm
  - ▷ ionisation: ≈ 20 eV/pair
  - $\rightarrow$ in calorimeters the ionisation charge is measured (dominantly)

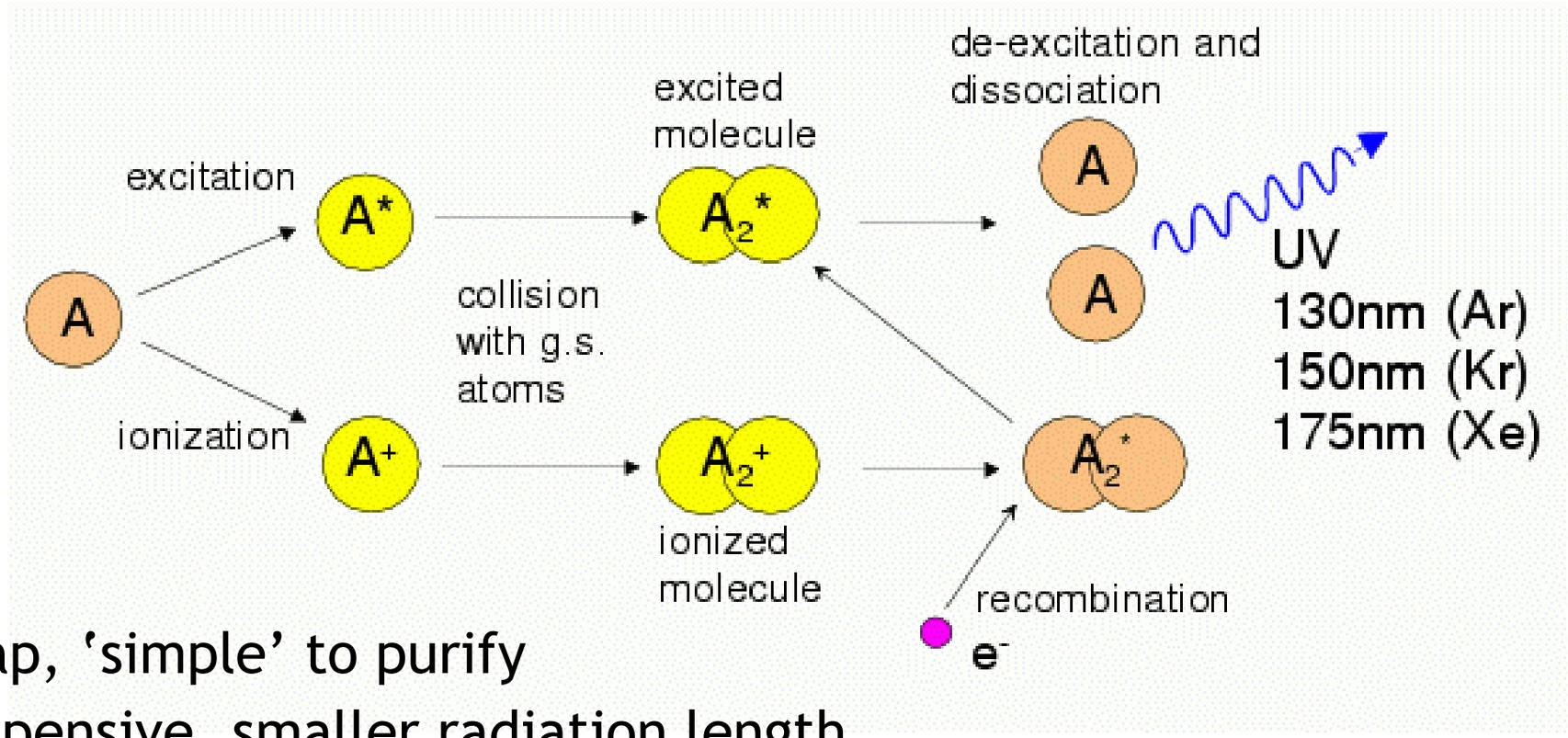

- Options
  - ▷ Argon: cheap, 'simple' to purify
  - ▷ Krypton: expensive, smaller radiation length
  - ▷ Xenon: very expensive

$\Rightarrow$ application in homogeneous and segmented calorimeters

Electromagnetic Shower

65 foot notes

Electromagnetic shower

- Electromagnetic calorimeter uses a successive generation of secondaries - EM shower.
- High energy photon occurs pair creation dominantly.
- High energy electron-positron pair loses its energy by bremsstrahlung.

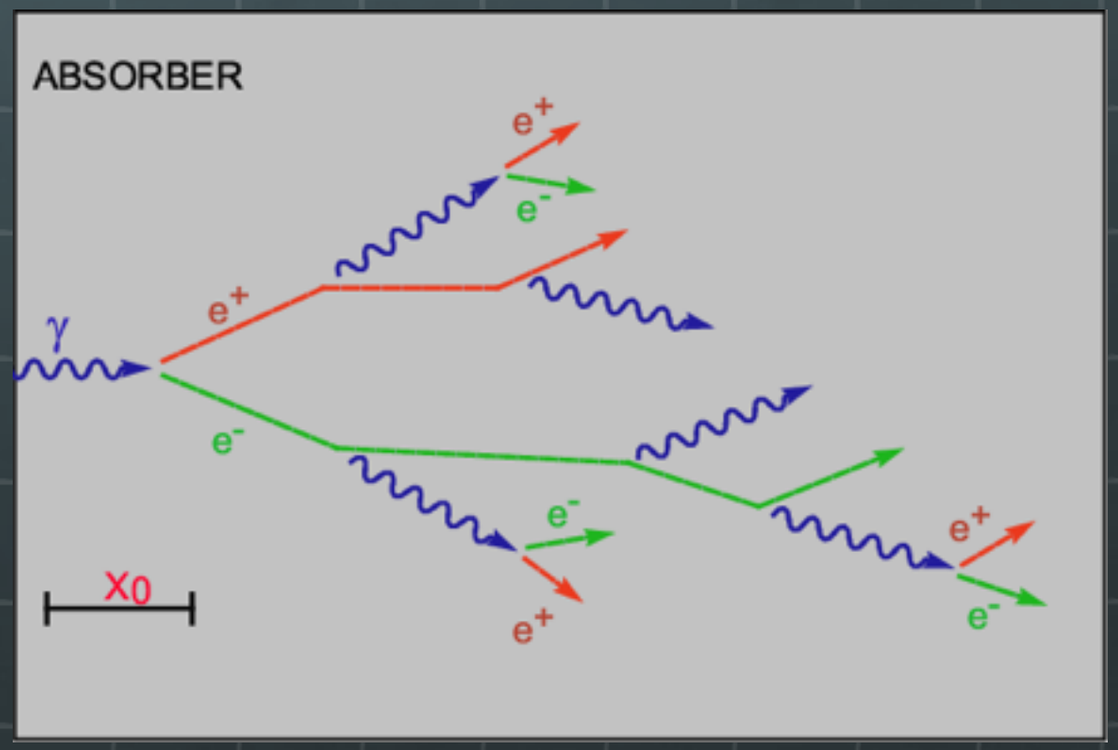

Radiation Length (Xo)

- Characteristic amount for energy loss of (high energy) photon and electron
  - mean distance over which a electron loses its energy as 1/e by bremsstrahlung
  - 7/9 of the mean free path for pair production by a photon

Longitudinal shower development

- **Number of secondaries**

$$N = 2^t$$

- **Average Energy**

$$E(t) = E_0/2^t$$

- **Shower development stops at**

$$E(t) = Ec$$

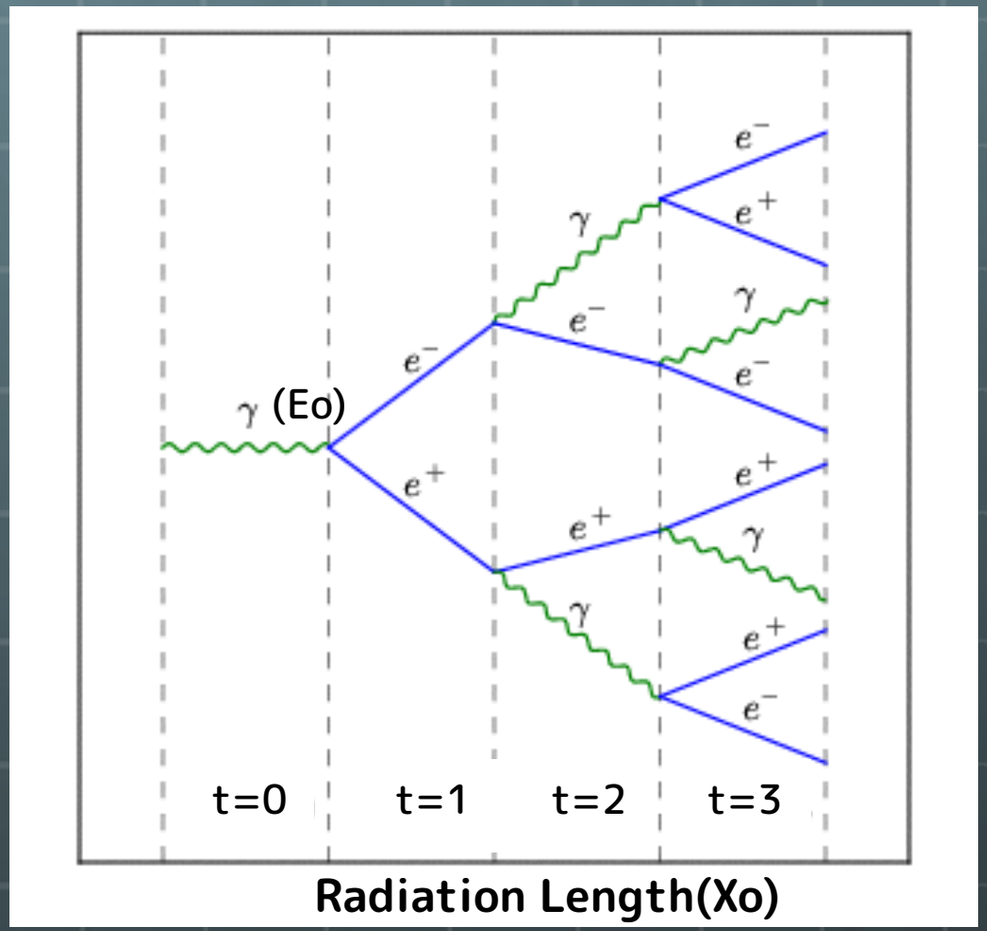

foot notes

Critical energy (Ec)

- Energy at which a electron losses its energy as same amount by bremsstrahlung and ionization.
- Energy at which the ionization loss per Xo is equal to the electron energy.

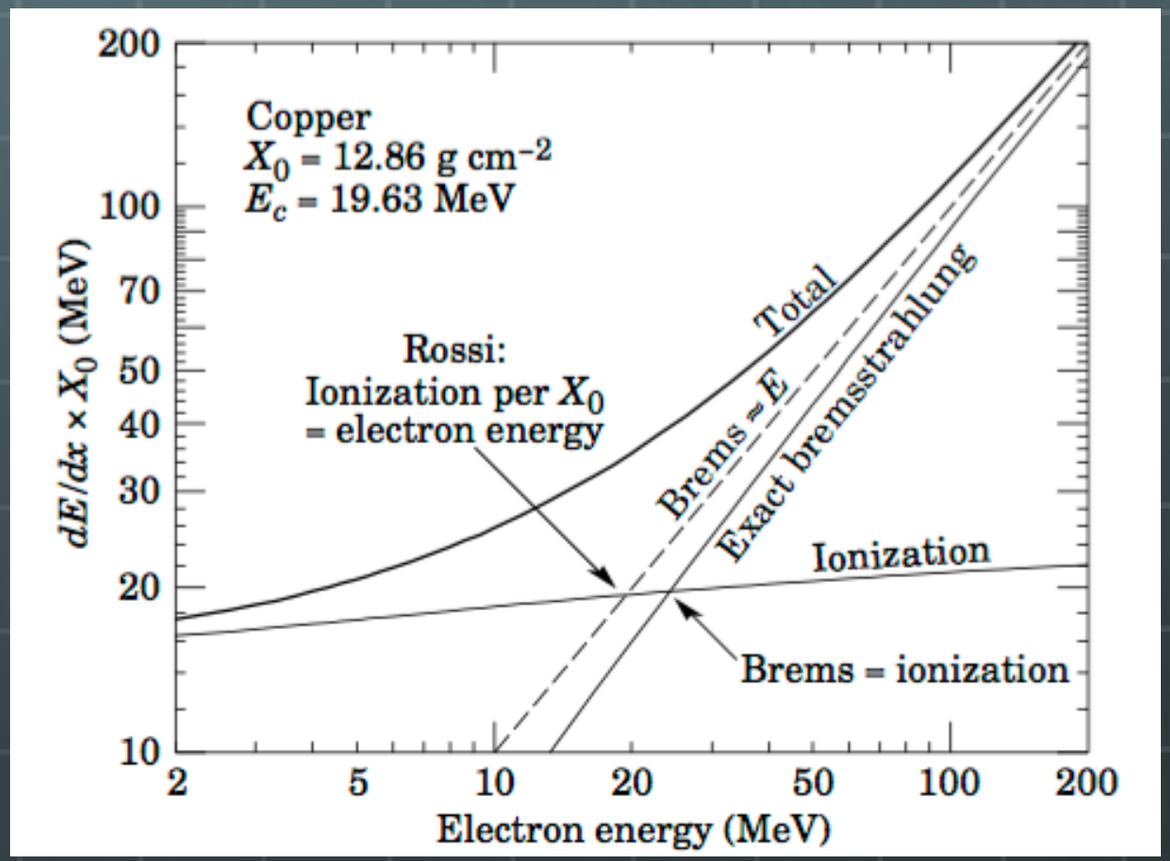

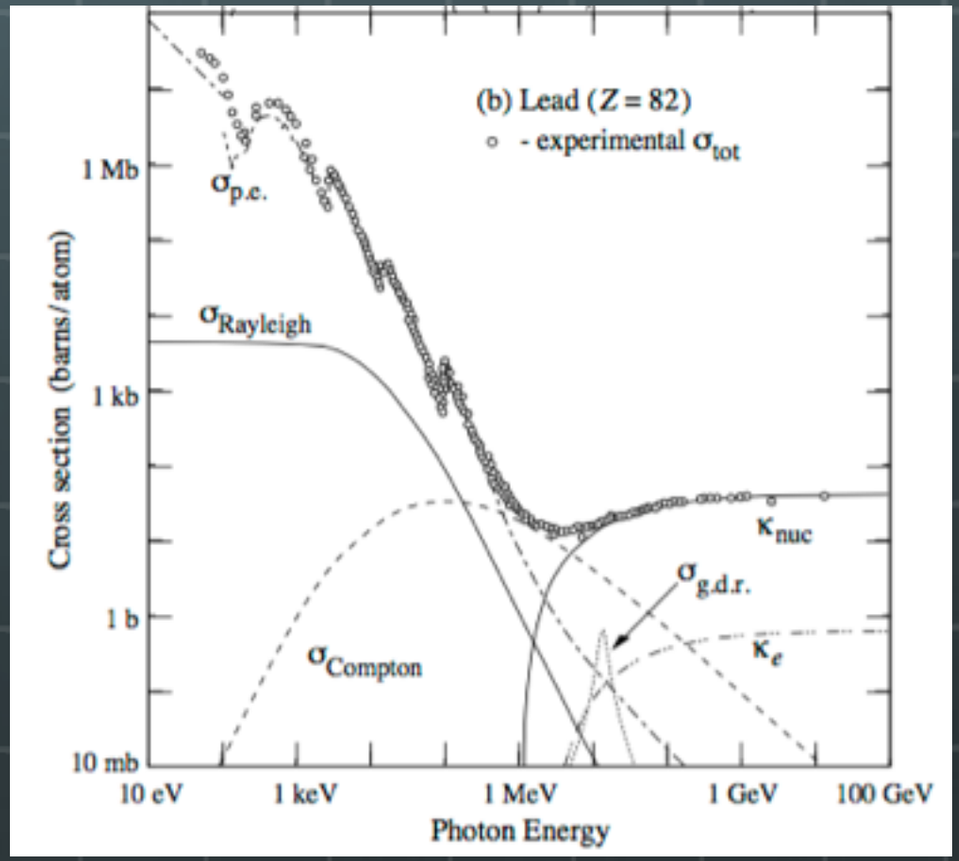

Longitudinal shower development

- **Number of secondaries**

$$N = 2^t$$

- **Average Energy**

$$E(t) = E_0/2^t$$

- **Shower development stops at**

$$E(t) = Ec$$

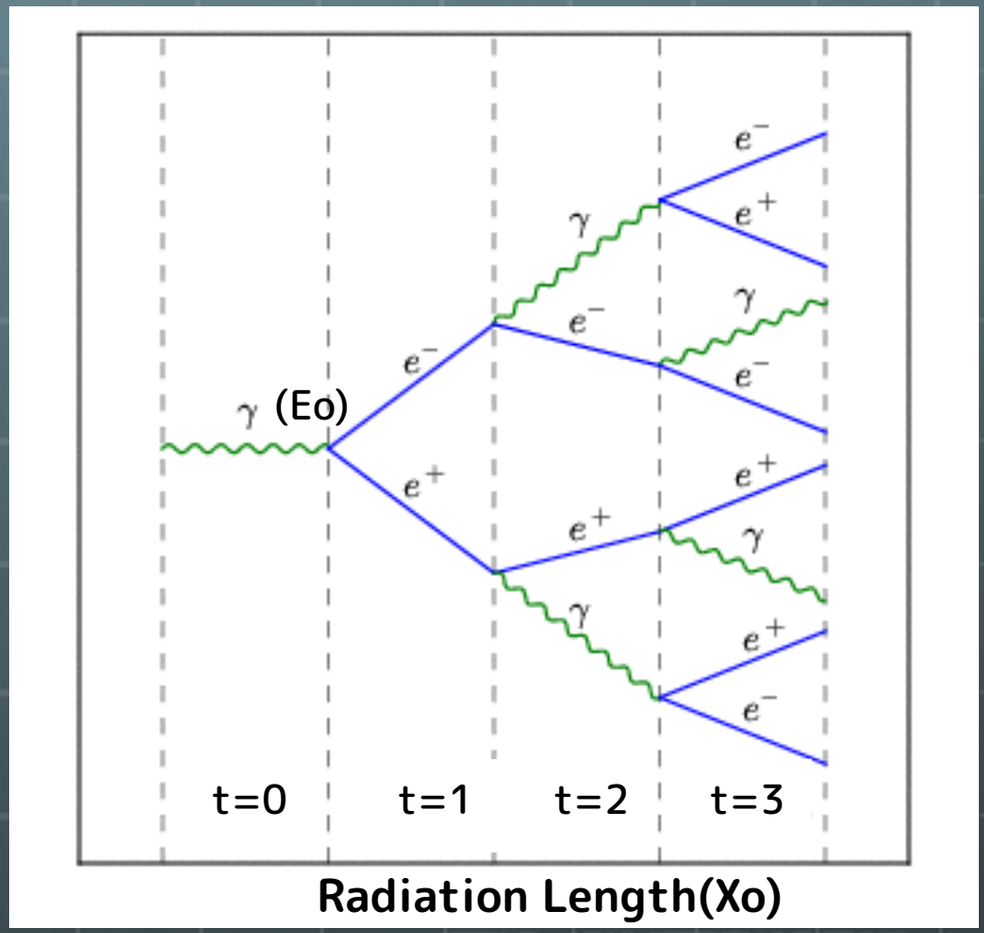

- **Maximum number of shower particles at which their energy is critical energy ;**

$$Ec = E_0/2^{t_{max}} \qquad t_{max} = \ln(\frac{E_0}{Ec})/\ln 2$$

Energy deposit

- Energy deposit ∝ total integrated charged track length

$$< T_i(E_0) >= \int_{(i-1)\Delta t}^{i\Delta t} N(E_0, E_{th}, t)dt$$

$$\frac{dE}{dx} = E_0 b \frac{(bt)^{(a-1)} e^{-bt}}{\Gamma(a)}$$

$$t_{max(\frac{dE}{dx})} = (a-1)/b$$
$$= \ln(\frac{E_0}{Ec}) + C_j$$

$$C_e = -0.5$$
$$C_\gamma = +0.5$$

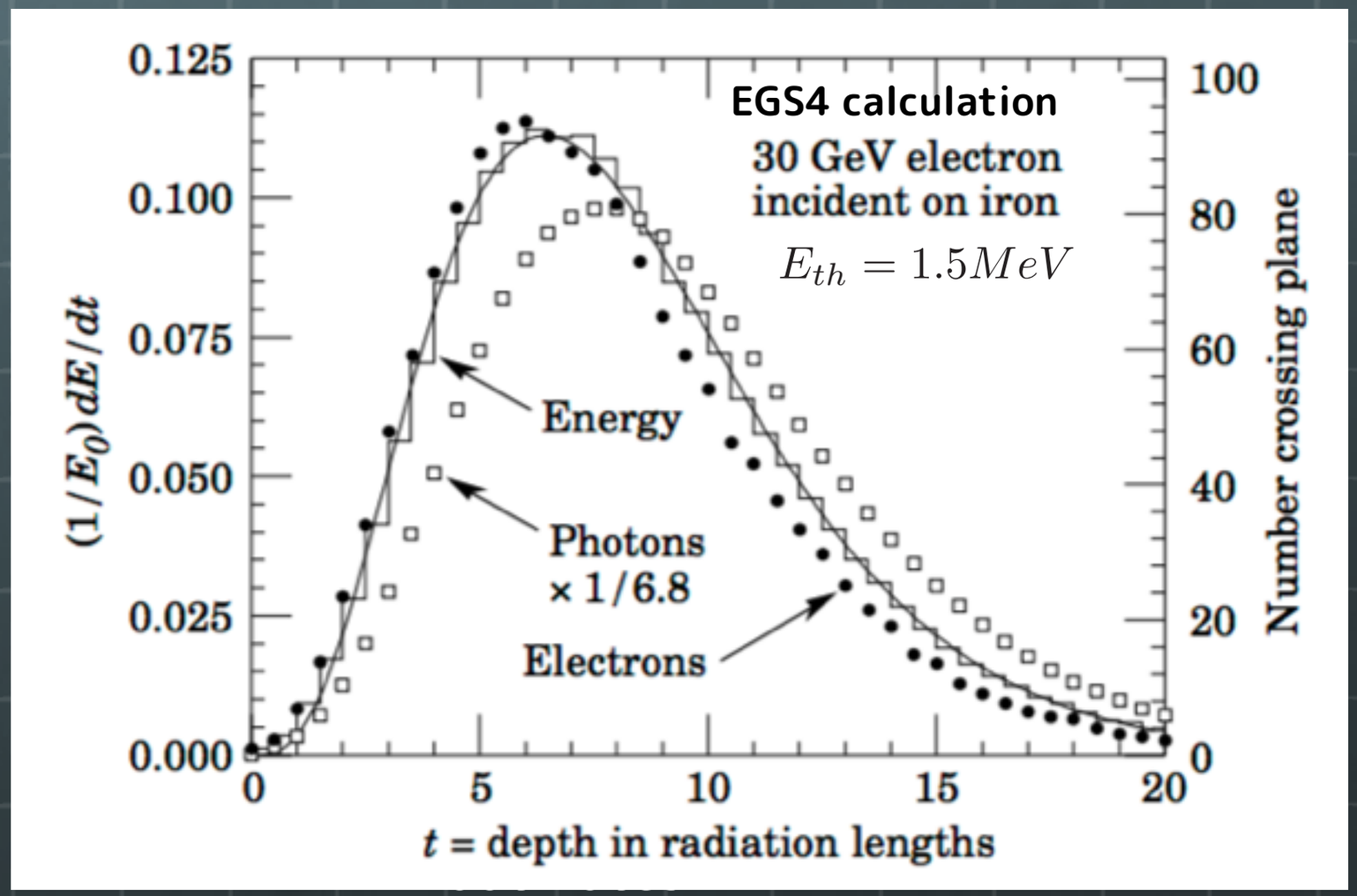

Longitudinal shower shape

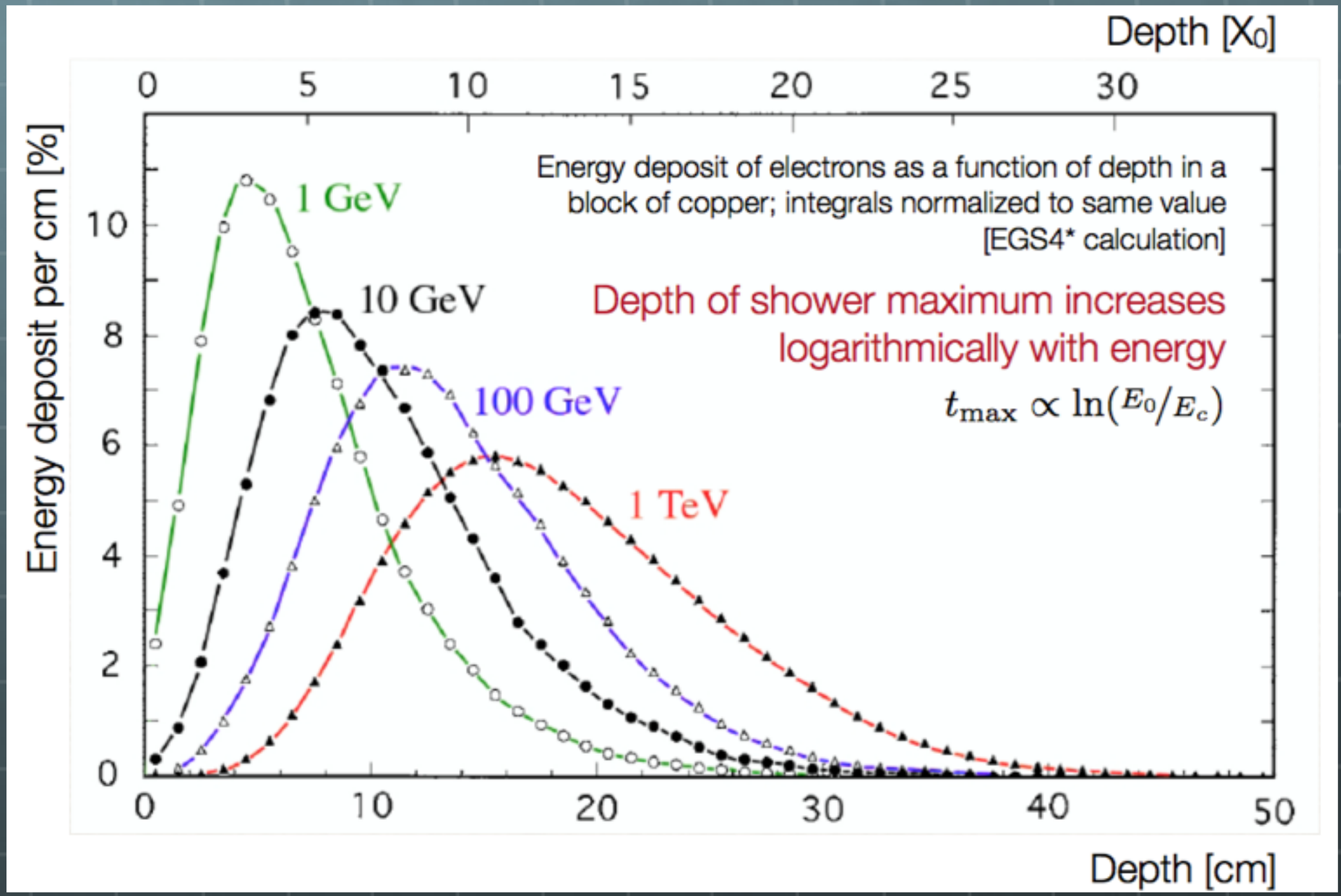

foot notes

Lateral development of EM

- Mainly due to multiple scattering of low energy electron.
- Moirère Radius (R_M)

$$R_M = \frac{21MeV}{E_c} X_0$$

$$\sim \frac{7A}{Z} [g/cm^2]$$

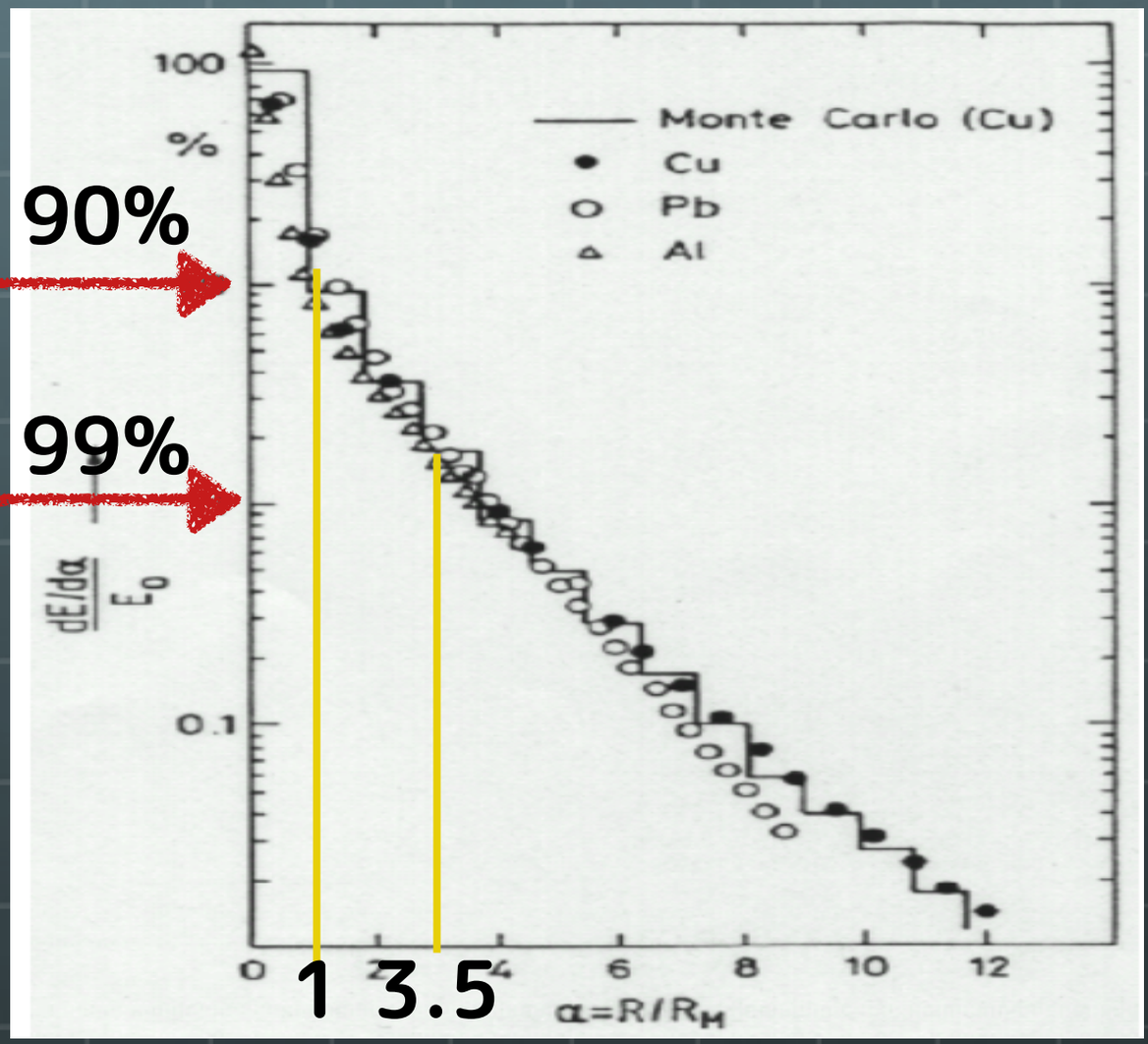

Hadronic Shower

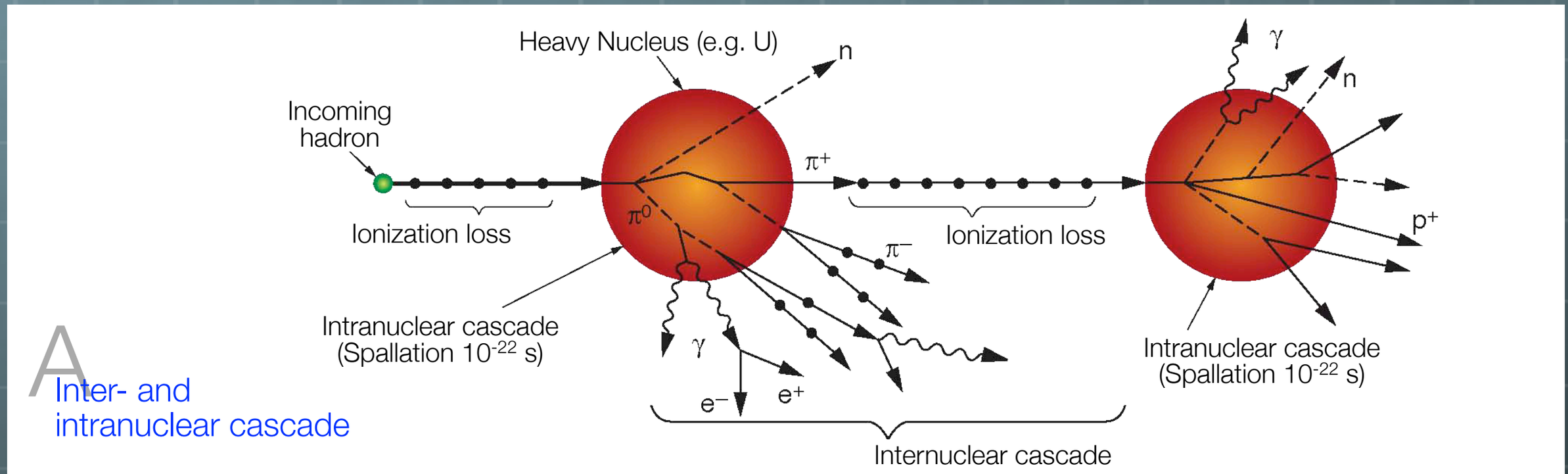

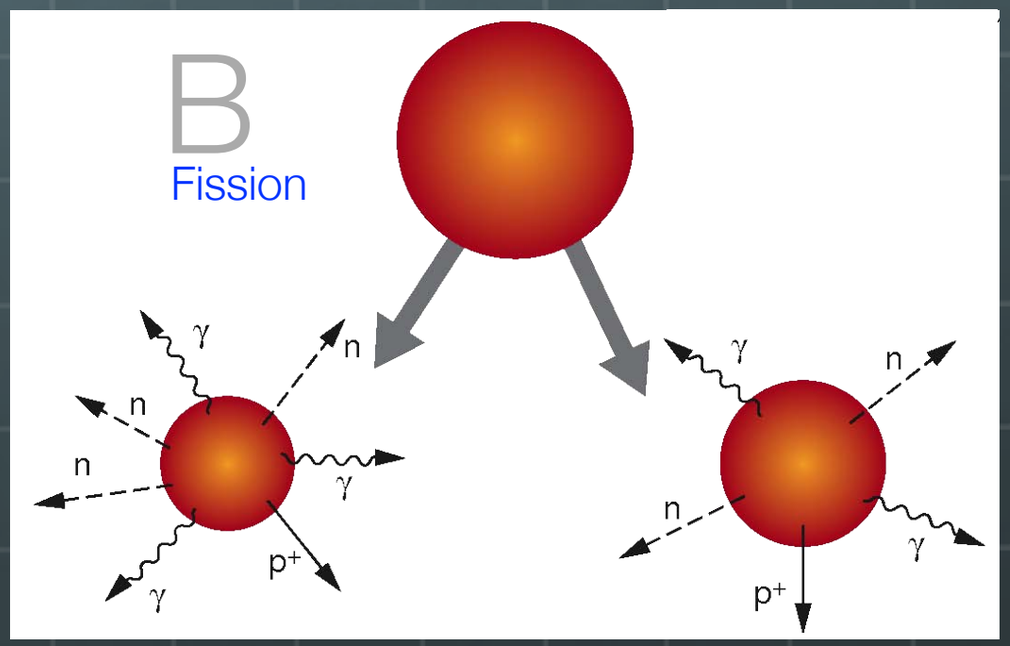

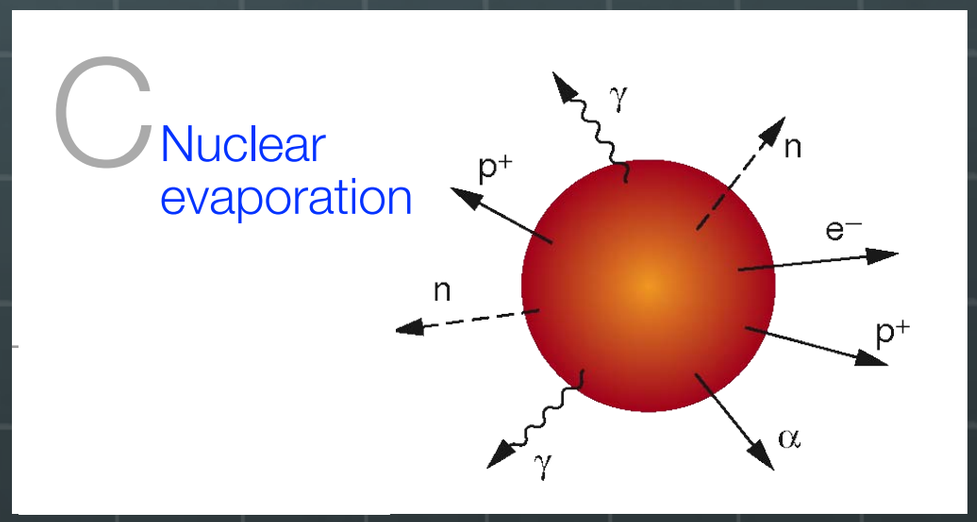

foot notes

Hadronic shower

$$\lambda_I \approx 35\ g/cm^2 \cdot A^{\frac{1}{3}}$$

$$N(x) = N_0 e^{-\frac{x}{\lambda_I}}$$

Typical
Longitudinal size: 6 ... 9 λ_{int}
[95% containment]

Typical
Transverse size: one λ_{int}
[95% containment]

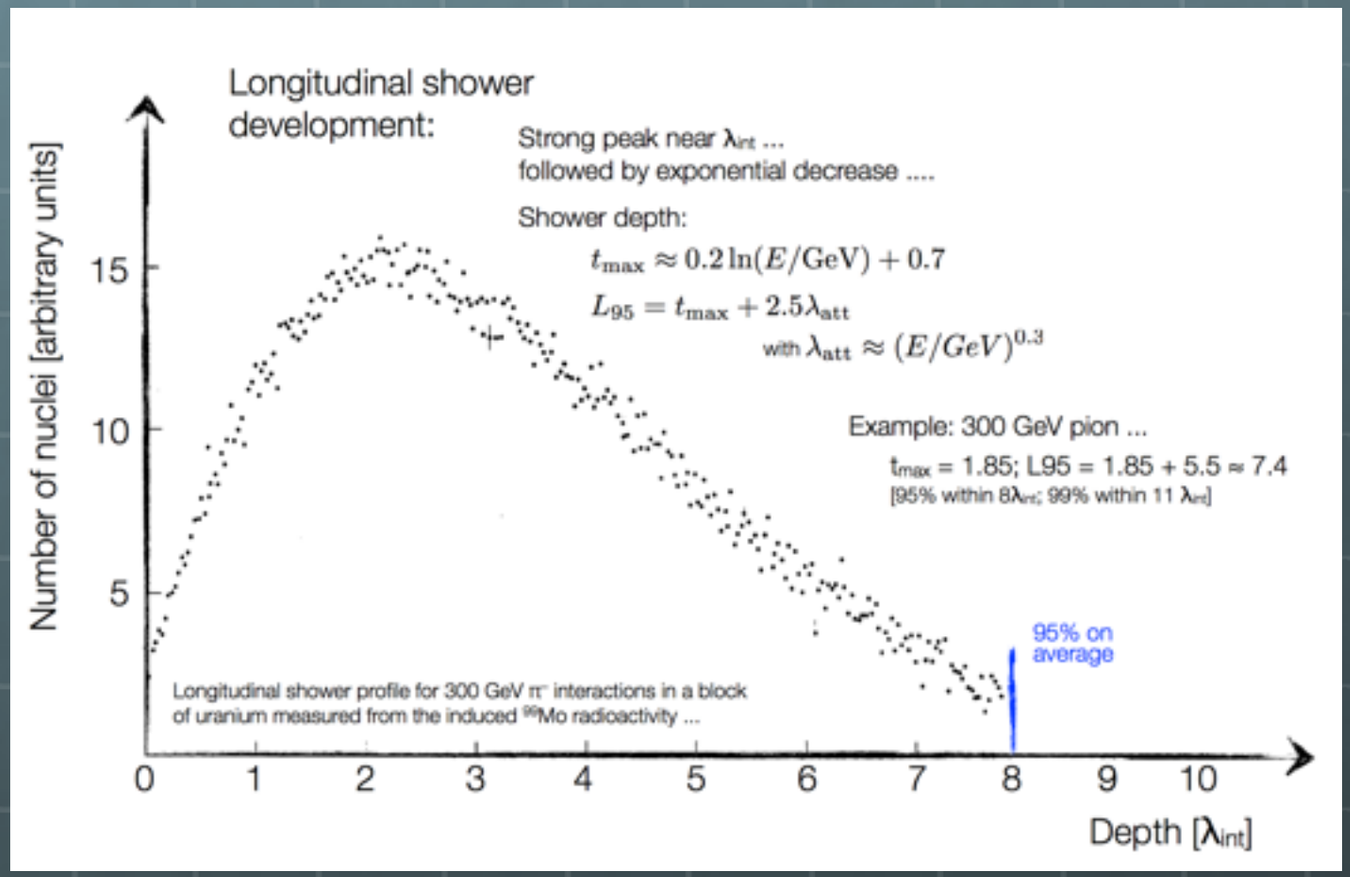

	λ_I	X_0	$R=(\lambda_I/X_0)$		λ_I	X_0	$R=(\lambda_I/X_0)$
Fe	16.78	1.76	9.54	Scin.	78.93	42.62	1.85
Cu	15.32	1.44	10.68	CsI	38.03	1.86	20.44
Pb	17.59	0.56	31.33	$PbWO_4$	20.28	0.89	22.77

Comparison hadronic vs EM showers

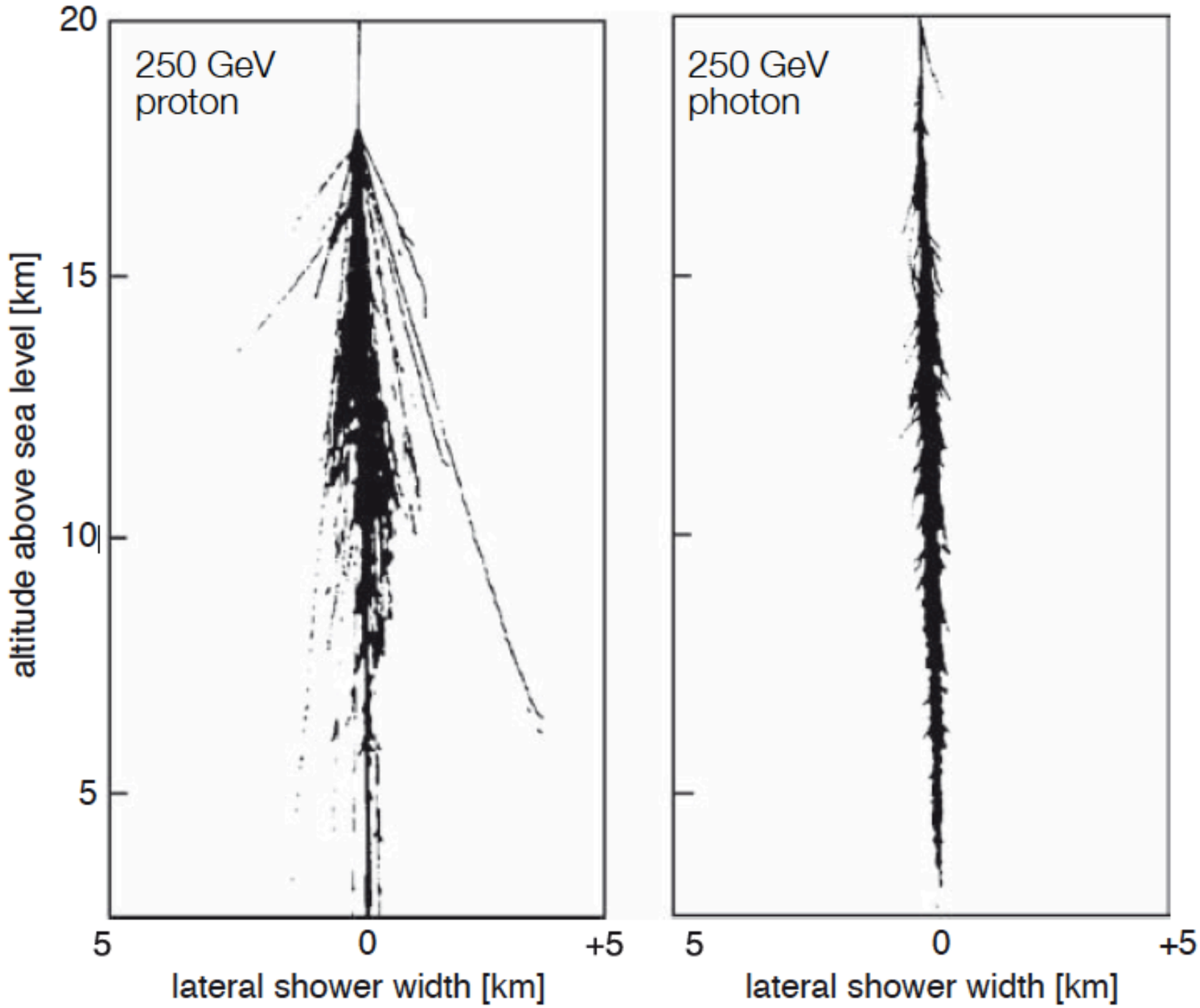

Simulated air showers

50

Calorimeter

Calorimeter

- A detector to measure particle's properties through total absorption.
  - Destructive absorption process, shower development, convert the particle energy into heat.:
    - Interaction of charged particles with matter.
- Both charged and neutral particles.
- Performance typically improves with increase energy.
- Use for triggering. Quick decision for event taking.

Tracker V.S. Calorimeter

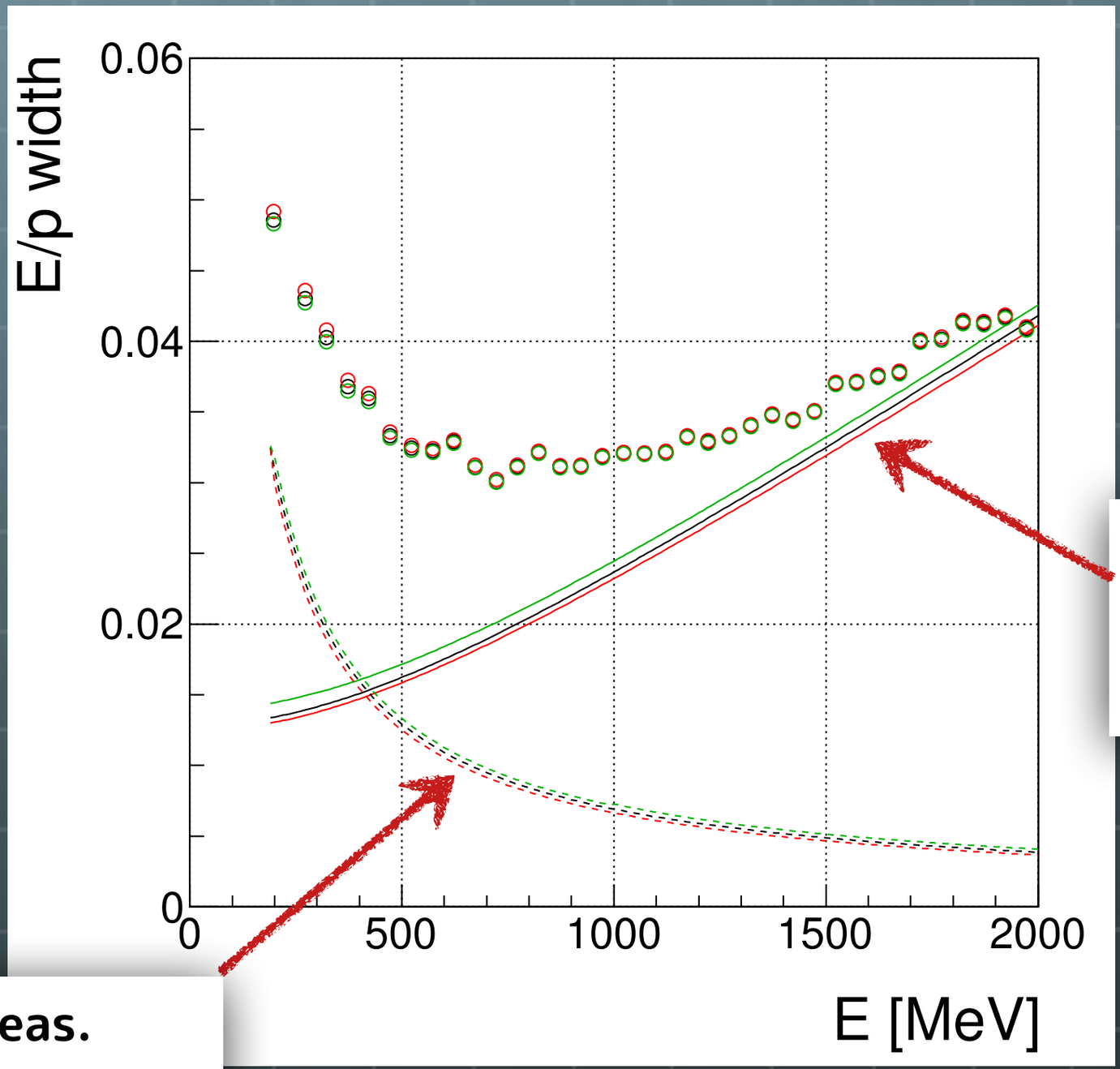

Momentum meas.
Better resolution
in Low energy

Energy meas.
Better resolution
in High energy

K. Sato Ph.D theses
2015, Osaka Univ.

Calorimeter

- Homogeneous Calorimeter
  - Assembled by modules of dense (inorganic) scintillator
    - Crystals, Liquid
  - Nice energy resolution, but expensive
- Sampling Calorimeter
  - Dense material generates shower particles
  - Detector (organic scintillator) detect shower particles
  - Worse energy resolution, however cheap
  - Large scale of calorimeter

Energy Resolution

- Fluctuation
  - Shower development
  - Number of photoelectrons
  - Shower leakage
  - Sampling fraction (for sampling calorimeter)
  - Path length (for sampling calorimeter)
  - Straggling (For sampling calorimeter)
- Noise term
- Constant Term

$$\frac{\sigma_E}{E} = \frac{a}{\sqrt{E}} \oplus \frac{b}{E} \oplus c$$

Energy Resolution

- Fluctuation

  Detected energy is proportional to number of shower particles, N.

$$E \propto N,\ N = \frac{E}{W}$$

$$\frac{\sigma_E}{E} \propto \frac{\sigma_N}{N} = \sqrt{\frac{FW}{E}}$$

$$\frac{\sigma_E}{E} \propto \frac{1}{\sqrt{N_{pe}}}$$

E: Incident energy

W: Mean energy for signal

F: Fano Factor

N_{pe}:Number of photoelectrons

Energy Resolution

- Path Length
  - Multiple scattering at the absorber.
  - Effective energy at the detector.

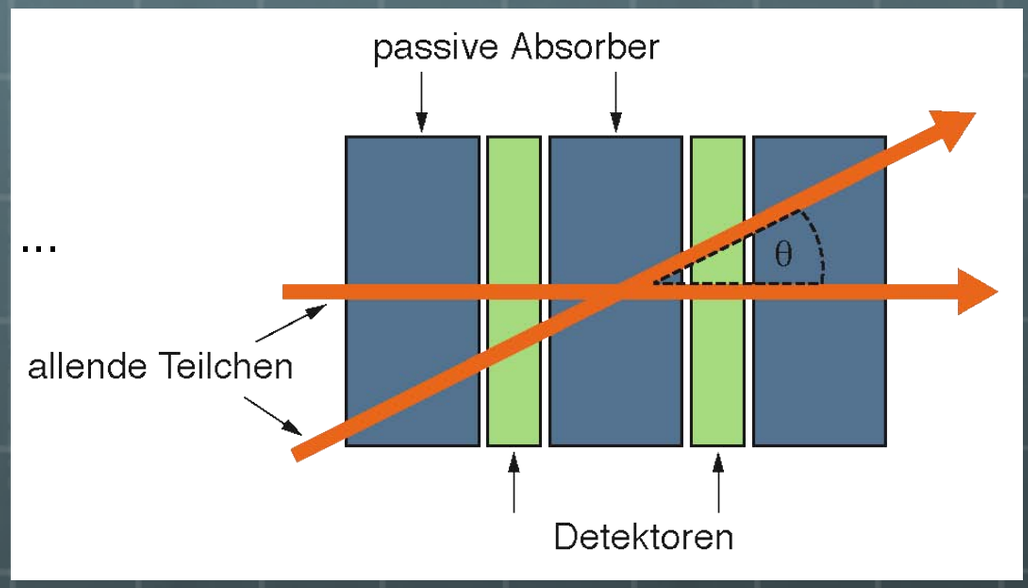

- Straggling
  - Thin detector (scintillator)
  - Sum of asymmetric energy deposit

Energy Resolution

- Fluctuation
- Noise term
  - Readout electronics
  - Import in low energy
- Constant Term
  - Inhomogeneity
  - Calibration constant
  - linearity
  - Shower leakage

$$\frac{\sigma_E}{E} = \frac{a}{\sqrt{E}} \oplus \frac{b}{E} \oplus c$$

Energy Resolution (hadron calorimeter)

$$\frac{\sigma_E}{E} = \frac{a}{\sqrt{E}} \oplus \frac{b}{E} \oplus c$$

- Fluctuation
- In addition…
- Nuclear excitation, fission, binding energy fluctuation
- Heavily ionizing particles

Compensation: e/h > 1 ➔ e/h ≈ 1
[Understanding of e/h ration allows optimization]

KOTO CsI Calorimeter

Fermilab

KTeV
CsI calorimeter

dismantled by December 2008

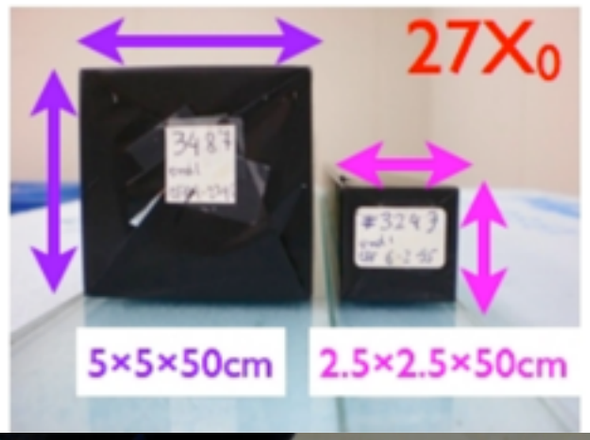

stacking

July 2010

October 2010:

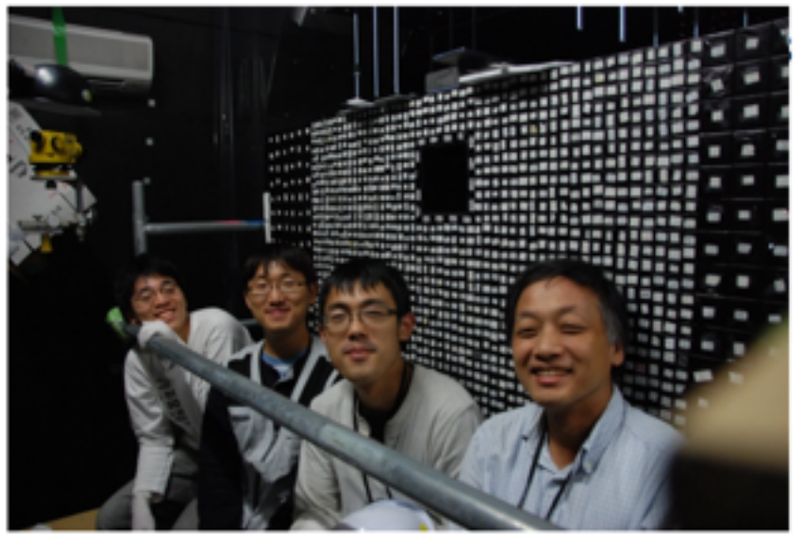

completed

J-PARC

KOTO
CsI calorimeter

2011.Feb.08 16:3

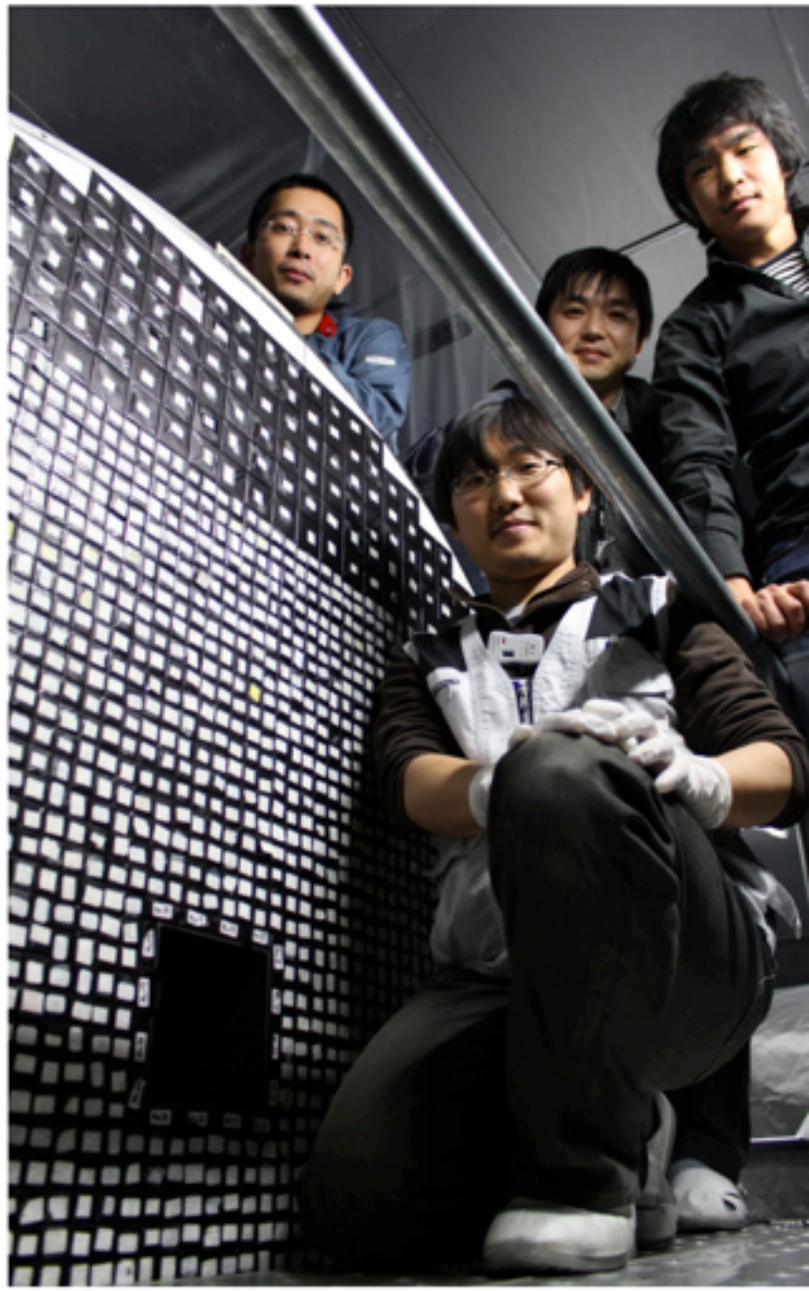

2716 crystals

CsI study with charged particle

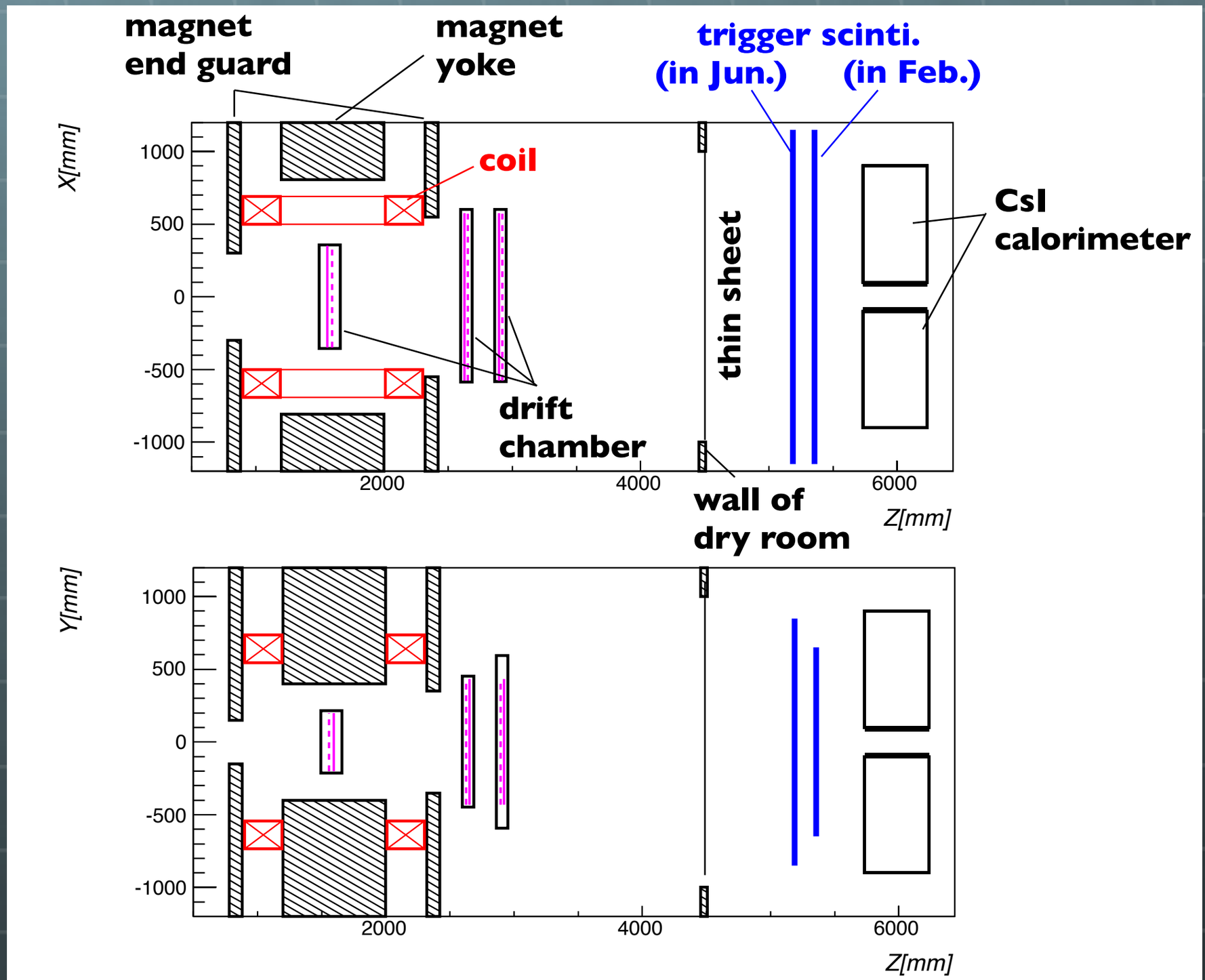

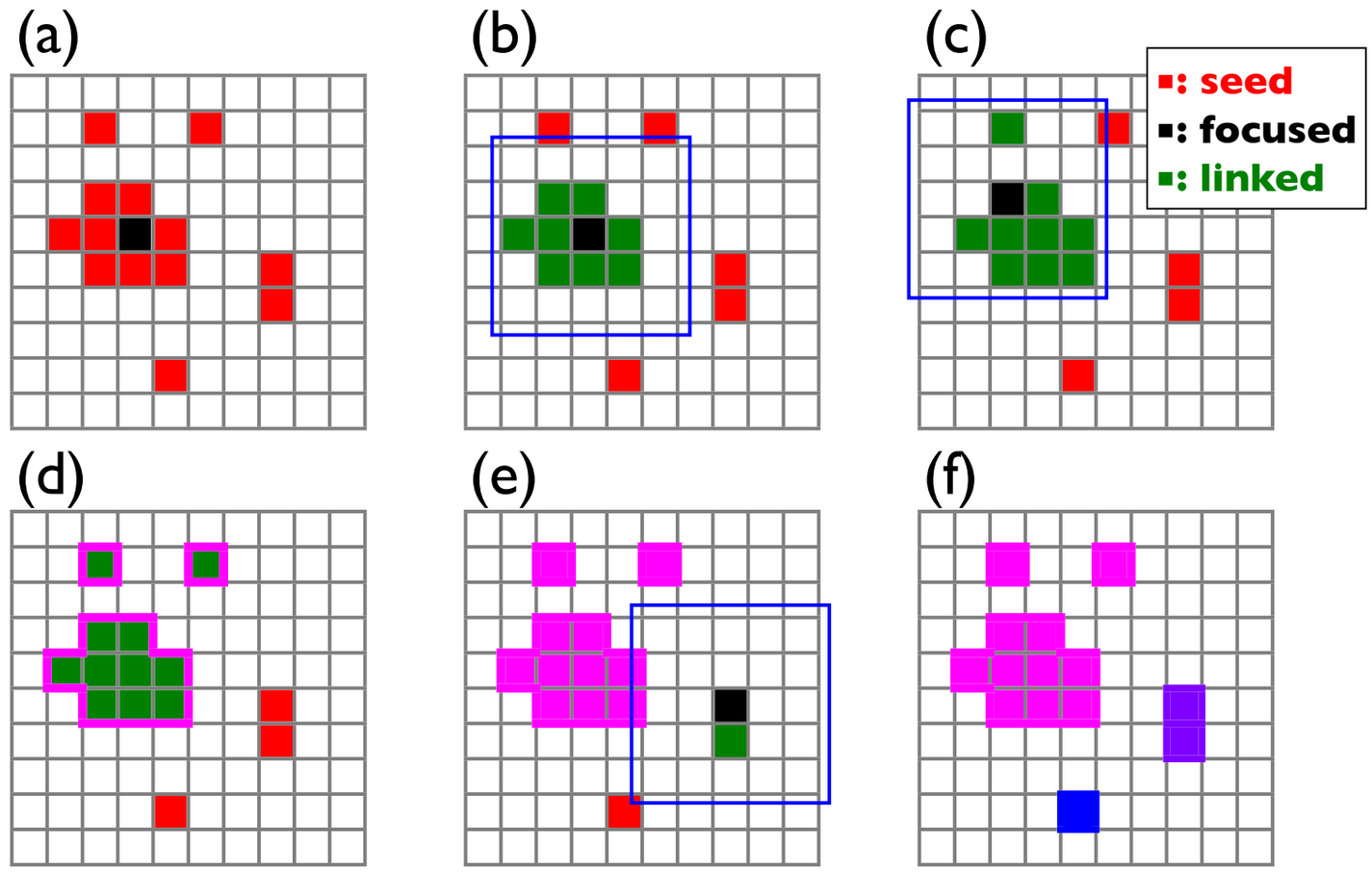

Figure 3.5: Illustration of the clustering process. (a) The CsI crystals with energy deposits more than 3 MeV are shown in red. They are defined as cluster seeds. The black block represents the seed with the maximum energy deposit. First we focused on the black block. (b) The 14×14 cm^2 square, drawn with blue line, is placed around the focused block. The seeds which were located in the square are linked with the focused seed. The linked crystals are filled with green. (c) We then move the focus to one of the linked crystals and seek the seed in the square centered on the focused block. (d) The process in (c) is iterated until no more seeds can be linked. The group of the linked crystals is defined as "cluster". (e) The processes (a)$\sim$(d) are iterated for the remaining seeds. (f) In this example, three clusters are finally found (Each of them are shown in magenta, purple and blue, respectively).

(a)

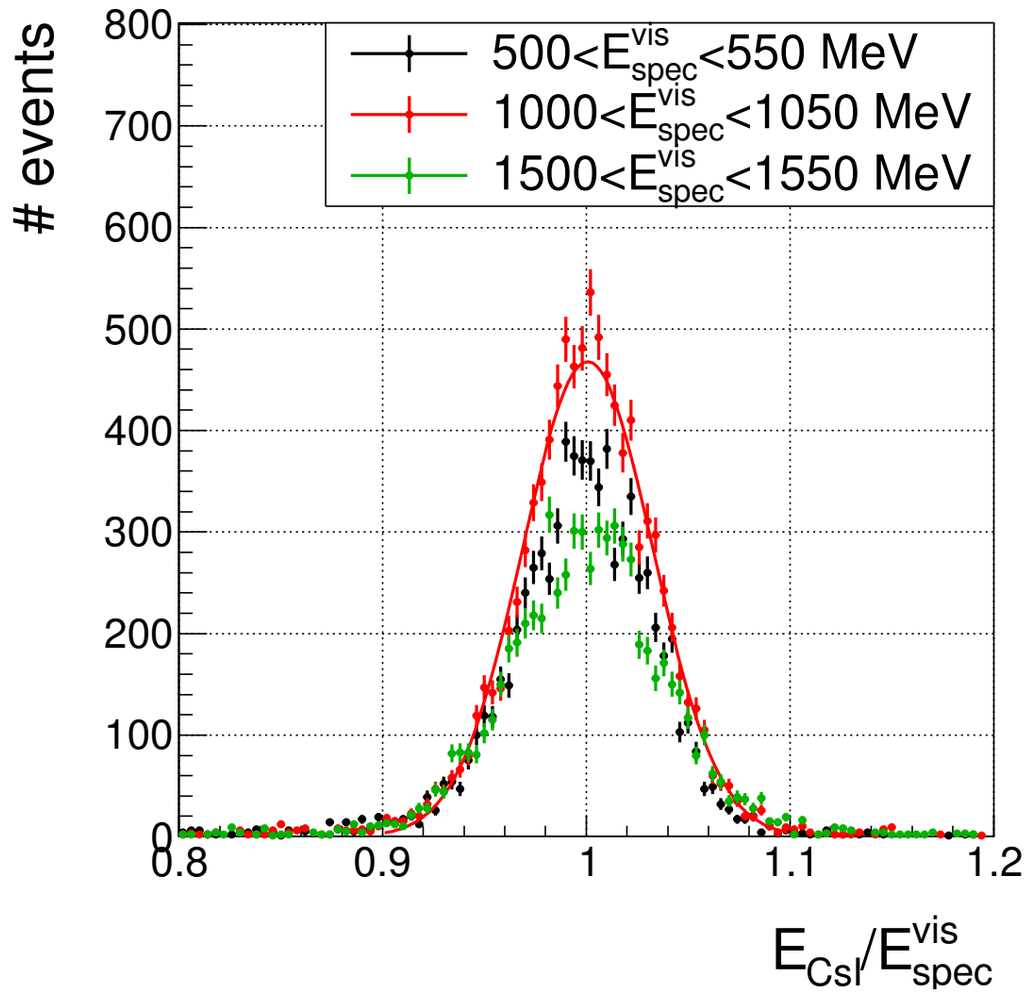

(b)

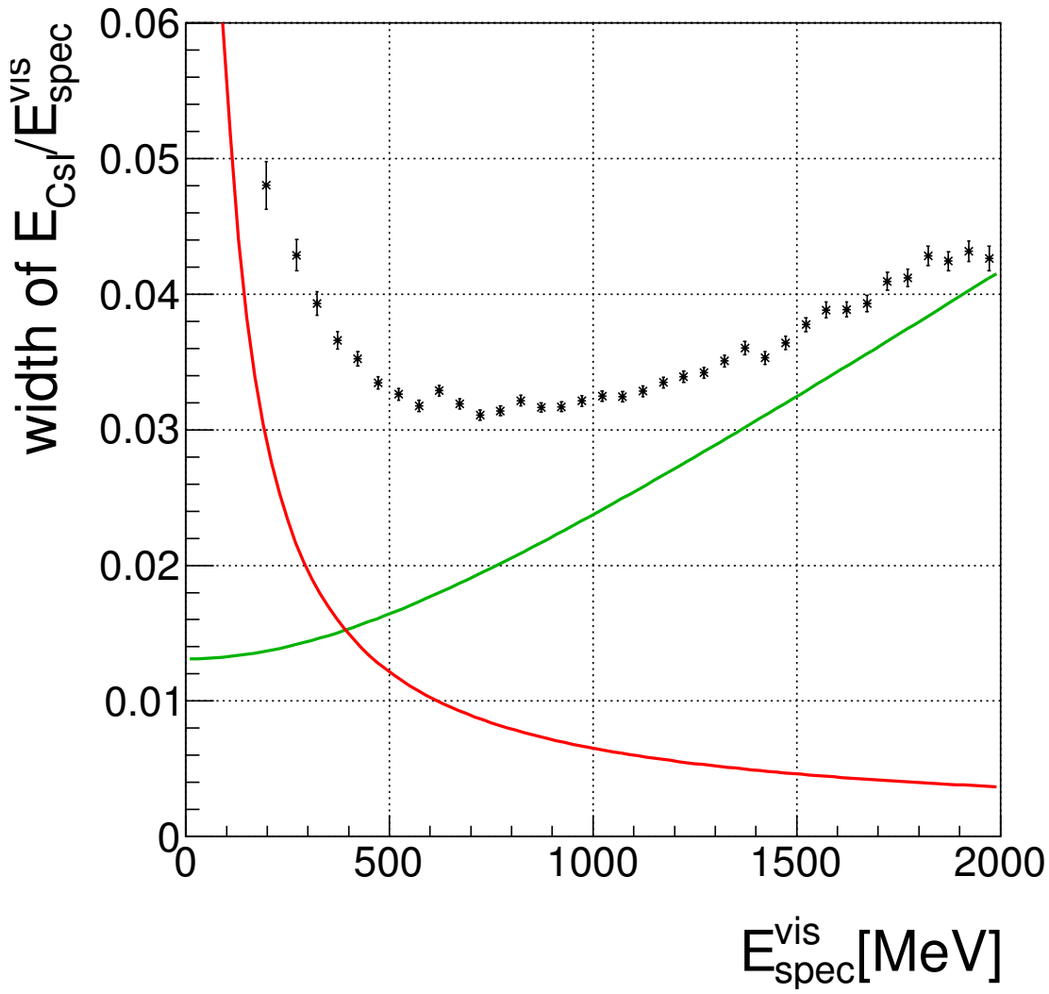

$$\frac{\sigma_E}{E} = p_1 \oplus \frac{p_2}{\sqrt{E[\mathrm{GeV}]}} \oplus \frac{p_3}{E[\mathrm{GeV}]}.$$

$p_1 = (0.66 \pm 0.12 \pm 0.51)\%,\ p_2 = (1.81 \pm 0.04 \pm 0.02)\%,\ p_3 = (0 \pm 0.15 \pm 0.00)\%$ **large Crystal**

$p_1 = (1.71 \pm 0.11 \pm 0.13)\%,\ p_2 = (1.31 \pm 0.10 \pm 0.01)\%,\ p_3 = (0 \pm 0.44 \pm 0.00)\%$ **small Crystal**

From January run

Calorimeter calibration 1 - cosmic ray

- E calibration before beam run using cosmic ray
  - Initial calibration
  - Also used for gain adjustment of each crystal (to use in trigger)

- E calibrations of other detectors were also done with cosmic ray data.
  (Except for detectors that are only sensitive to particles in the beam direction.)

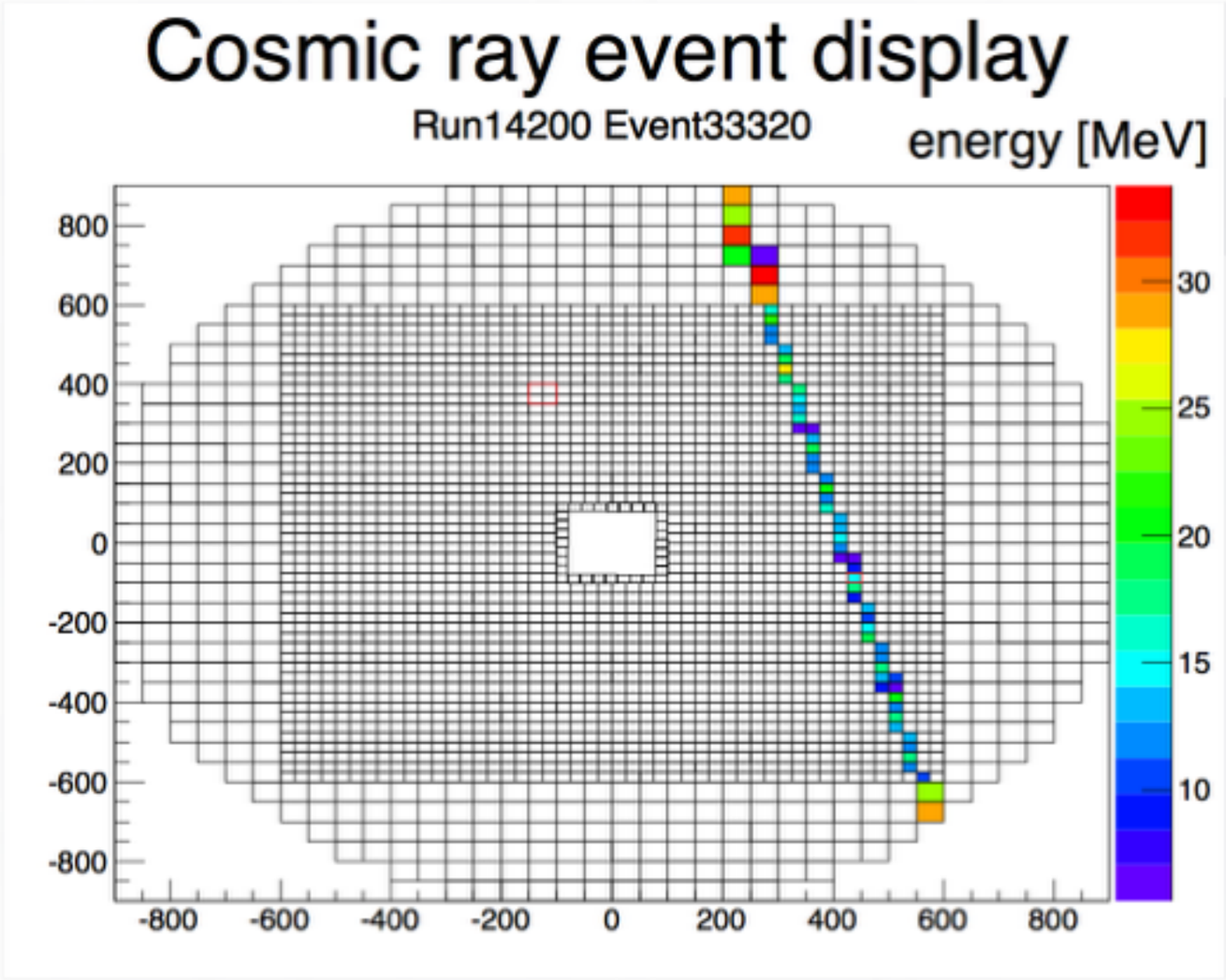

$K_L \rightarrow \pi^0\pi^0\pi^0$

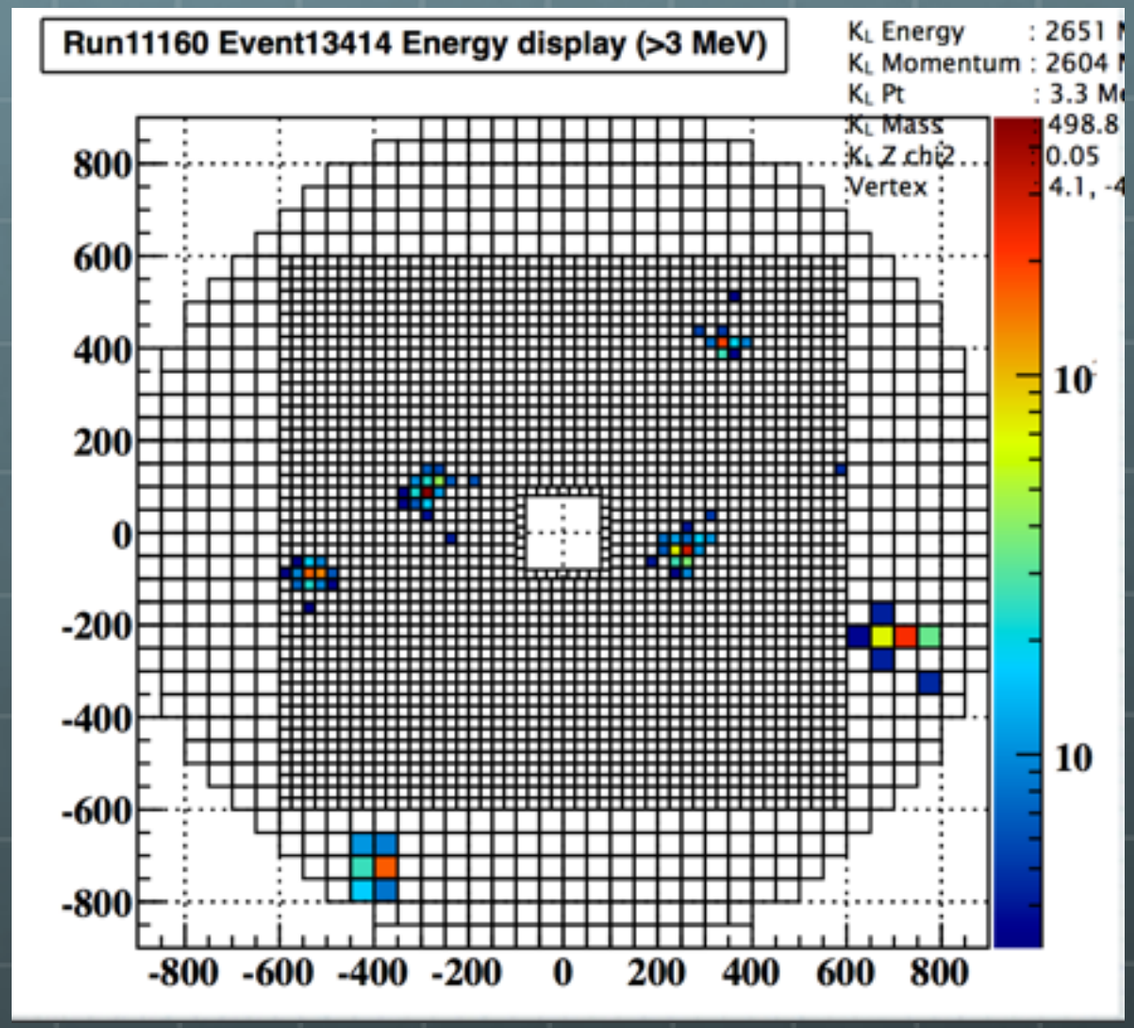

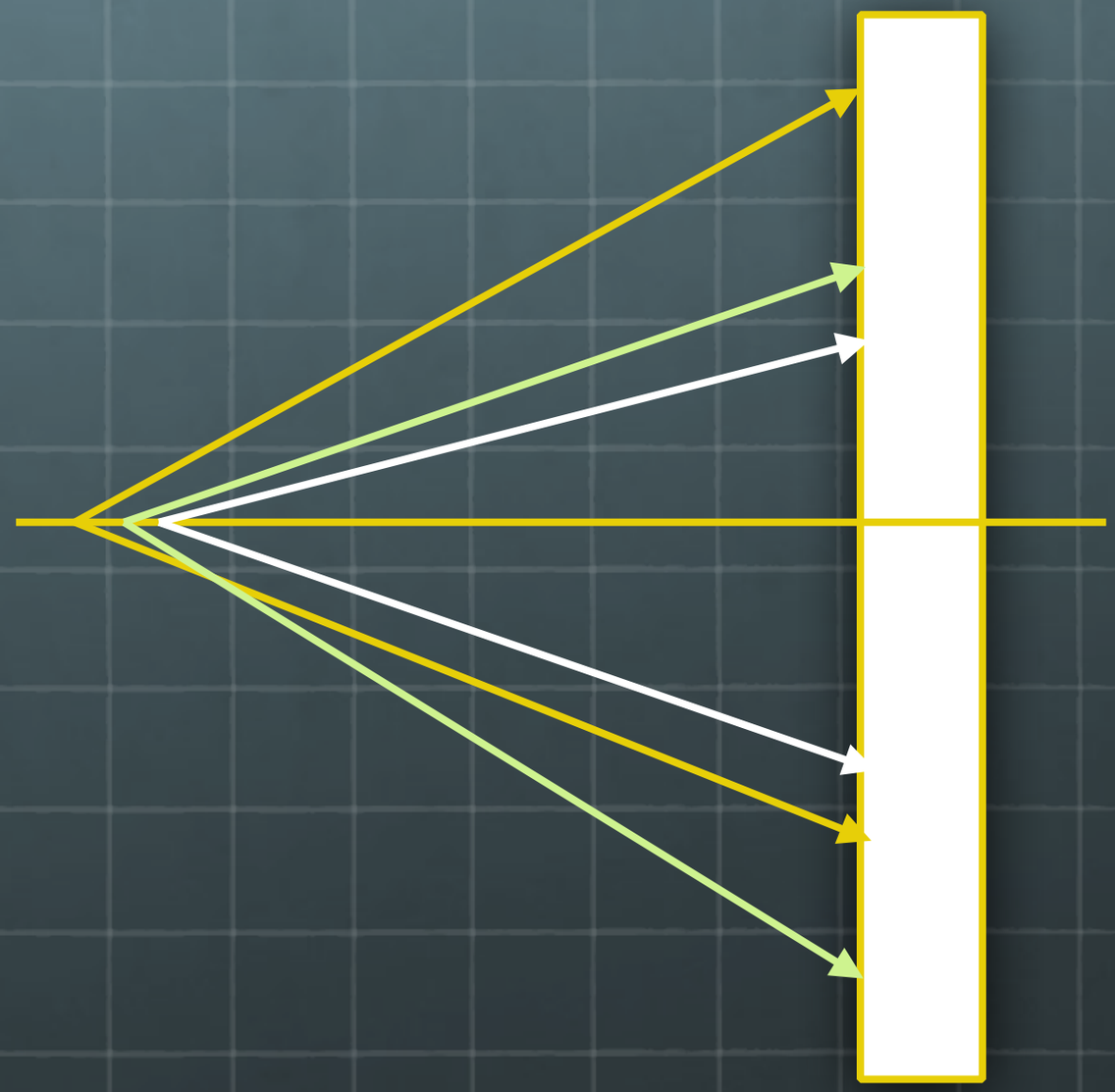

π^0 reconstruction

- EM calorimeter provides energies and incident positions of two photons
- With an assumption that π^0 decays at beam center and π^0 rest mass, we can obtain a distance between calorimeter and decaying vertex.
- Pair of neutrinos take away transverse momentum (P_T)

$$\cos\theta = 1 - \frac{M_{\pi^0}^2}{2E_1E_2}$$

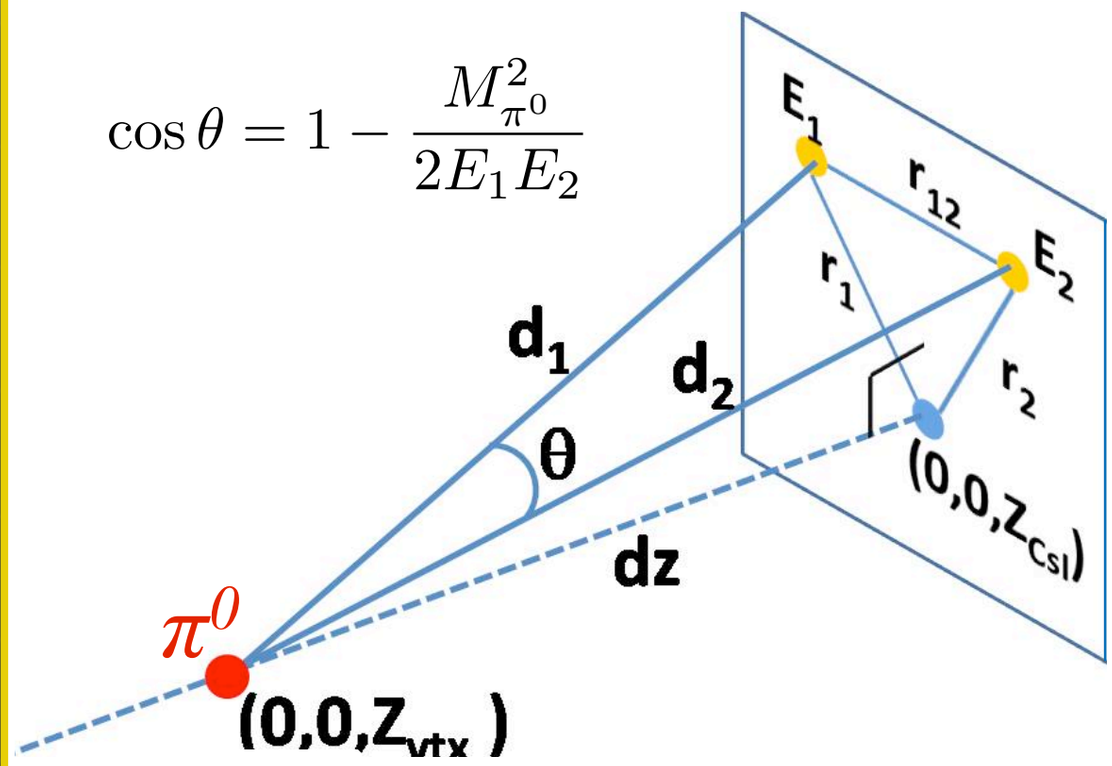

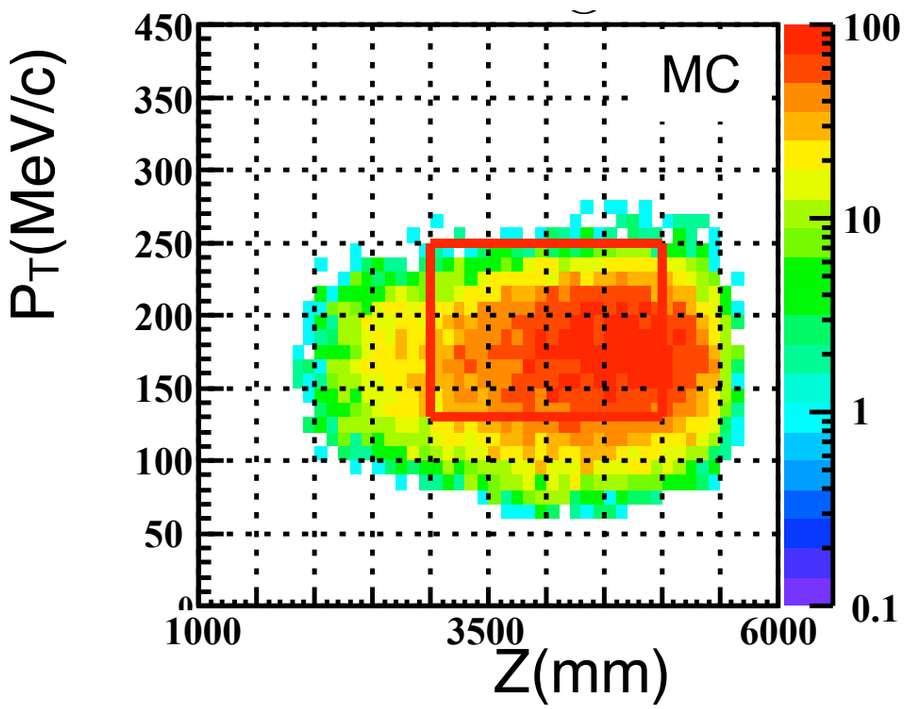

$K_L \rightarrow \pi^0\pi^0\pi^0$

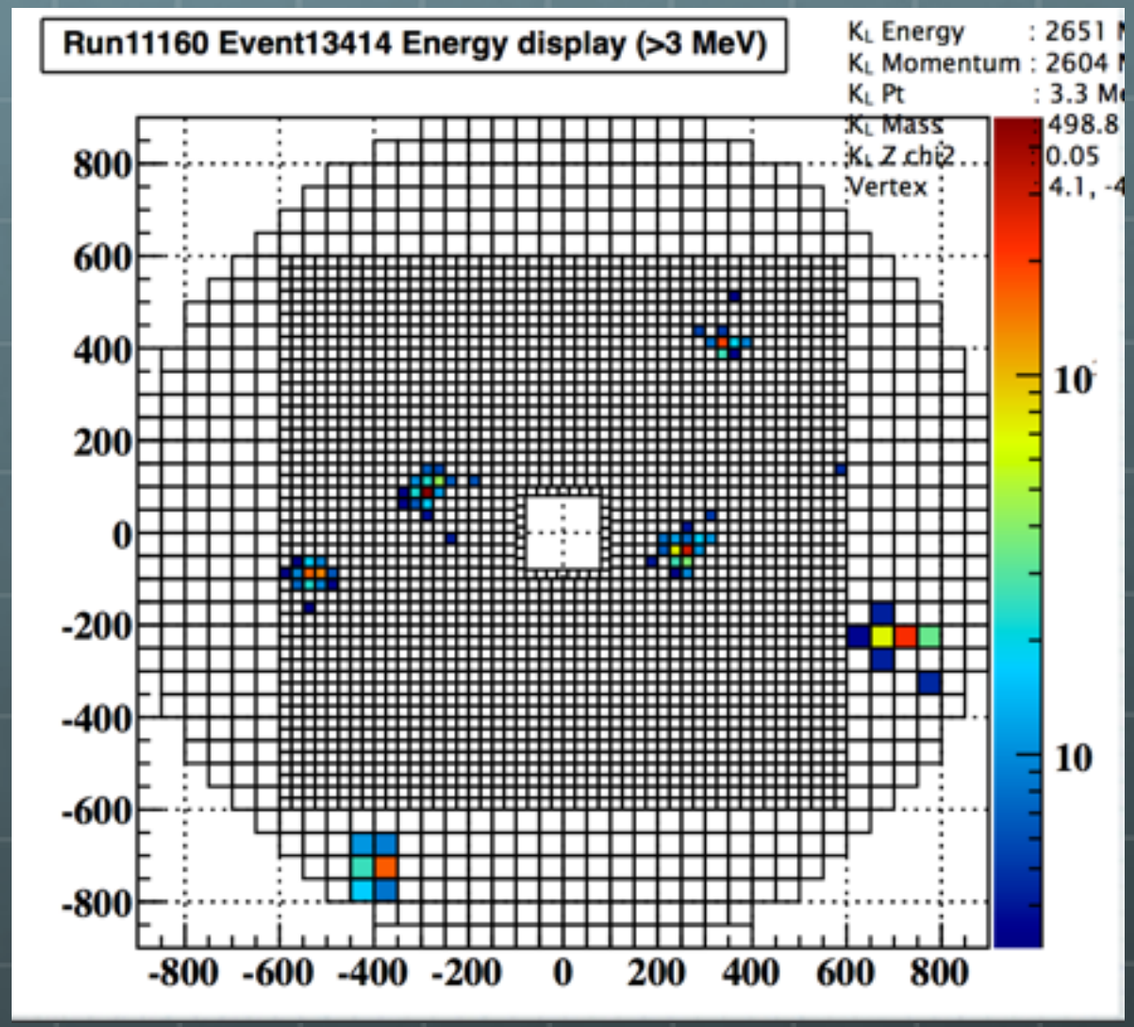

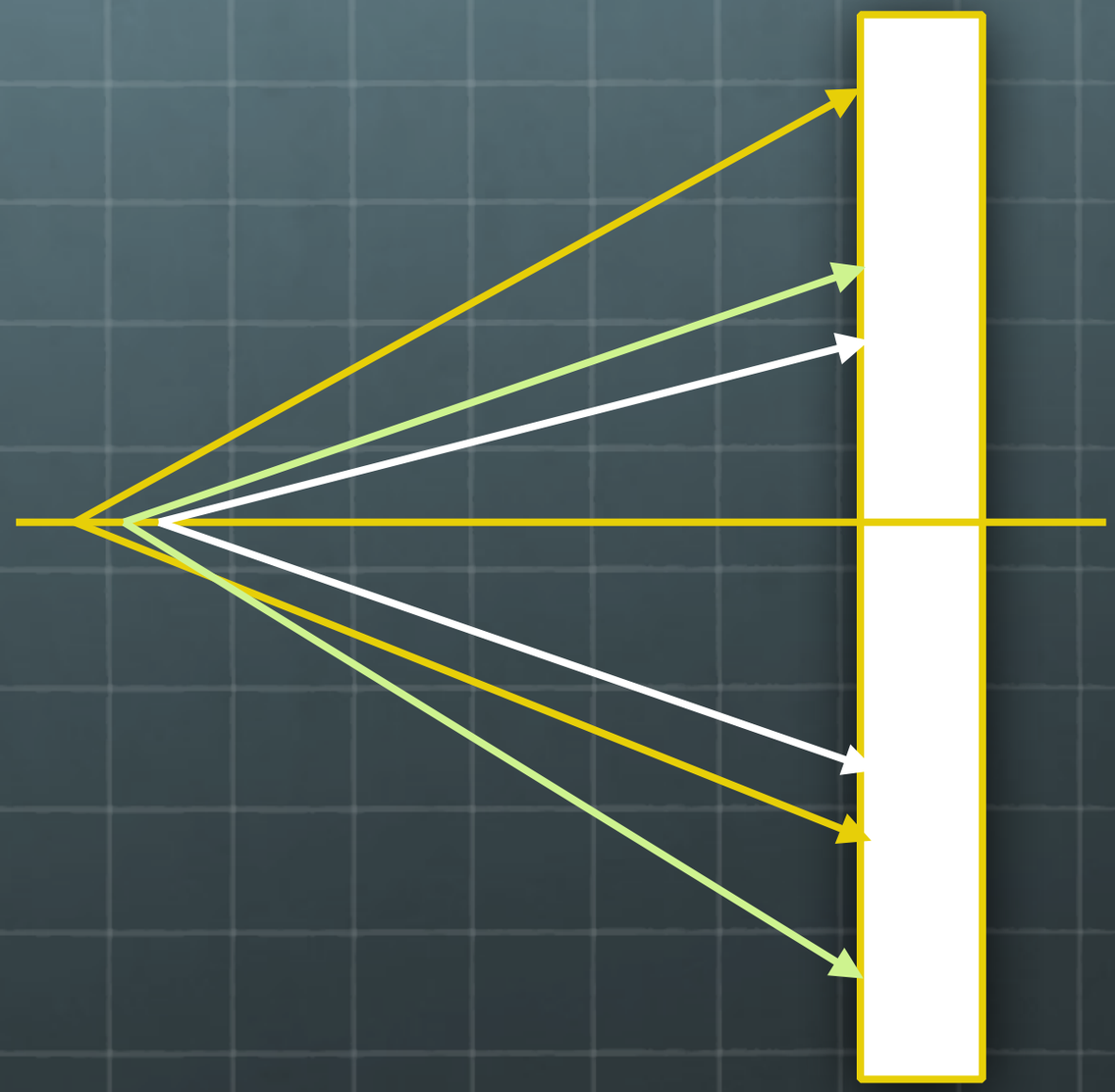

From January run

Calorimeter calibration 3 - $K_L \rightarrow 3\pi^0$

- Relative calibration using 6γ from $K_L \rightarrow 3\pi^0$
- Constraint fitting with
  4 parameters and
  6 constraints

parameters:
- decay vertex: v_x, v_y, v_z
- E of i-th photon

constraints:
- mass of 3 pairs = $M_{\pi 0}$
- mass of 6γ = M_{KL}
- vertex x,y correlate with COE

$$(E_0+E_1)^2-(\vec{P}_0+\vec{P}_1)^2=M_{\pi^0}{}^2$$
$$(E_2+E_3)^2-(\vec{P}_2+\vec{P}_3)^2=M_{\pi^0}{}^2$$
$$(E_4+E_5)^2-(\vec{P}_4+\vec{P}_5)^2=M_{\pi^0}{}^2$$
$$\left(\sum_{i=0}^{5}E_i\right)^2-\left(\sum_{i=0}^{5}P_i\right)^2=M_{K_L}{}^2$$
$$\sum_{i=0}^{5}x_i\cdot E_i=v_x\cdot\sum_{i=0}^{5}E_i$$
$$\sum_{i=0}^{5}y_i\cdot E_i=v_y\cdot\sum_{i=0}^{5}E_i$$

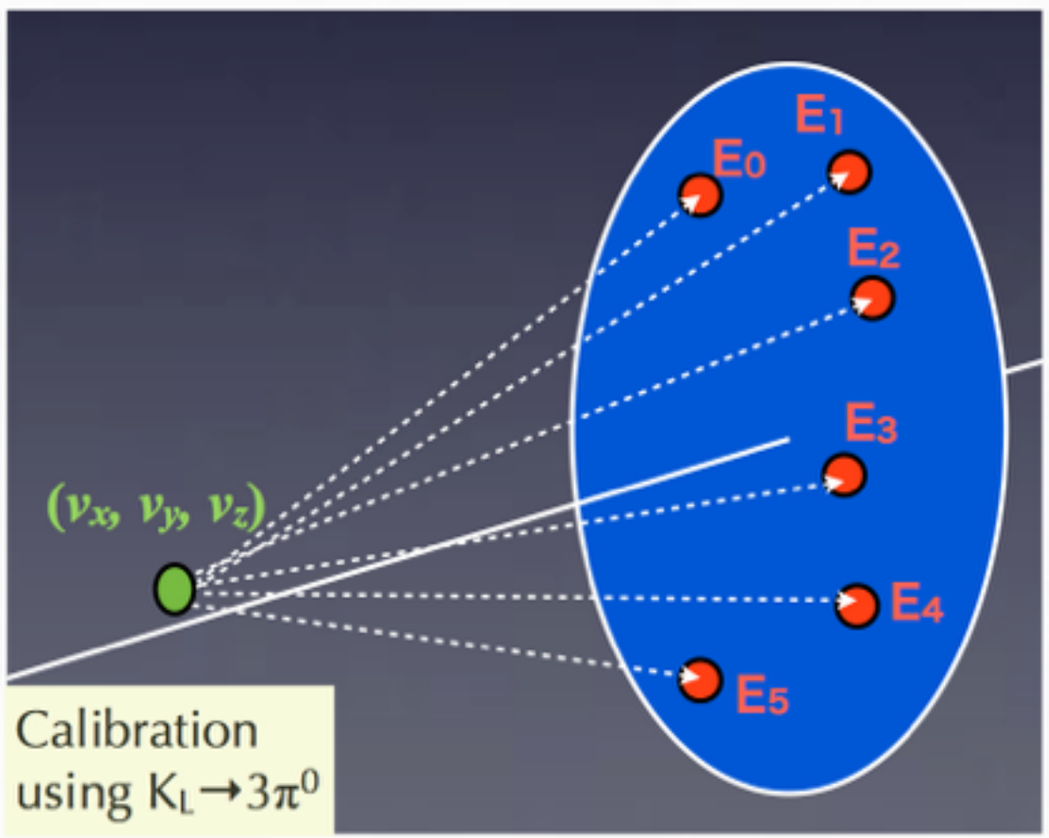

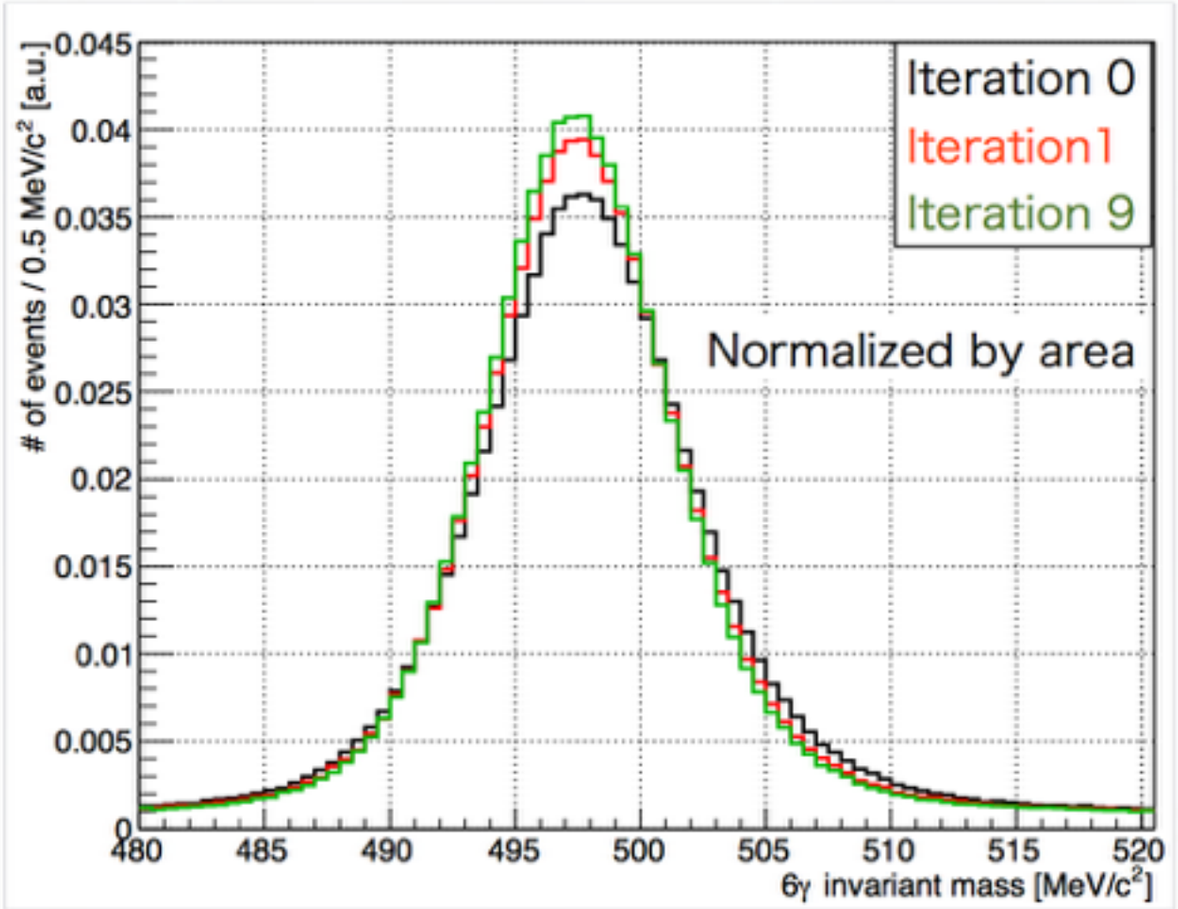

From January run

Calorimeter calibration 2 - Al target

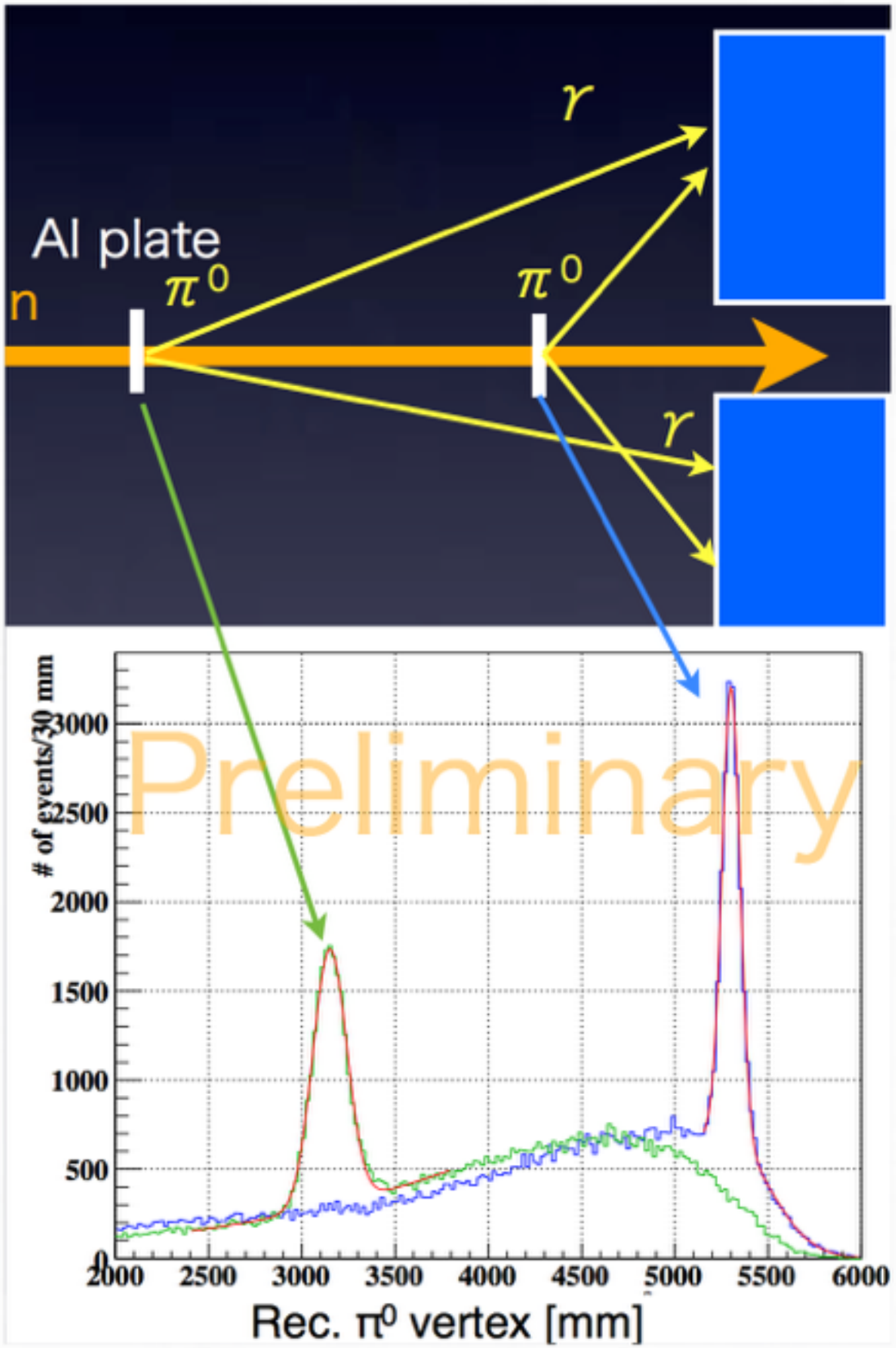

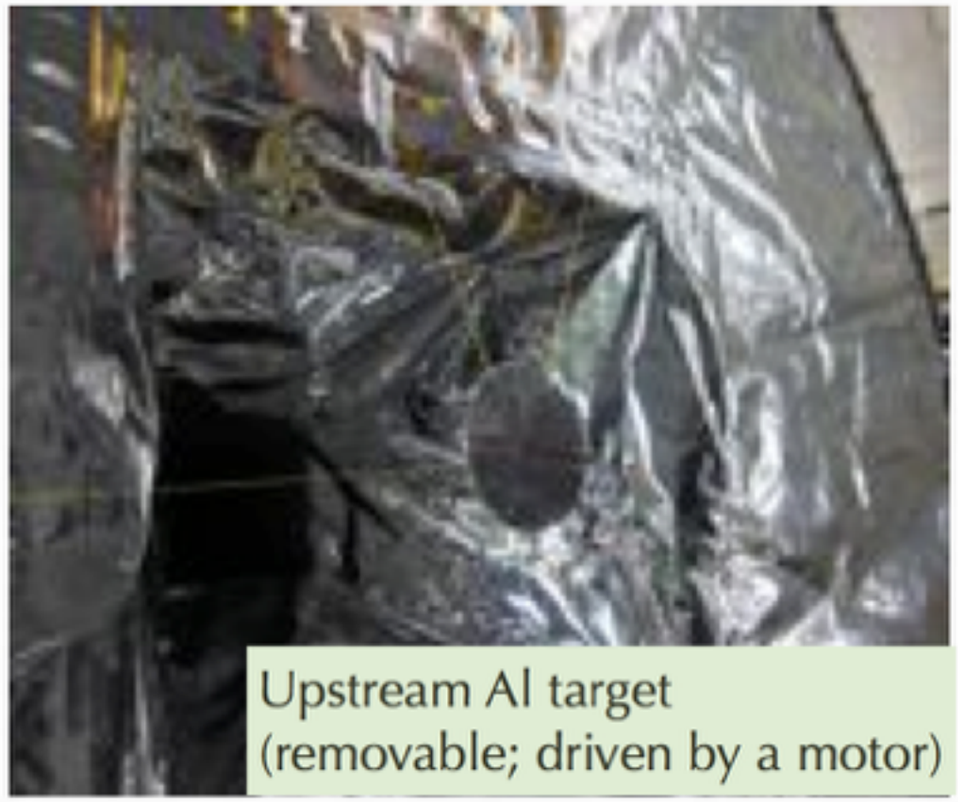

Upstream Al target
(removable; driven by a motor)

- 5mm Al target inserted in the neutral beam
  - π^0 production at known z position
- Absolute energy scale can be obtained.
  (If π0 mass is assumed, a peak can be observed at corresponding z position.)

Results of May 2013

- Removed B.G. events learned from the E391a.
  (π^0 production at the detectors)
- We found two new sources of the B.G.
- Upgraded detector for run 2015

$$\mathrm{S.E.S} = 1.29 \times 10^{-8}$$

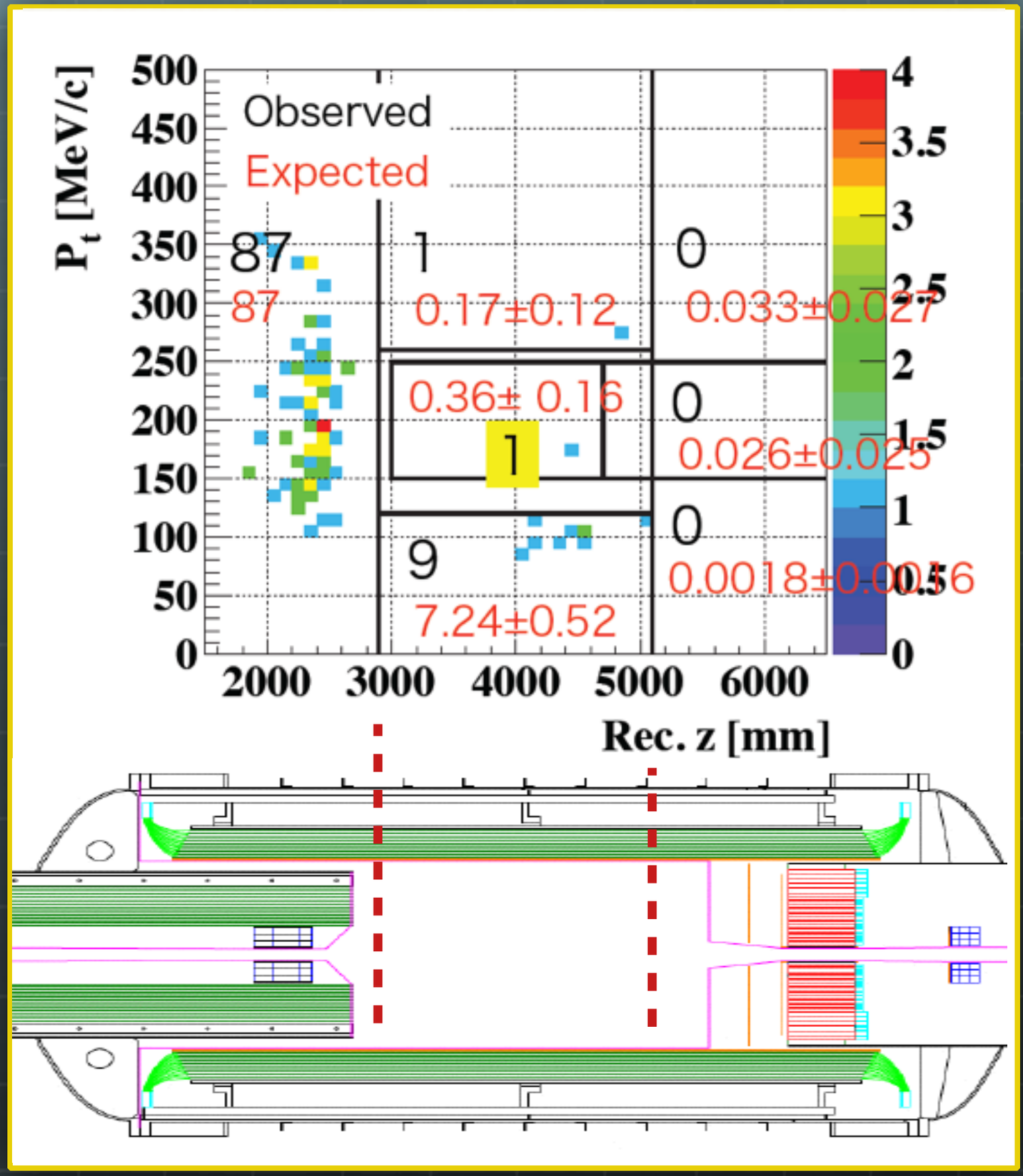

M.C. for gamma with High statistics

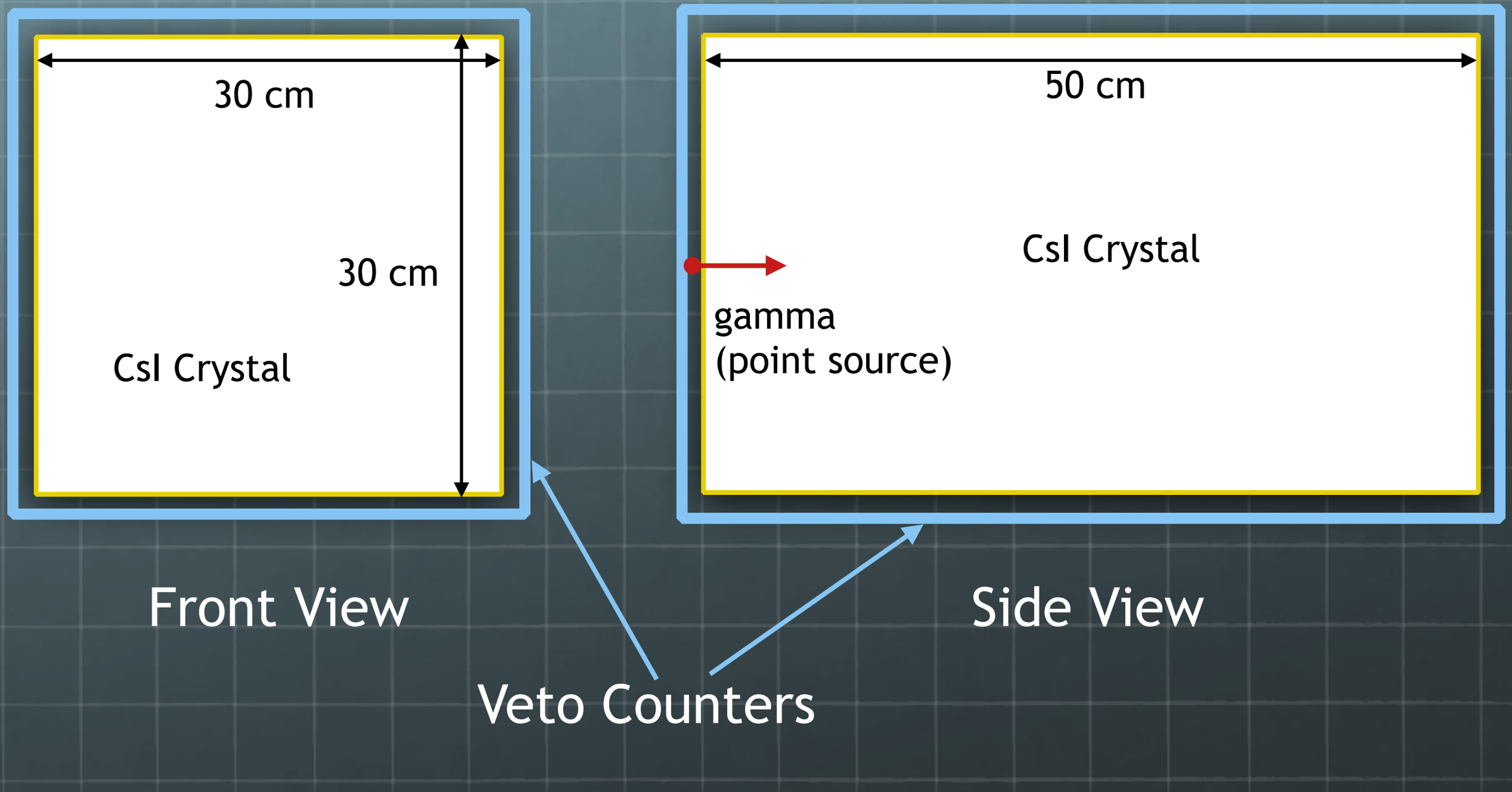

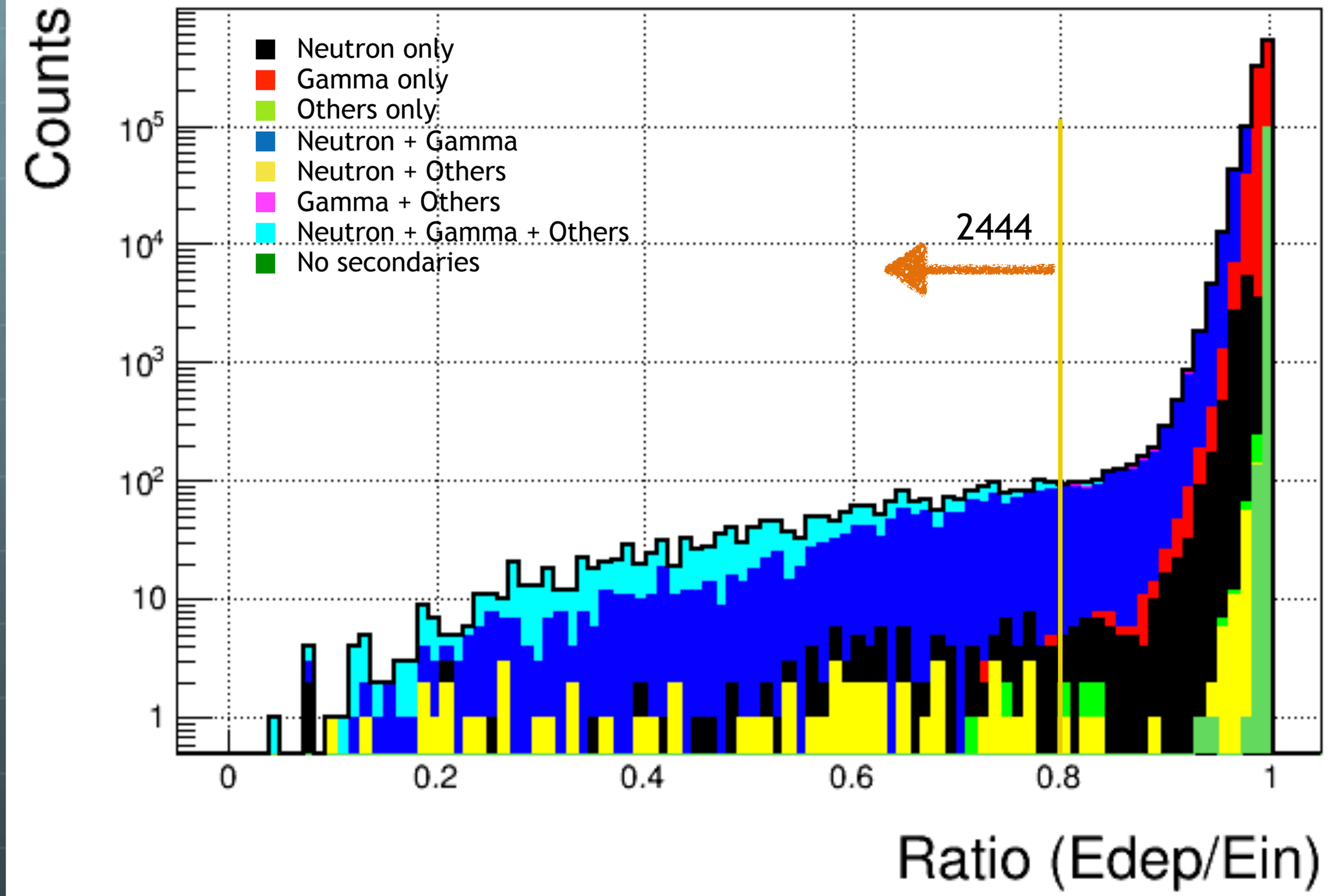
Counts
Neutron only
Gamma only
Others only
Neutron + Gamma
Neutron + Others
Gamma + Others
Neutron + Gamma + Others
No secondaries
2444
10^5
10^4
10^3
10^2
10
1
0
0.2
0.4
0.6
0.8
1
Ratio (Edep/Ein)

Election Incident

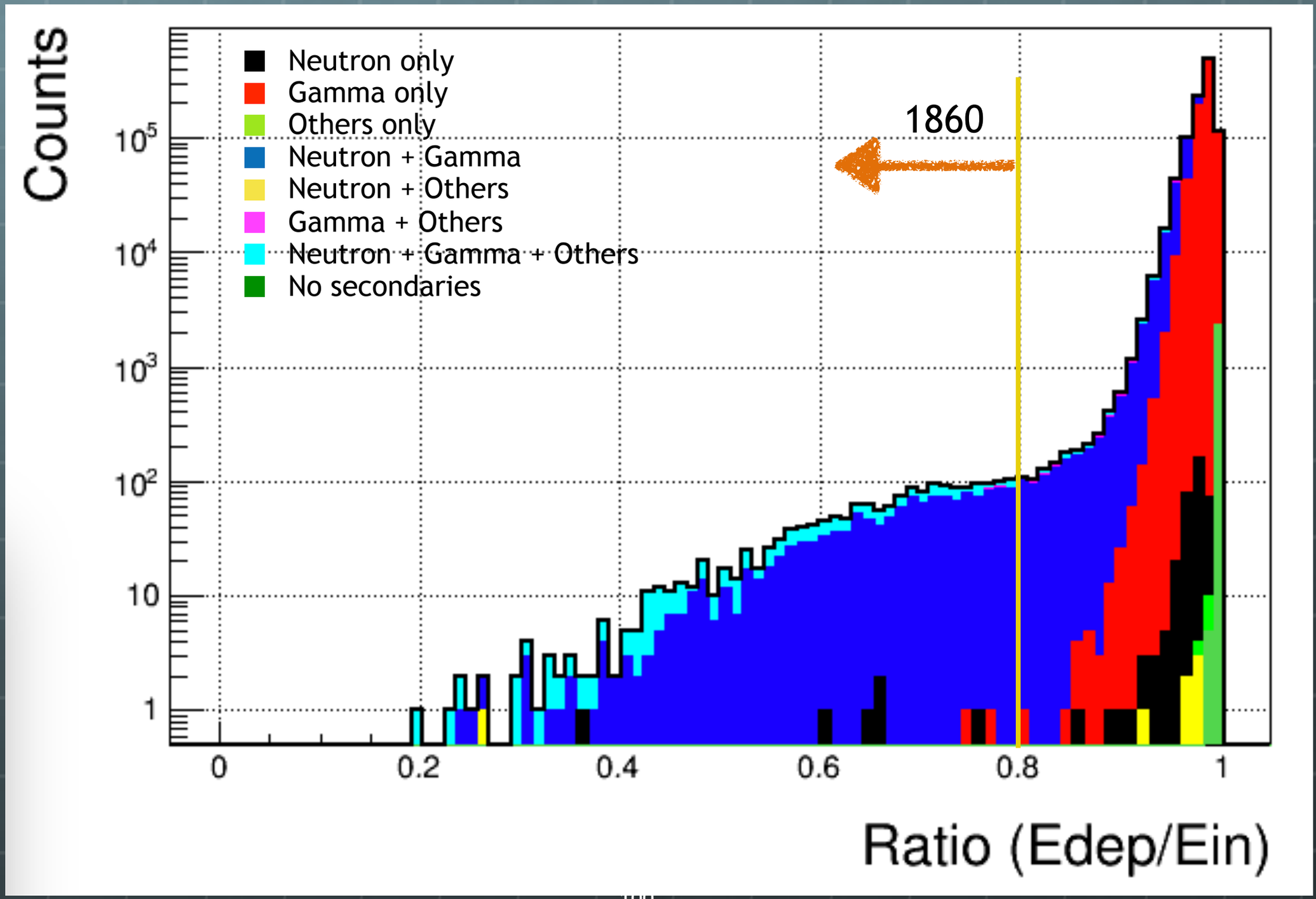

J-PARC

(Japan Proton Accelerate Research Complex)

Location of J-PARC

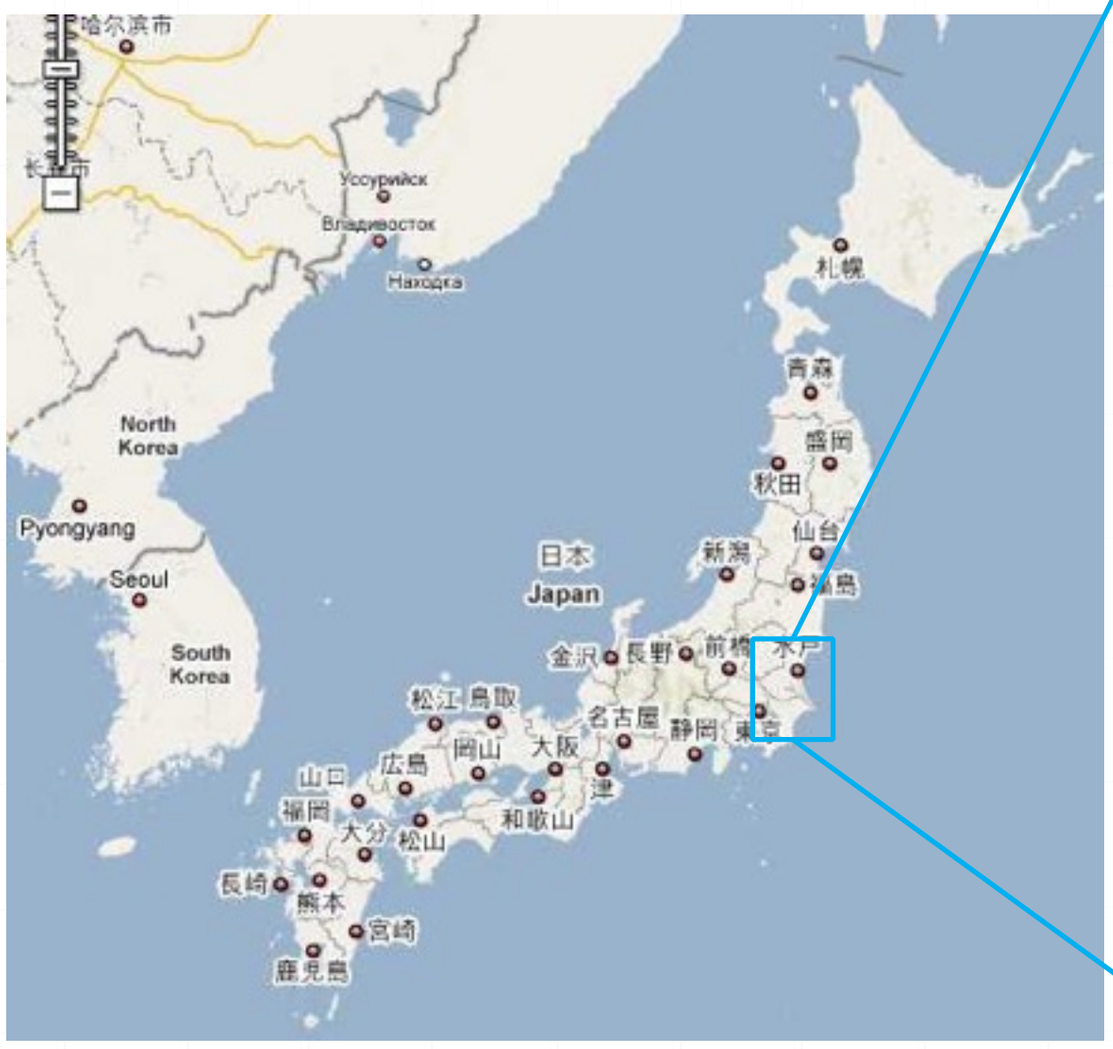

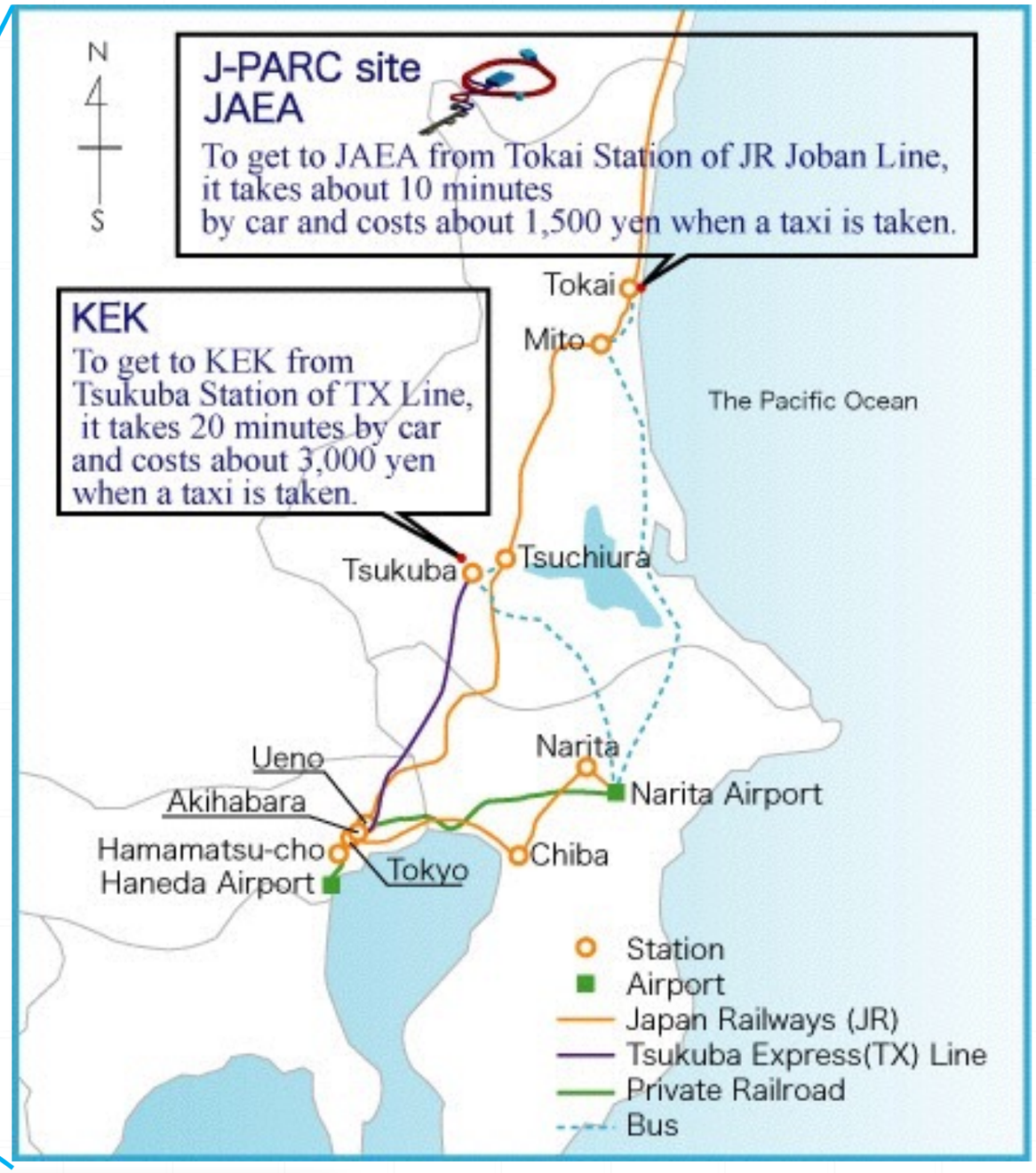

http://j-parc.jp/index-e.html

J-PARC Facility

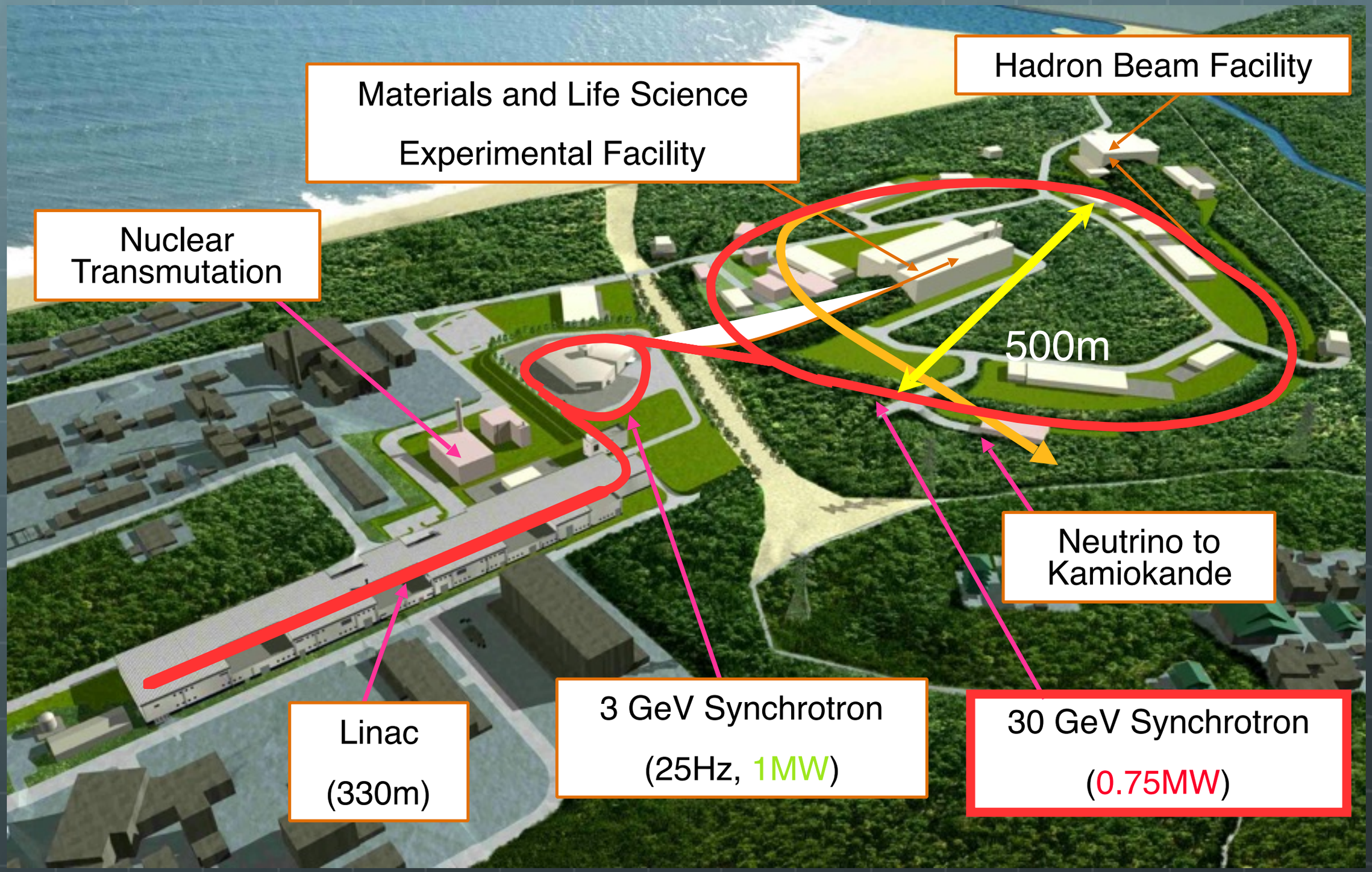

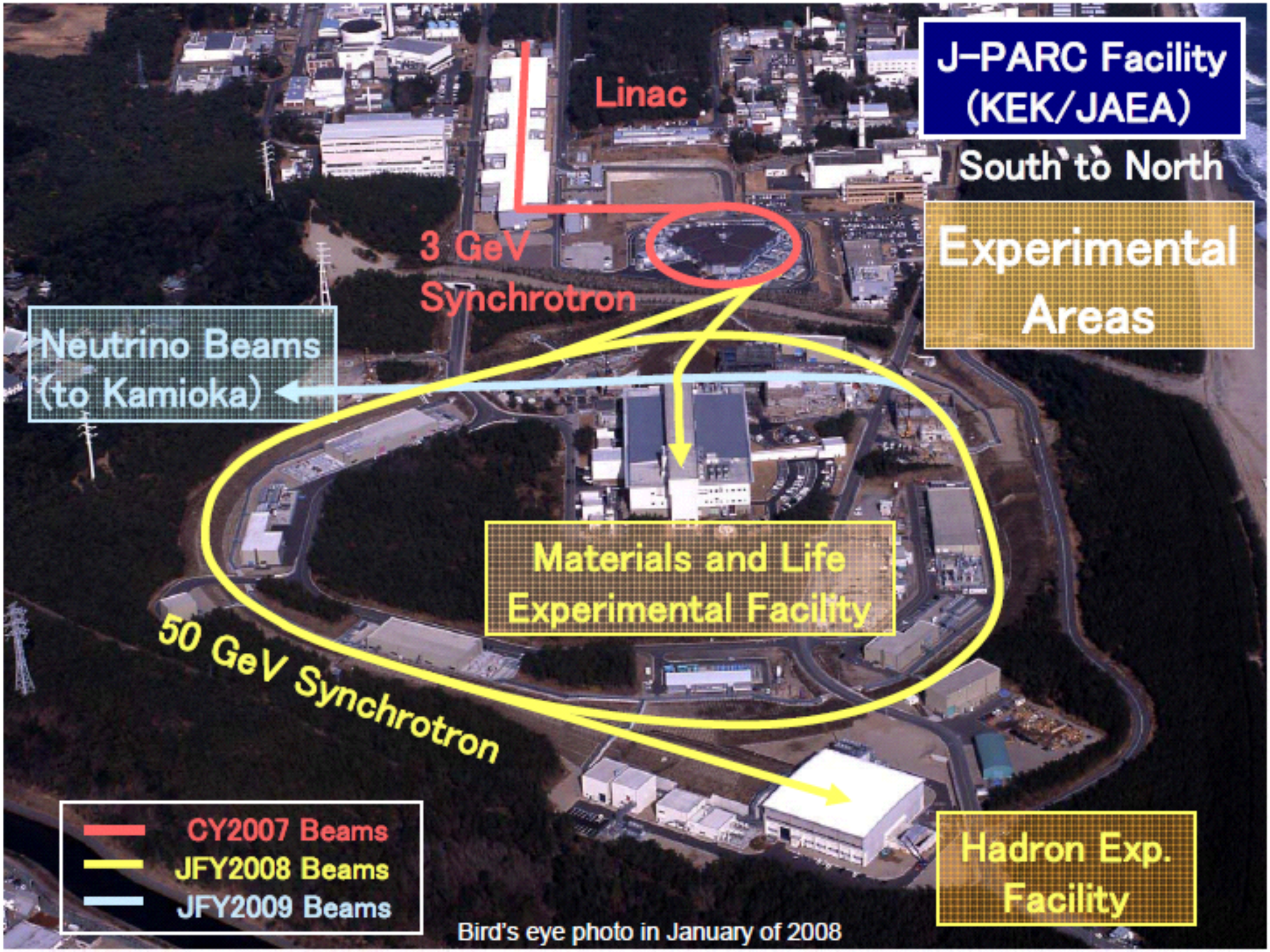
J-PARC Facility
(KEK/JAEA)
South to North
Linac
3 GeV
Synchrotron
Experimental
Areas
Neutrino Beams
(to Kamioka)
Materials and Life
Experimental Facility
50 GeV Synchrotron
CY2007 Beams
JFY2008 Beams
JFY2009 Beams
Hadron Exp.
Facility
Bird's eye photo in January of 2008

EXPERIMENTS

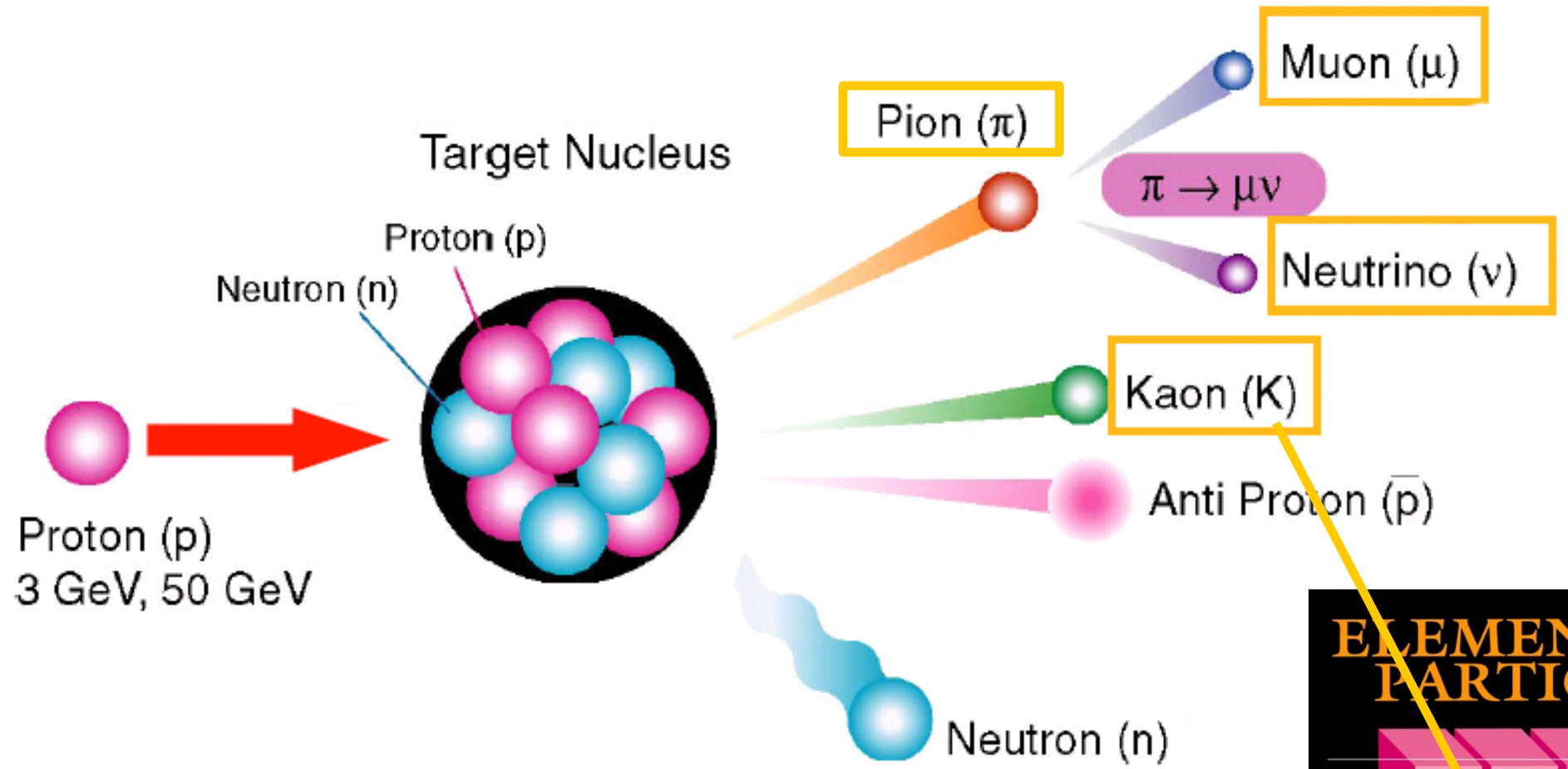

To study various phenomena with high intensity secondary particles.

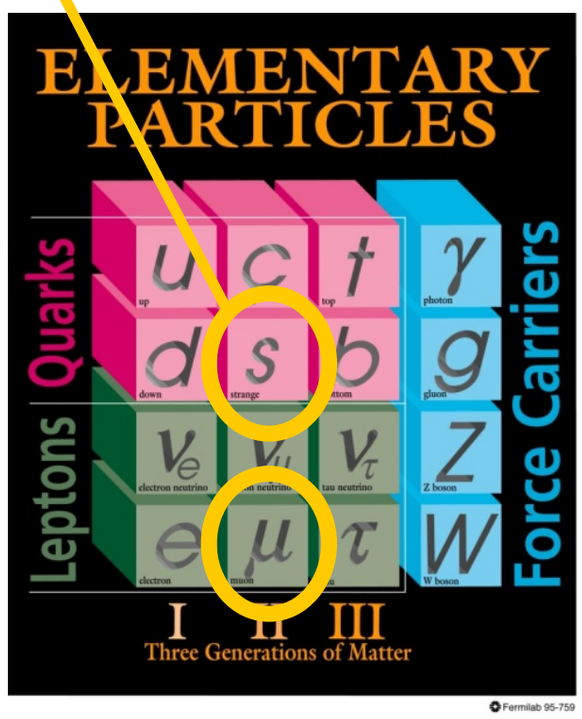

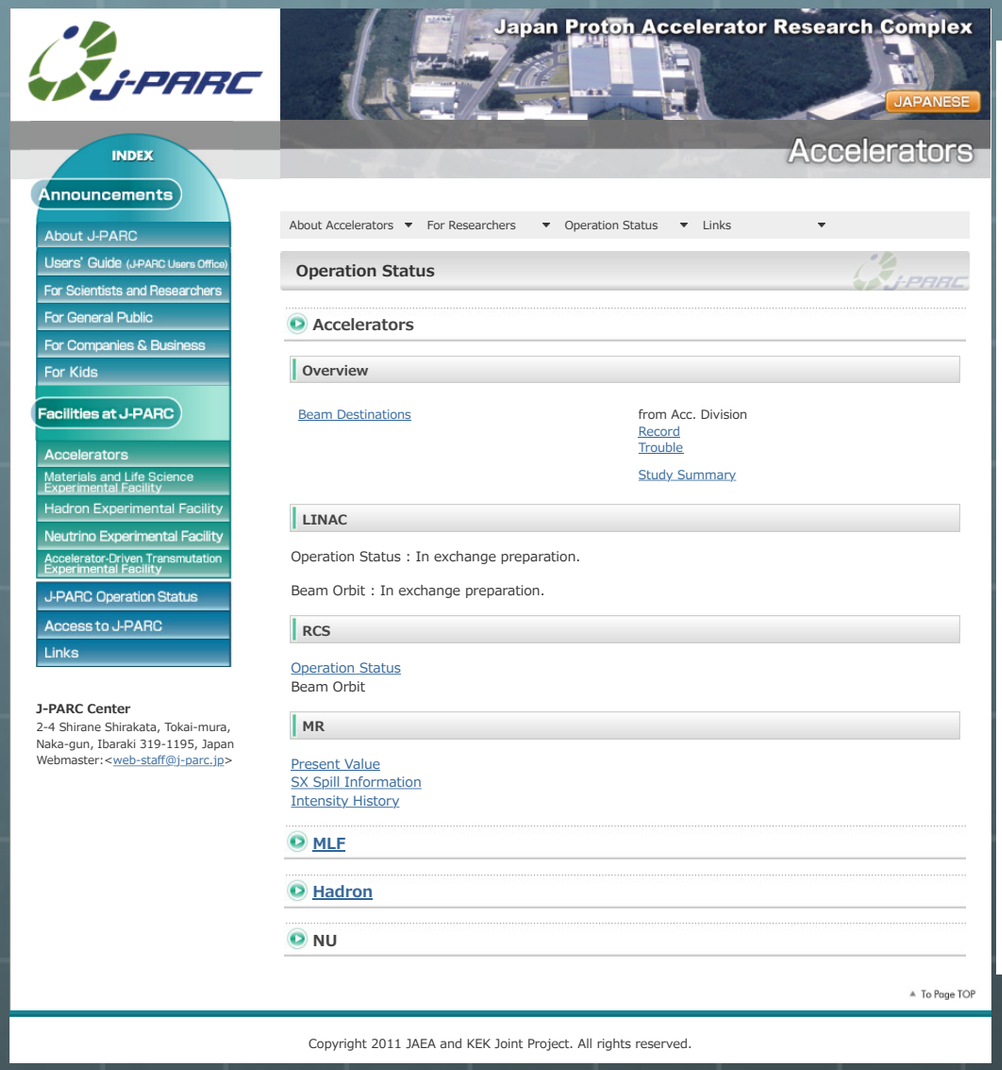

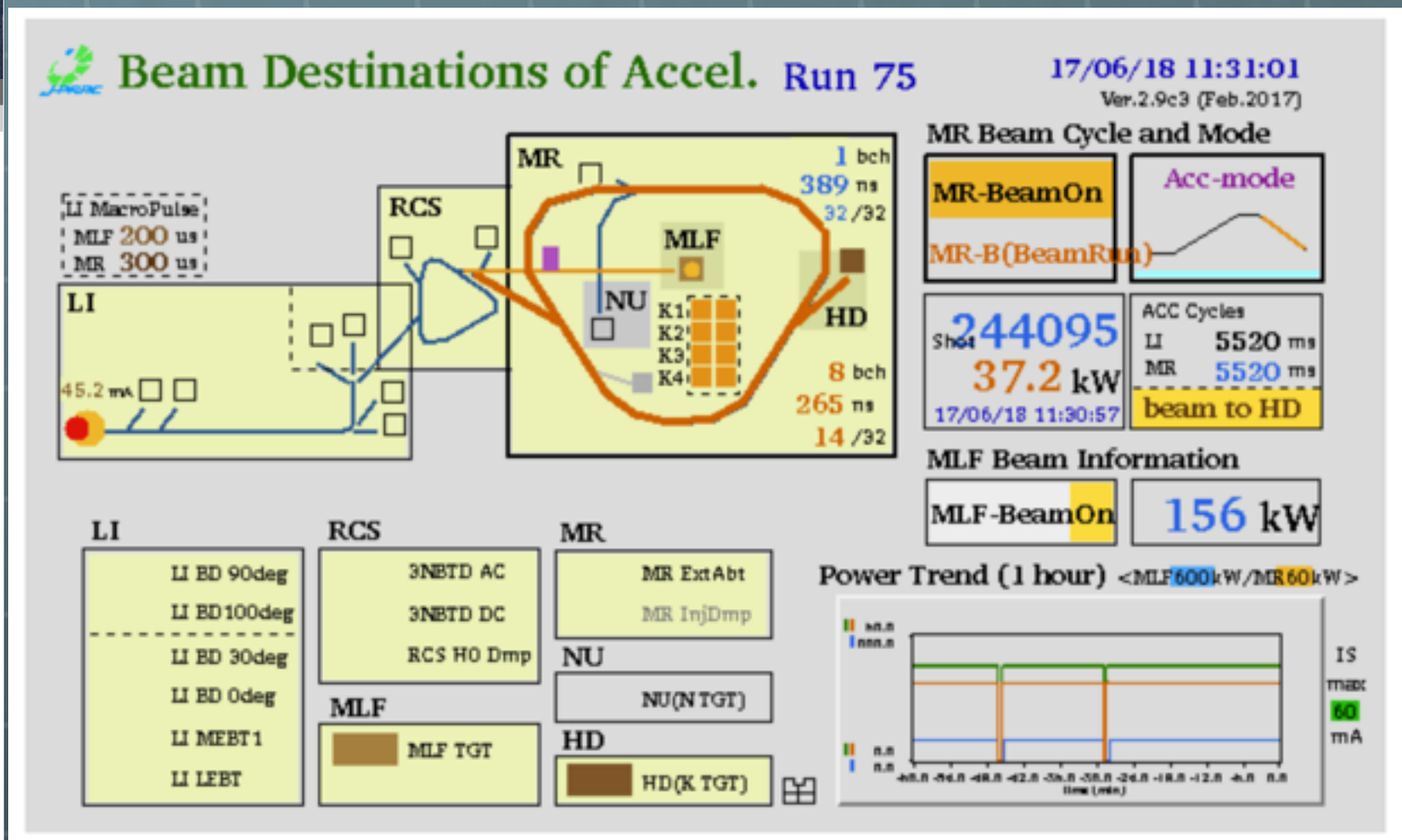

http://j-parc.jp/Acc/en/operation.html

42 kW Beam

$$42kW = 30GeV \cdot 1.4\mu A$$

$$1.4\mu A = 8.74 \times 10^{12}\ protons/s$$

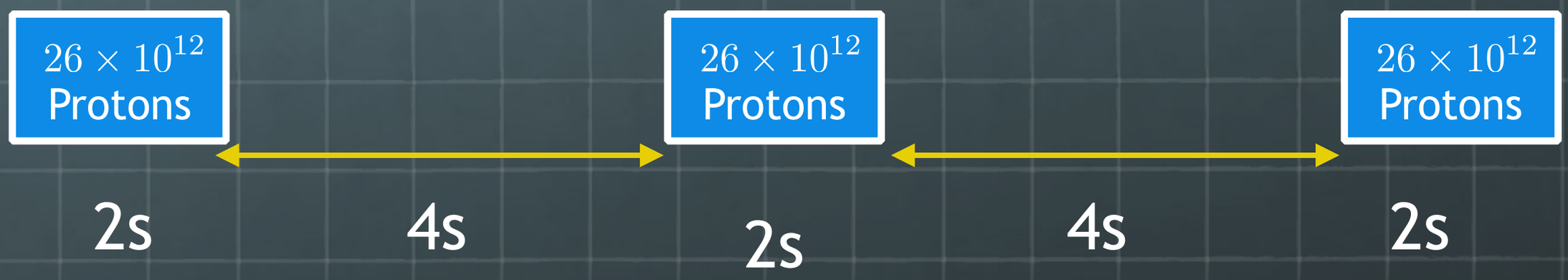

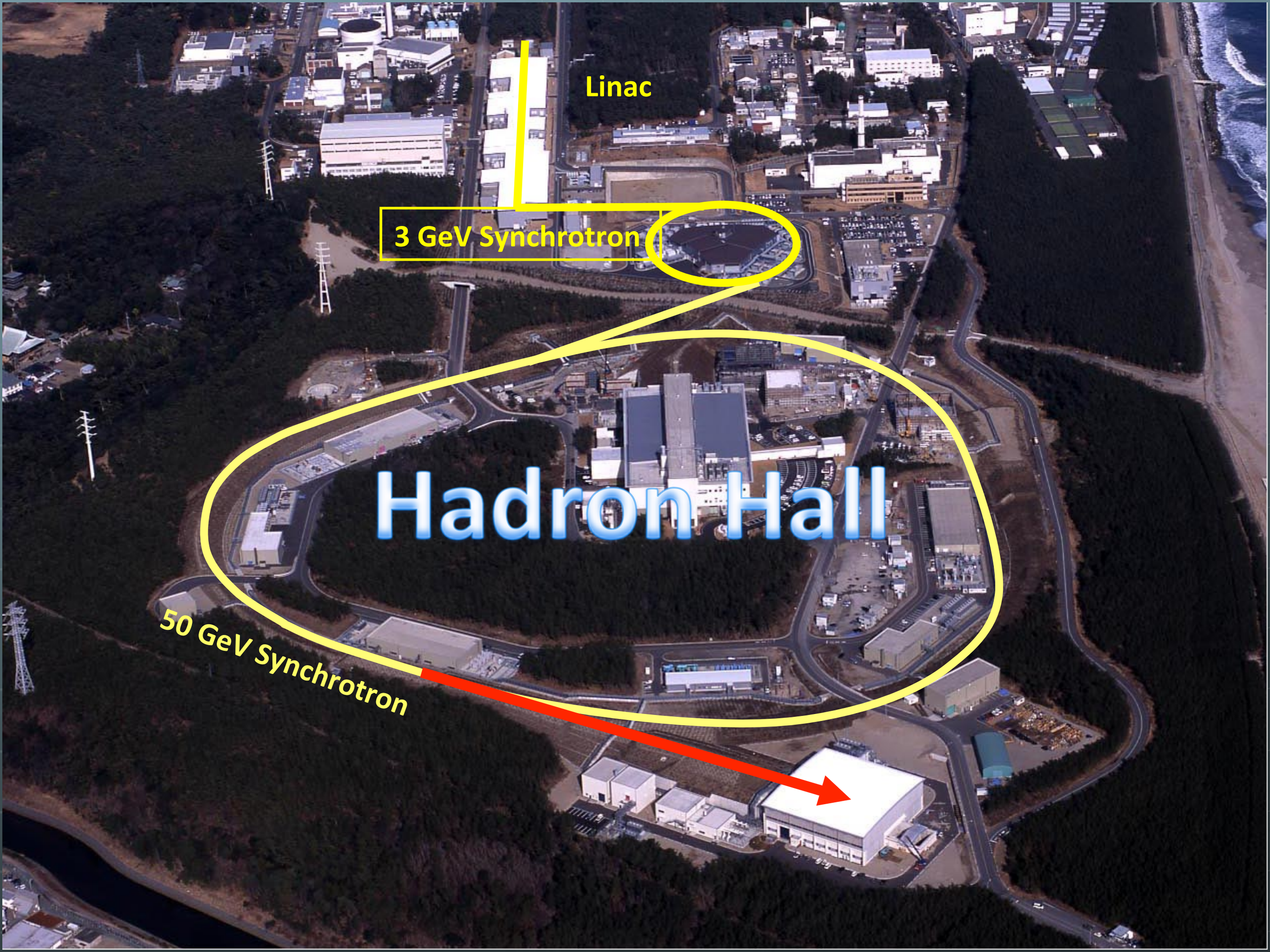
Linac
3 GeV Synchrotron
Hadron Hall
50 GeV Synchrotron

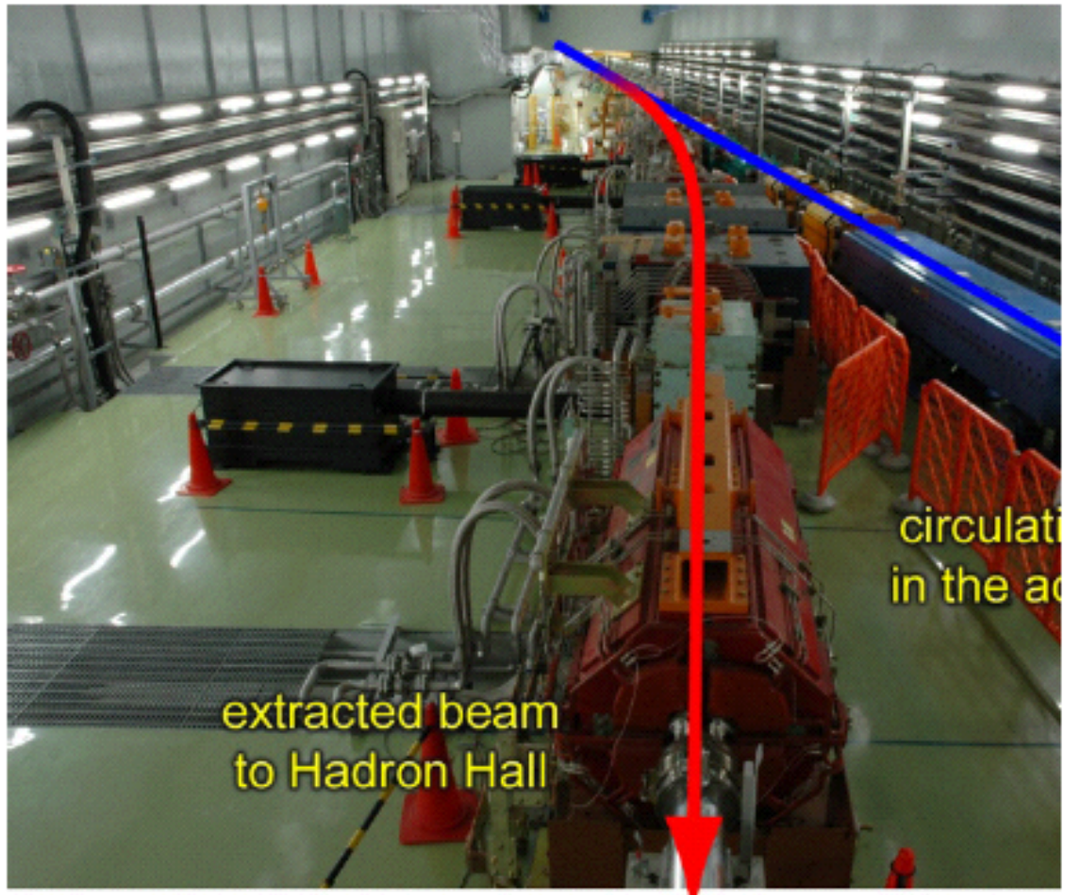

beam extraction
to Hadron Hall

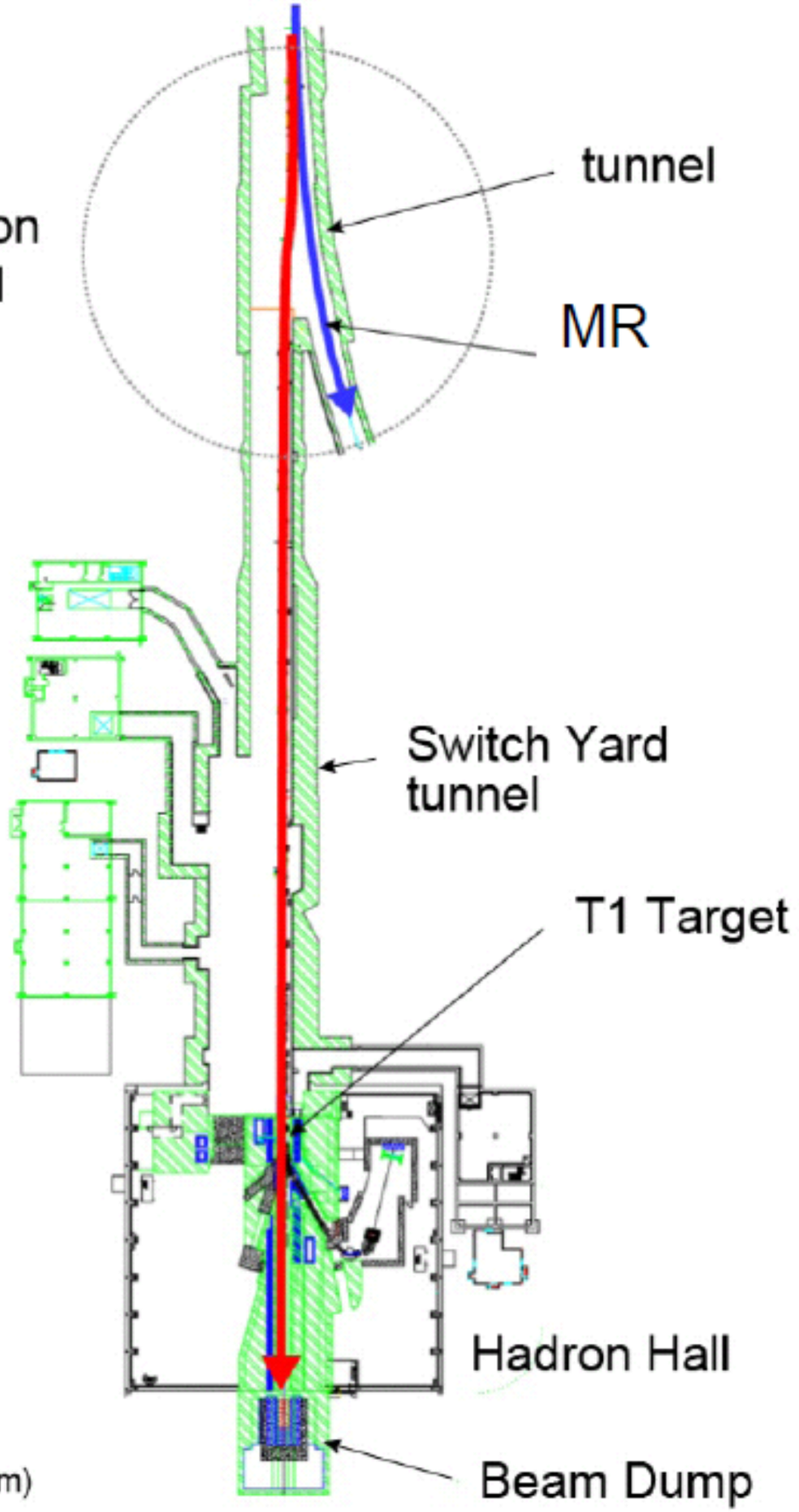

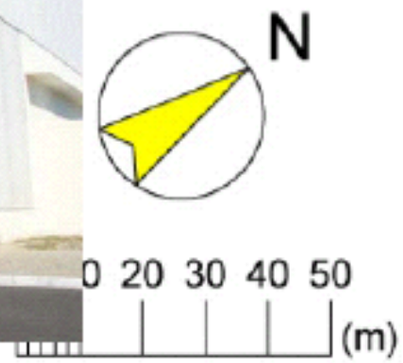

Hadron Hall

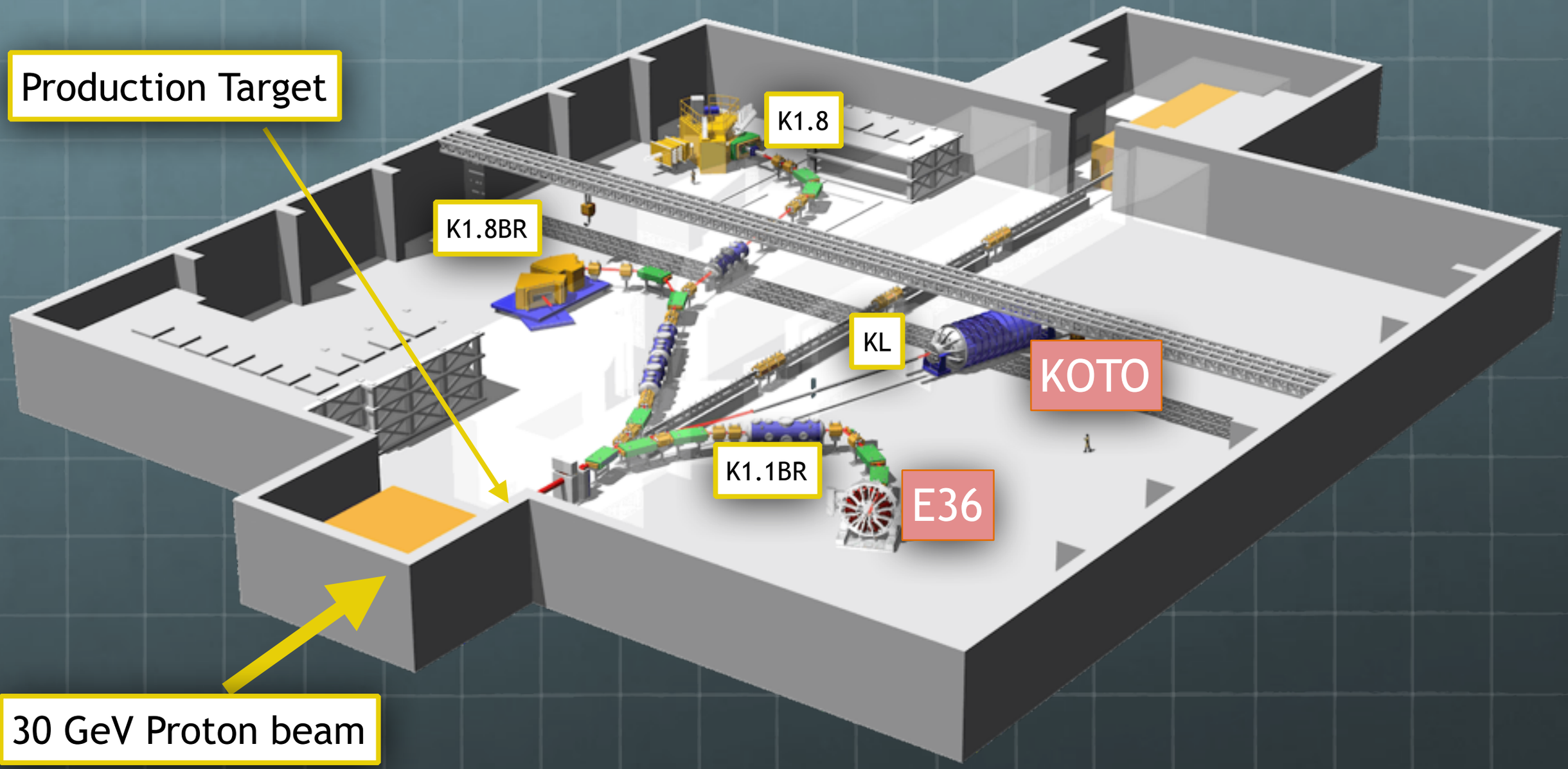
Production Target
K1.8
K1.8BR
KL
KOTO
K1.1BR
E36
30 GeV Proton beam

Hadron Hall after 2017

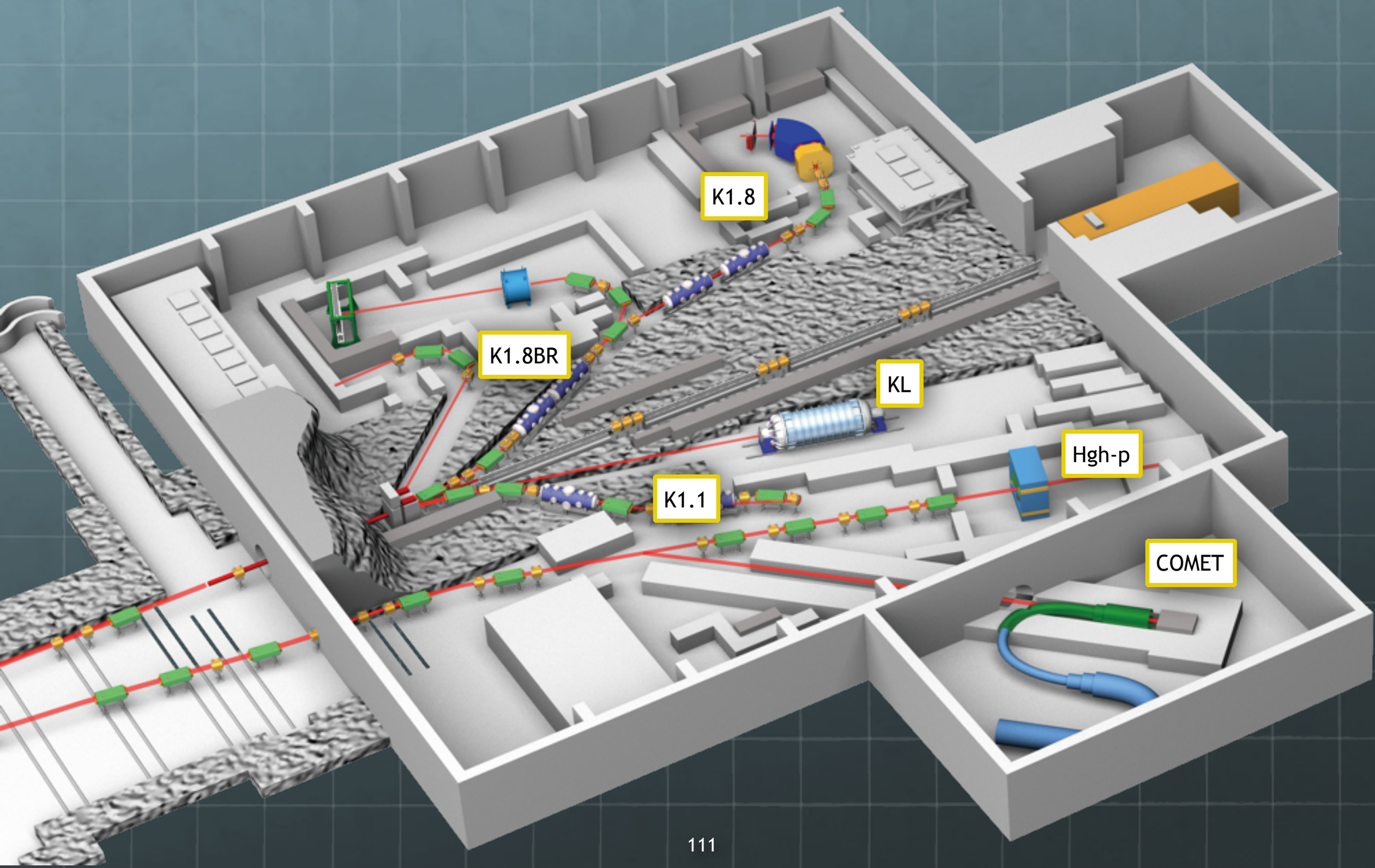

Searching for the $K_L \to \pi^0 \nu\bar{\nu}$ *decay*

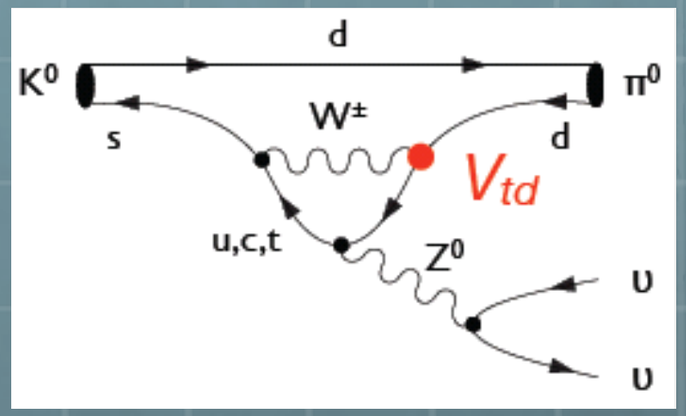

K0 at TOkai

Search for new physics

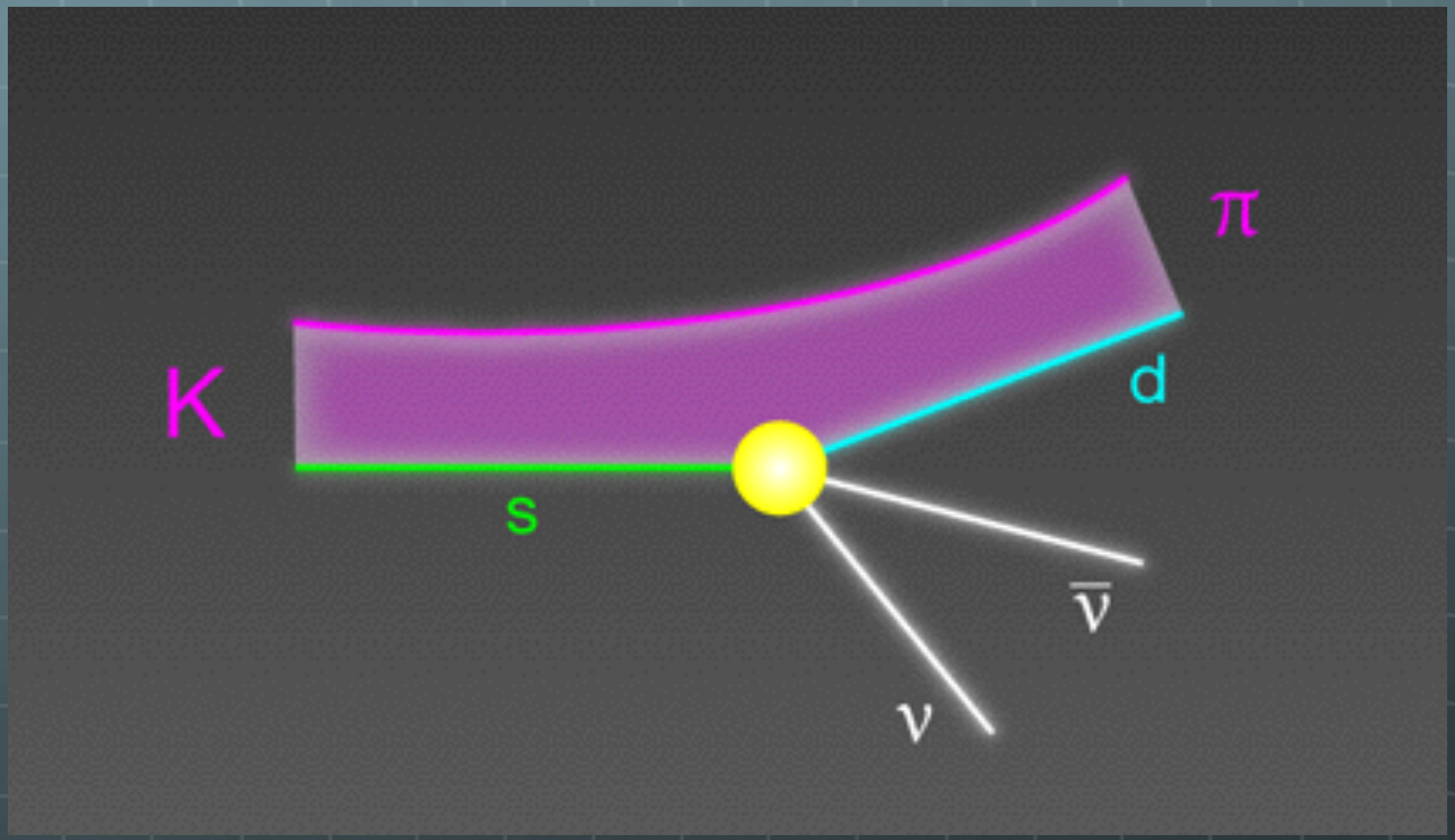

Rare precess : $\Delta t \cdot \Delta E \sim \hbar$

Studies on kaon decays
- Cornerstone of the SM -

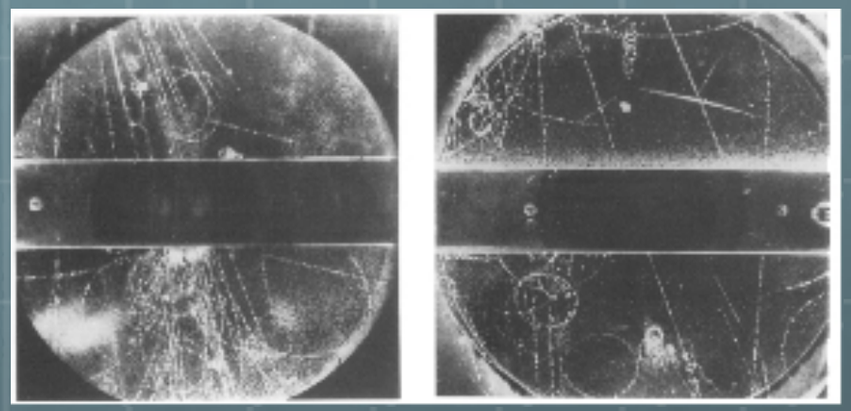

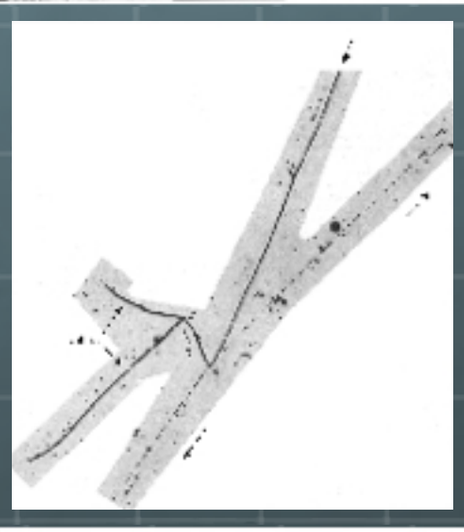

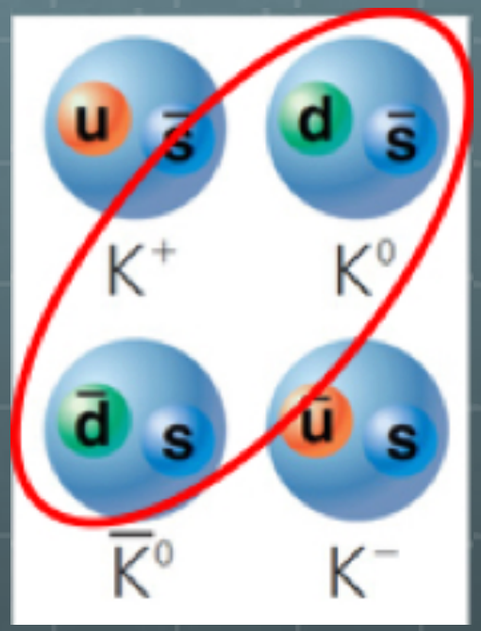

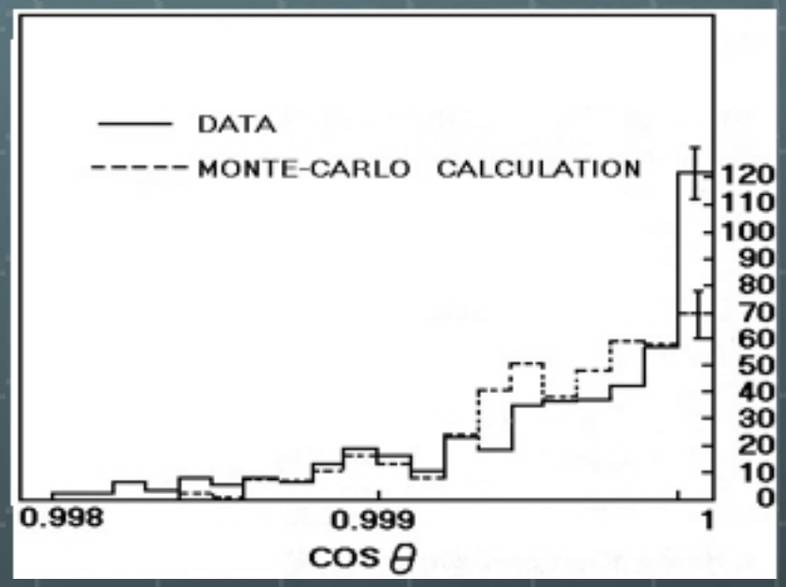

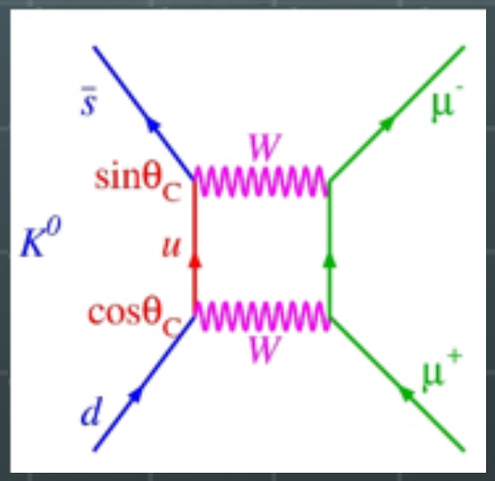

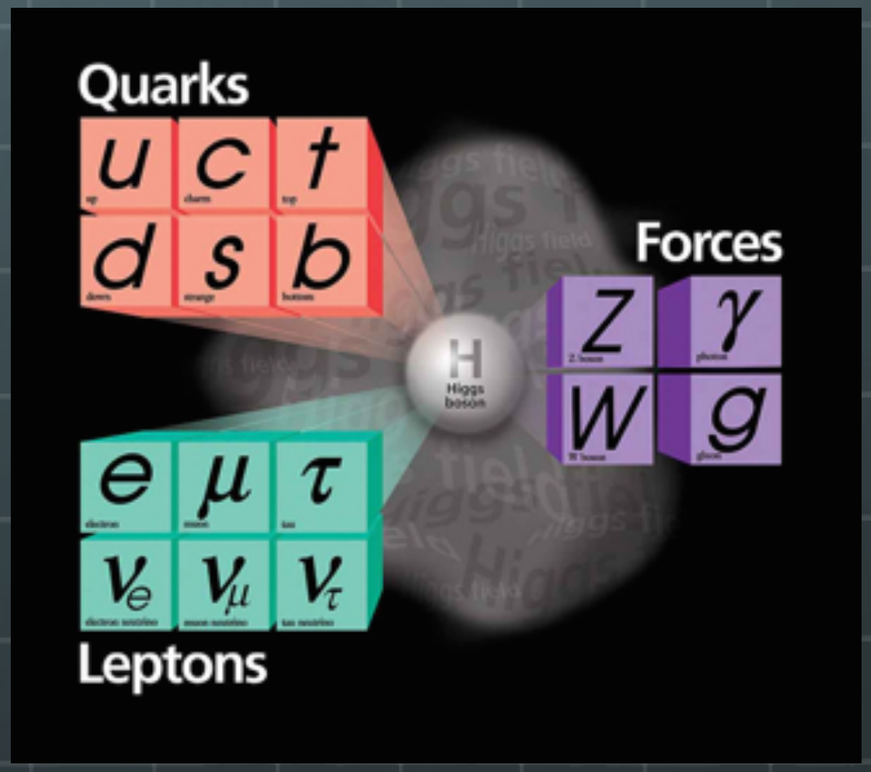

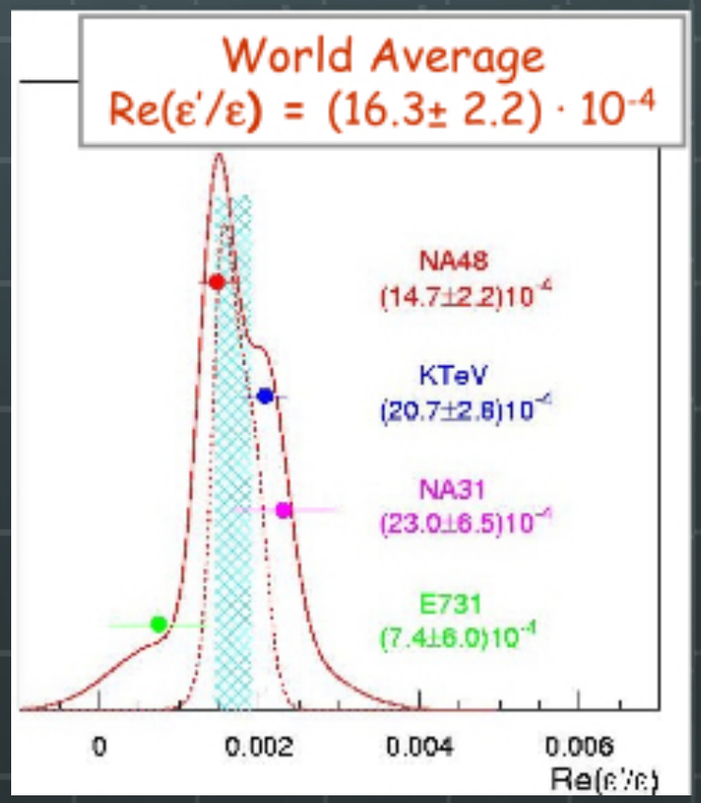

perhaps new world(s) of SM replicas

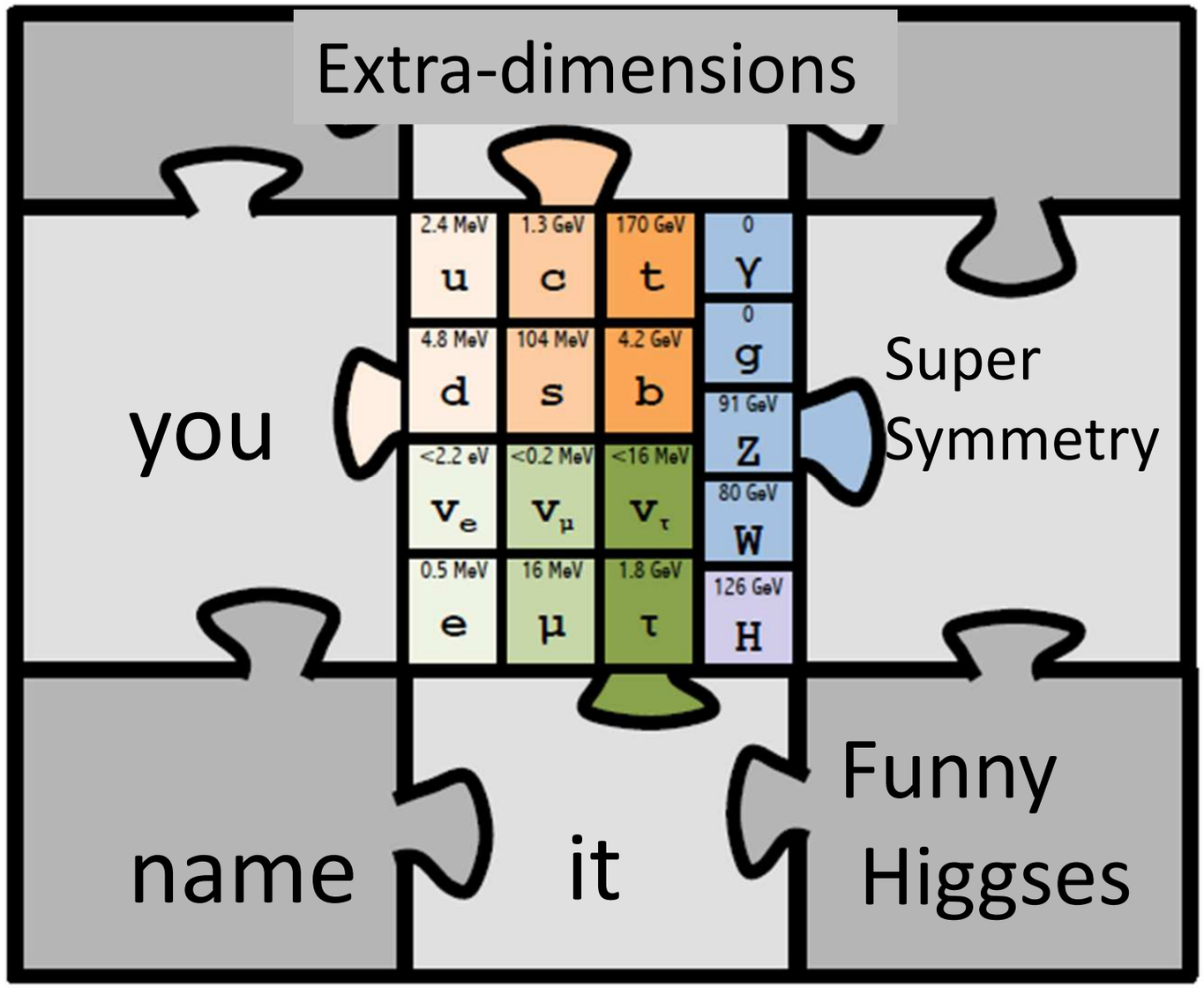

Typically supersymmetry, same couplings as the Standard Model
Can generate $\mu \rightarrow e\gamma$ $Z \rightarrow \mu\tau$ anomalies in CKM measurements, etc. etc…
Dark Matter and BAU. High intensity and luminosity:
Many parameters but must be protected otherwise Higgs mass goes to infinity

Searching for $K_L \to \pi^0 \nu\bar{\nu}$ Decay

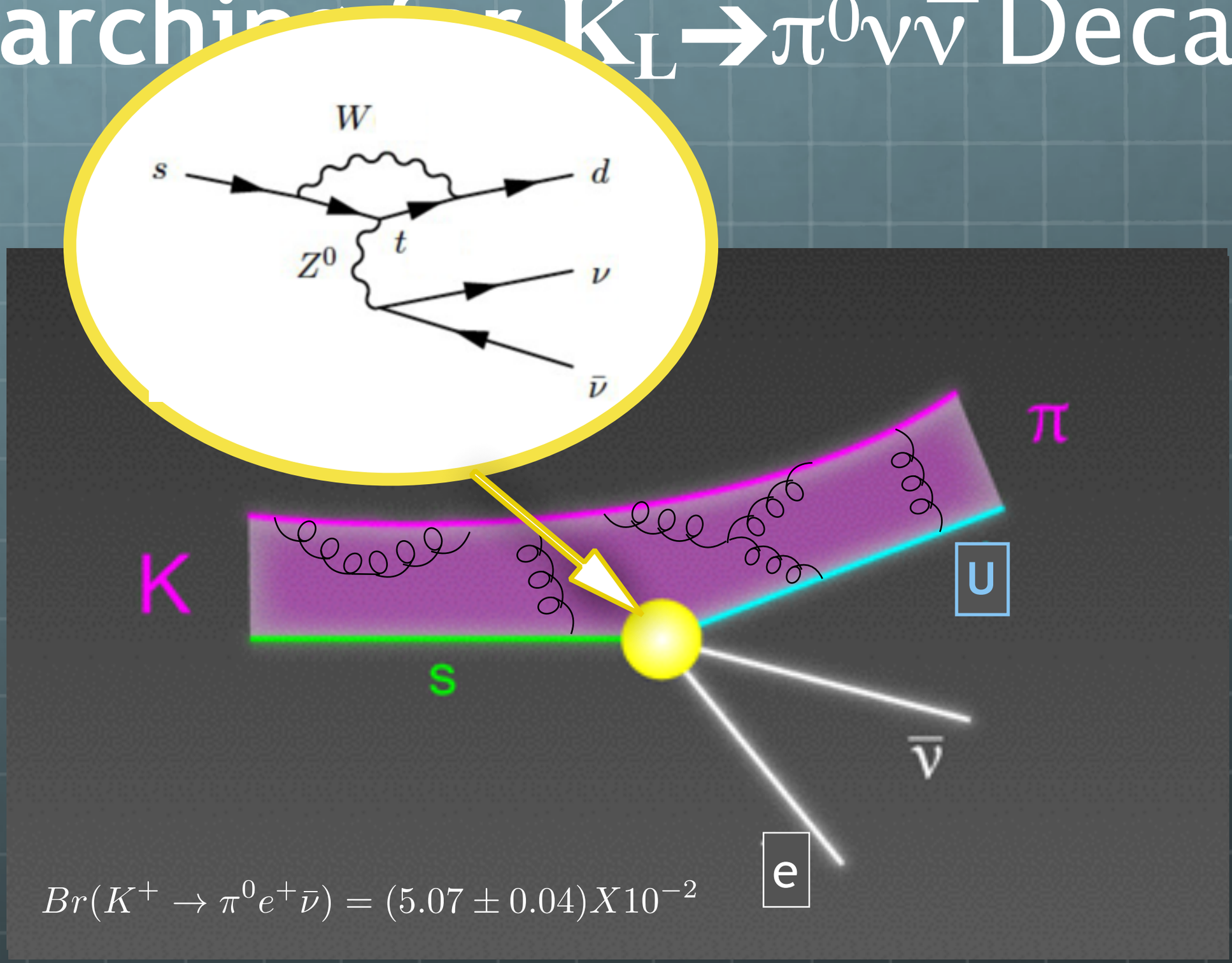

The most suppressed FCNC

$$\underbrace{|V_{ts}^* V_{td}|}_{K \text{ system}} \sim 5 \cdot 10^{-4} \ll \underbrace{|V_{tb}^* V_{td}|}_{B_d \text{ system}} \sim 10^{-2} < \underbrace{|V_{tb}^* V_{ts}|}_{B_s \text{ system}} \sim 4 \cdot 10^{-2},$$

The largest deviations from the SM prediction in Kaon sector.

LHT : Littlest Higgs model with T-parity

RSc : Randall-Sundrum model

LR : General left-right model

M. Blanke, arXiv:1305.5671v1

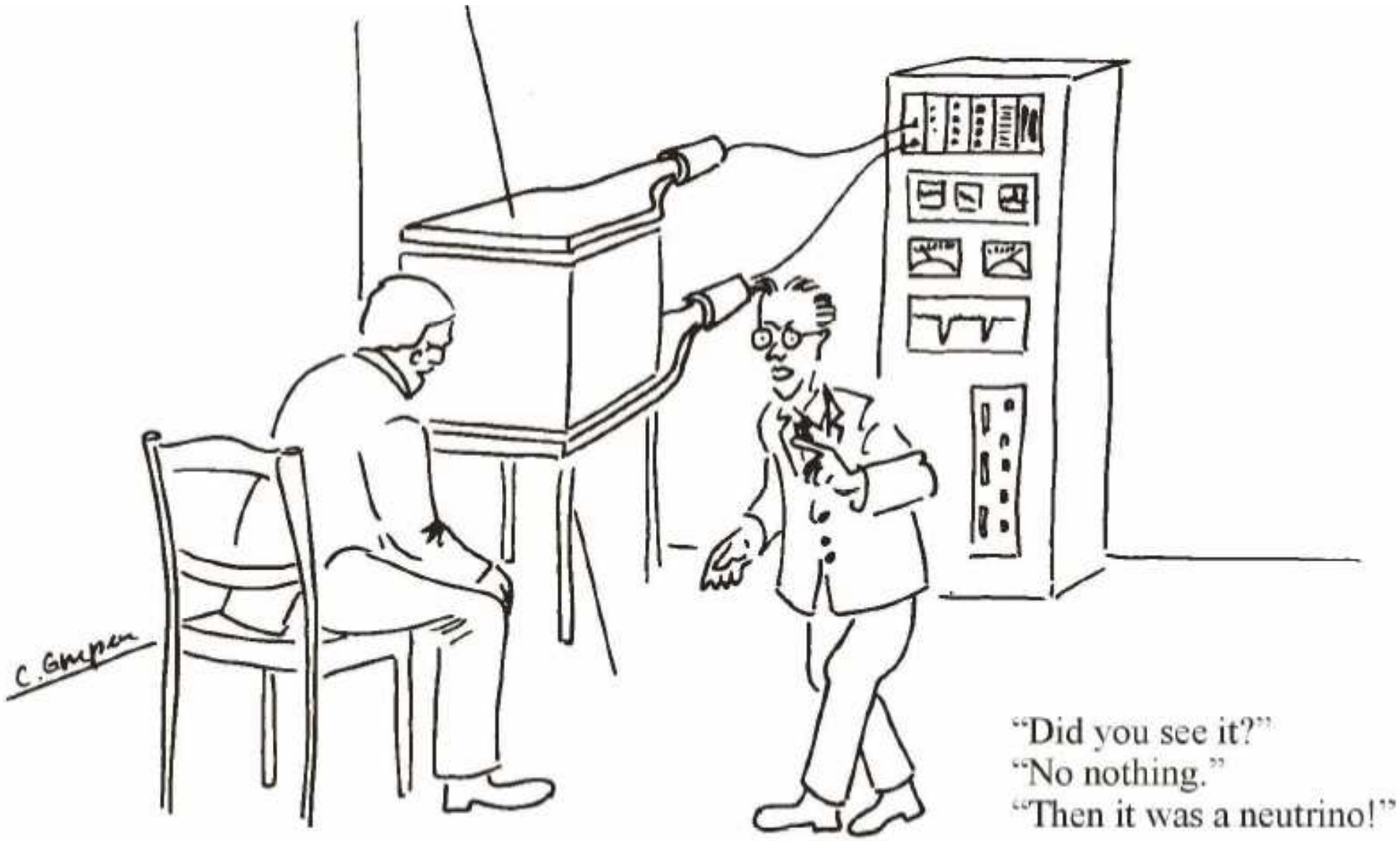

I.Dumanoglu,Calorimeters in HEP,
Bodrum Accelerator School 2006

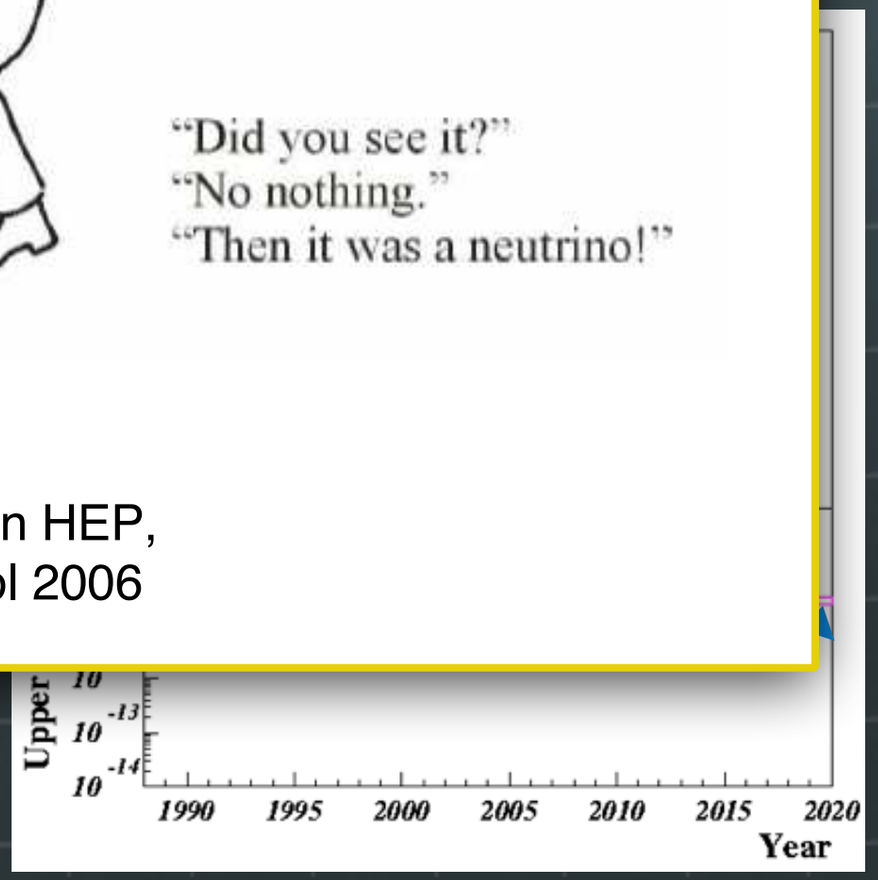

Experimental Method

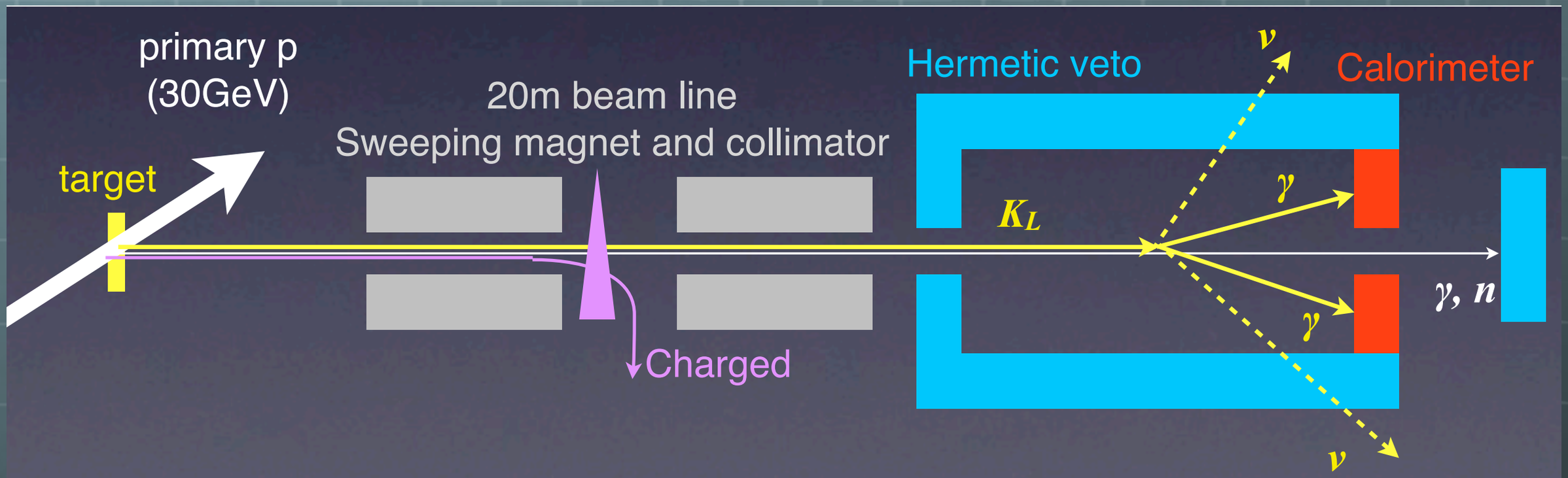

2γ+ Nothing

List of KL decay modes

K^0_L DECAY MODES		Fraction (Γ_i/Γ)	Scale factor/ Confidence level	p (MeV/c)
Semileptonic modes				
$\pi^\pm e^\mp \nu_e$ Called K^0_{e3}.	[p]	(40.55 ±0.11) %	S=1.7	229
$\pi^\pm \mu^\mp \nu_\mu$ Called $K^0_{\mu 3}$.	[p]	(27.04 ±0.07) %	S=1.1	216
$(\pi\mu\text{atom})\nu$		(1.05 ±0.11) × 10^{-7}		188
$\pi^0\pi^\pm e^\mp \nu$	[p]	(5.20 ±0.11) × 10^{-5}		207
$\pi^\pm e^\mp \nu e^+ e^-$	[p]	(1.26 ±0.04) × 10^{-5}		229
Hadronic modes, including Charge conjugation×Parity Violating (*CPV*) modes				
$3\pi^0$		(19.52 ±0.12) %	S=1.6	139
$\pi^+\pi^-\pi^0$		(12.54 ±0.05) %		133
$\pi^+\pi^-$	*CPV* [r]	(1.967±0.010) × 10^{-3}	S=1.5	206
$\pi^0\pi^0$	*CPV*	(8.64 ±0.06) × 10^{-4}	S=1.8	209
Semileptonic modes with photons				
$\pi^\pm e^\mp \nu_e \gamma$	[g,p,s]	(3.79 ±0.06) × 10^{-3}		229
$\pi^\pm \mu^\mp \nu_\mu \gamma$		(5.65 ±0.23) × 10^{-4}		216
Hadronic modes with photons or $\ell\bar{\ell}$ pairs				
$\pi^0\pi^0\gamma$		< 2.43 × 10^{-7}	CL=90%	209
$\pi^+\pi^-\gamma$	[g,s]	(4.15 ±0.15) × 10^{-5}	S=2.8	206
$\pi^+\pi^-\gamma$(DE)		(2.84 ±0.11) × 10^{-5}	S=2.0	206
$\pi^0 2\gamma$	[s]	(1.273±0.033) × 10^{-6}		230
$\pi^0\gamma e^+ e^-$		(1.62 ±0.17) × 10^{-8}		230

Other modes with photons or $\ell\bar{\ell}$ pairs				
2γ		(5.47 ±0.04) × 10^{-4}	S=1.1	249
3γ		< 7.4 × 10^{-8}	CL=90%	249
$e^+ e^-\gamma$		(9.4 ±0.4) × 10^{-6}	S=2.0	249
$\mu^+\mu^-\gamma$		(3.59 ±0.11) × 10^{-7}	S=1.3	225
$e^+ e^-\gamma\gamma$	[s]	(5.95 ±0.33) × 10^{-7}		249
$\mu^+\mu^-\gamma\gamma$	[s]	(1.0 $^{+0.8}_{-0.6}$) × 10^{-8}		225
Charge conjugation × Parity (*CP*) or Lepton Family number (*LF*) violating modes, or $\Delta S = 1$ weak neutral current (*S1*) modes				
$\mu^+\mu^-$	*S1*	(6.84 ±0.11) × 10^{-9}		
$e^+ e^-$	*S1*	(9 $^{+6}_{-4}$) × 10^{-12}		
$\pi^+\pi^- e^+ e^-$	*S1* [r]	(3.11 ±0.19) × 10^{-7}		
$\pi^0\pi^0 e^+ e^-$	*S1*	< 6.6 × 10^{-9}		
$\pi^0\pi^0\mu^+\mu^-$	*S1*	< 9.2 × 10^{-11}		
$\mu^+\mu^- e^+ e^-$	*S1*	(2.69 ±0.27) × 10^{-9}		
$e^+ e^- e^+ e^-$	*S1*	(3.56 ±0.21) × 10^{-8}		
$\pi^0\mu^+\mu^-$	*CP,S1* [s]	< 3.8 × 10^{-10}		
$\pi^0 e^+ e^-$	*CP,S1* [s]	< 2.8 × 10^{-10}		
$\pi^0\nu\bar{\nu}$	*CP,S1* [t]	< 2.6 × 10^{-8}		
$\pi^0\pi^0\nu\bar{\nu}$	*S1*	< 8.1 × 10^{-7}		
$e^\pm\mu^\mp$	*LF* [o]	< 4.7 × 10^{-12}		
$e^\pm e^\pm\mu^\mp\mu^\mp$	*LF* [o]	< 4.12 × 10^{-11}		
$\pi^0\mu^\pm e^\mp$	*LF* [o]	< 7.6 × 10^{-11}		
$\pi^0\pi^0\mu^\pm e^\mp$	*LF*	< 1.7 × 10^{-10}		

$K_L \rightarrow \pi^0 \pi^0$ Background ?

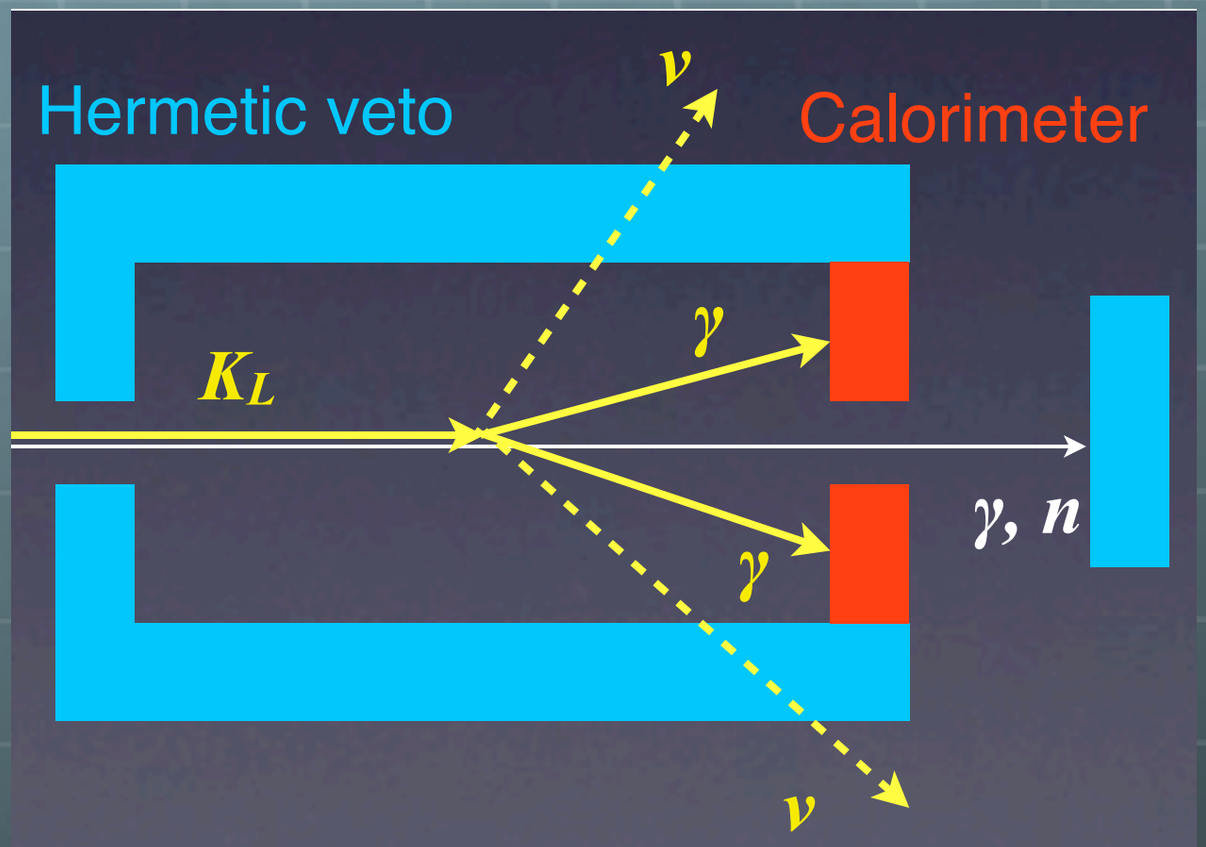

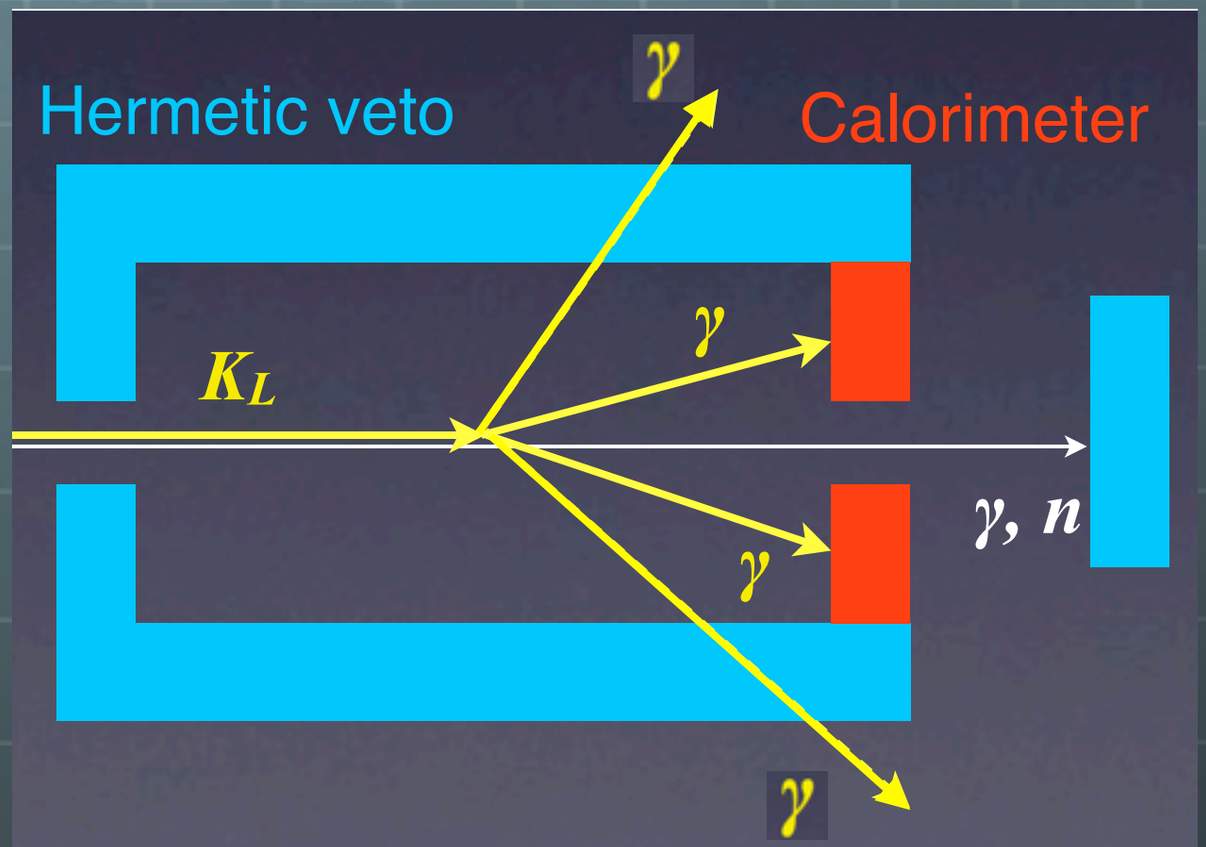

- When we miss 2 gammas among 4 gammas generated at the $K_L \rightarrow \pi^0 \pi^0$ decay.
- $Br(K_L \rightarrow \pi^0 \pi^0)/Br(K_L \rightarrow \pi^0 \nu\bar{\nu}) = 2.6 \times 10^{7}$
- We have to detect gamma with inefficiency less than 10^{-4}

Why we miss the gamma ?

- Punch-through

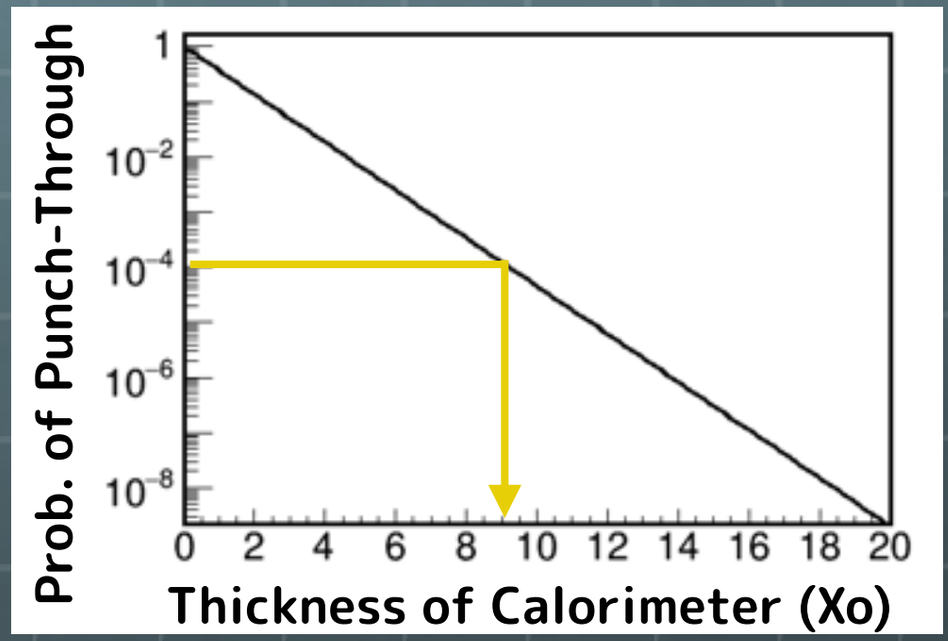

Detailed study using M.C.

- Photo-nuclear

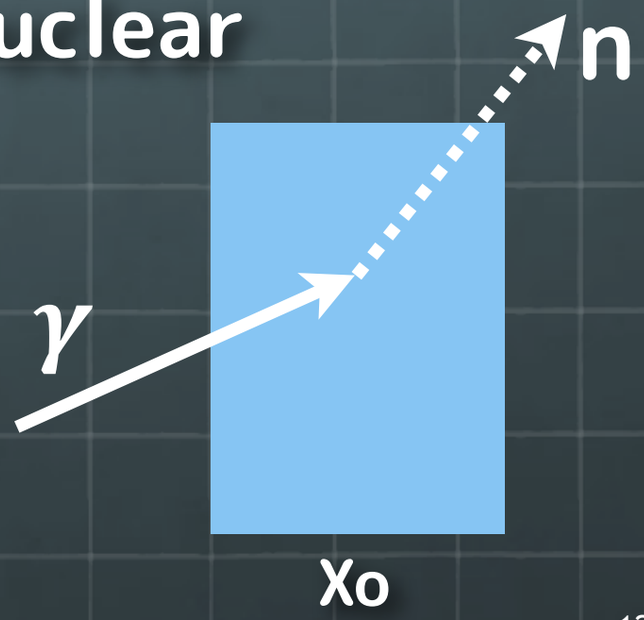

Energy dependent

(GDR and Delta resonate)

Doubtable M.C. calculation

Inefficiency measurement

Electron beam from INS 1.3-GeV ES

Photon tagging system,

32 +8 (backing) counters,

detects recoil electrons after bremsstrahlung.)

Samples were placed behind a shield through active collimation.

Still not so perfect photon-tagging to make a direct measurement of inefficiency. 1~0.1% mis-tagging exists

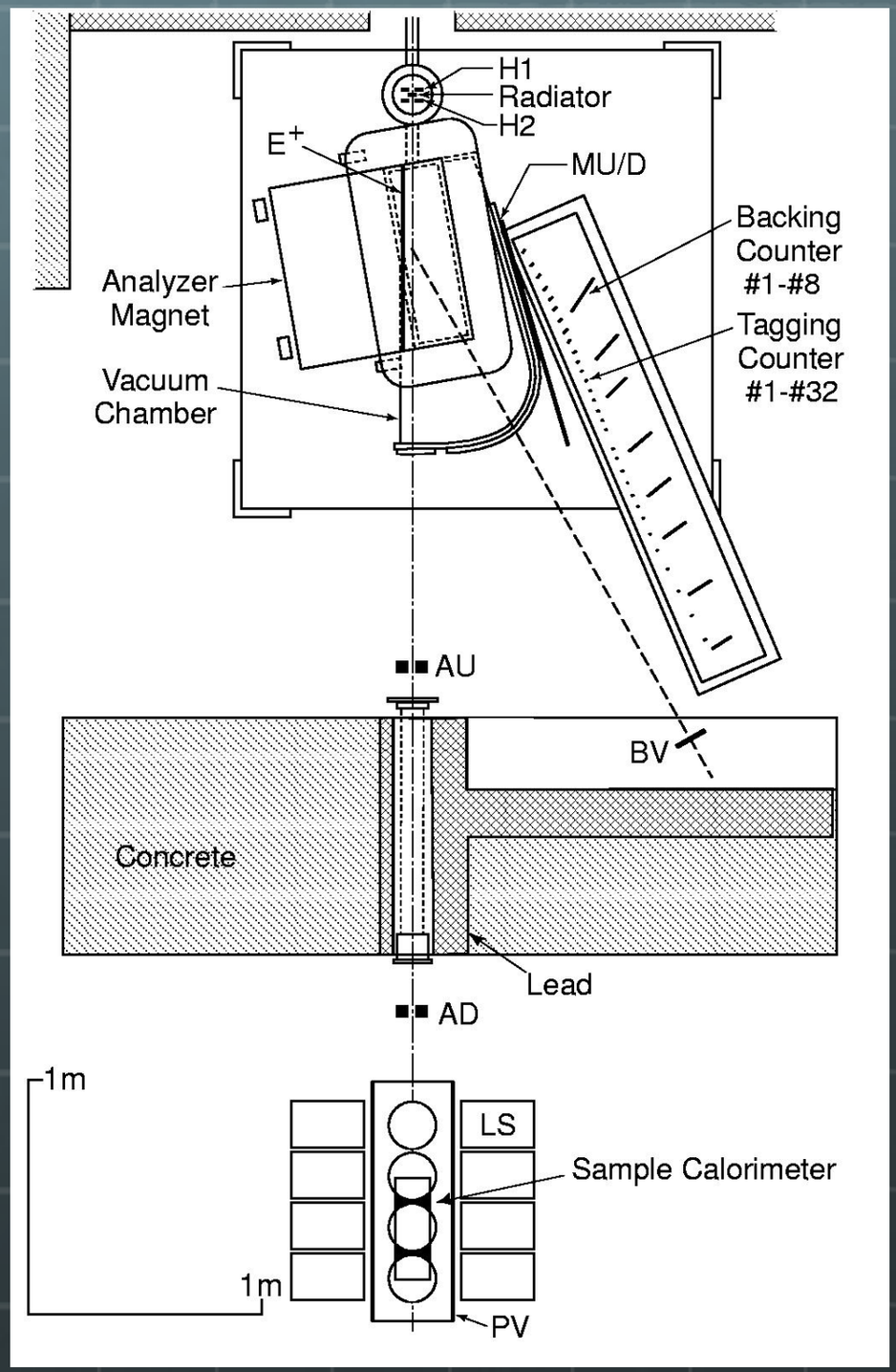

CsI Calorimeter

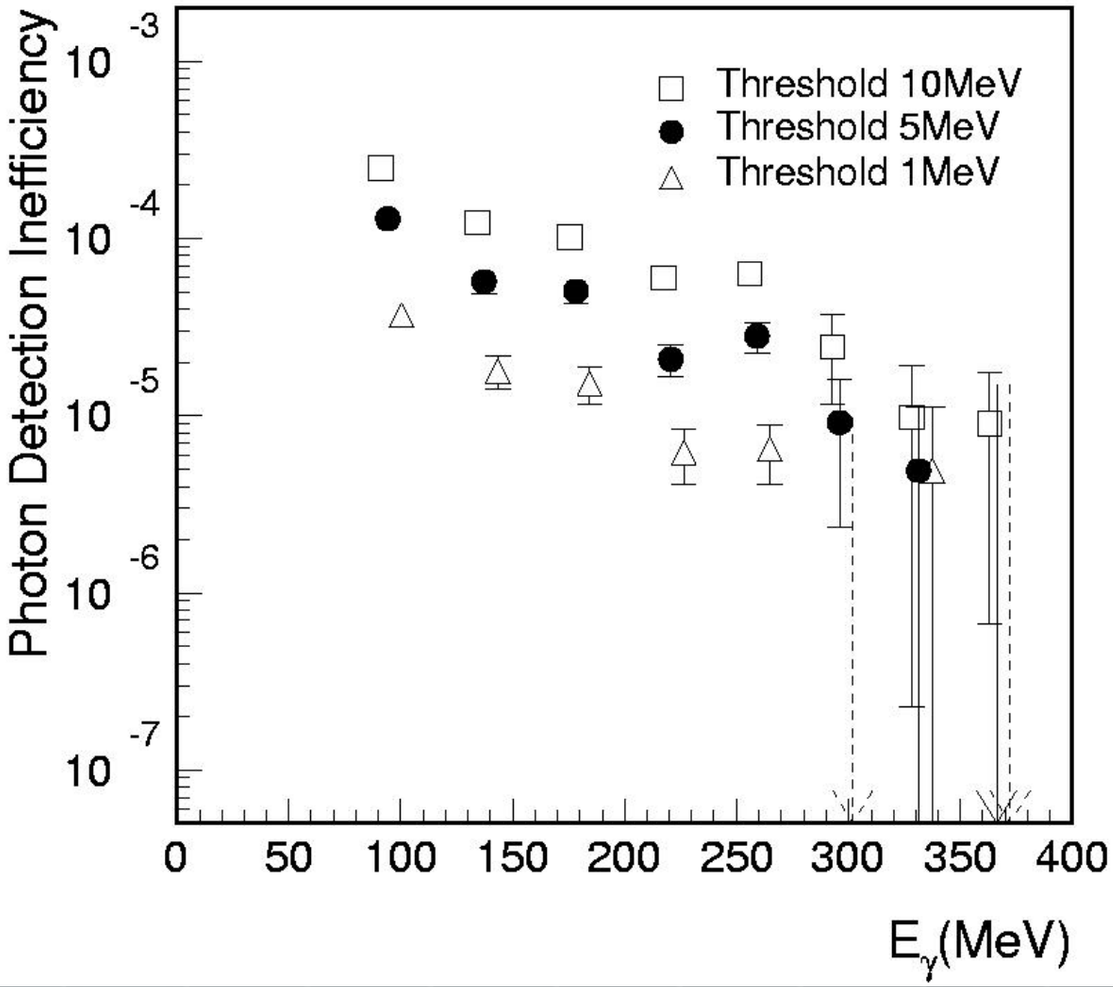

Lead-Scin. Sampling calorimeter

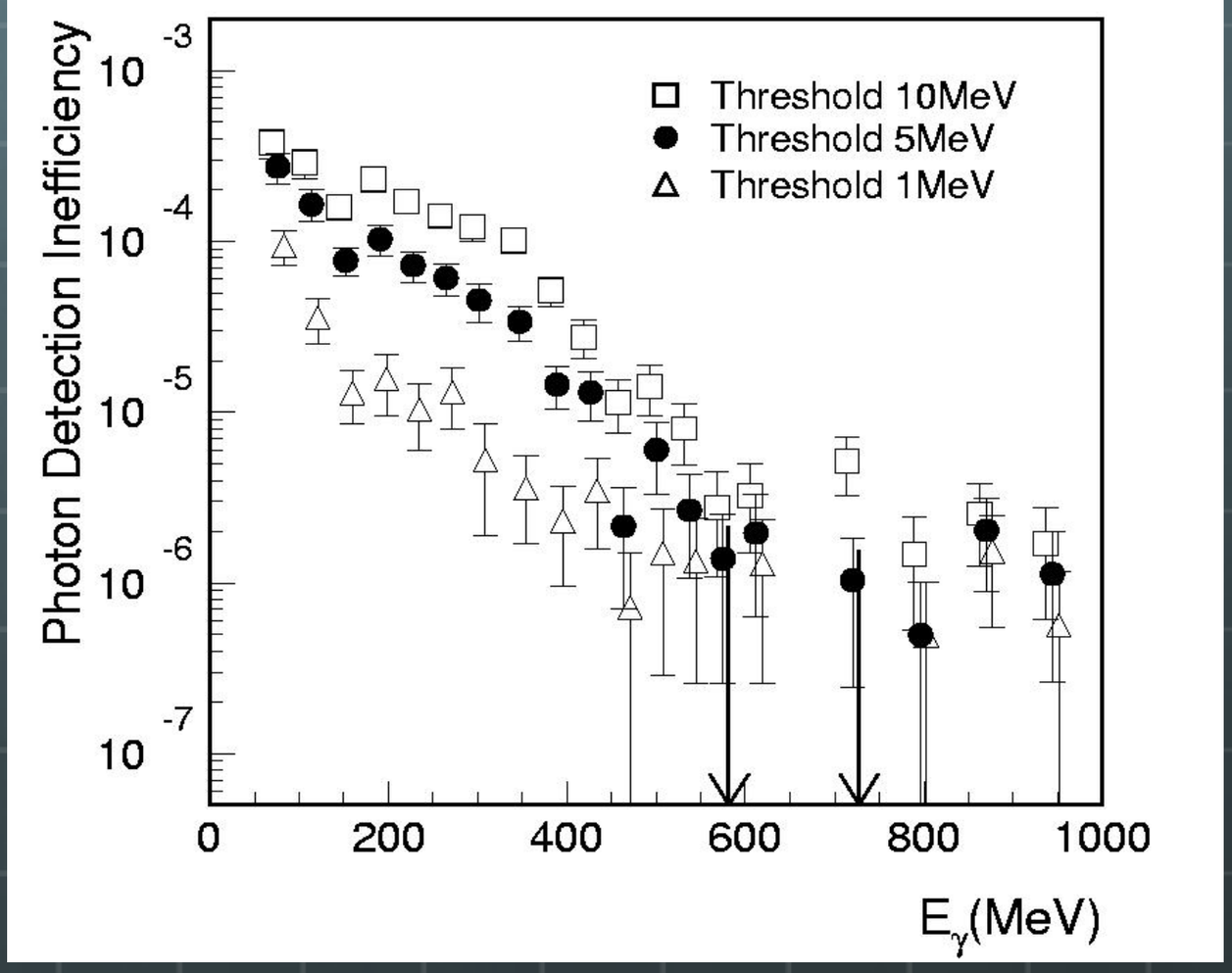

Why we miss the gamma ?

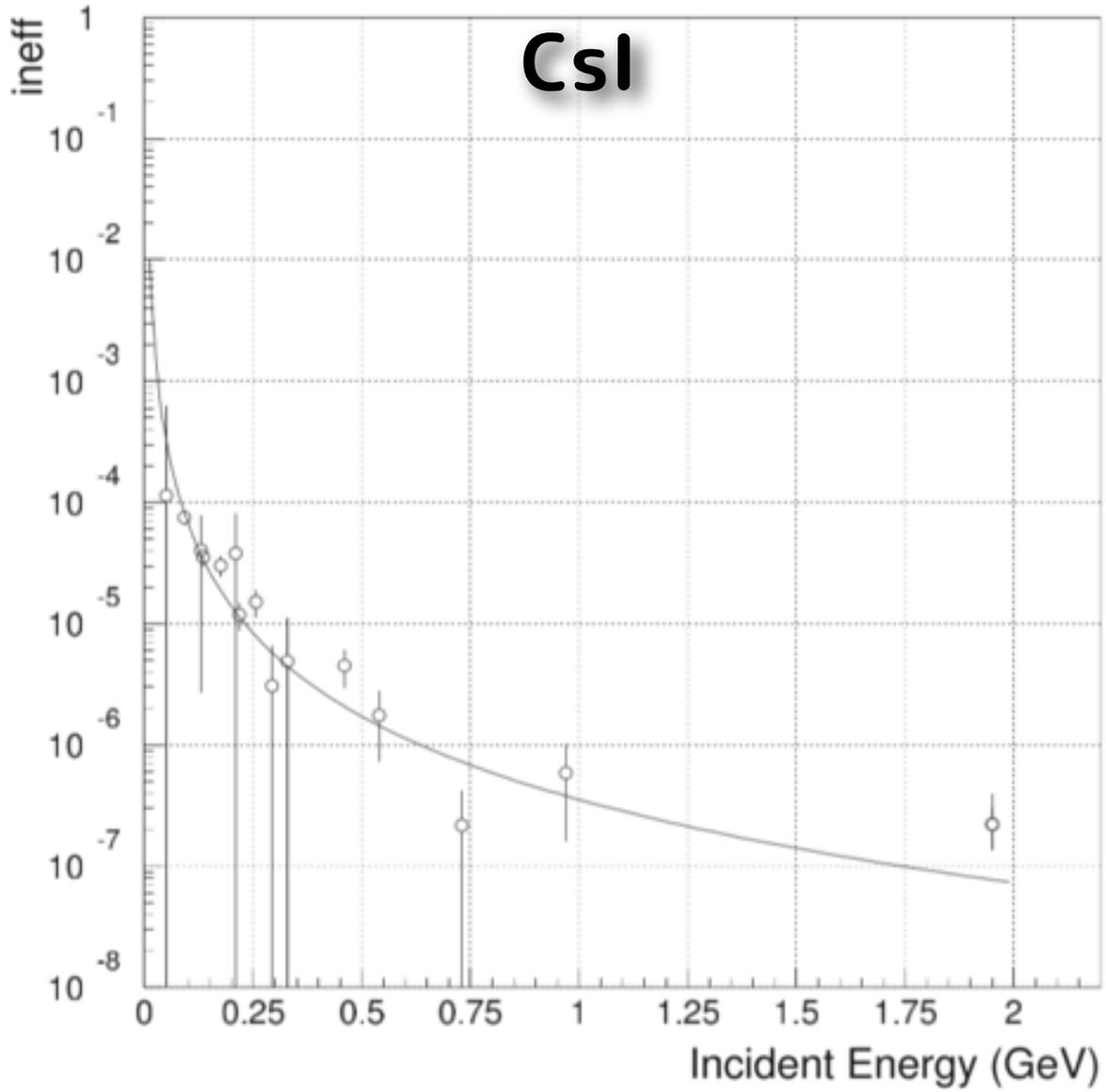

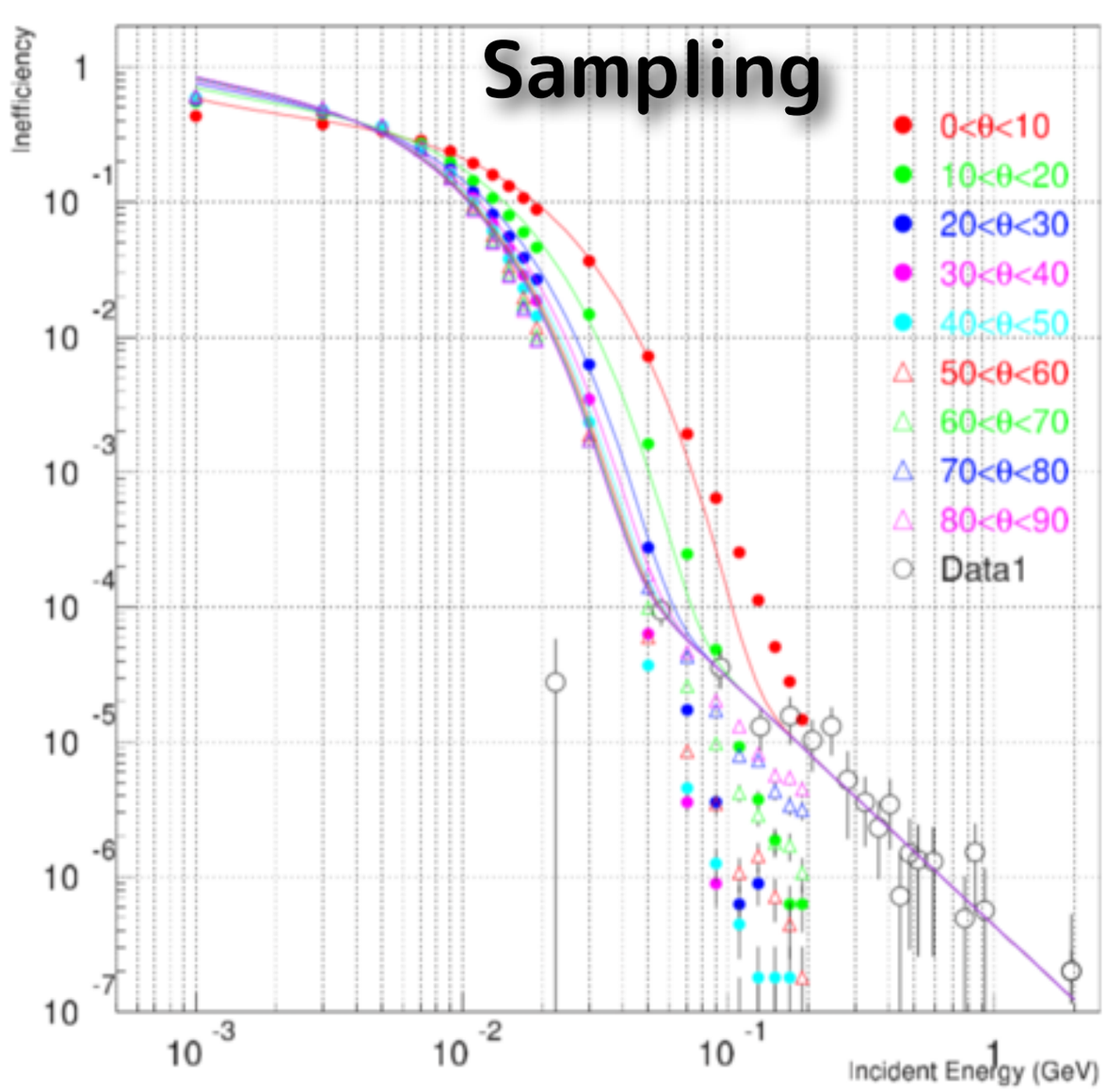

Detector

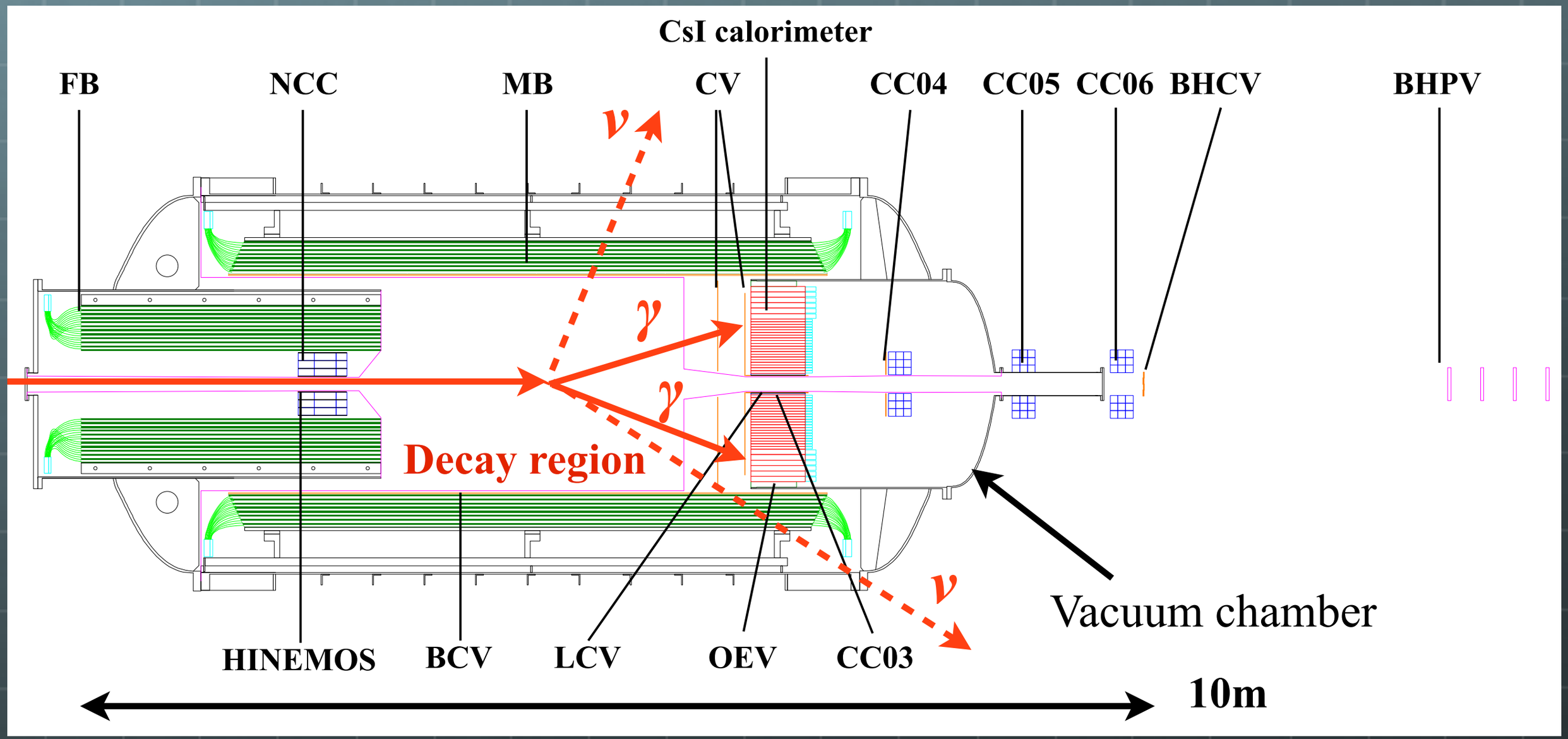
CsI calorimeter
FB
NCC
MB
CV
CC04
CC05
CC06
BHCV
BHPV
ν
γ
γ
Decay region
ν
Vacuum chamber
HINEMOS
BCV
LCV
OEV
CC03
10m

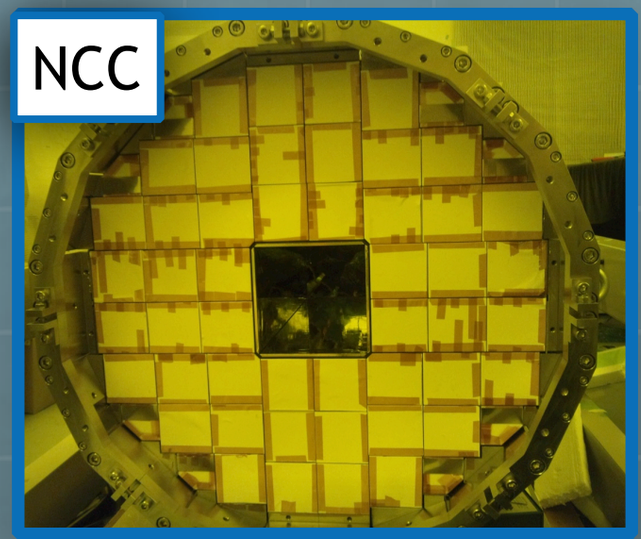
NCC

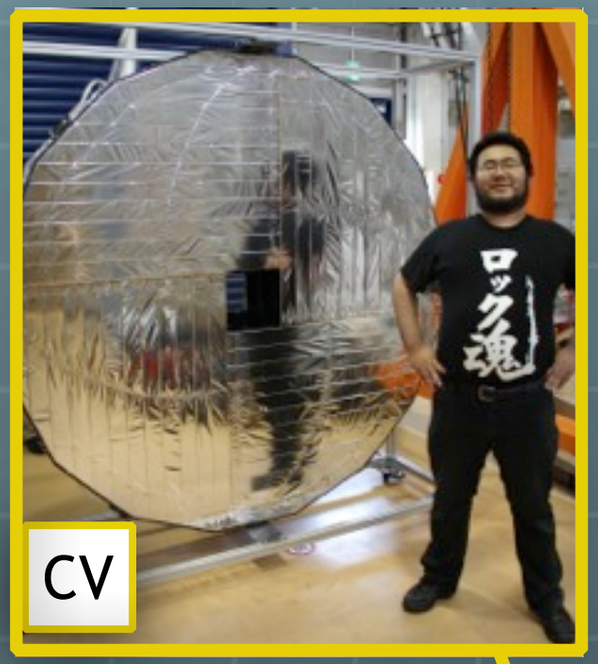
CV


CsI

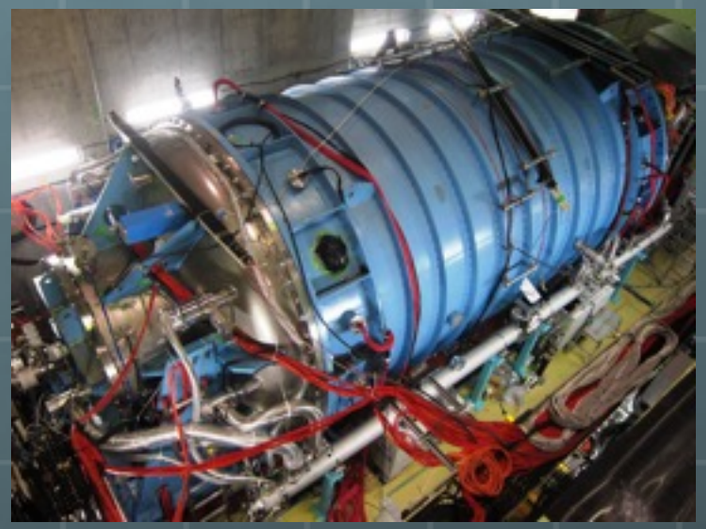

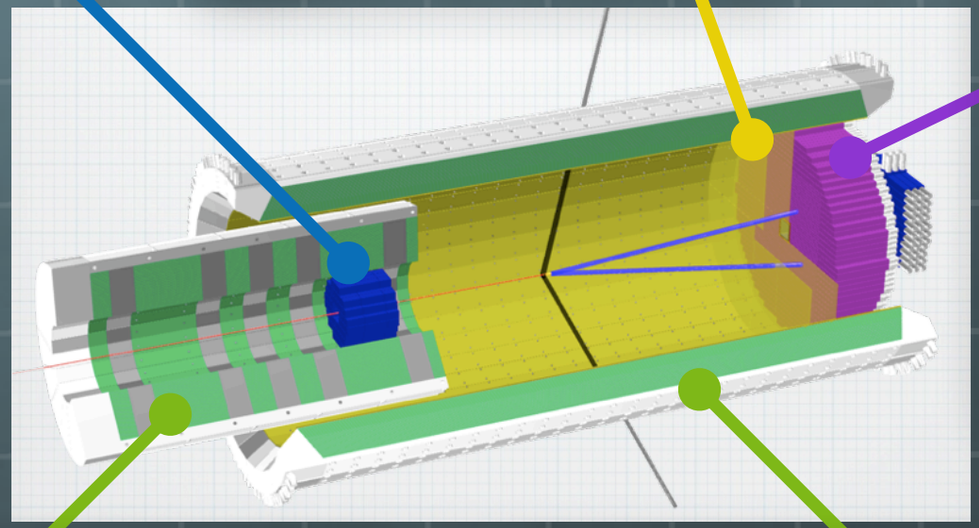


FB


MB

Timeline of KOTO

2009

Beamline construction finished (2009 Aug)

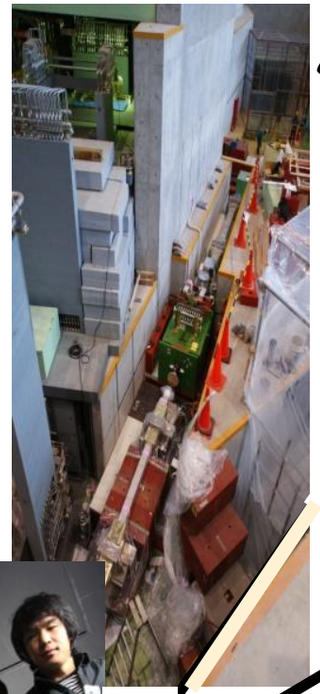

2010

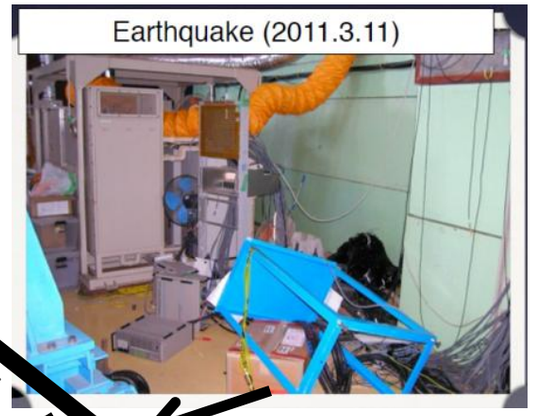

2011

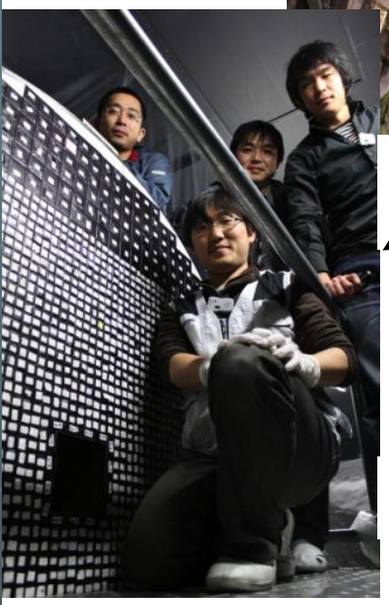

CsI calorimeter stacking finished (2011 Feb)

Charged Veto installation (2012 June)

2012

NCC installation (2012 Nov)

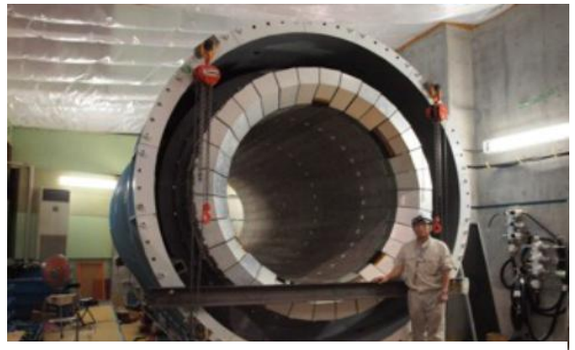

Main Barrel installation (2012 Dec)

Closing vacuum chamber (2012 Dec)

2013

FB installation (2012 Nov)

Sub detectors (CC04 etc.) Installation (2012 Dec)

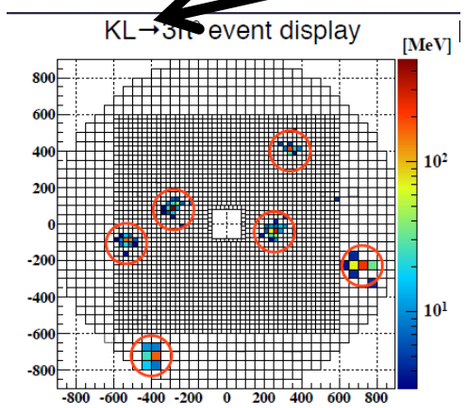

2013 Jan engineering run

2014

1st physics run 2013 May

Detector

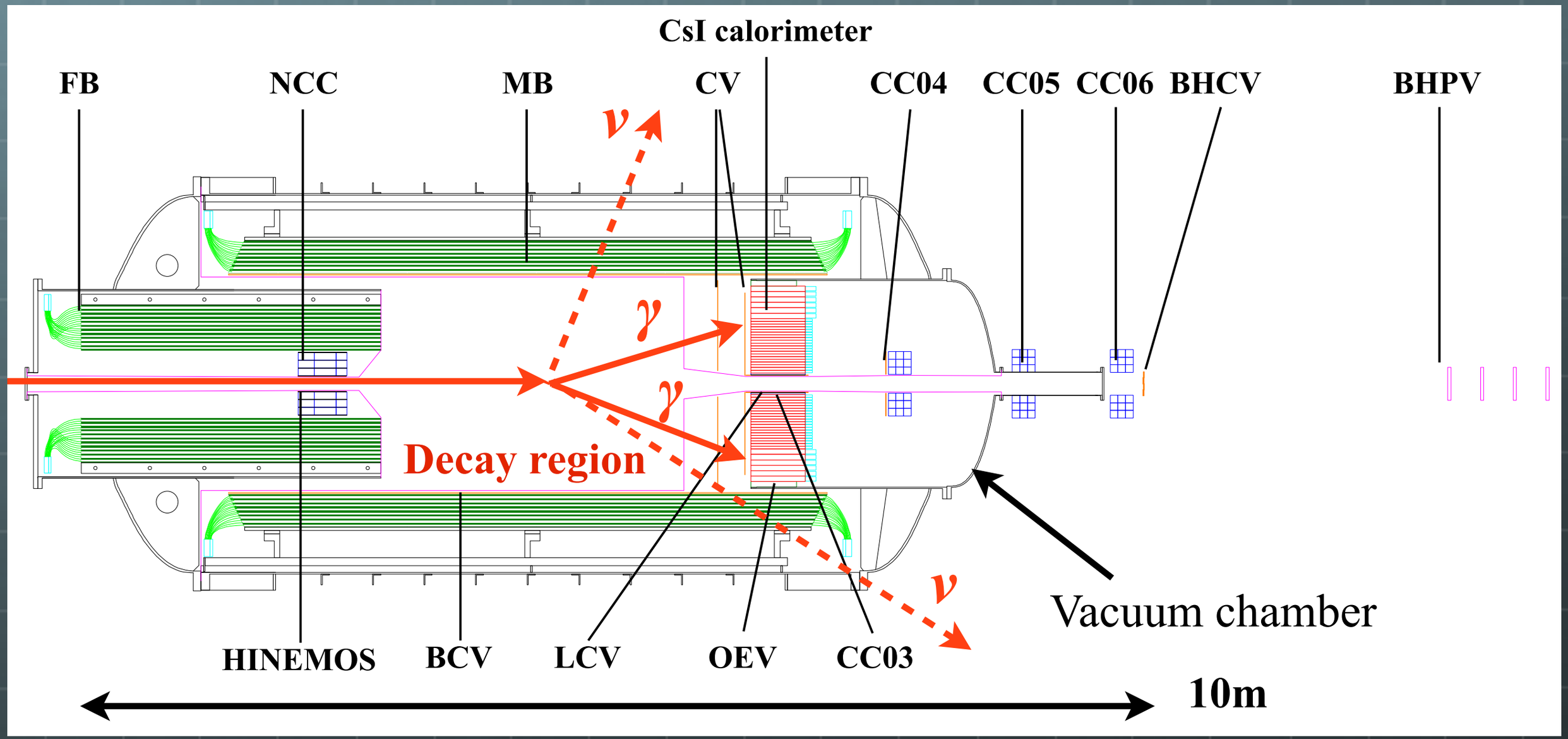
CsI calorimeter
FB
NCC
MB
CV
CC04
CC05
CC06
BHCV
BHPV
ν
γ
γ
Decay region
ν
Vacuum chamber
HINEMOS
BCV
LCV
OEV
CC03
10m

Detector

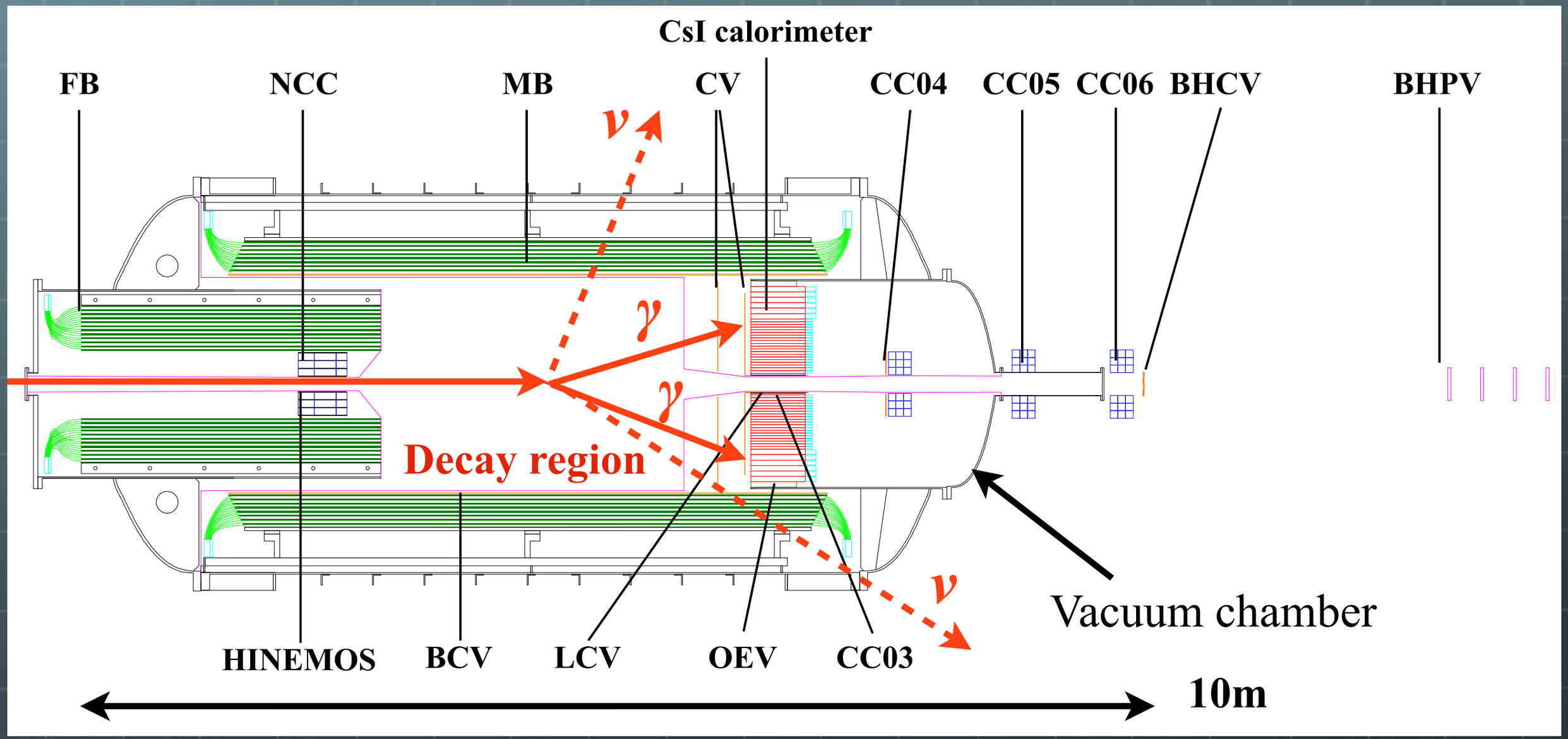
CsI calorimeter
FB
NCC
MB
CV
CC04
CC05
CC06
BHCV
BHPV
ν
γ
γ
Decay region
ν
Vacuum chamber
HINEMOS
BCV
LCV
OEV
CC03
10m

rel

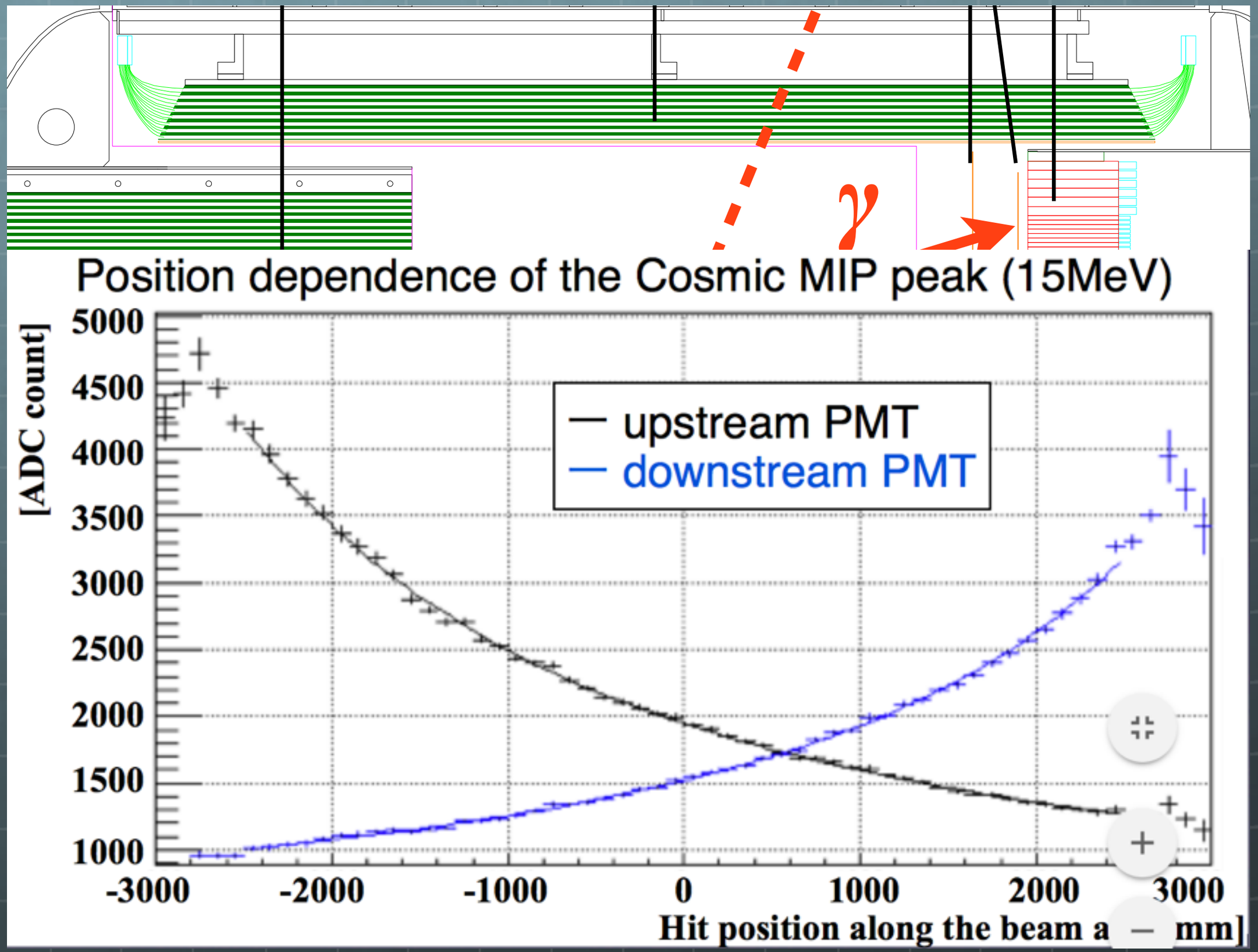
γ
Position dependence of the Cosmic MIP peak (15MeV)
[ADC count]
5000
4500
4000
3500
3000
2500
2000
1500
1000
upstream PMT
downstream PMT
-3000
-2000
-1000
0
1000
2000
3000
Hit position along the beam a mm]

Inner Barrel

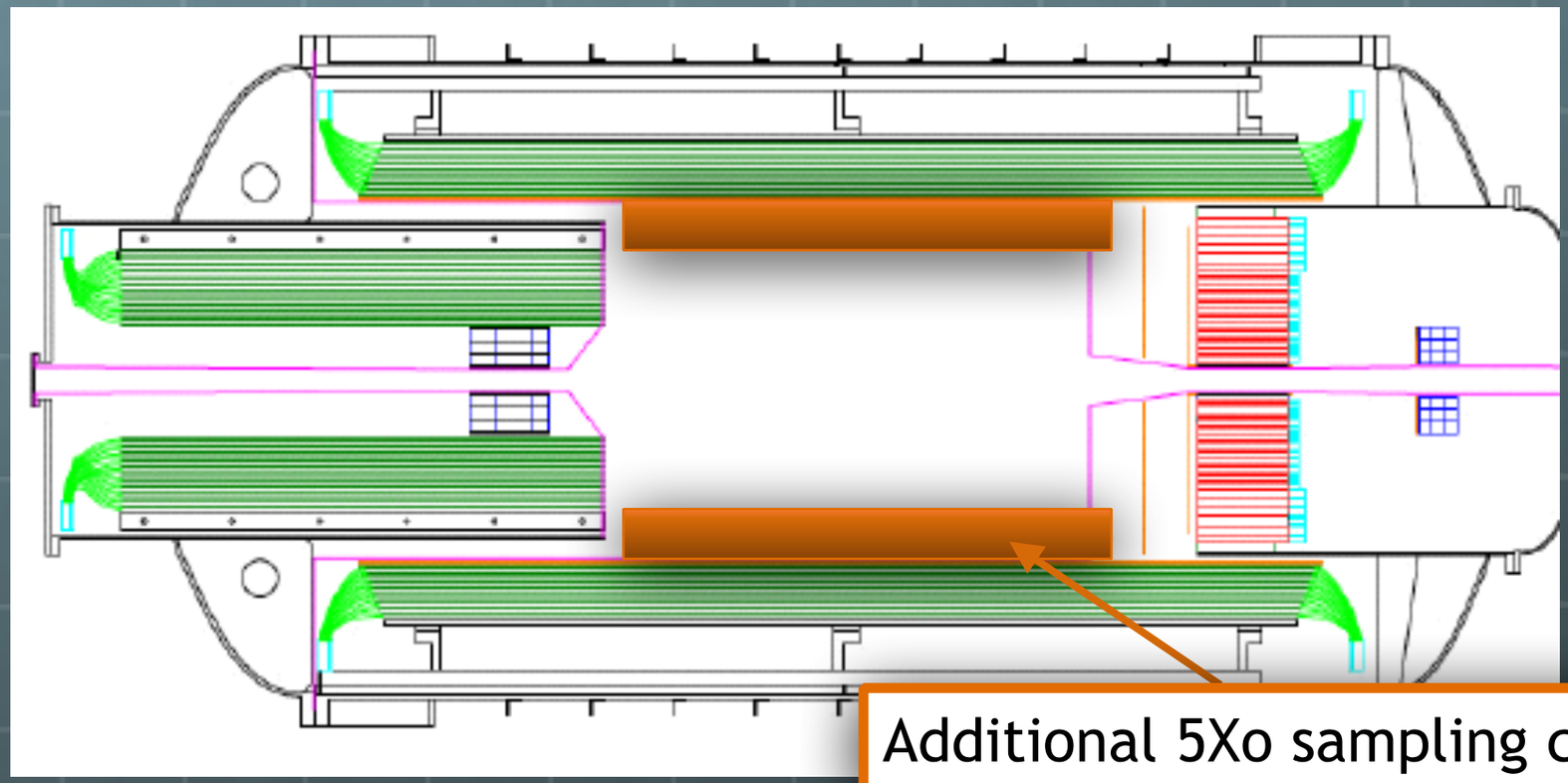

- Additional reduction for detection inefficiency due to punch-through as a factor of 50
- Increase better visible ration portion
- Reduction of Kpi2 background as a factor of three

Glueing Process

1. string WLS fibers

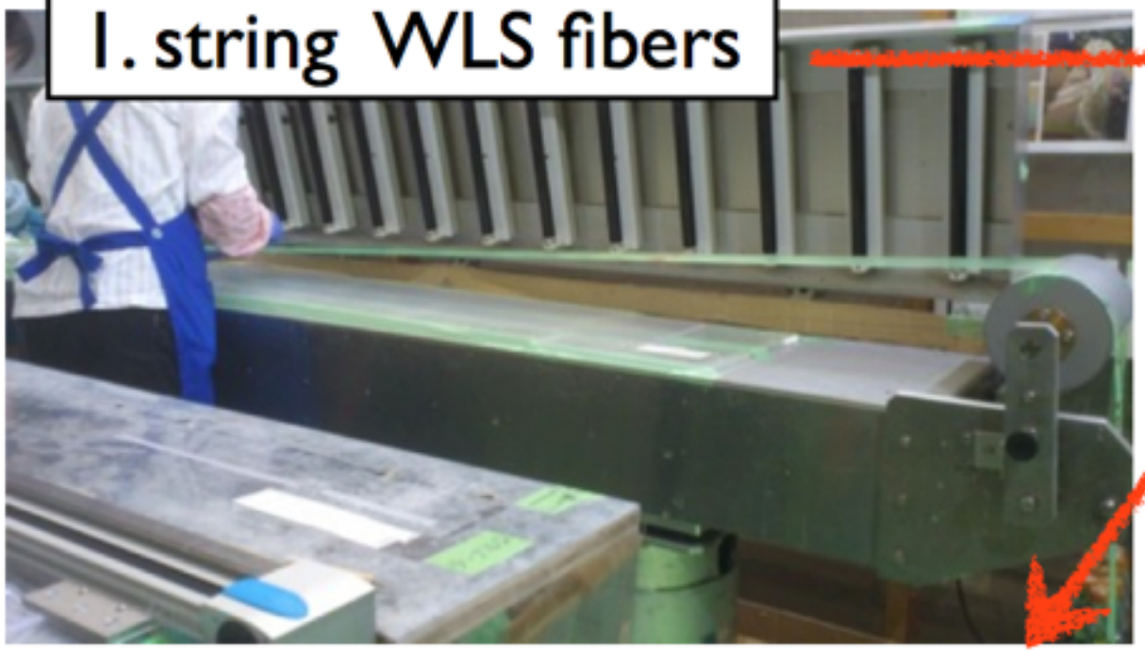

2. inject glue into grooving

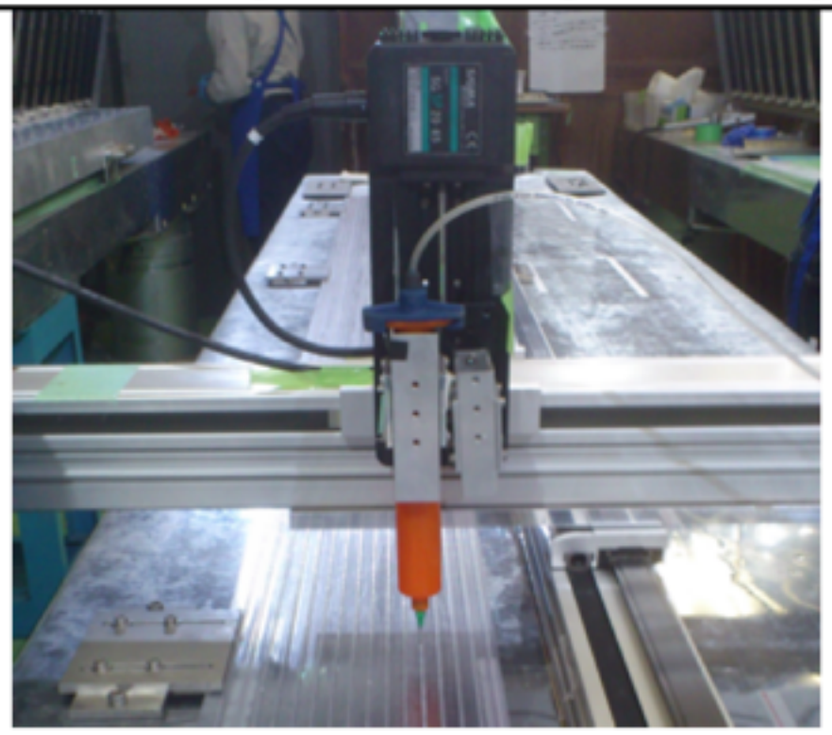

3. set the WLS fibers on the scintillator

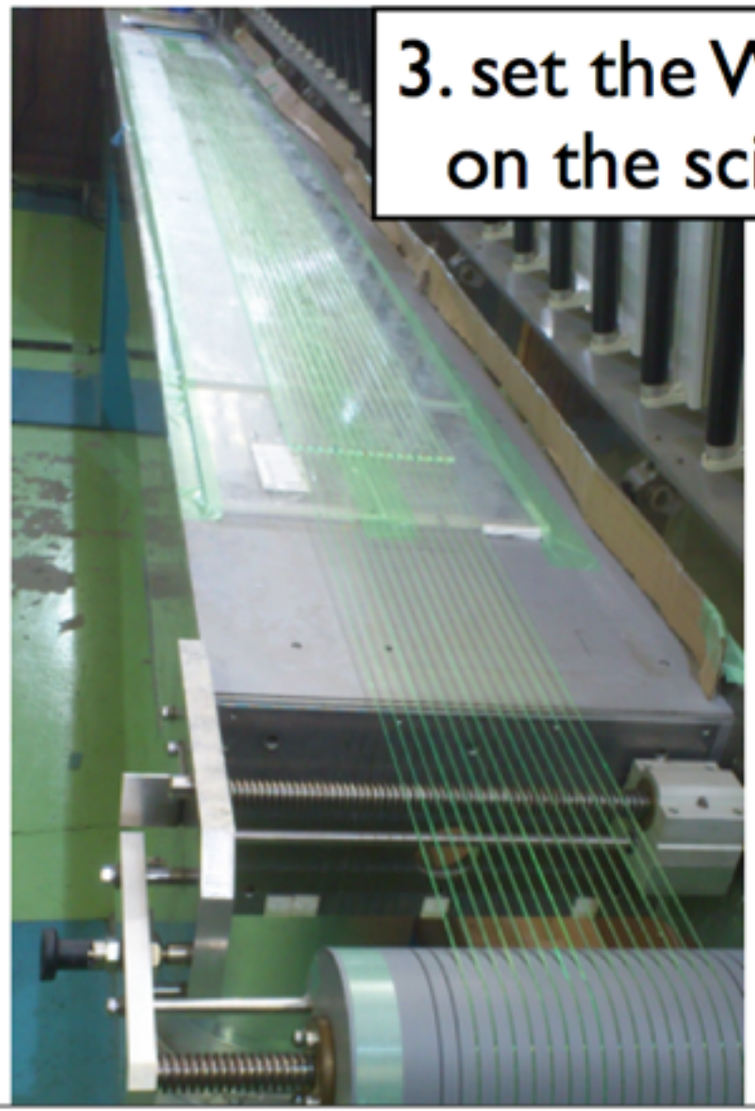

4. irradiate UV light to harden the glue

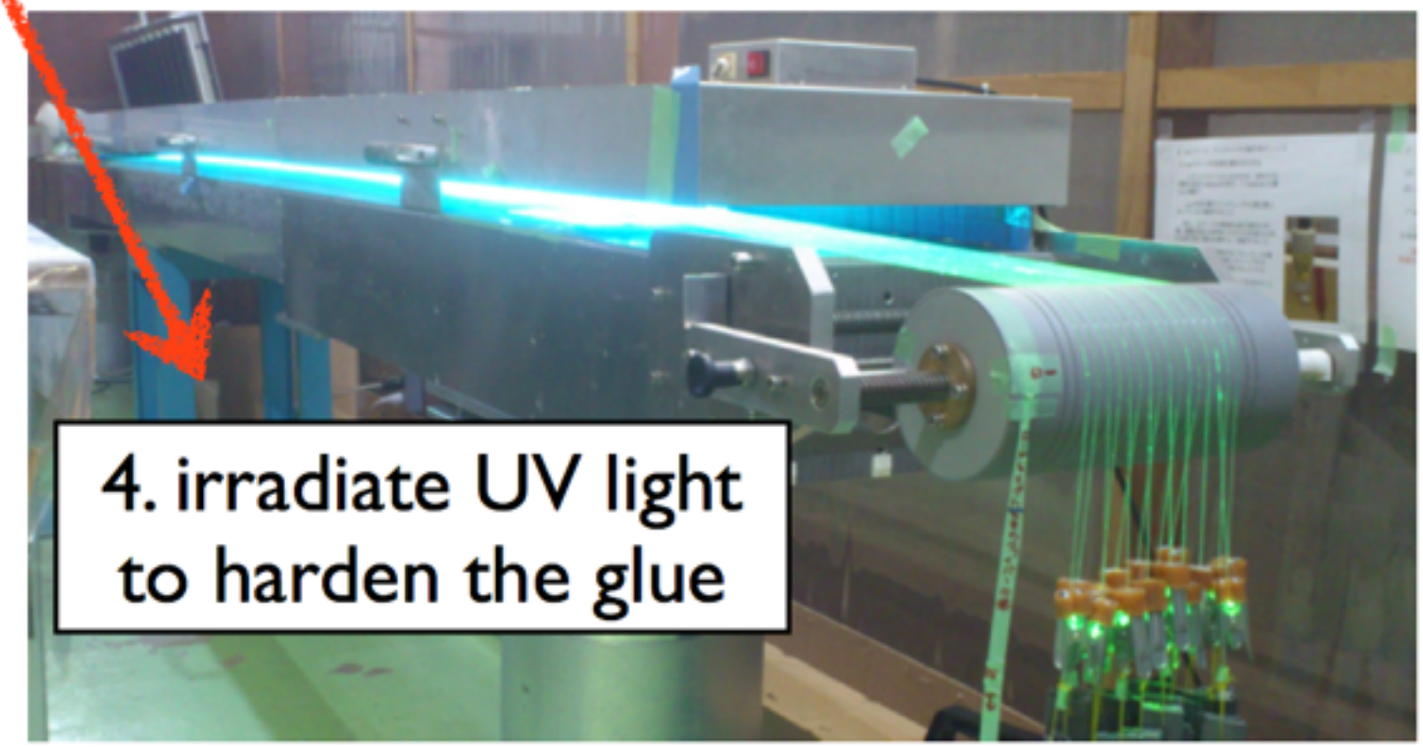

ファーストモジュールの準備

＊積層&バンド締め　・積層~1日(3人)

・バンド締め~4時間(2人)

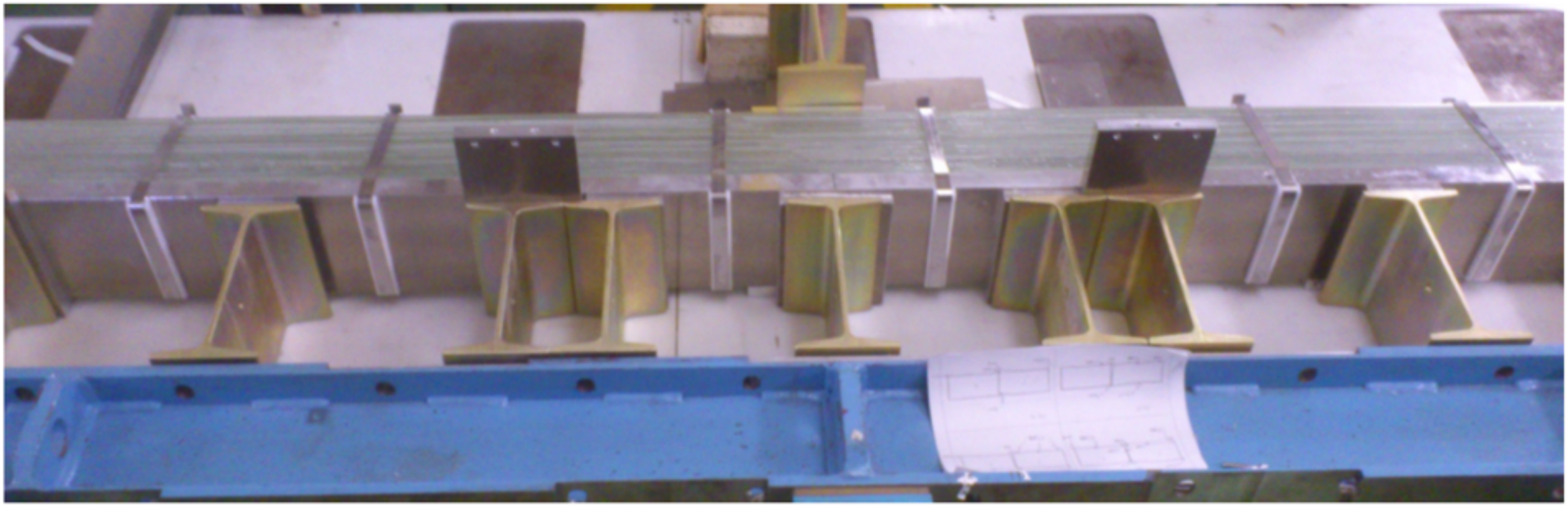

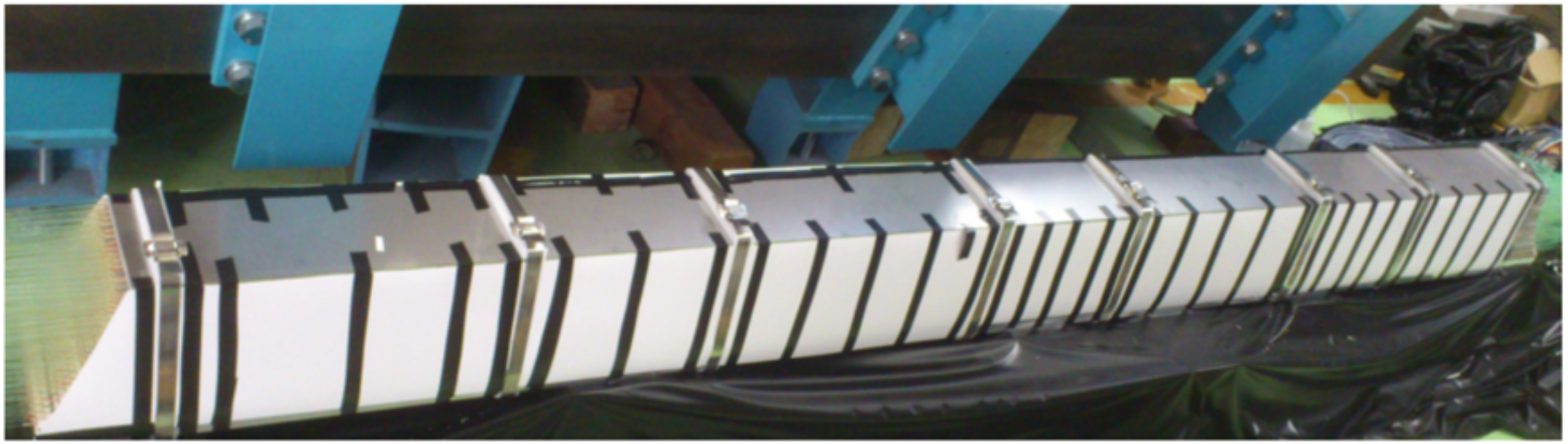

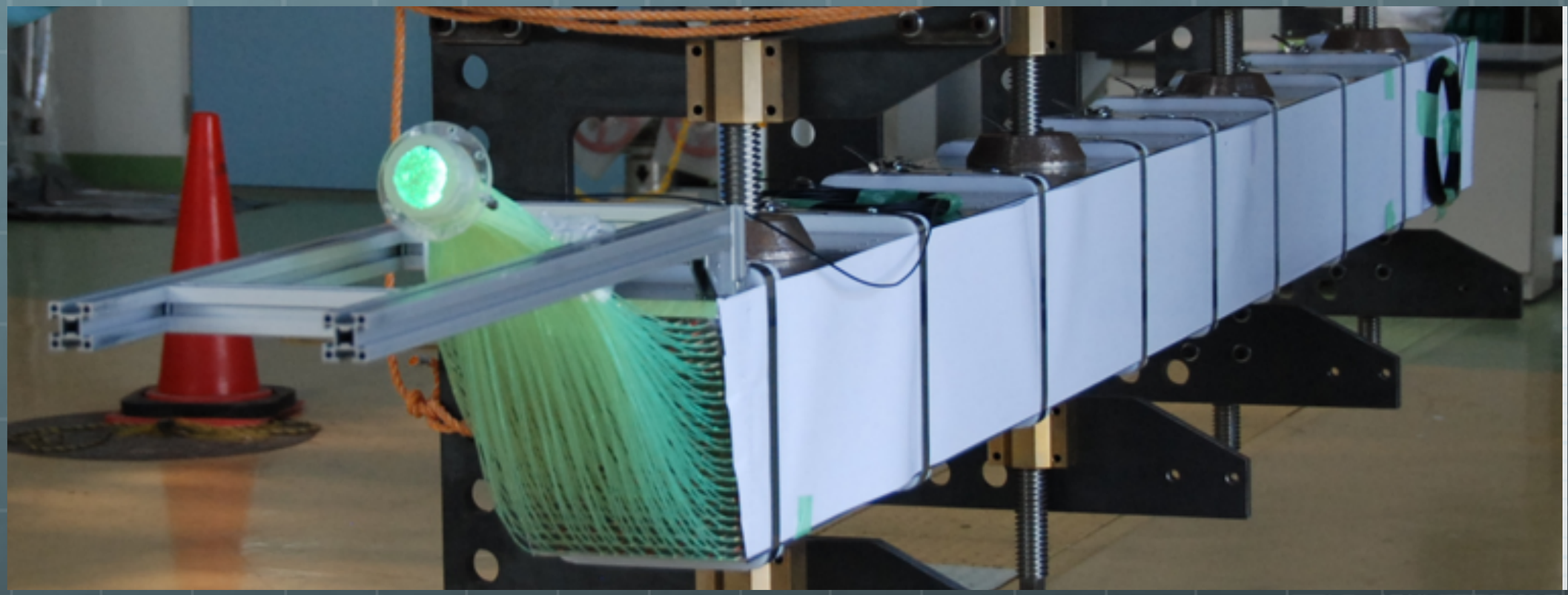

- Alternation lead sheet (1mm) and plastic scintillator(5mm)
- Wave length shifting fiber read-out (BCF-92, ϕ1.5mm)

Inner Main Barrel

M8 bolts : (8X8+8X7)X32=3840

Moved to J-PARC
Feb. 17, 2016

Installed
April 1, 2016

$K_L \to \pi^0\pi^0\pi^0$ Reconstruction

Using 5γ on CsI and 1γ on Barrel

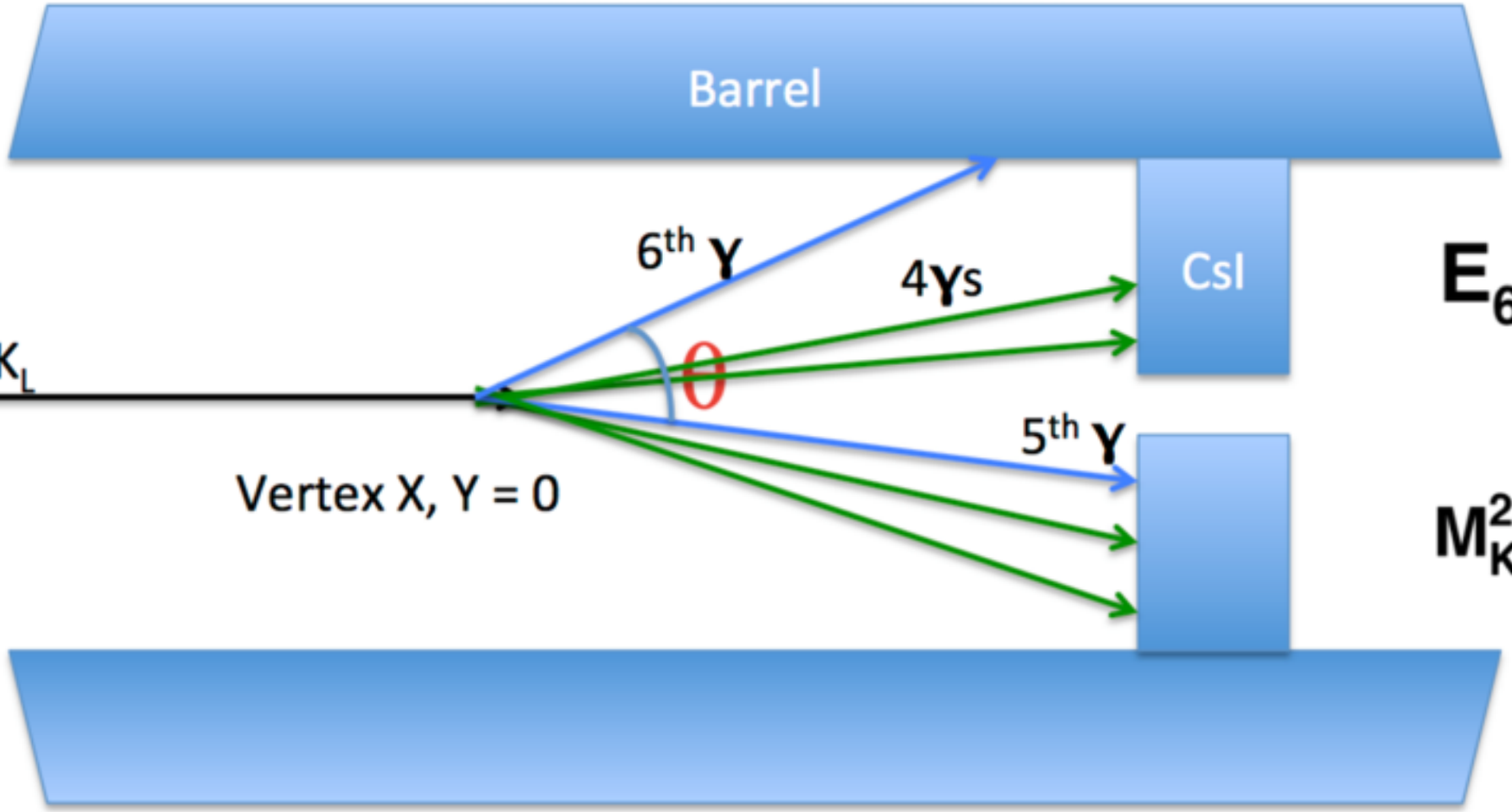

$$E_6 = \frac{M_\pi^2}{2E_5(1-\cos\theta)}$$

$$M_{K_L}^2 = \left(\sum_{i=1}^{6} E_i\right)^2 - \left(\sum_{i=1}^{6} \vec{p}_i\right)^2$$

- $K_L \to \pi^0\pi^0\pi^0$ decay samples with 5γs on CsI and 1γ on Barrel
- Reconstruction of $2\pi^0$ from 4γs on CsI
- 1γ Reconstruction from hit information of Barrel (timing and Module ID)
- Reconstruction of the last π^0 from 1γ on CsI and 1γ on Barrel

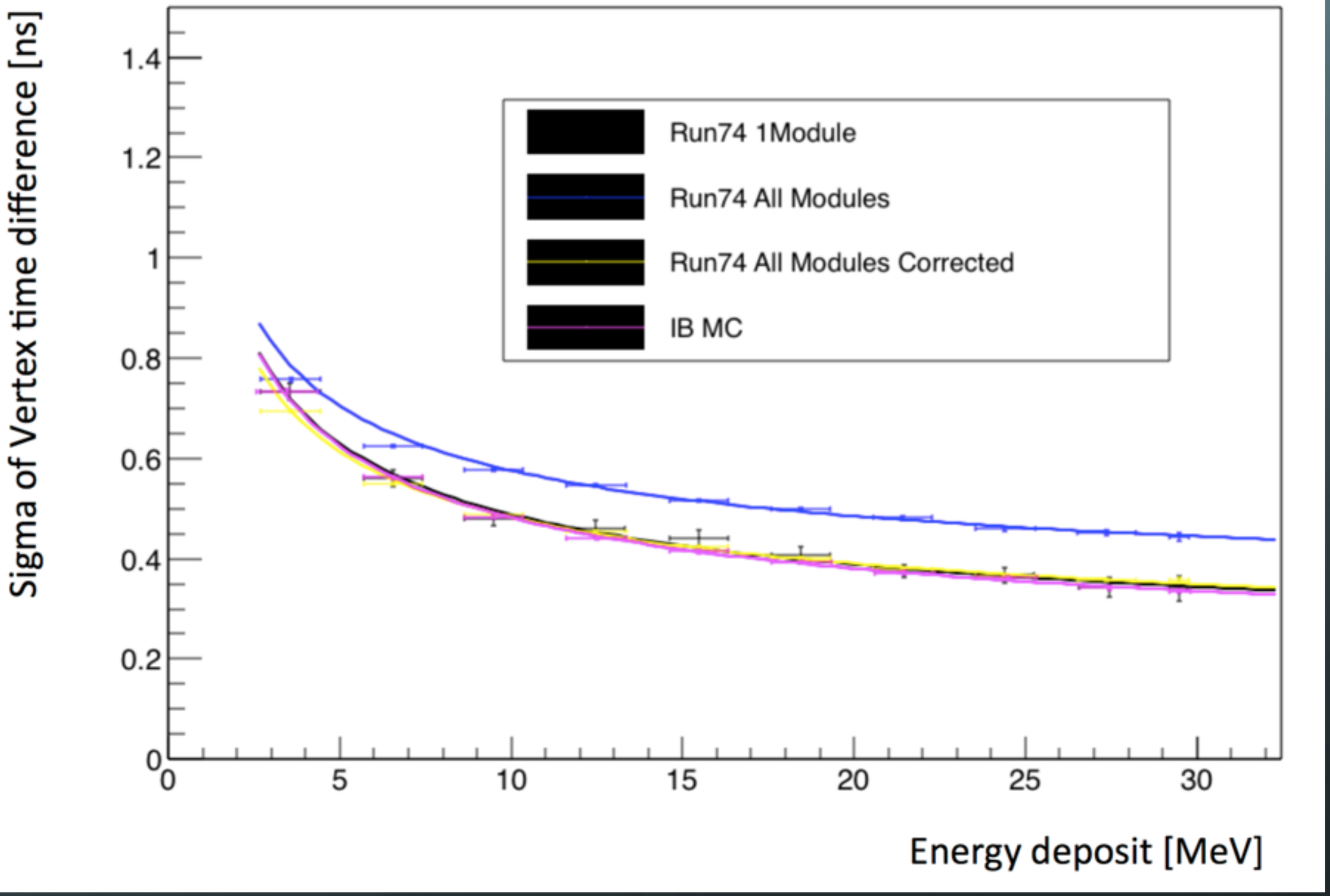
Sigma of Vertex time difference [ns]
1.4
1.2
1
0.8
0.6
0.4
0.2
0
0
5
10
15
20
25
30
Energy deposit [MeV]
Run74 1Module
Run74 All Modules
Run74 All Modules Corrected
IB MC

Data : Run65 Min. bias trigger (Black)

M.C. : KL3pi0 with Run65 Acc. (Red)

Deposited energy, Incident energy

***IMB**

Energy Deposit

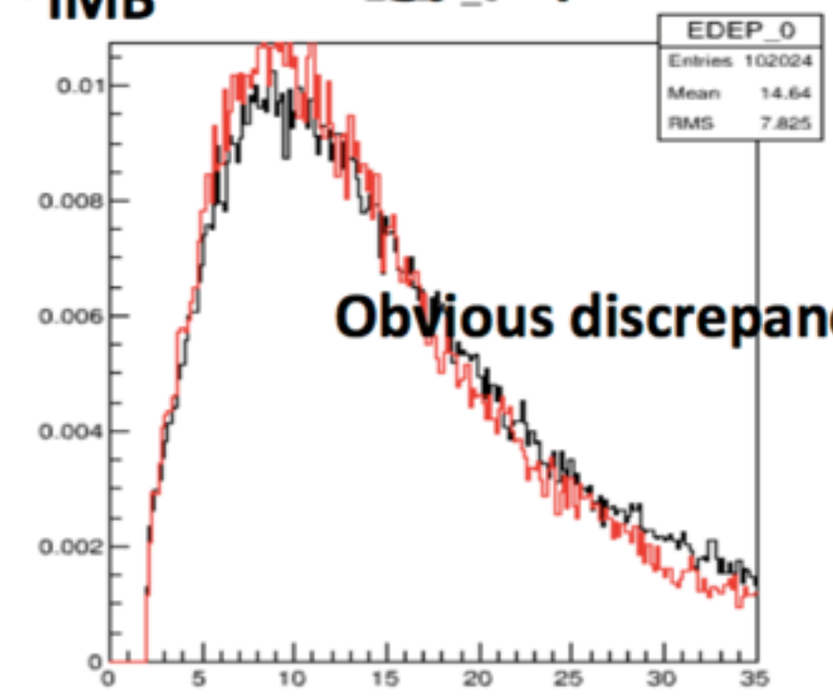

Incident Energy

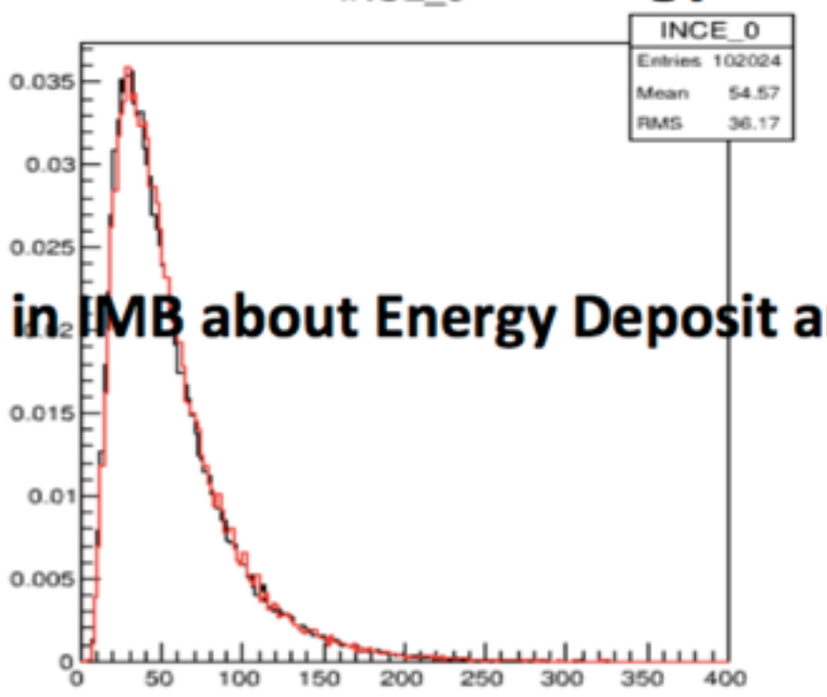

Energy Deposit / Incident Energy

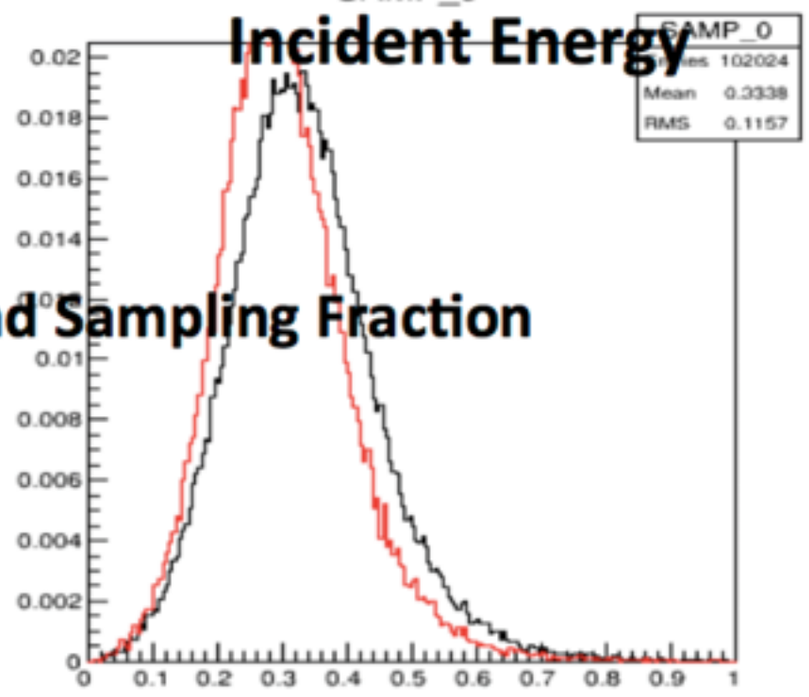

Obvious discrepancy in IMB about Energy Deposit and Sampling Fraction

***OMB**

Energy Deposit

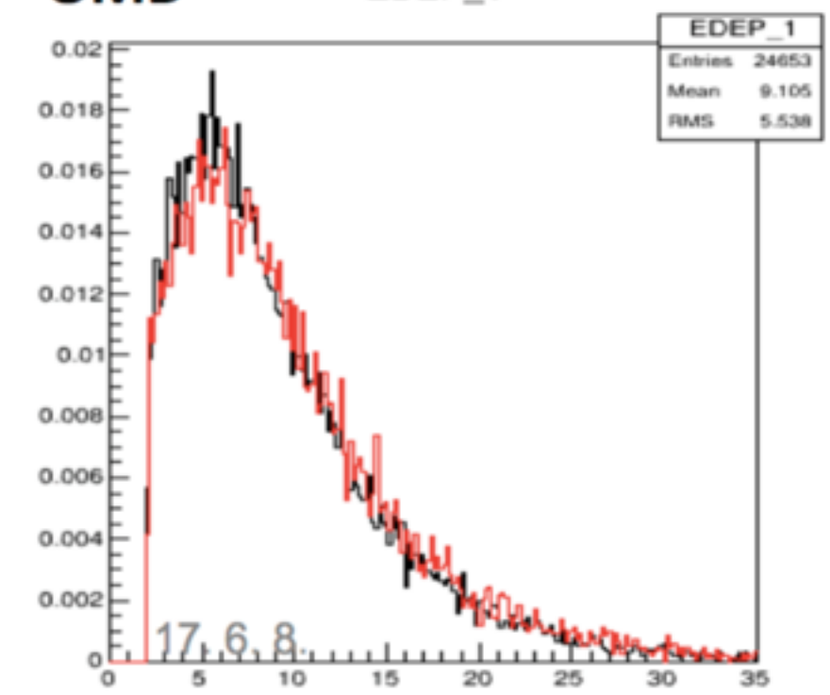

Incident Energy

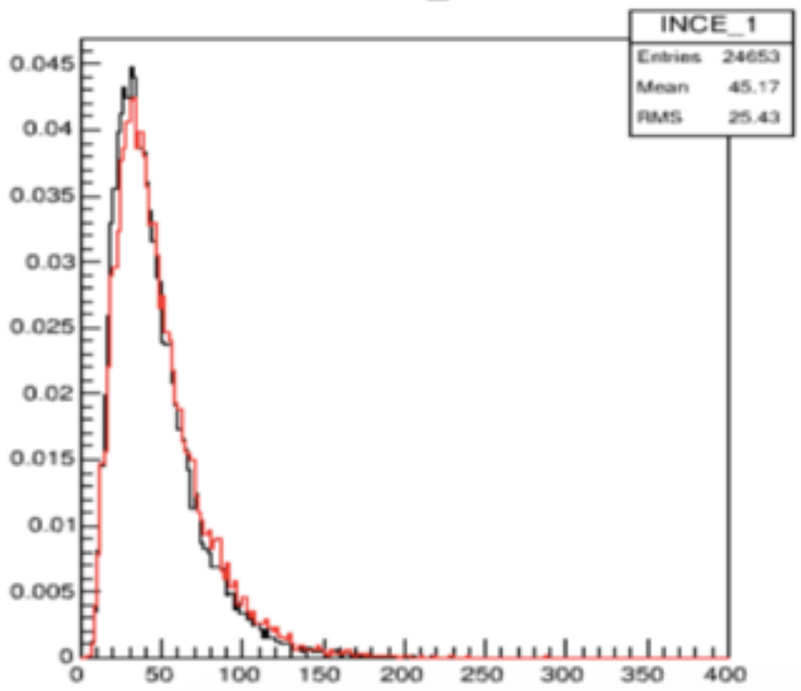

Energy Deposit / Incident Energy

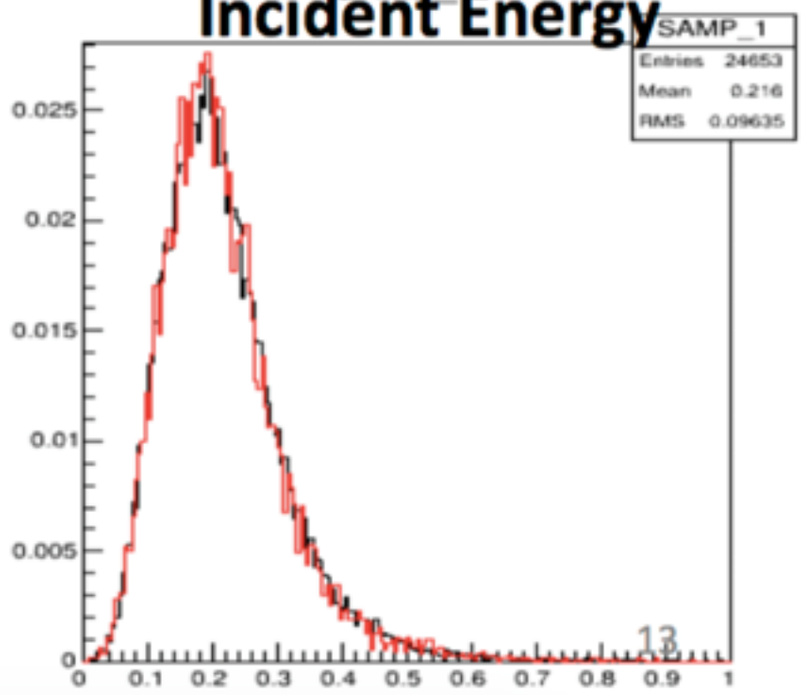

Detector

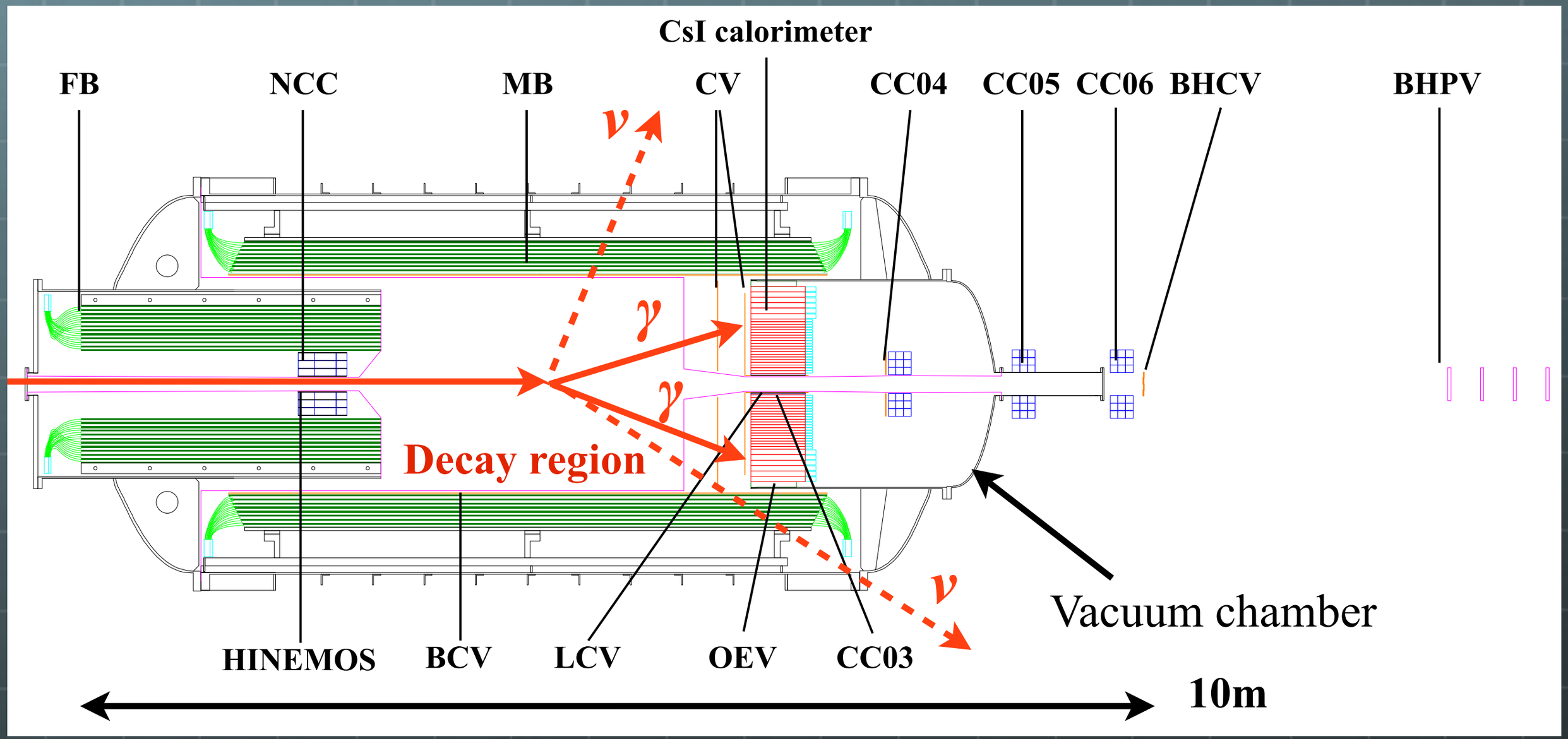
CsI calorimeter
FB
NCC
MB
CV
CC04
CC05
CC06
BHCV
BHPV
ν
γ
γ
Decay region
ν
Vacuum chamber
HINEMOS
BCV
LCV
OEV
CC03
10m

Neutron Meas.

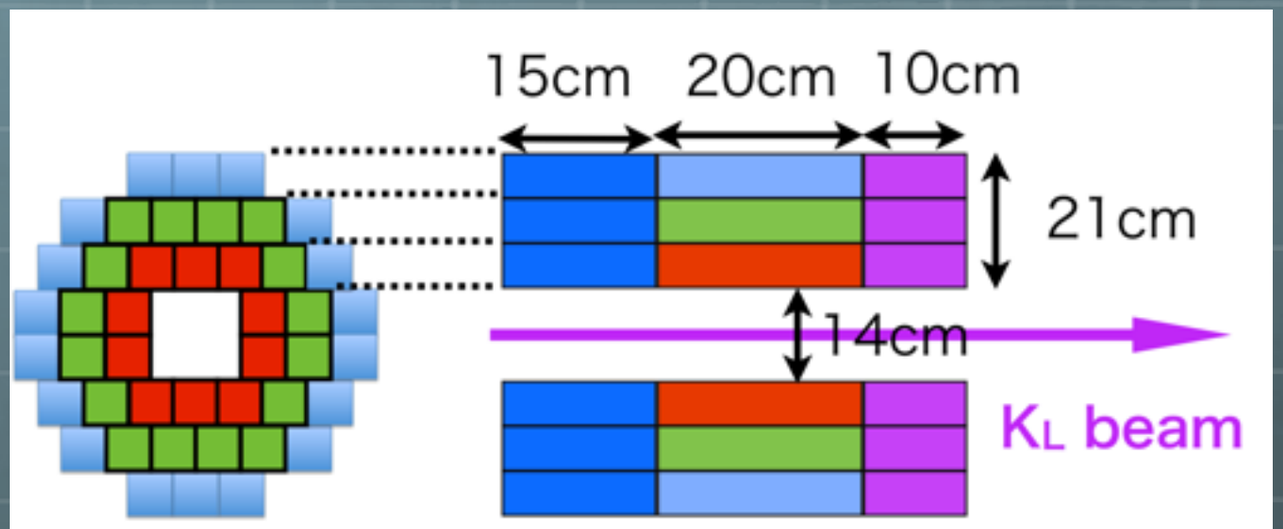

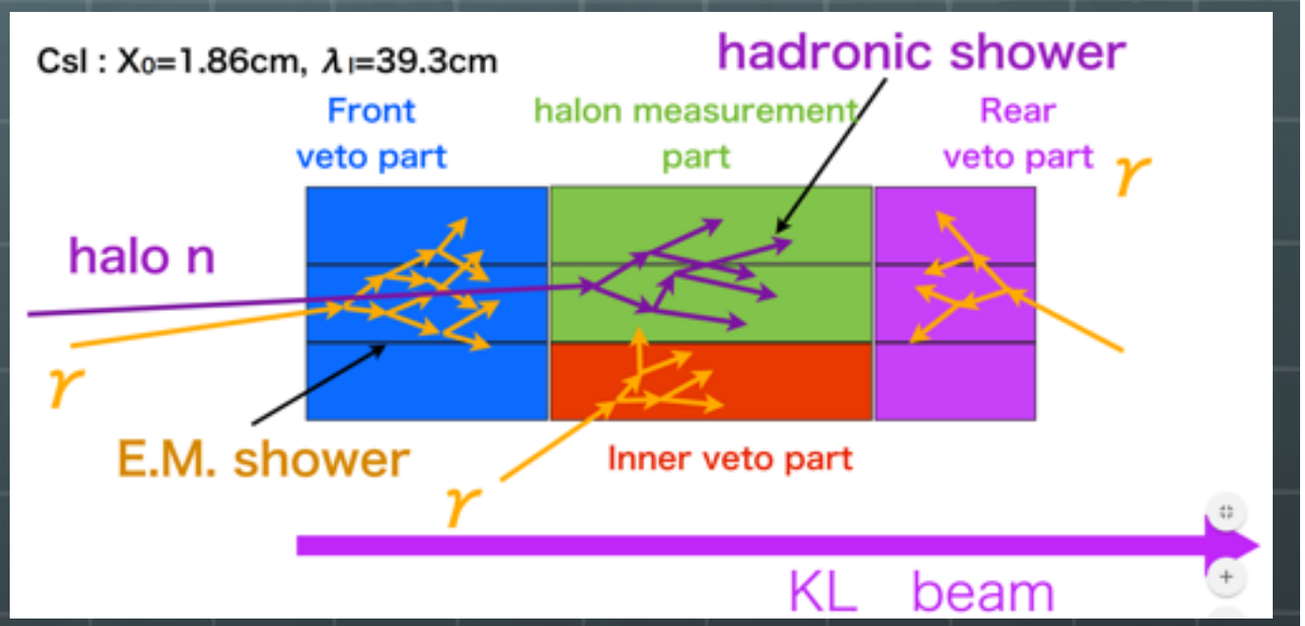

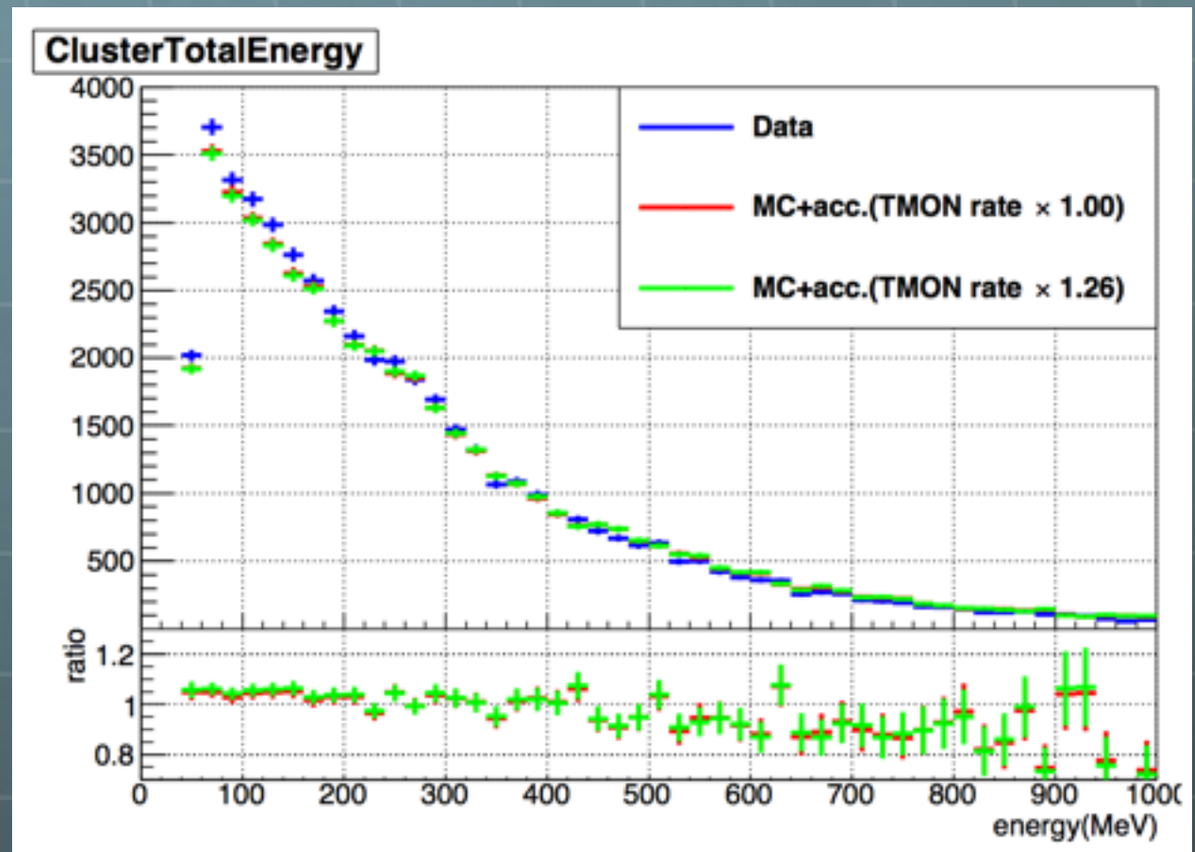

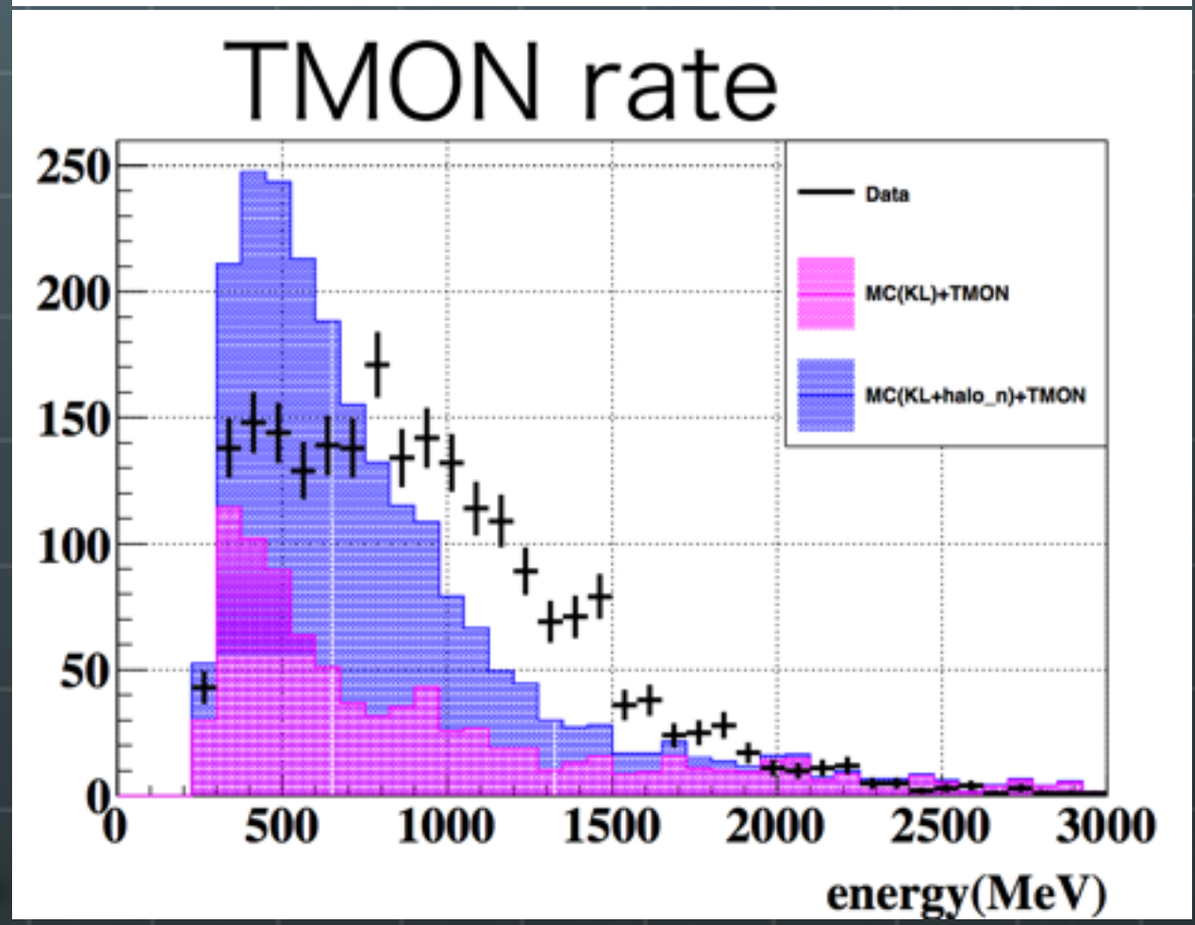

Results of May 2013

- Removed B.G. events learned from the E391a.
  (π^0 production at the detectors)
- We found two new sources of the B.G.
- Upgraded detector for run 2015

$$\mathrm{S.E.S} = 1.29 \times 10^{-8}$$

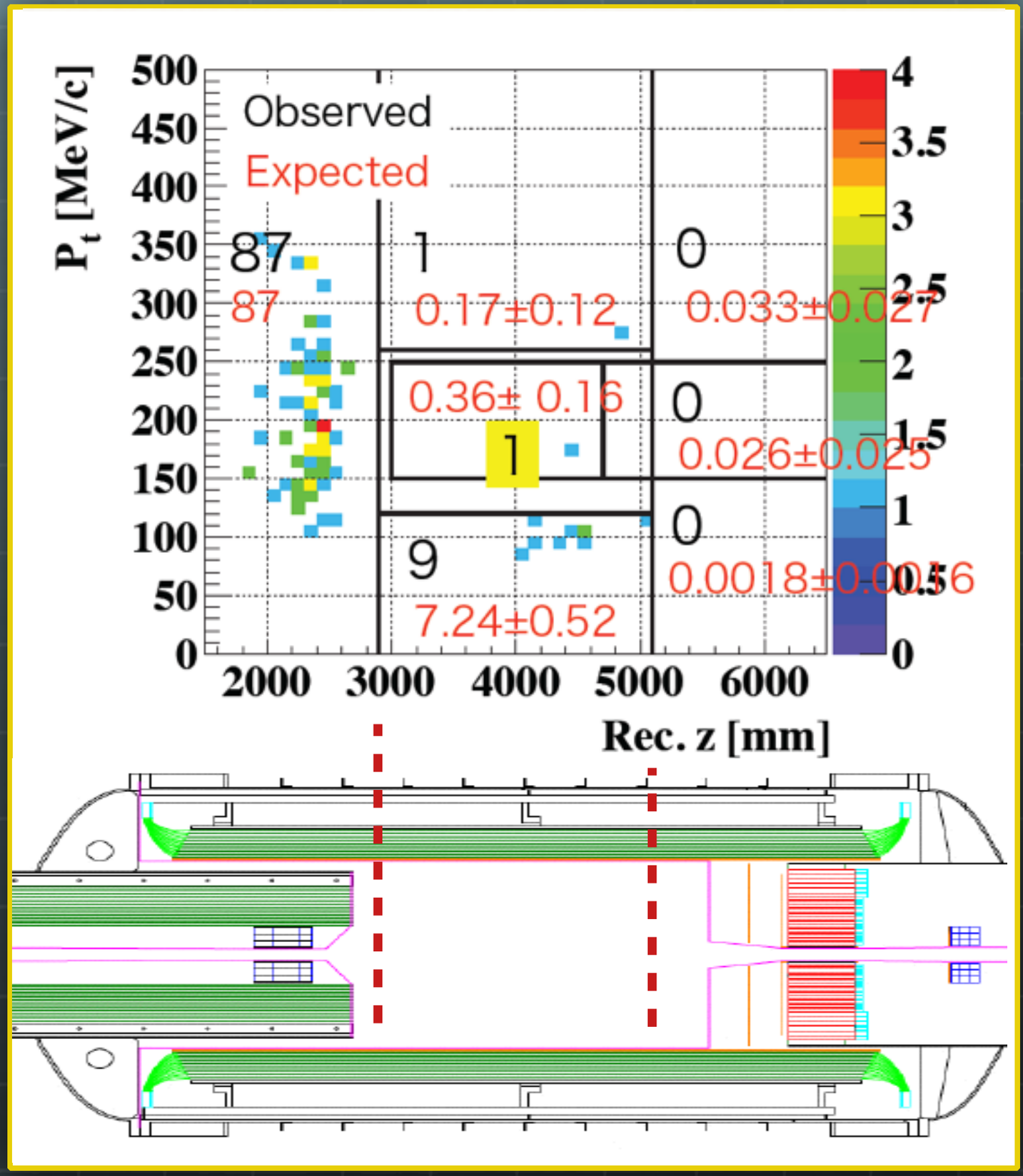

From Now

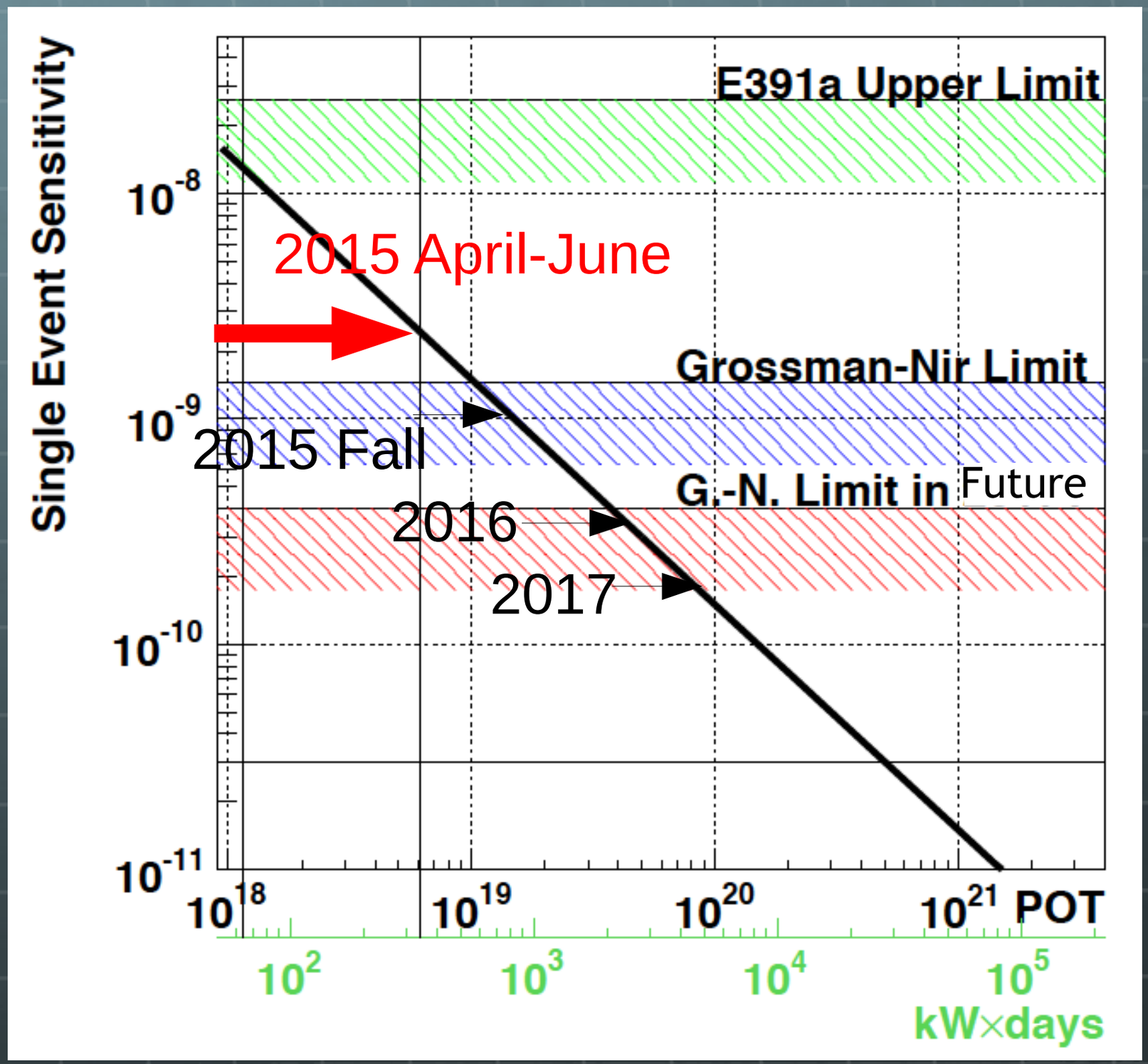
Single Event Sensitivity
E391a Upper Limit
10^{-8}
2015 April-June
Grossman-Nir Limit
10^{-9}
2015 Fall
G.-N. Limit in Future
2016
2017
10^{-10}
10^{-11}
10^{18}
10^{19}
10^{20}
10^{21} POT
10^{2}
10^{3}
10^{4}
10^{5}
kW×days

Halo neutron events

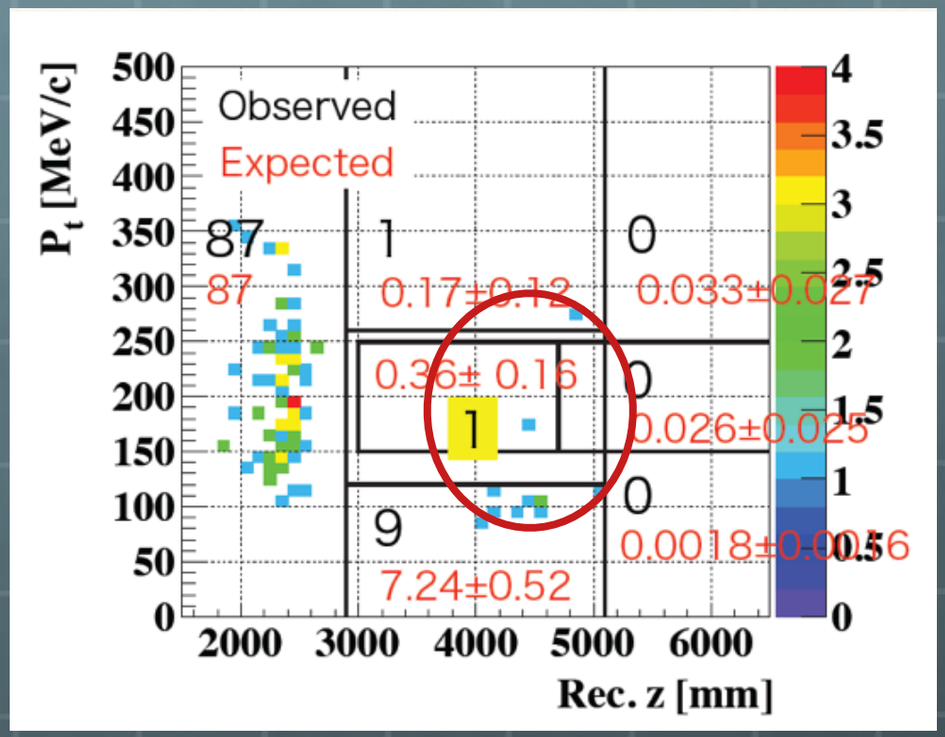

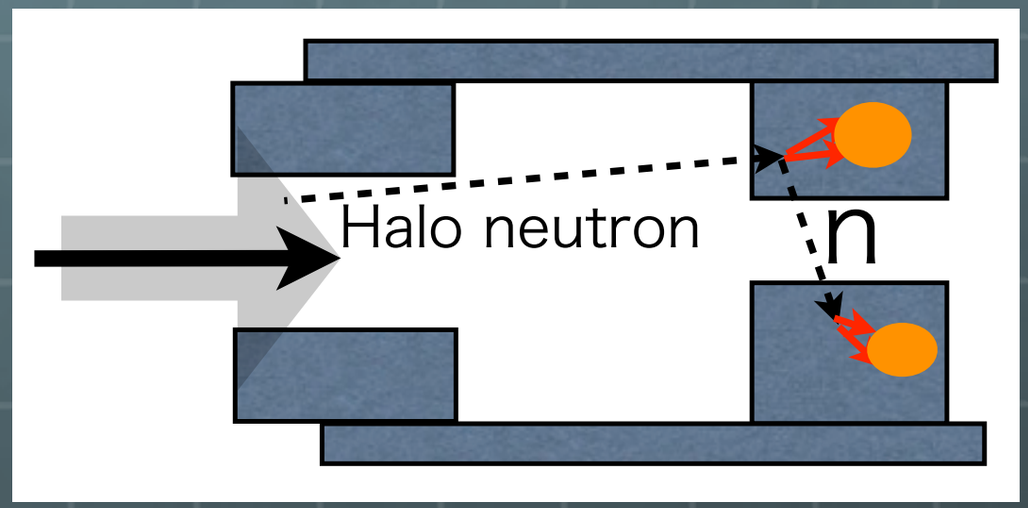

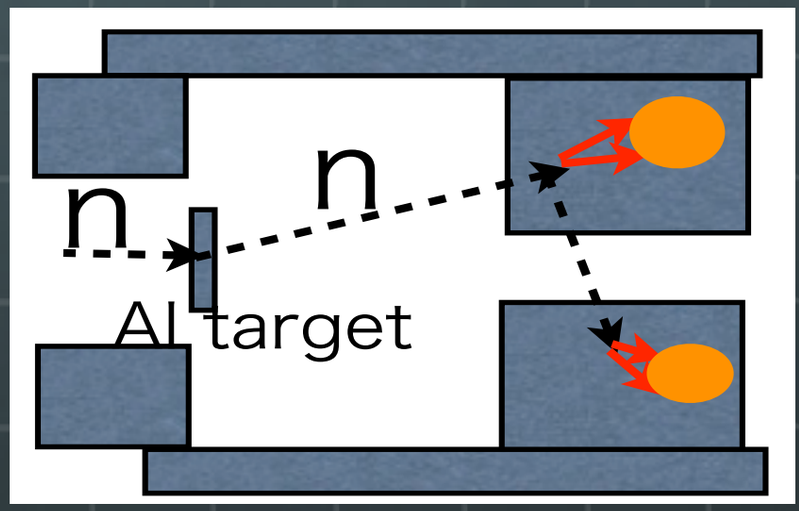

- Single neutron produce two clusters
  - Newly founded background source
  - Studied by using aluminum target data

Reduction of the Halo neutron events

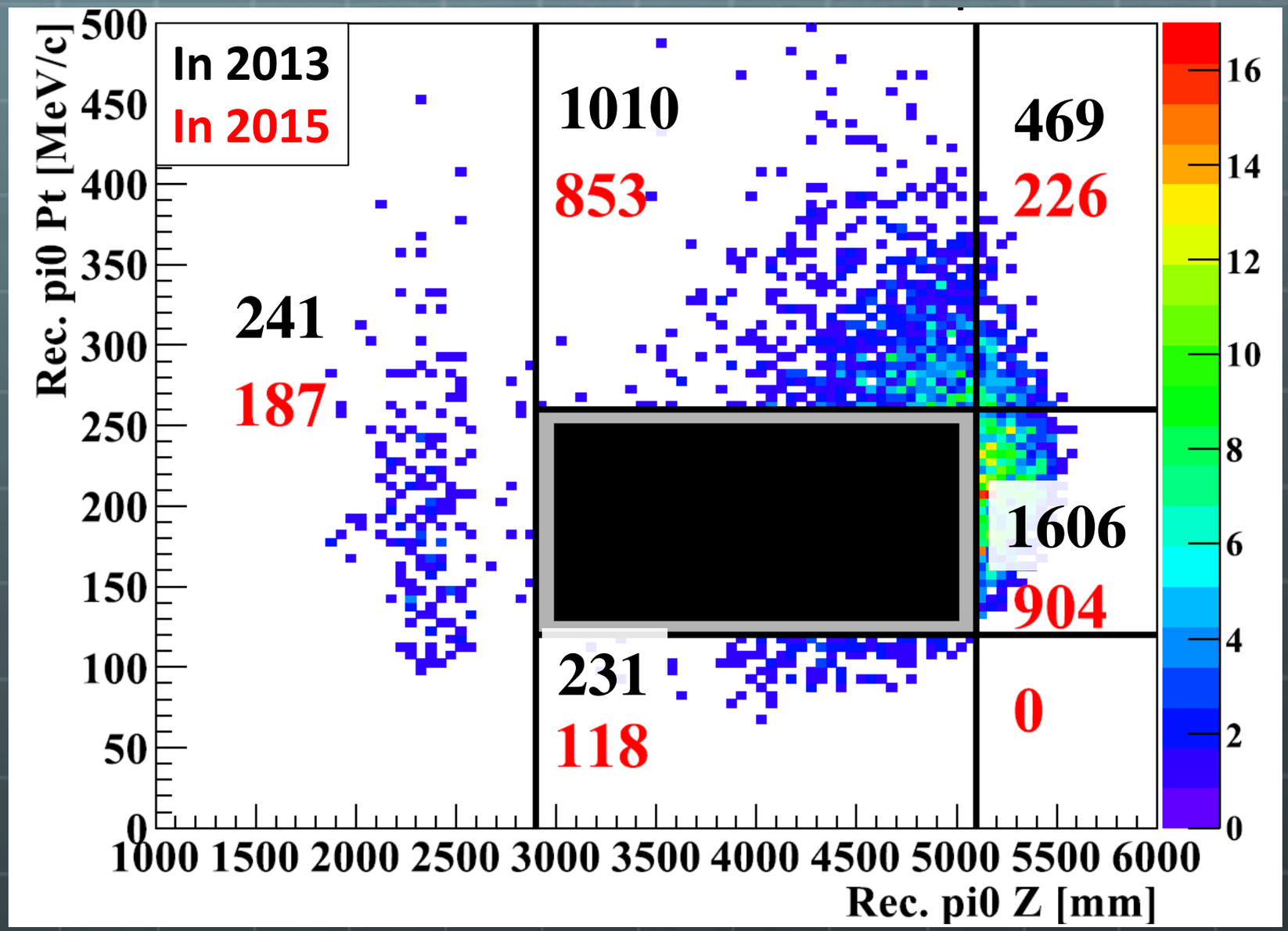

Halo neutron events

- To reduce scattering source
- To take data for enhanced neutron events

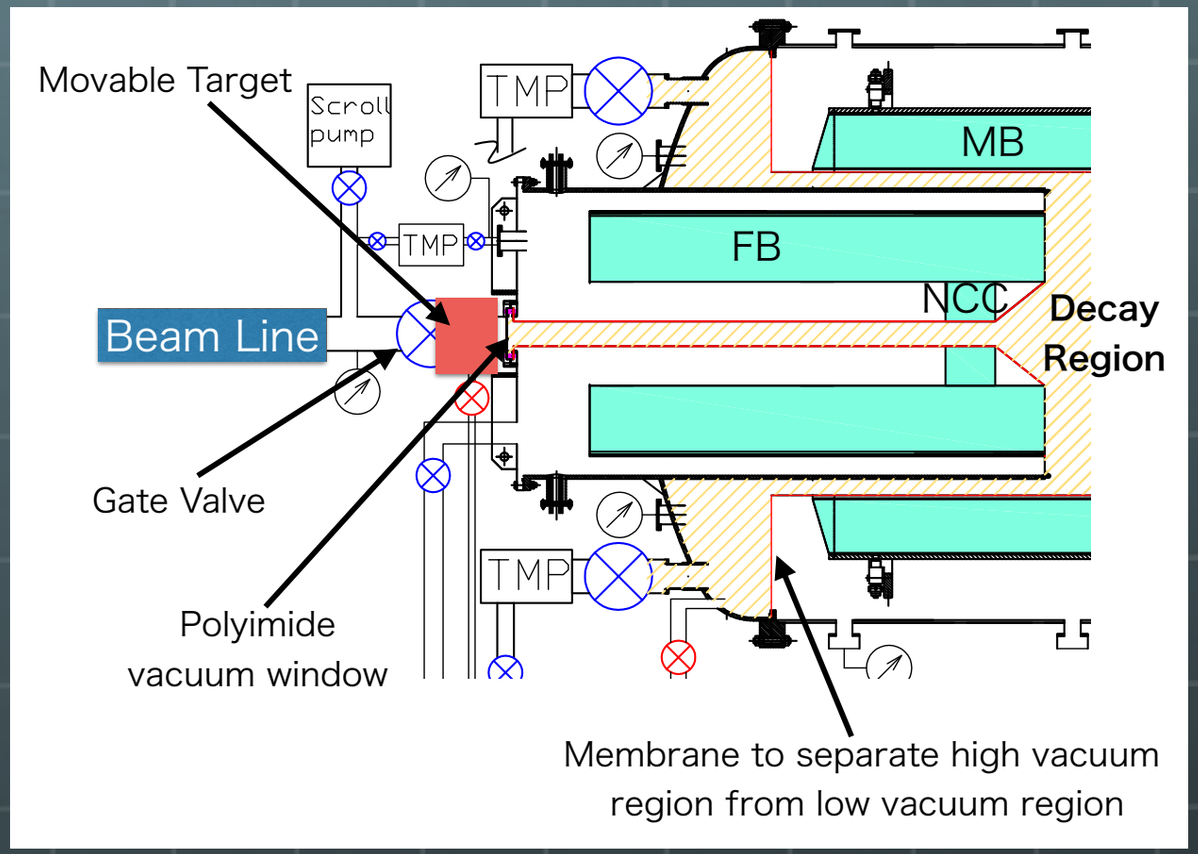

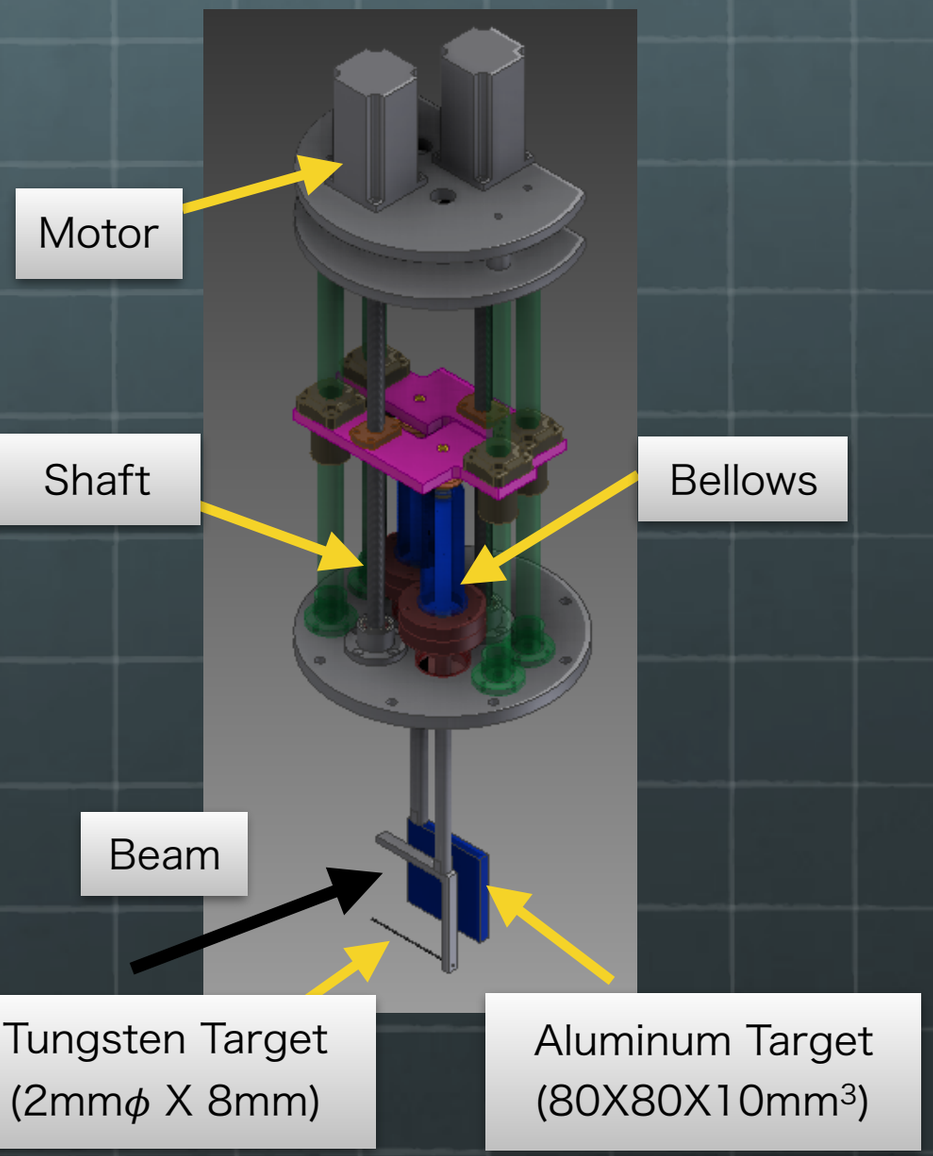

Enhanced neutron events

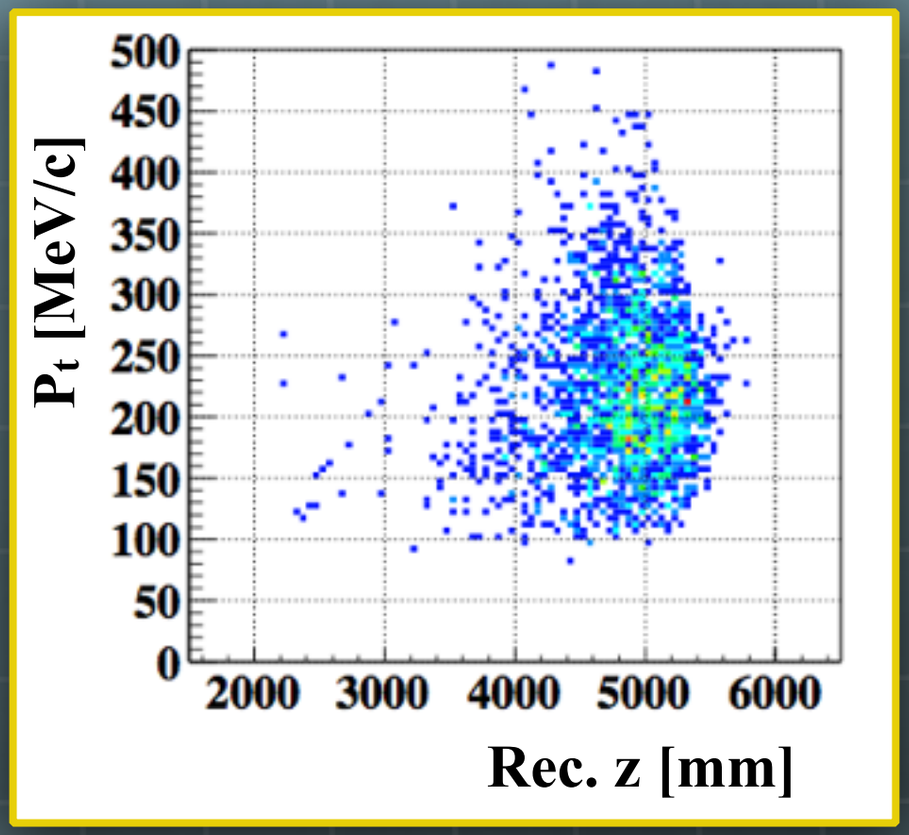

- 70-hour data taking with Al-target (>15 times more than May 2013)
- To study cluster and pulse shape in the calorimeter
- To develop a method to discriminate neutron induced events from the π^0 events

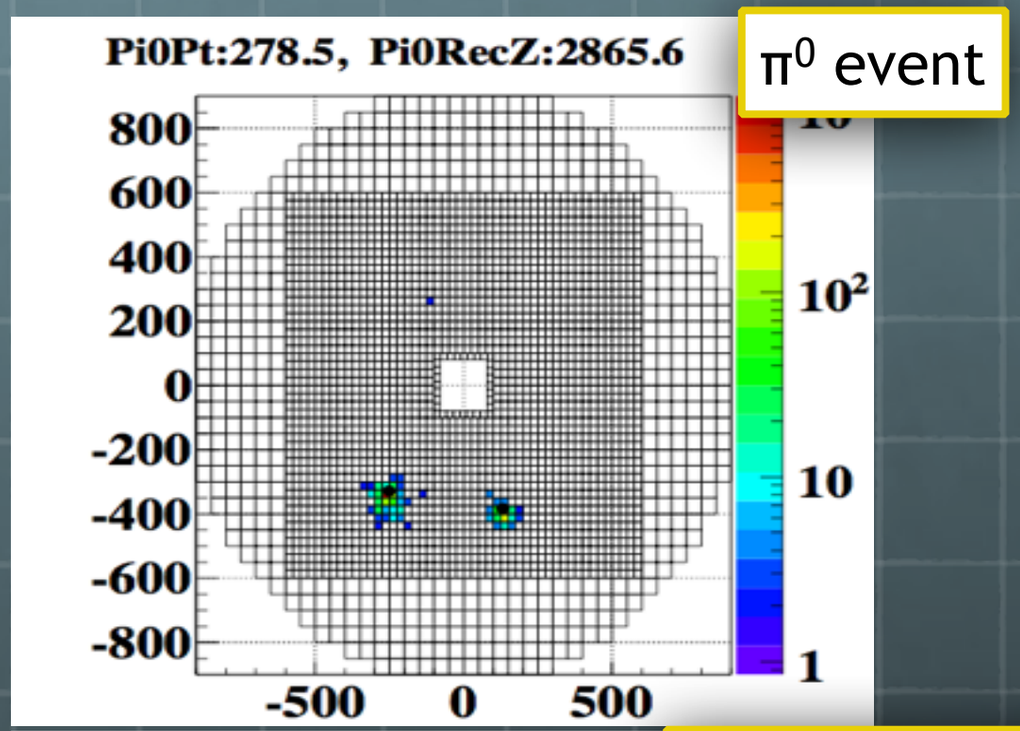

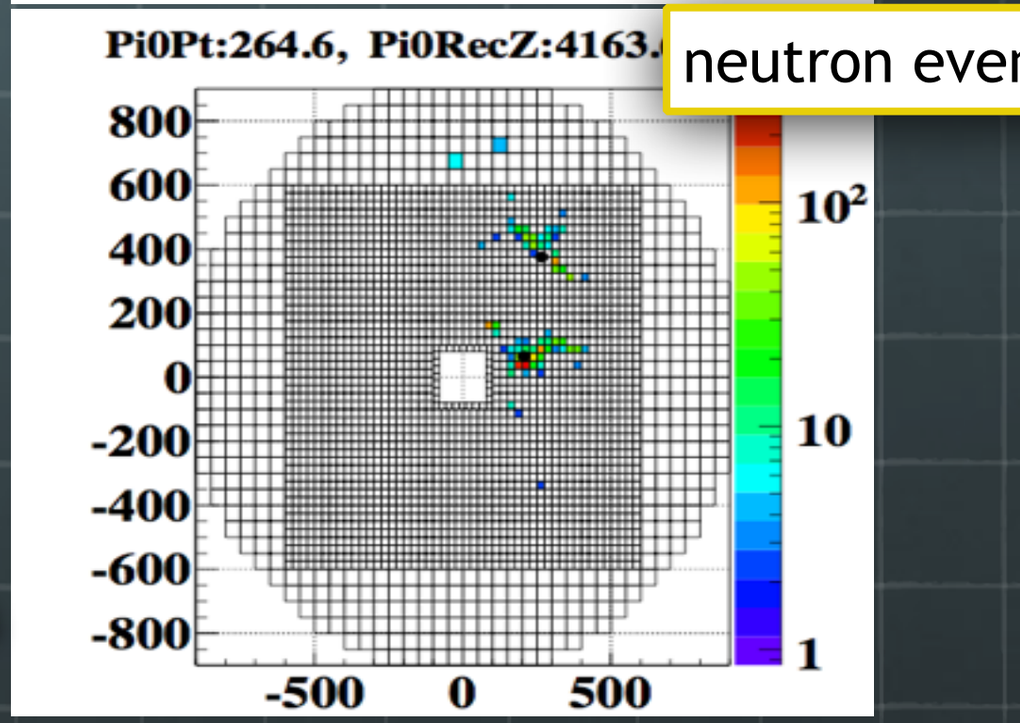

Shower Shape analysis

- Compare cluster energy & timing to library from MC

Template of Gamma Cluster from MC

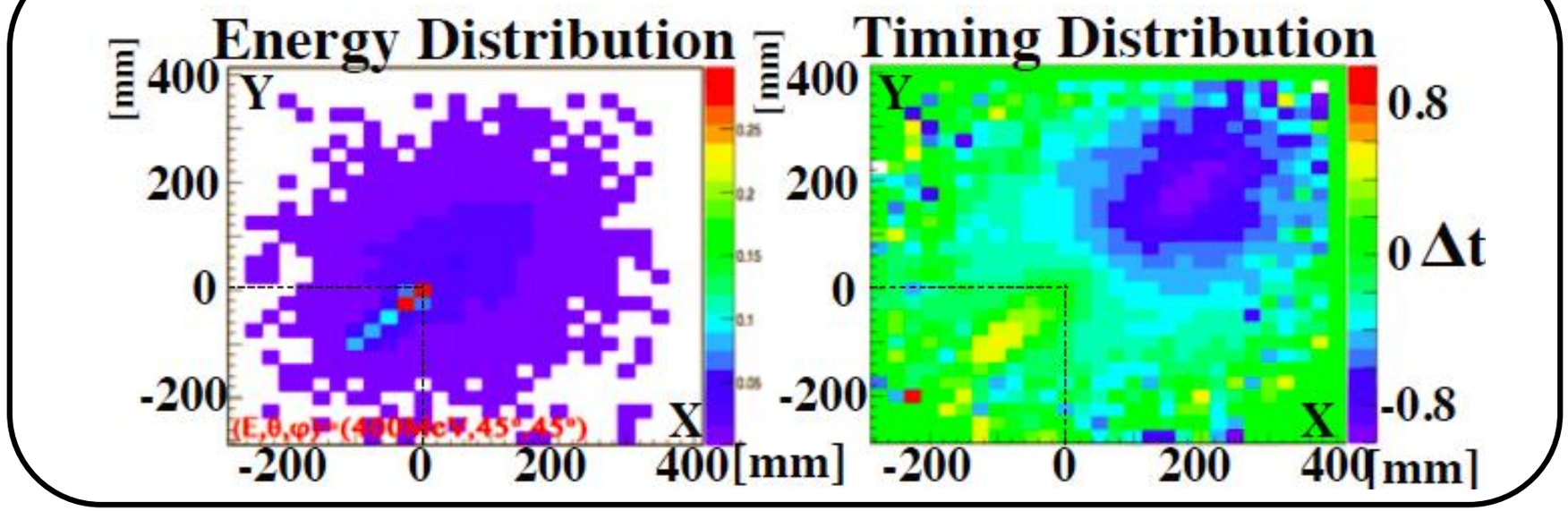

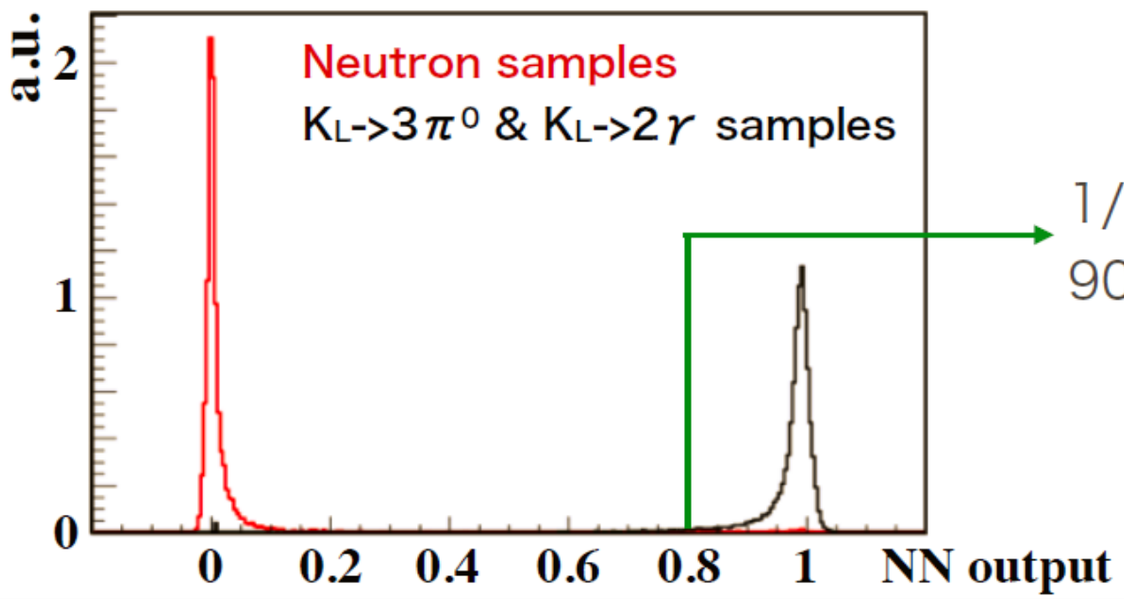

1/1500 BG reduction &
90% signal acceptance

Pulse Shape analysis

Signal waveform of calorimeter

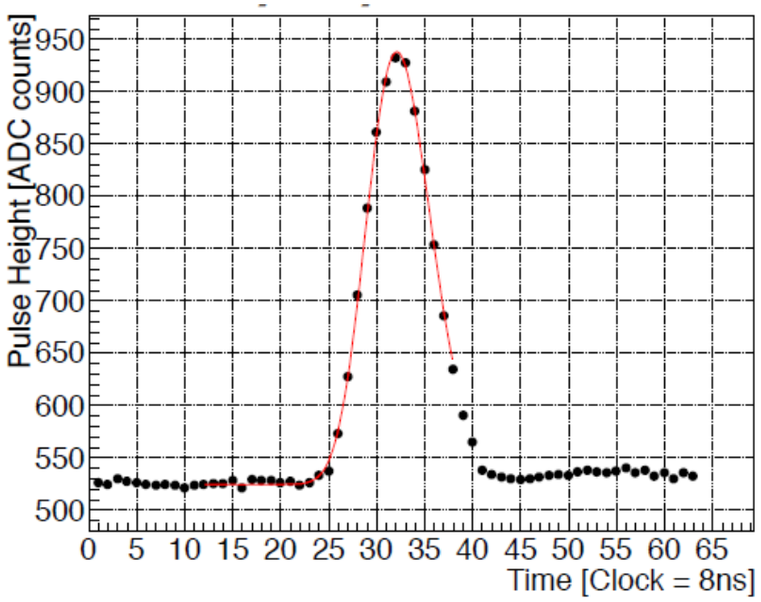

$$A(t) = |A| \exp\left(-\frac{(t-t_0)^2}{2\sigma(t)^2}\right),$$

$$\sigma(t) = \sigma_0 + a(t-t_0)$$

σ_0 vs Log_{10}(PulseHeight)

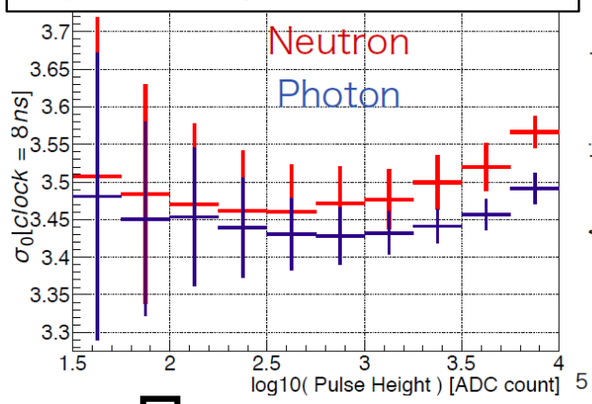

a vs Log_{10}(PulseHeight)

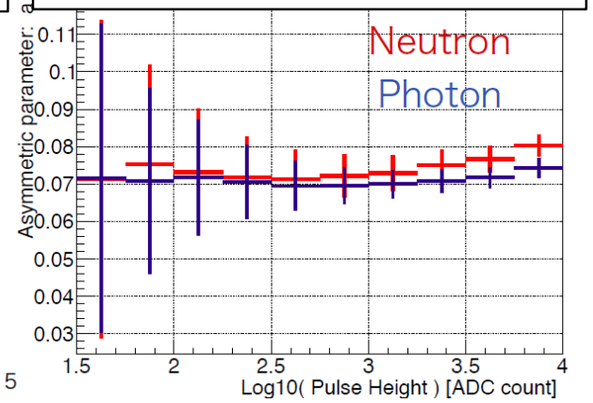

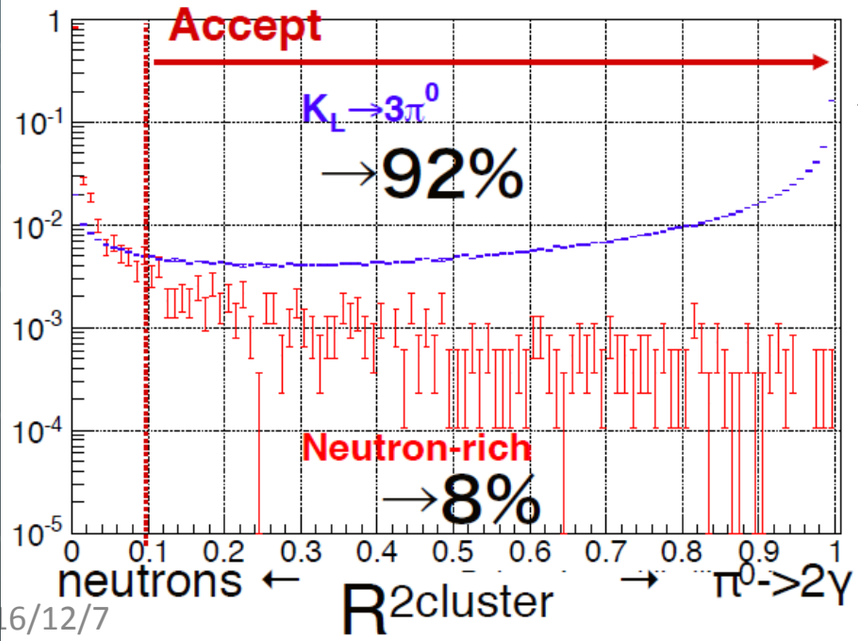

Summing up in all the crystals

Likelihood Ratio

$$R_\gamma^{2cluster} = \frac{L_\gamma^{2cluster}}{L_\gamma^{2cluster} + L_n^{2cluster}}$$

Likelihood for gamma clusters

Likelihood for neutron clusters

Reduction Neutron background

	Reduction Factor
Shape χ2 && Cluster Shape Discrimination	$3.4^{+2.1}_{-0.9} \times 10^3$
Pulse Shape Likelihood	$11.1^{+0.4}_{-0.9}$

Total Reduction Factor = $3.8^{+2.4}_{-1.1} \times 10^4$

Al Target Data (before neutron cut)

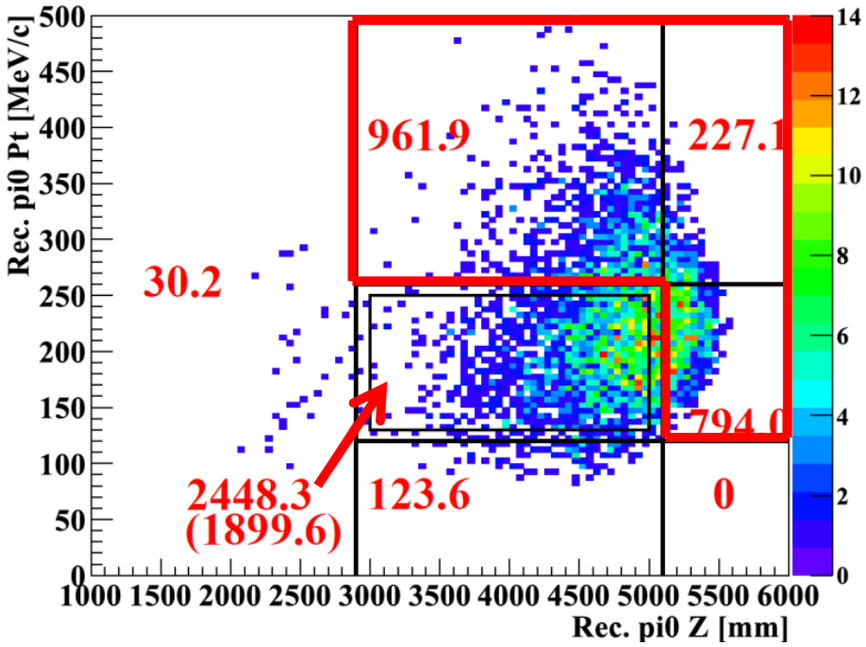

Physics Data (before neutron cut)

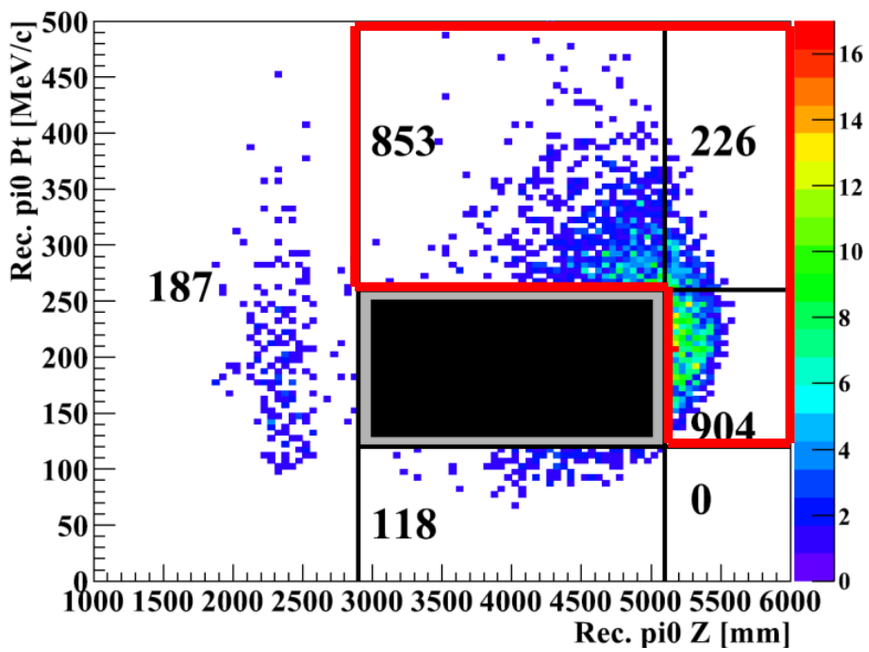

Normalized with the number of events in red box

For further X10 reductio

- CsI Both-End read-out

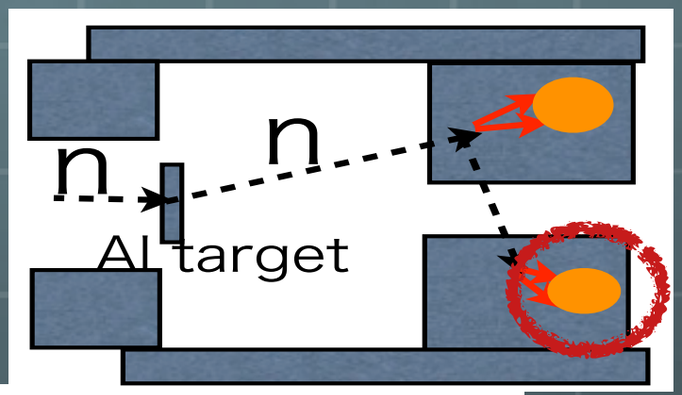

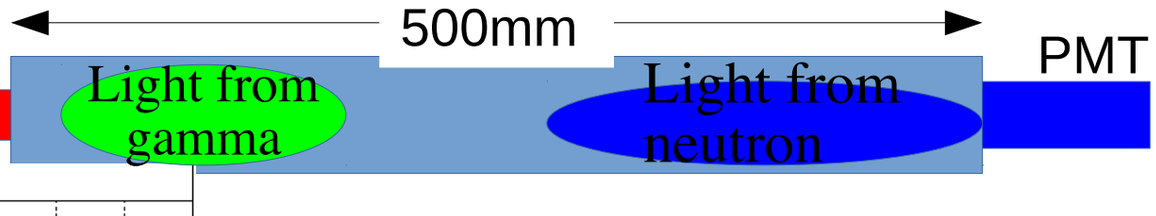

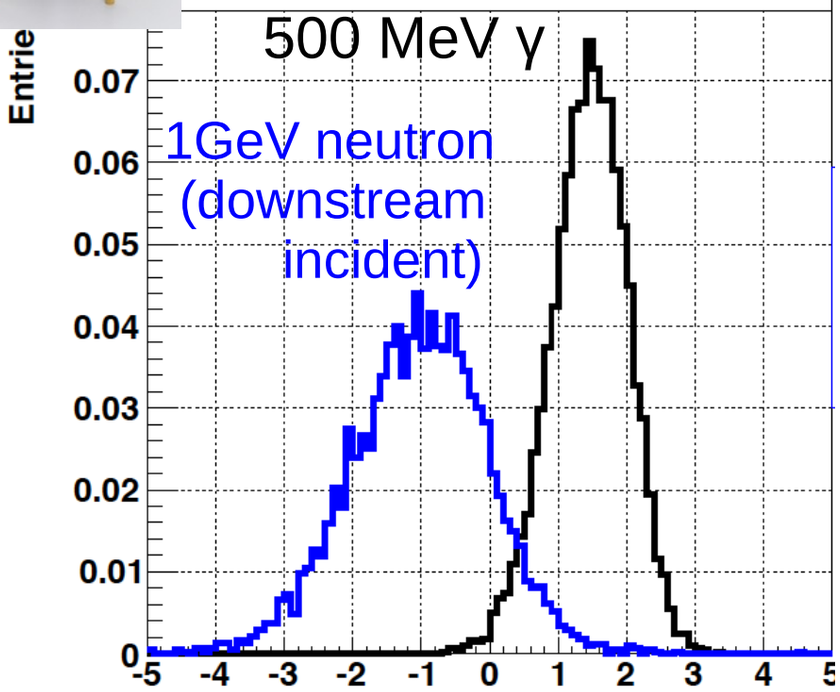

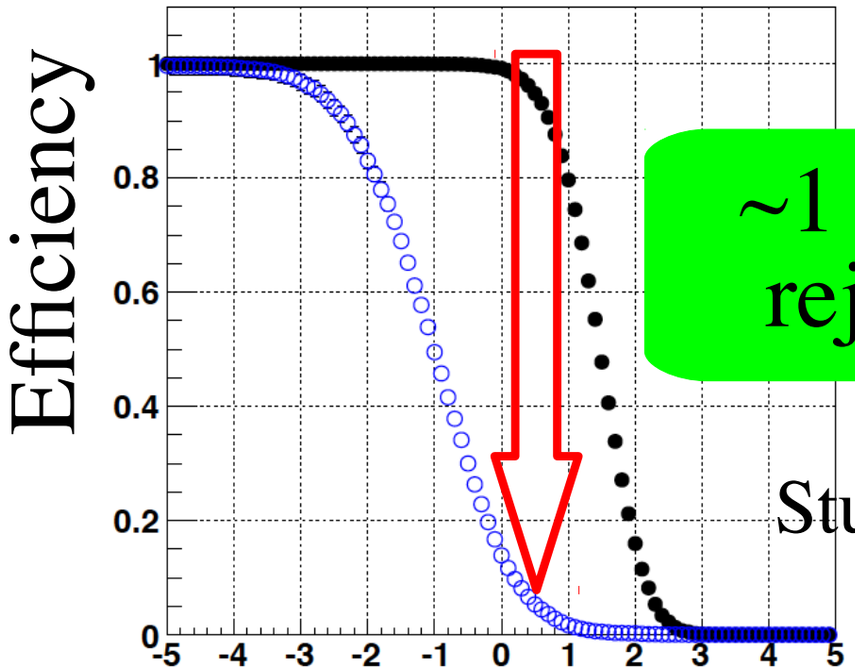

~1 order rejection!

Study on going

Hadron Hall Extension

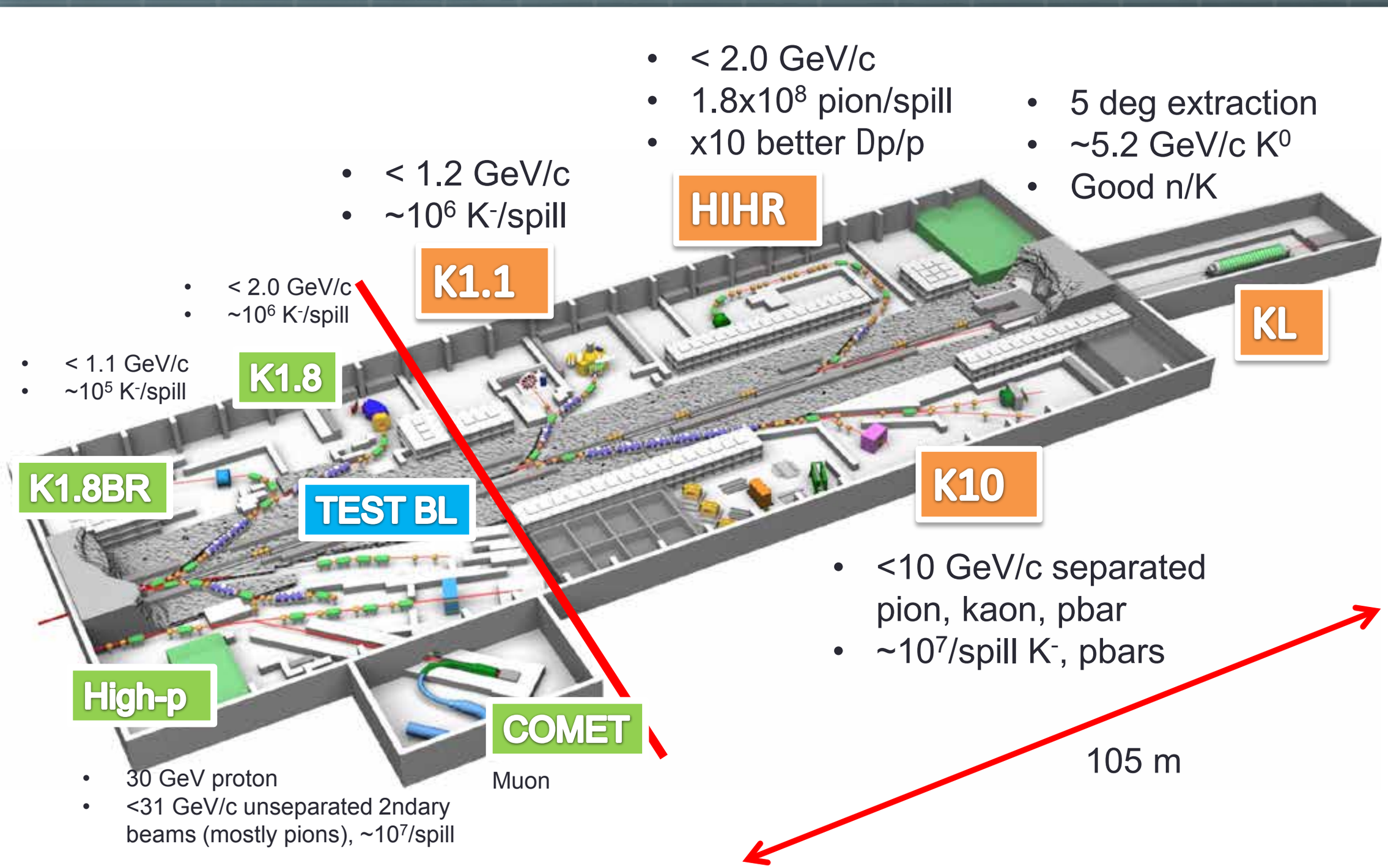

In near future

- To perform precise measurement of the branching ratio (KOTO II)
- It is worth to design an experiment to determine branching ratio with comparable uncertainty to that of the theoretical calculation
- For the experiment
  - Correct understanding all background sources
  - Higher beam intensity
  - Larger detector acceptance

Summary

- The J-PARC is providing high intensity proton beam to study variety fields of science.
- KOTO aims at the precise measurement of branching ratio of the $K_L \rightarrow \pi^0\nu\nu$ decay
  - Important role to understand new physics effects
  - Step-by-step approach to determine its branching ratio precisely.
- With the hadron hall extension
  - KOTO-II will be performed

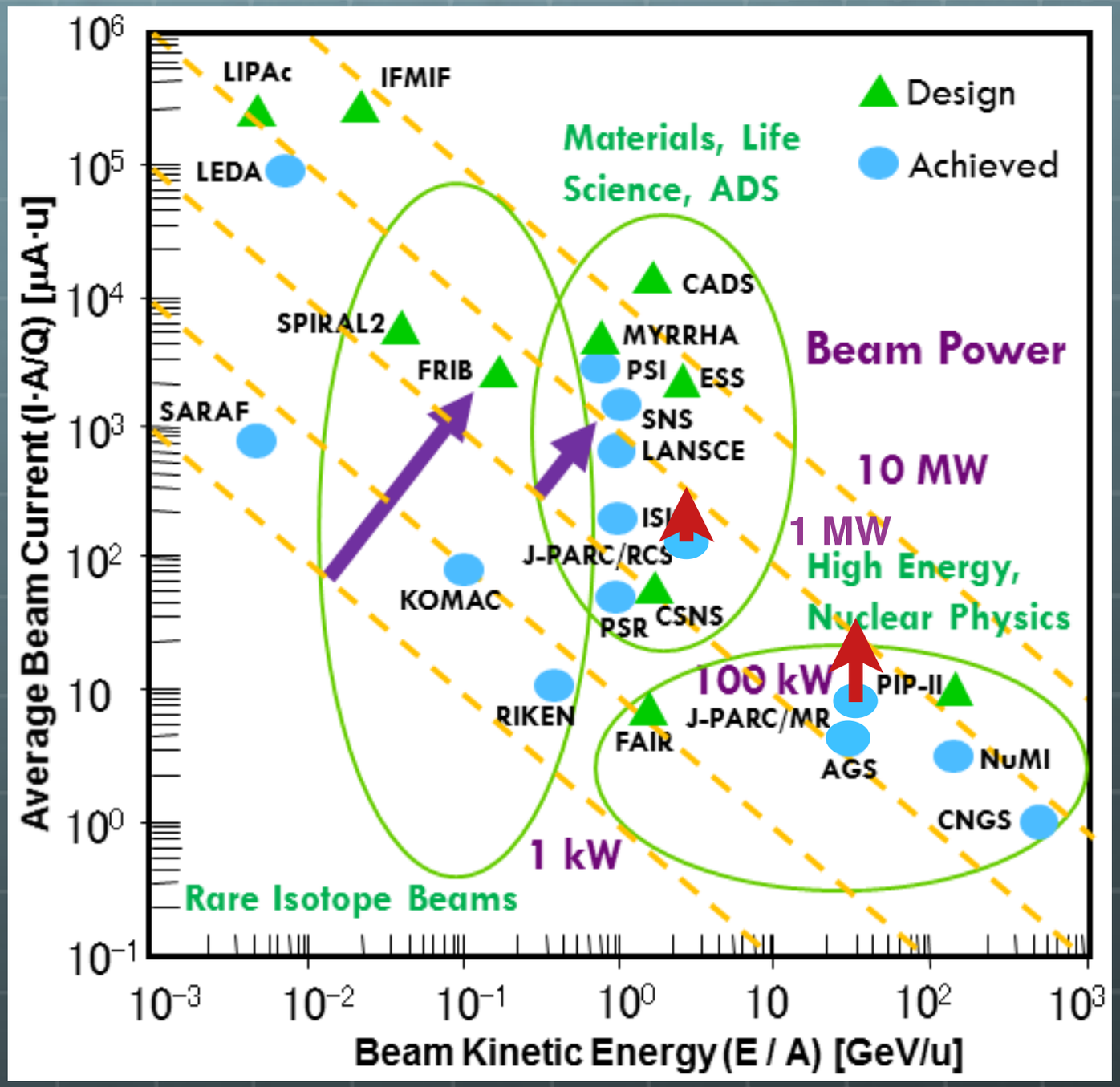

Jie Wei / Y.Yamazaki

High intensity

Precision Meas. Rare phenomena

New Science

E391a : 2600

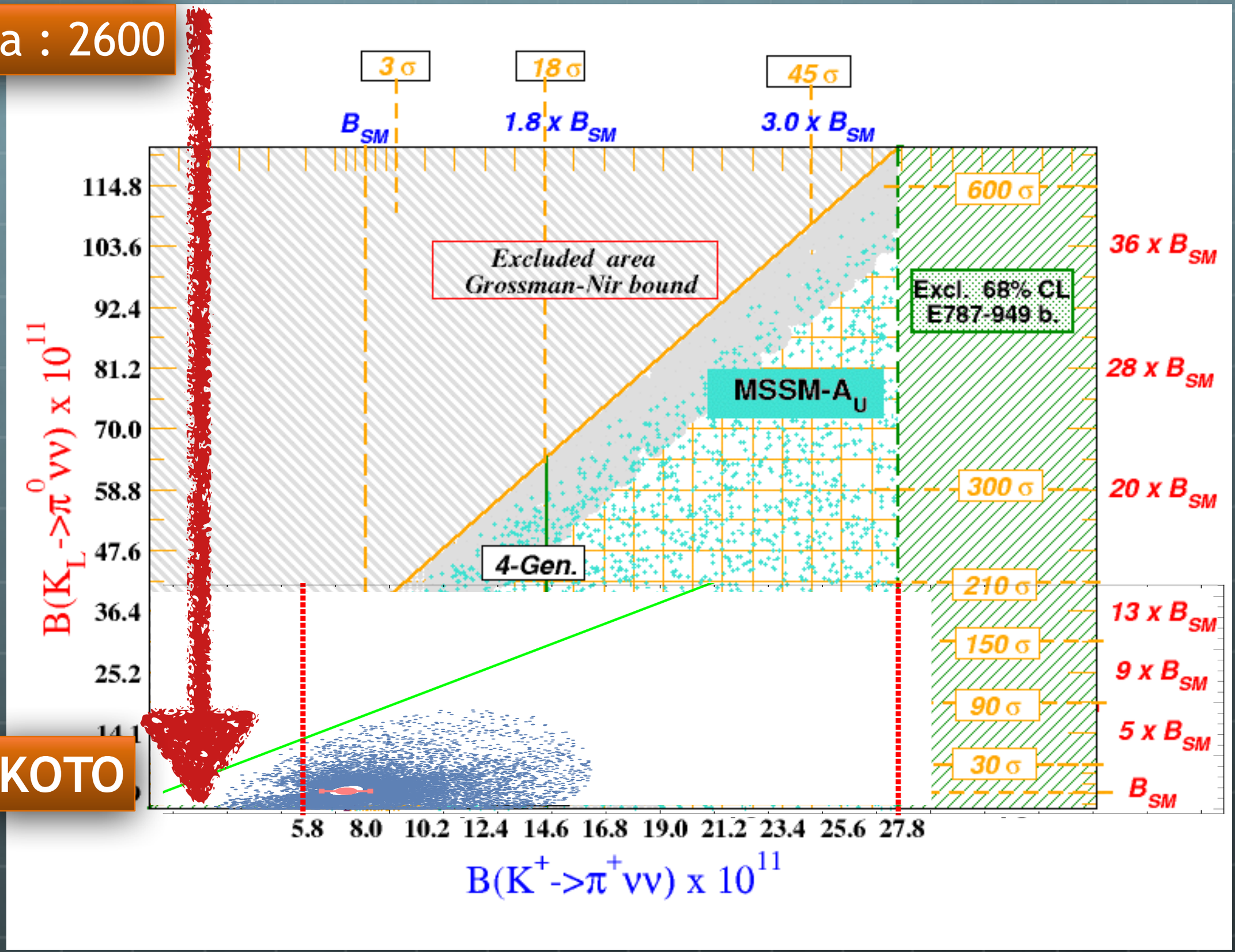

KOTO

http://www.lnf.infn.it/wg/vus/content/Krare.html

Operator Production Expansion

$$A(M \to F) = \langle F|\mathcal{H}_{eff}|M\rangle = \frac{G_F}{\sqrt{2}} \sum_i V^i_{CKM} C_i(\mu) \langle F|Q_i(\mu)|M\rangle$$

Operator Product Expansion, Renormalization Group and Weak Decays *

Andrzej J. Buras

arXiv:hep-ph/9901409v1 26 Jan 1999

PHYSICAL REVIEW VOLUME 179, NUMBER 5 25 MARCH 1969

Non-Lagrangian Models of Current Algebra*

KENNETH G. WILSON†
Laboratory of Nuclear Studies, Cornell University, Ithaca, New York 14850
(Received 25 November 1968)

An alternative is proposed to specific Lagrangian models of current algebra. In this alternative there are no explicit canonical fields, and operator products at the same point [say, $j_\mu(x)j^\mu(x)$] have no meaning. Instead, it is assumed that scale invariance is a broken symmetry of strong interactions, as proposed by Kastrup and Mack. Also, a generalization of equal-time commutators is assumed: Operator products at short distances have expansions involving local fields multiplying singular functions. It is assumed that the dominant fields are the $SU(3)\times SU(3)$ currents and the $SU(3)\times SU(3)$ multiplet containing the pion field. It is assumed that the pion field scales like a field of dimension Δ, where Δ is unspecified within the range $1\leq\Delta<4$; the value of Δ is a consequence of renormalization. These hypotheses imply several qualitative predictions: The second Weinberg sum rule does not hold for the difference of the K^* and axial-K^* propagators, even for exact $SU(2)\times SU(2)$; electromagnetic corrections require one subtraction proportional to the $I=1$, $I_z=0$ σ field; $\eta\to 3\pi$ and $\pi_0\to 2\gamma$ are allowed by current algebra. Octet dominance of nonleptonic weak processes can be understood, and a new form of superconvergence relation is deduced as a consequence. A generalization of the Bjorken limit is proposed.

Amplitude for a decay of a given meson M into a final state F is given as

$$A(M \to F) = \langle F|\mathcal{H}_{eff}|M\rangle = \frac{G_F}{\sqrt{2}} \sum_i V^i_{CKM} C_i(\mu) \langle F|Q_i(\mu)|M\rangle$$

G_F Fermi Constant : Universal gauge coupling of the Weak int.

V_{CKM} CKM Matrix Element : Quark mixing

$C_i(\mu)$ Wilson Coefficient : Short distance (perturbative) contribution

$< F|Q_i(\mu)|M >$ Hadronic matrix elements : Long distance (non-perturbative)

$$M : K_L \longrightarrow F : \pi^0 \nu\bar{\nu}$$

Branching ratio

$$\mathbf{Br}(K_L \to \pi^0 \nu\bar{\nu}) = \kappa_L (\frac{\mathbf{Im}\lambda_t}{\lambda^5} X(x_t))^2$$

$\lambda_t = V_{ts}^* V_{td}$ ⟵ From measured values

$\lambda = 0.2252(9)$ Precise measured Cabibbo angle

$$\kappa_L = 2.231 \pm 0.013 \cdot 10^{-10} [\frac{\lambda}{0.225}]$$

Branching ratio

$$\mathbf{Br}(K_L \to \pi^0 \nu\bar{\nu}) = \kappa_L \left(\frac{\mathbf{Im}\lambda_t}{\lambda^5} X(x_t)\right)^2$$

$\lambda_t = V_{ts}^* V_{td}$ ⟵ From measured values

$\lambda = 0.2252(9)$ Precise measured Cabibbo angle

$\kappa_L = 2.231 \pm 0.013 \cdot 10^{-10} \left[\frac{\lambda}{0.225}\right]$

Long distance contribution

$X(x_t)$ Lim-Inami function
Short distance contribution

To get the matrix-elements of these operators, and to carry out the phase-spa integration. parametrization with Ke3 dec

Progress of Theoretical Physics, Vol. 65, No. 1, January 1981

Effects of Superheavy Quarks and Leptons in Low-Energy Weak Processes $K_L \to \mu\bar{\mu}$, $K^+ \to \pi^+ \nu\bar{\nu}$ and $K^0 \leftrightarrow \bar{K}^0$

TAKEO INAMI and C. S. LIM

Institute of Physics, University of Tokyo, Komaba, Tokyo 153

(Received October 13, 1980)

We investigate potentially important effects due to the existence of superheavy quarks and leptons of the sequential type in higher-order weak processes at low energies. The second-order $\Delta S \neq 0$ neutral-current processes $K_L \to \mu\bar{\mu}$, $K^+ \to \pi^+ \nu\bar{\nu}$ and K_L-K_S mass difference are analysed allowing for fermions of masses comparable to or larger than the weak-boson mass in the Kobayashi-Maskawa scheme and in the general sequential scheme with an arbitrary number of generations. Possible connection between heavy-quark masses and light-heavy quark mixing are also examined. The requirement that the rare decay processes such as $K_L \to \mu\bar{\mu}$ and $K^+ \to \pi^+ \nu\bar{\nu}$ be absent up to order αG_F yields a rather stringent bound on the magnitude of light-heavy quark mixing: Such mixing has to be less than m_W/m_{Quark} times a factor much smaller than unity.

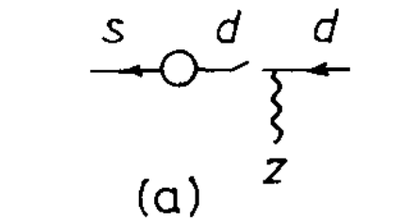

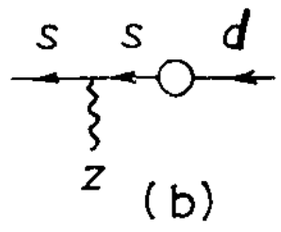

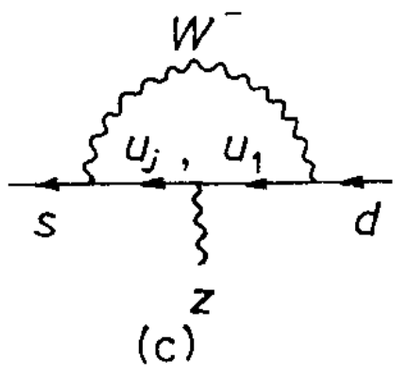

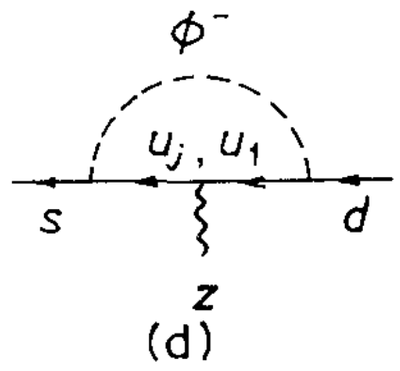

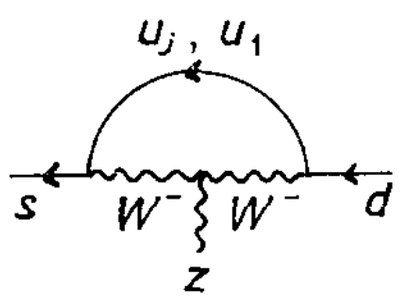

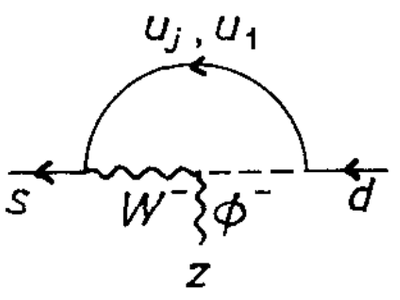

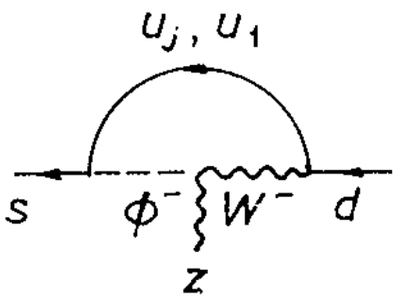

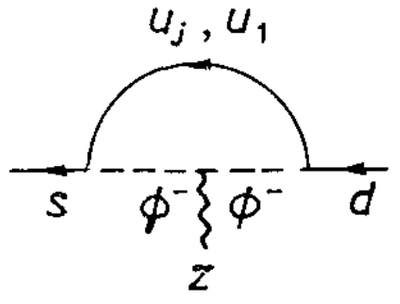

$$\Gamma_z \equiv \sum_{i=1}^{h} \Gamma^{(i)} = \frac{1}{4} x_j - \frac{3}{8} \frac{1}{x_j - 1} + \frac{3}{8} \frac{2x_j^2 - x_j}{(x_j - 1)^2} \ln x_j + \gamma(x_j, \xi) - (x_j \to x_1).$$

The $K_L \to \mu^+ \mu^-$ decay and the $n\lambda Z$-vertex in the Weinberg–Salam model

M. B. Voloshin

Moscow Physico-Technical Institute
(Submitted November 19, 1975)
Yad. Fiz. **24**, 810–819 (October 1976)

The $n\lambda Z$ vertex in the Weinberg–Salam model is calculated using two independent methods in the one-loop approximation for free quarks. The results of these calculations are used to estimate the $K_L \to \mu^+ \mu^-$ decay amplitude and the mass of the c quark.

PACS numbers: 13.20.Eb, 12.30.Cx

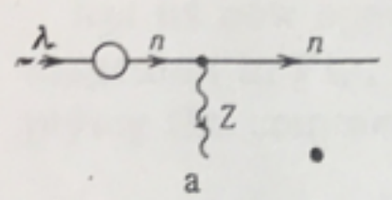

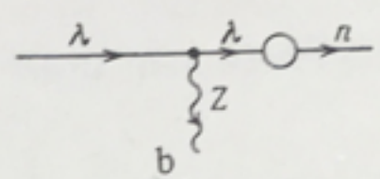

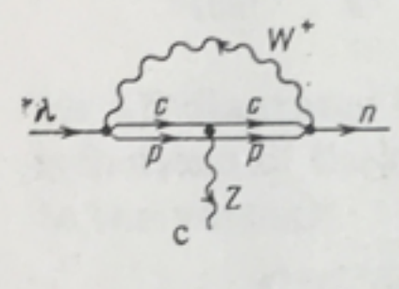

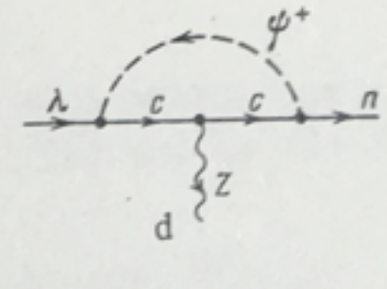

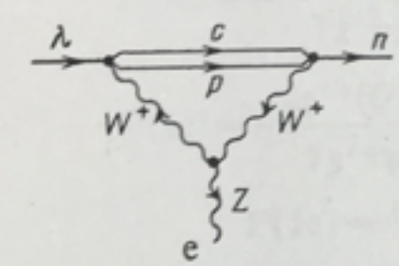

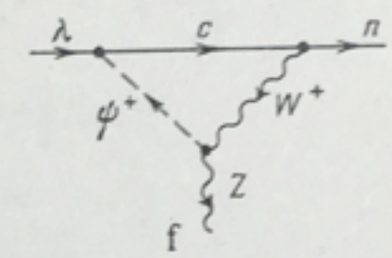

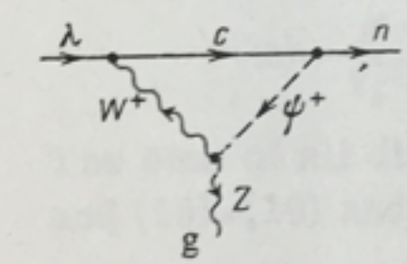

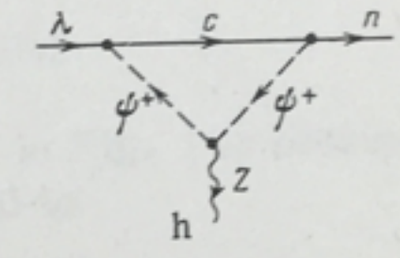

$$x_j \equiv m_{uj}^2 / m_W^2$$

Determination of the Br.
- Using loop-level observables -

	$\{\lvert\varepsilon_K\rvert, \Delta M_d/\Delta M_s, S_{\psi K_S}\}_{\rm SM}$	$\{\Delta M_d, \Delta M_s, S_{\psi K_S}\}_{\rm SM}$	$\{\lvert\varepsilon_K\rvert, \Delta M_d, \Delta M_s, S_{\psi K_S}\}_{\rm SM}$
$\lvert V_{cb}\rvert\ [10^{-3}]$	$42.59^{+1.41}_{-1.26}$	$41.30^{+2.65}_{-2.47}$	$42.35^{+1.25}_{-1.13}$
$\lvert V_{ub}\rvert\ [10^{-3}]$	$3.62^{+0.15}_{-0.14}$	$3.51^{+0.27}_{-0.25}$	$3.61^{+0.15}_{-0.14}$
$\lvert V_{td}\rvert\ [10^{-3}]$	$8.96^{+0.28}_{-0.28}$	$8.68^{+0.66}_{-0.62}$	$8.95^{+0.27}_{-0.28}$
$\lvert V_{ts}\rvert\ [10^{-3}]$	$41.79^{+1.43}_{-1.27}$	$40.52^{+2.60}_{-2.42}$	$41.55^{+1.27}_{-1.14}$
$\mathcal{B}(K^+ \to \pi^+\nu\bar{\nu})\ [10^{-11}]$	$9.18^{+0.79}_{-0.71}$	$8.39^{+1.76}_{-1.41}$	$9.08^{+0.74}_{-0.68}$
$\mathcal{B}(K_L \to \pi^0\nu\bar{\nu})\ [10^{-11}]$	$3.01^{+0.33}_{-0.29}$	$2.66^{+0.84}_{-0.63}$	$2.98^{+0.32}_{-0.28}$
$\overline{\mathcal{B}}(B_s \to \mu^+\mu^-)\ [10^{-9}]$	$3.69^{+0.30}_{-0.26}$	$3.46^{+0.49}_{-0.43}$	$3.64^{+0.27}_{-0.24}$
$\mathcal{B}(B_d \to \mu^+\mu^-)\ [10^{-10}]$	$1.09^{+0.08}_{-0.08}$	$1.02^{+0.17}_{-0.15}$	$1.09^{+0.08}_{-0.08}$
$\mathrm{Im}(\lambda_t)\ [10^{-4}]$	$1.43^{+0.08}_{-0.07}$	$1.35^{+0.20}_{-0.17}$	$1.42^{+0.07}_{-0.07}$
$\mathrm{Re}(\lambda_t)\ [10^{-4}]$	$-3.46^{+0.18}_{-0.19}$	$-3.25^{+0.40}_{-0.45}$	$-3.43^{+0.17}_{-0.18}$

A. Buras, arXiv:1503.02693

Grossman-Nir Limit

$K_L \to \pi^0 \nu \bar{\nu}$ beyond the Standard Model ⋆

Yuval Grossman [a], Yosef Nir [b]

[a] *Stanford Linear Accelerator Center, Stanford University, Stanford, CA 94309, USA*
[b] *Department of Particle Physics, Weizmann Institute of Science, Rehovot 76100, Israel*

Received 29 January 1997
Editor: M. Dine

Abstract

We analyze the decay $K_L \to \pi^0 \nu \bar{\nu}$ in a model independent way. If lepton flavor is conserved the final state is (to a good approximation) purely CP even. In that case this decay mode goes mainly through CP violating interference between mixing and decay. Consequently, a theoretically clean relation between the measured rate and electroweak parameters holds in any given model. Specifically, $\Gamma(K_L \to \pi^0 \nu \bar{\nu})/\Gamma(K^+ \to \pi^+ \nu \bar{\nu}) = \sin^2 \theta$ (up to known isospin corrections), where θ is the relative CP violating phase between the $K - \bar{K}$ mixing amplitude and the $s \to d \nu \bar{\nu}$ decay amplitude. The experimental bound on $\mathrm{BR}(K^+ \to \pi^+ \nu \bar{\nu})$ provides a model independent upper bound: $\mathrm{BR}(K_L \to \pi^0 \nu \bar{\nu}) < 1.1 \times 10^{-8}$. In models with lepton flavor violation, the final state is not necessarily a CP eigenstate. Then CP conserving contributions can dominate the decay rate.

Physics Letters B 398 (1997) 163–168

BNL E787 : Search for $K^+ \to \pi^+ \nu\bar{\nu}$

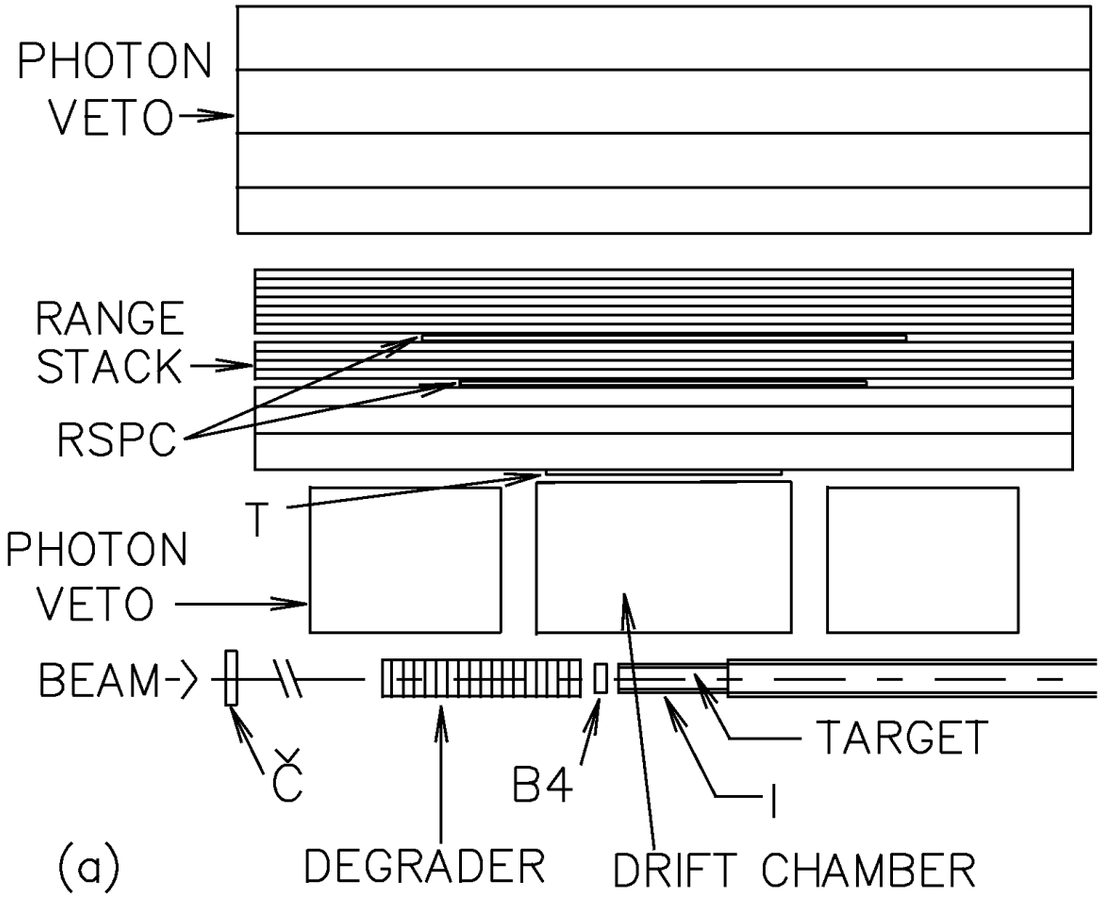

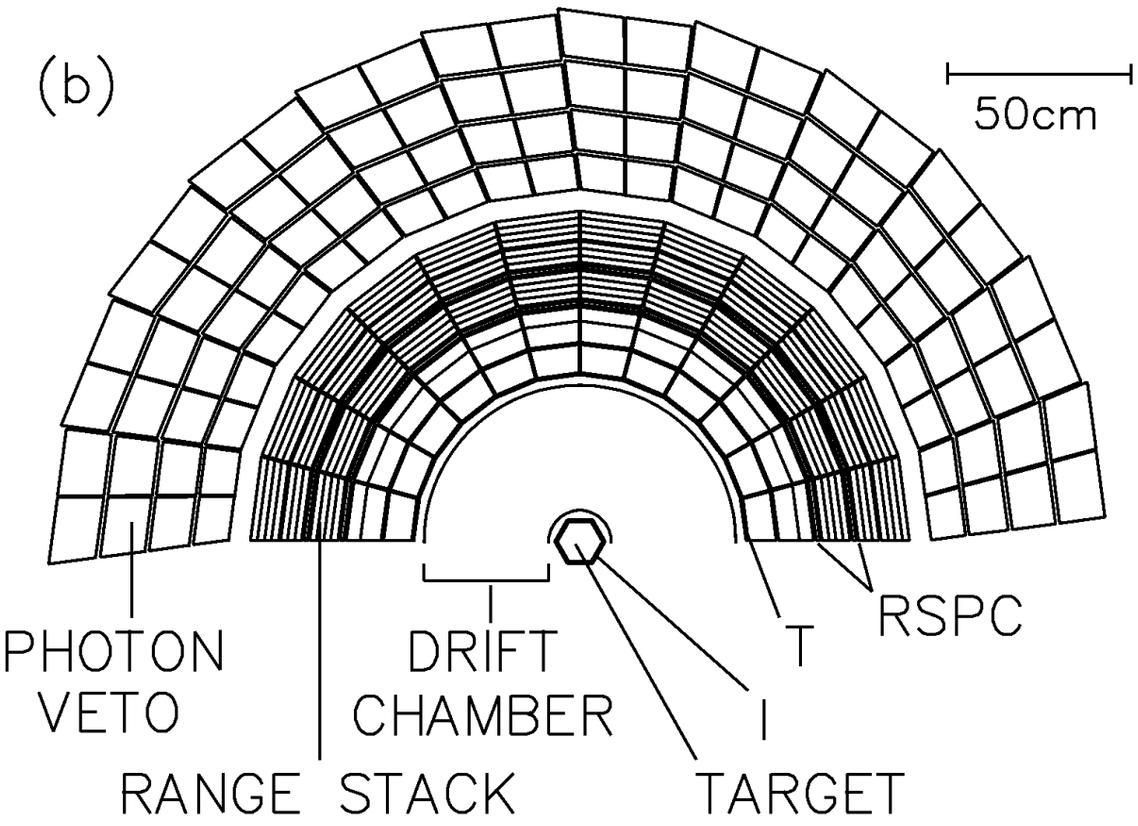

- Stopped Kaon (800 MeV/c) in target
- Main Backgrounds: $K^+ \to \pi^+\pi^0$ $K^+ \to \mu^+\nu$
- K^+ incident, only one charged particle, π^+

BNL E787 Experiment

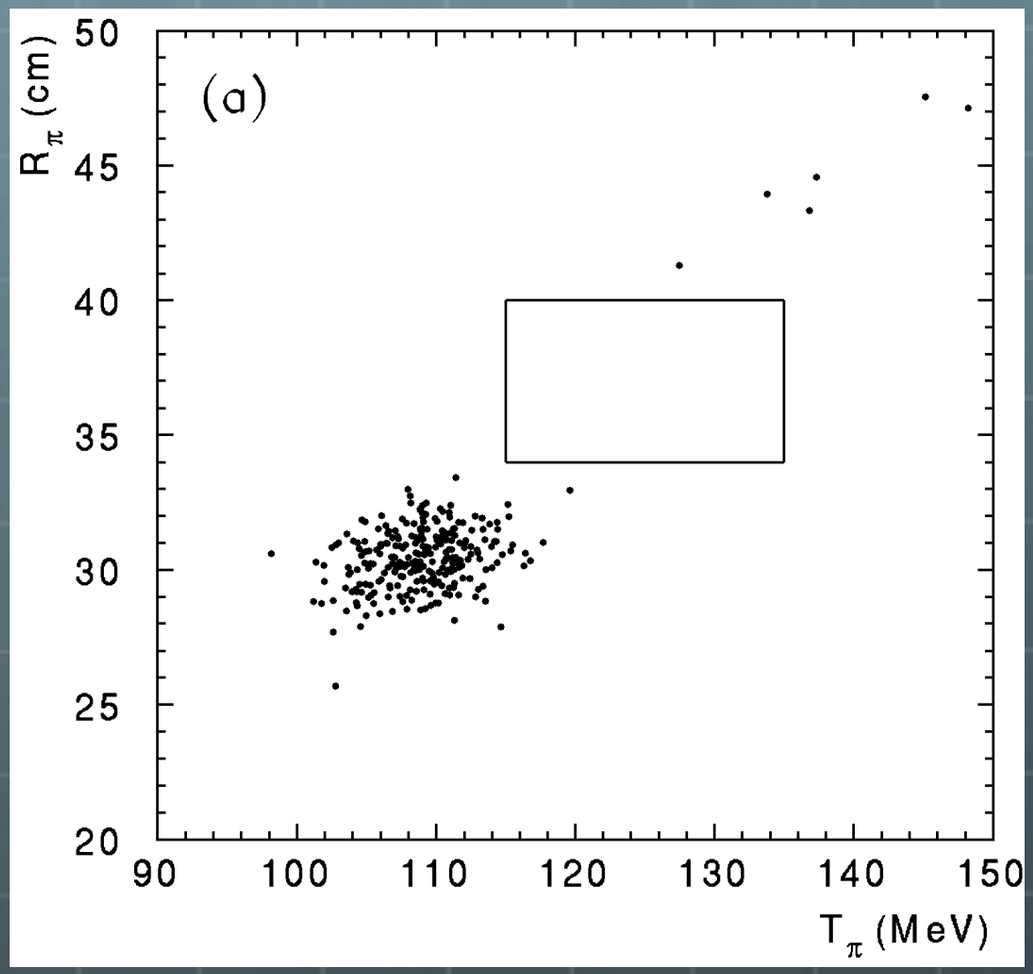

PRL 76, 1421 (1996)

$$\mathbf{Br}(K^+ \to \pi^+ \nu\bar{\nu}) < 2.4 \times 10^{-9}$$

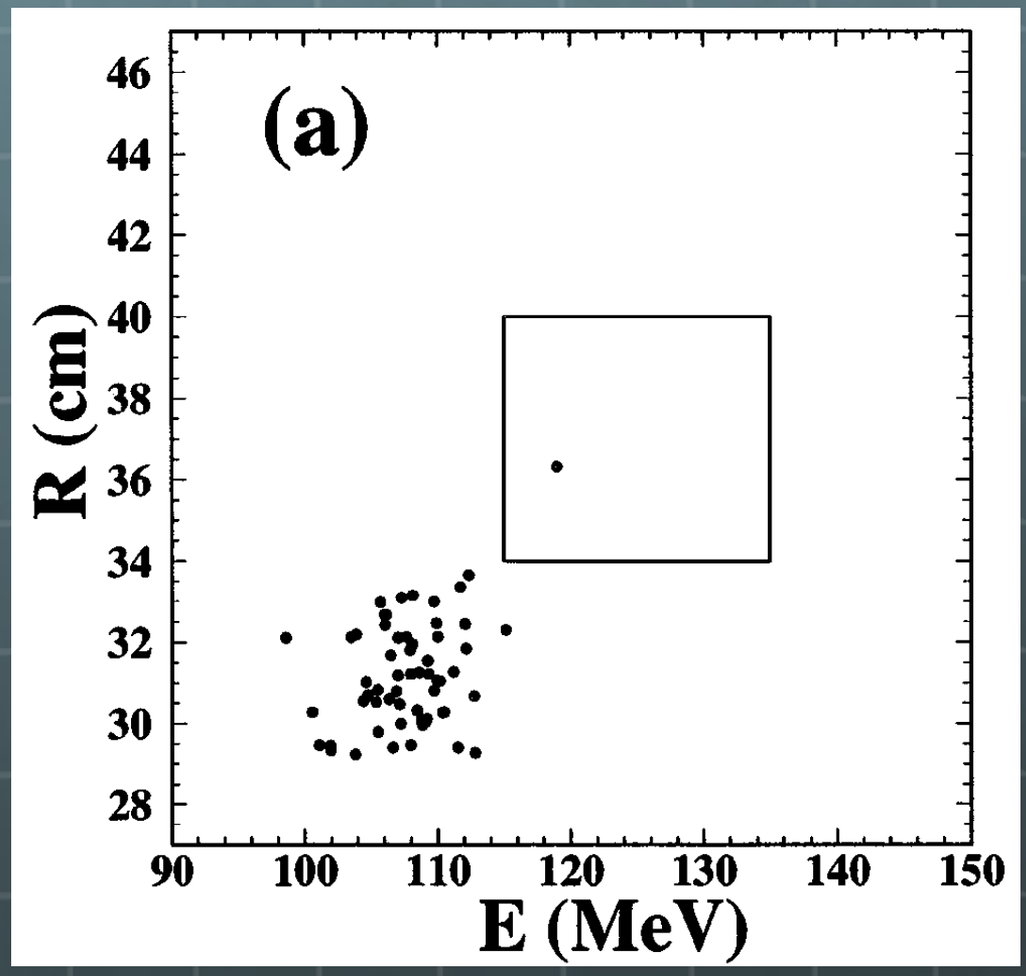

PRL 79, 2204 (1997)

$$\mathbf{Br}(K^+ \to \pi^+ \nu\bar{\nu}) = 4.2^{+9.7}_{-3.5} \times 10^{-10}$$

Decay amplitude

$$A = \langle \pi^0 \nu\bar{\nu} | H | K^0 \rangle, \quad \bar{A} = \langle \pi^0 \nu\bar{\nu} | H | \bar{K}^0 \rangle.$$

$|\bar{A}/A| = 1$ CP Limit (CP symmetry is exact)

$$|K1> = \frac{1}{\sqrt{2}}(|K^0> - |\bar{K}^0>) \qquad |K2> = \frac{1}{\sqrt{2}}(|K^0> + |\bar{K}^0>)$$

CP EVEN CP ODD

$$|K_S\rangle = \frac{1}{\sqrt{1+|\epsilon|^2}}(|K_1\rangle + \epsilon|K_2\rangle),$$

$$|K_L\rangle = \frac{1}{\sqrt{1+|\epsilon|^2}}(|K_2\rangle + \epsilon|K_1\rangle),$$

$$|q/p| \neq 1$$

Indirect CP Violation

$$|K_{L,S}\rangle = p|K^0\rangle \mp q|\bar{K}^0\rangle$$

$$\langle \pi^0 \nu\bar{\nu} | H | K_{L,S} \rangle = pA \mp q\bar{A}$$

$$\lambda \equiv \frac{q}{p}\frac{\bar{A}}{A}$$

$$\frac{\Gamma(K_L \to \pi^0 \nu\bar{\nu})}{\Gamma(K_S \to \pi^0 \nu\bar{\nu})} = \frac{1 + |\lambda|^2 - 2\mathrm{Re}\,\lambda}{1 + |\lambda|^2 + 2\mathrm{Re}\,\lambda}$$

PHYSICAL REVIEW D VOLUME 39, NUMBER 11 1 JUNE 1989

CP-violating decay $K_L^0 \to \pi^0 \nu\bar{\nu}$

Laurence S. Littenberg
Department of Physics, Brookhaven National Laboratory, Upton, New York 11973
(Received 6 January 1989)

The process $K_L^0 \to \pi^0 \nu\bar{\nu}$ offers perhaps the clearest window yet proposed into the origin of *CP* violation. The largest expected contribution to this decay is a direct *CP*-violating term at $\approx$few$\times 10^{-12}$. The indirect *CP*-violating contribution is some *3 orders of magnitude* smaller, and *CP*-conserving contributions are also estimated to be extremely small. Although this decay has never been directly probed, a branching ratio upper limit of $\sim 1\%$ can be extracted from previous data on $K_L^0 \to 2\pi^0$. This leaves an enormous range in which to search for new physics. If the Kobayashi-Maskawa (KM) model prediction can be reached, a theoretically clean determination of the KM product $\sin\theta_2 \sin\theta_3 \sin\delta$ can be made.

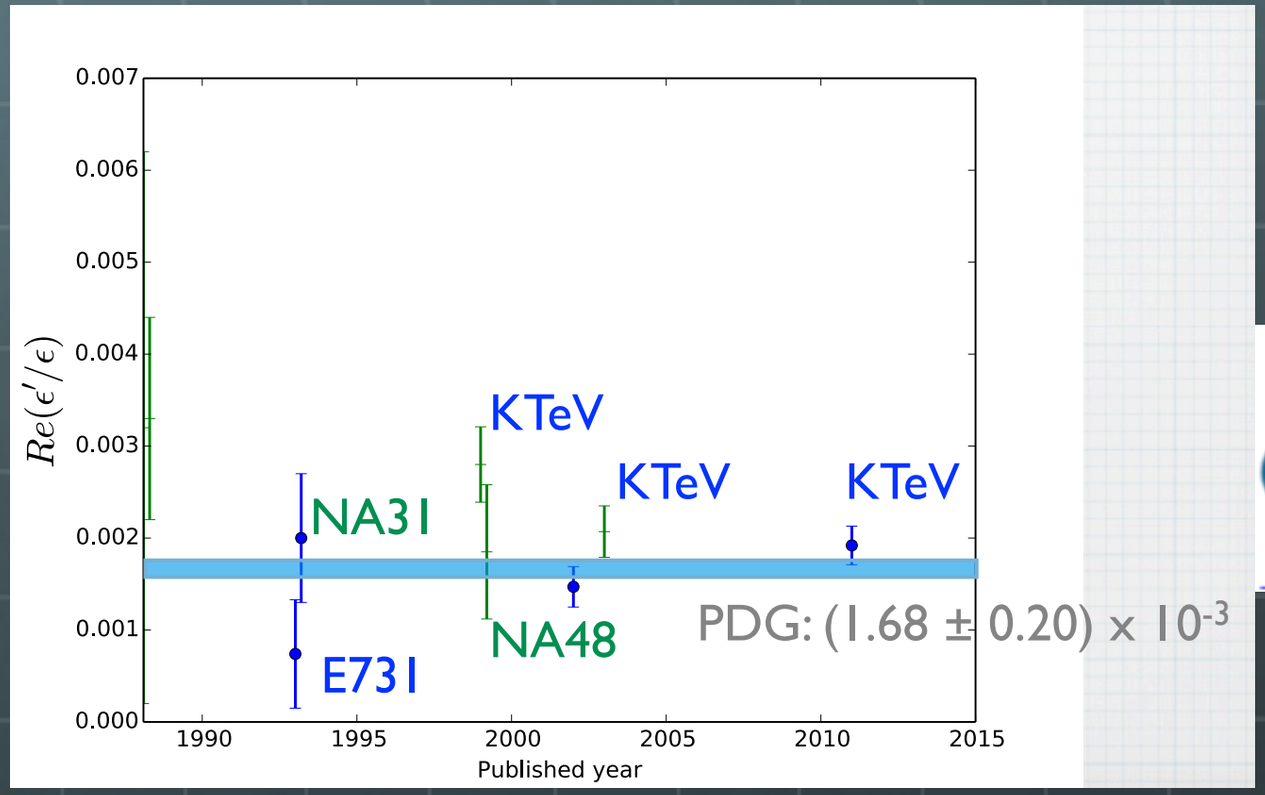

Direct CP-violation

Welcome to the **KLOE** Experiment at the DAFNE accelerator of the INFN LNF

INFN Istituto Nazionale di Fisica Nucleare Laboratori Nazionali di Frascati

T. Yamanaka , 50 Years of CP Violation

$$|\lambda| = 1 \text{ to } \mathcal{O}(10^{-3}) \text{ accuracy.}$$

Leading CP Violation effect : Phase

Arbitrary phase between Direct and Indirect CP Violation

$$\lambda = e^{2i\theta}$$

$$\frac{\Gamma(K_L \to \pi^0 \nu\bar{\nu})}{\Gamma(K_S \to \pi^0 \nu\bar{\nu})} = \frac{1 - \cos 2\theta}{1 + \cos 2\theta} = \tan^2\theta$$

$$a_{\rm CP} \equiv r_{\rm is} \frac{\Gamma(K_L \to \pi^0 \nu\bar{\nu})}{\Gamma(K^+ \to \pi^+ \nu\bar{\nu})}$$
$$= \frac{1 - \cos 2\theta}{2} = \sin^2\theta,$$

$$\frac{A(K^0 \to \pi^0 \nu\bar{\nu})}{A(K^+ \to \pi^+ \nu\bar{\nu})} = \frac{1}{\sqrt{2}}$$

$$\mathrm{BR}(K_L \to \pi^0 \nu\bar{\nu}) < 4.4 \times \mathrm{BR}(K^+ \to \pi^+ \nu\bar{\nu})$$

$\tau_{K_L}/\tau_{K^+} = 4.17$

$r_{is} = 0.954$

PHYSICAL REVIEW D VOLUME 39, NUMBER 11 1 JUNE 1989

CP-violating decay $K_L^0 \to \pi^0 \nu\bar{\nu}$

Laurence S. Littenberg
Department of Physics, Brookhaven National Laboratory, Upton, New York 11973
(Received 6 January 1989)

The process $K_L^0 \to \pi^0 \nu\bar{\nu}$ offers perhaps the clearest window yet proposed into the origin of *CP* violation. The largest expected contribution to this decay is a direct *CP*-violating term at $\approx$few$\times 10^{-12}$. The indirect *CP*-violating contribution is some *3 orders of magnitude* smaller, and *CP*-conserving contributions are also estimated to be extremely small. Although this decay has never been directly probed, a branching ratio upper limit of $\sim 1\%$ can be extracted from previous data on $K_L^0 \to 2\pi^0$. This leaves an enormous range in which to search for new physics. If the Kobayashi-Maskawa (KM) model prediction can be reached, a theoretically clean determination of the KM product $\sin\theta_2 \sin\theta_3 \sin\delta$ can be made.

Searching for Direct CP-violation

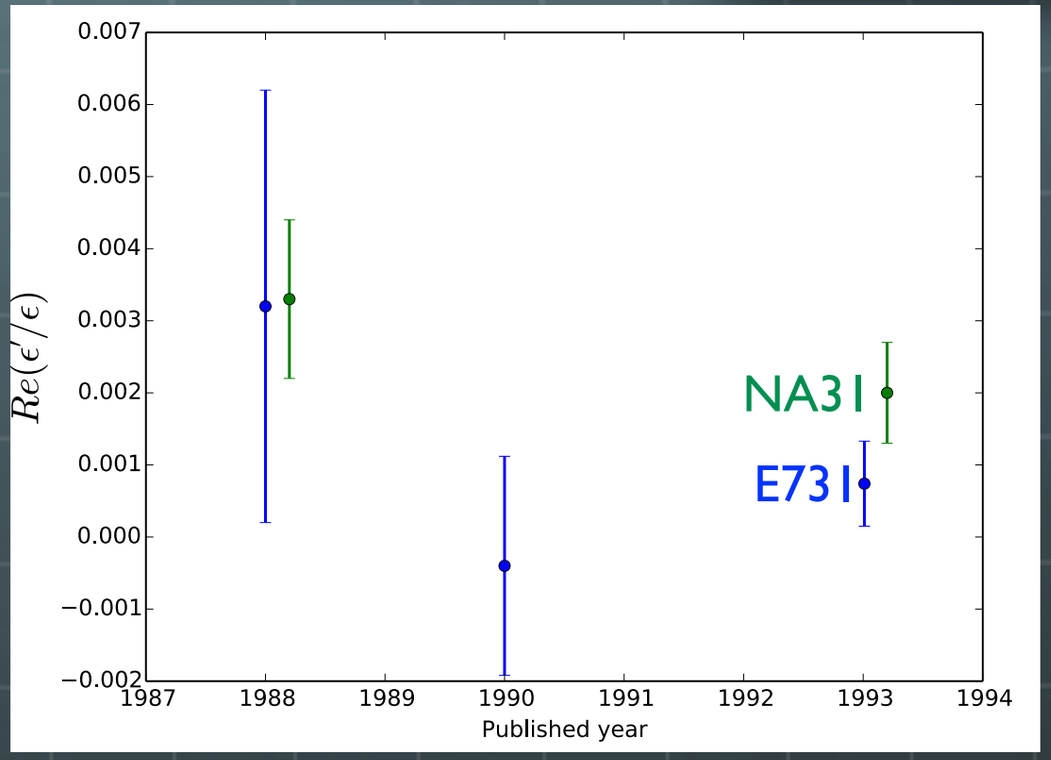

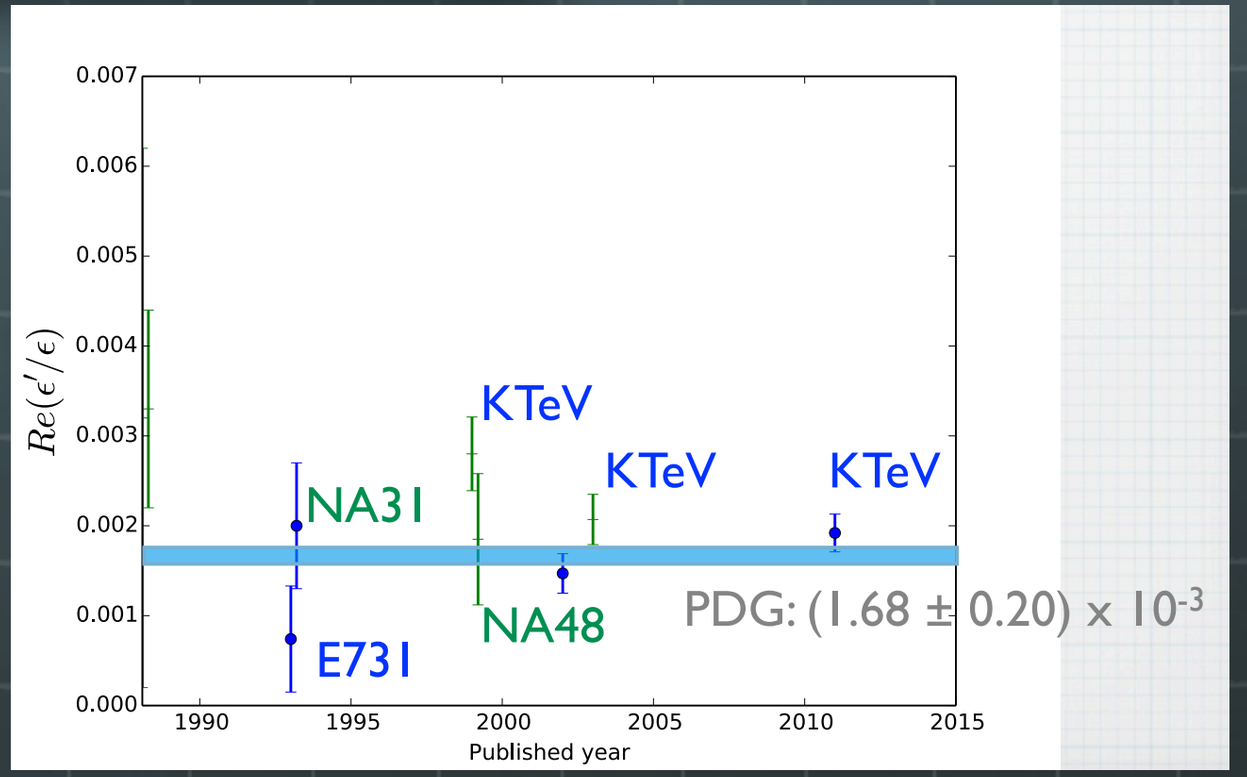

T. Yamanaka , 50 Years of CP Violation

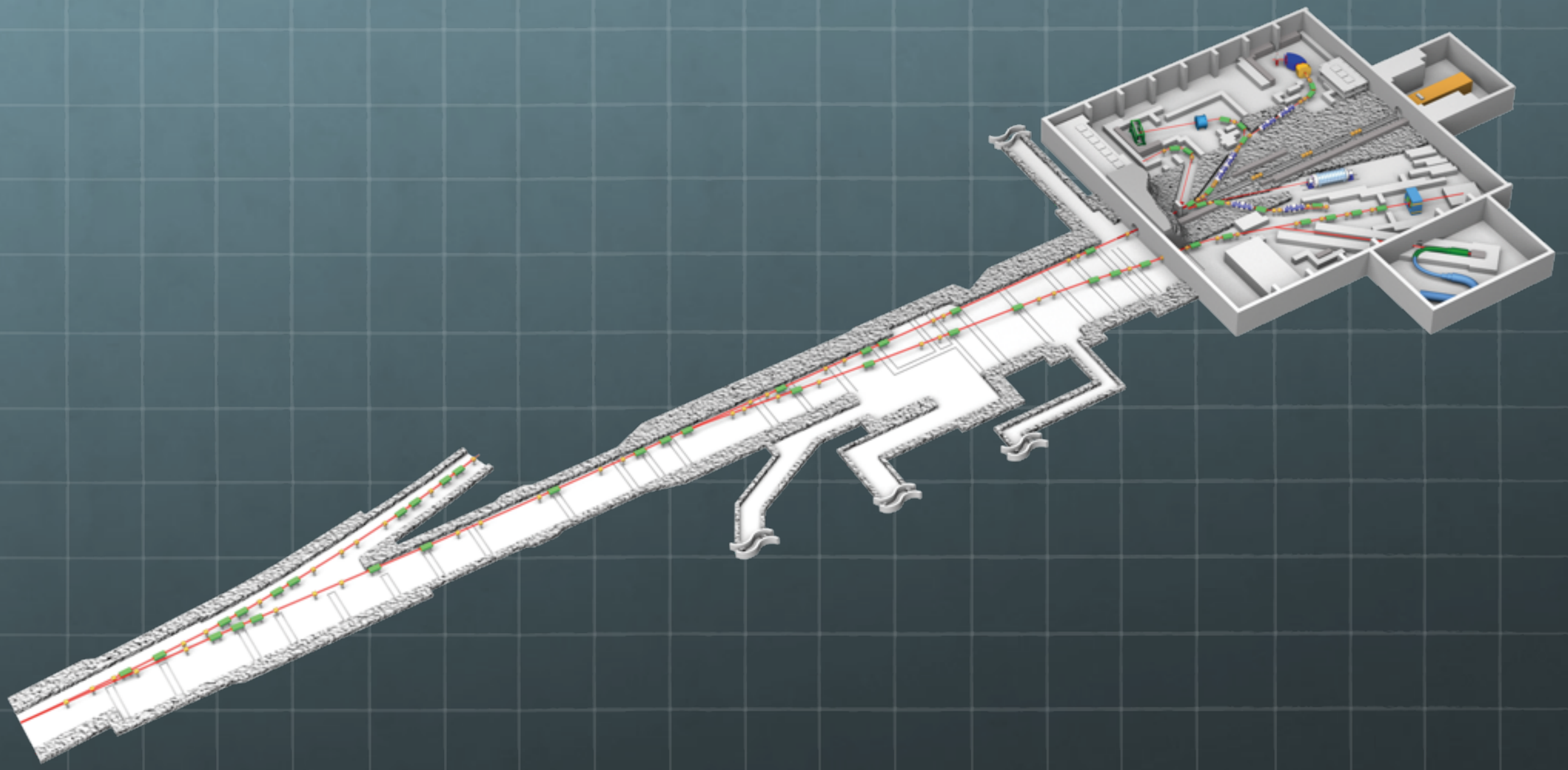

Kaon Physics

To understand building blocks of our universe and interaction among them by using various K-meson decays

Kaon rare decay $K_L \rightarrow \pi^0 \nu\nu$

What is K-meason ?

Matter made of quark-antiquark including s-quark

Baryon

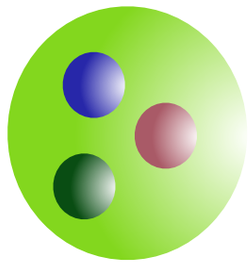

Proton · Neutron · Lambda

(uud) (ddu) (uds)

Meson

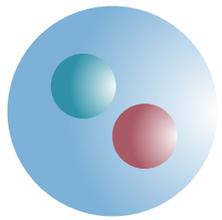

Pion · Kaon · B-Meson

(ud)... (su)... (bd)...

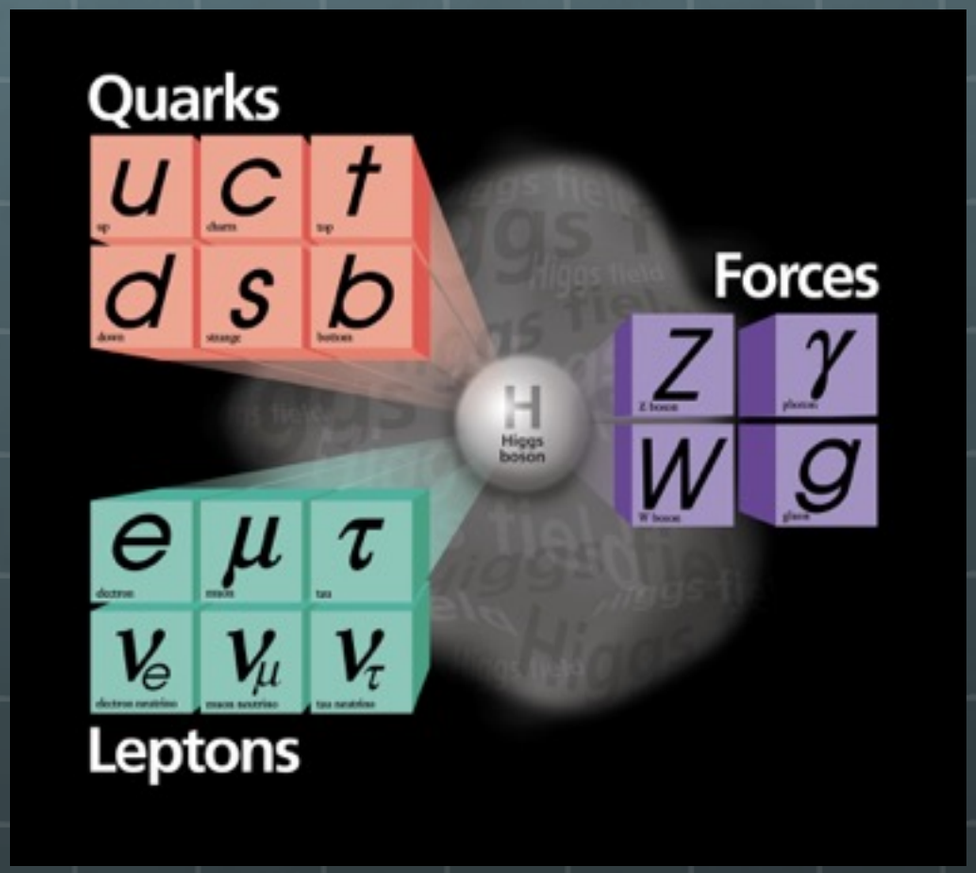

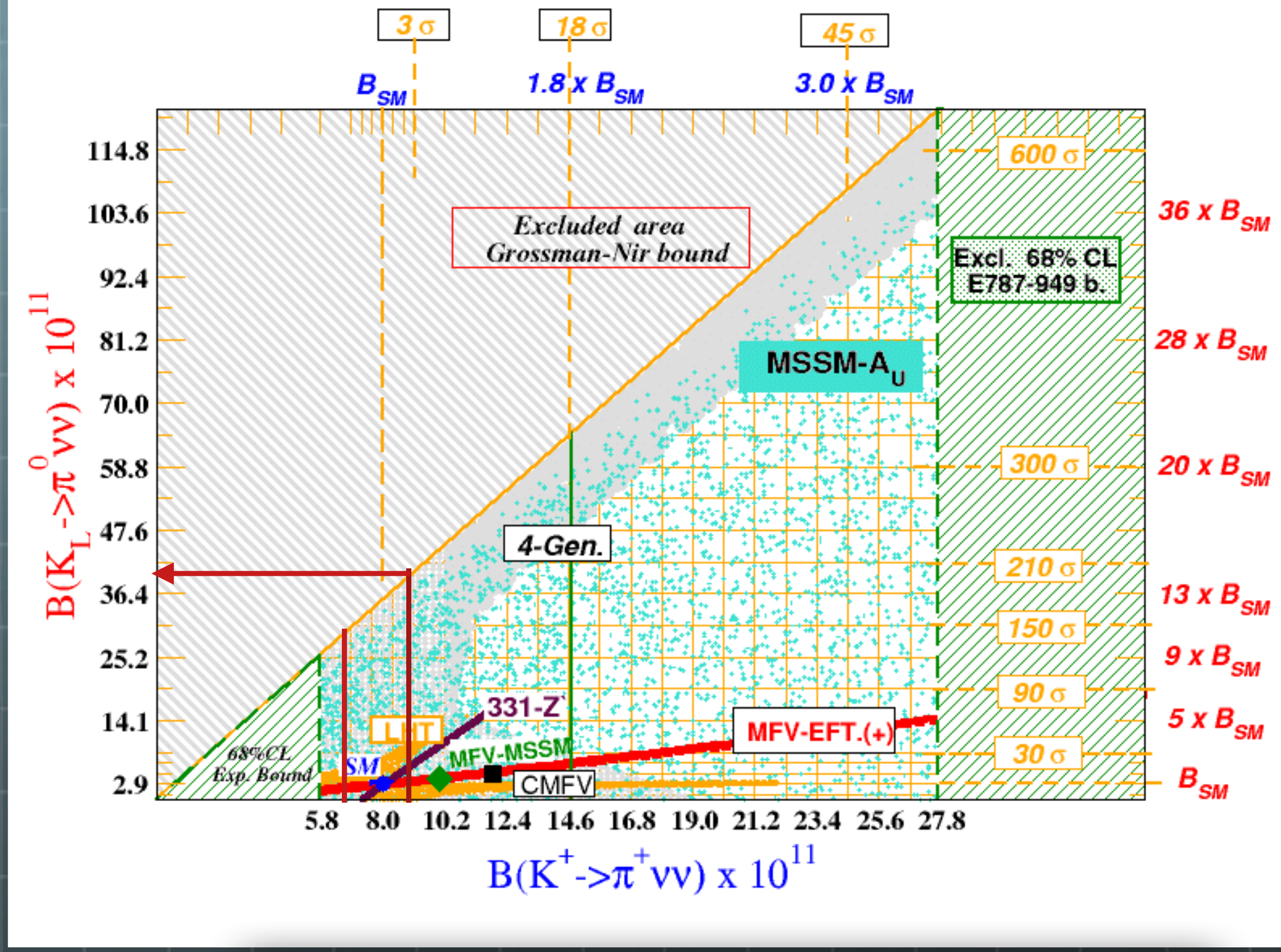

http://www.lnf.infn.it/wg/vus/content/Krare.html

3 years from now

- Up-graded detector System
- Higher beam intensity of J-PARC

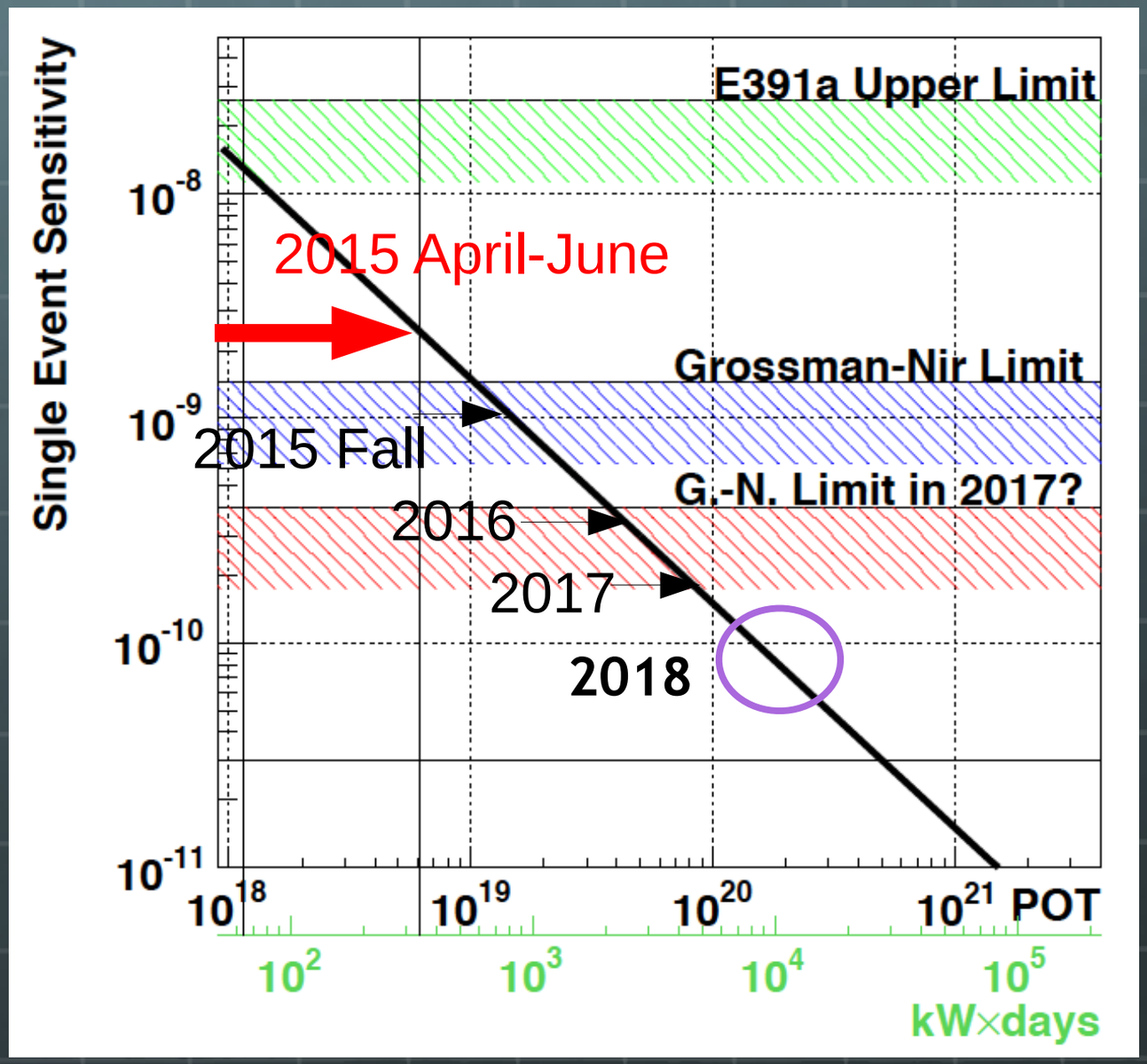

Experimental Status

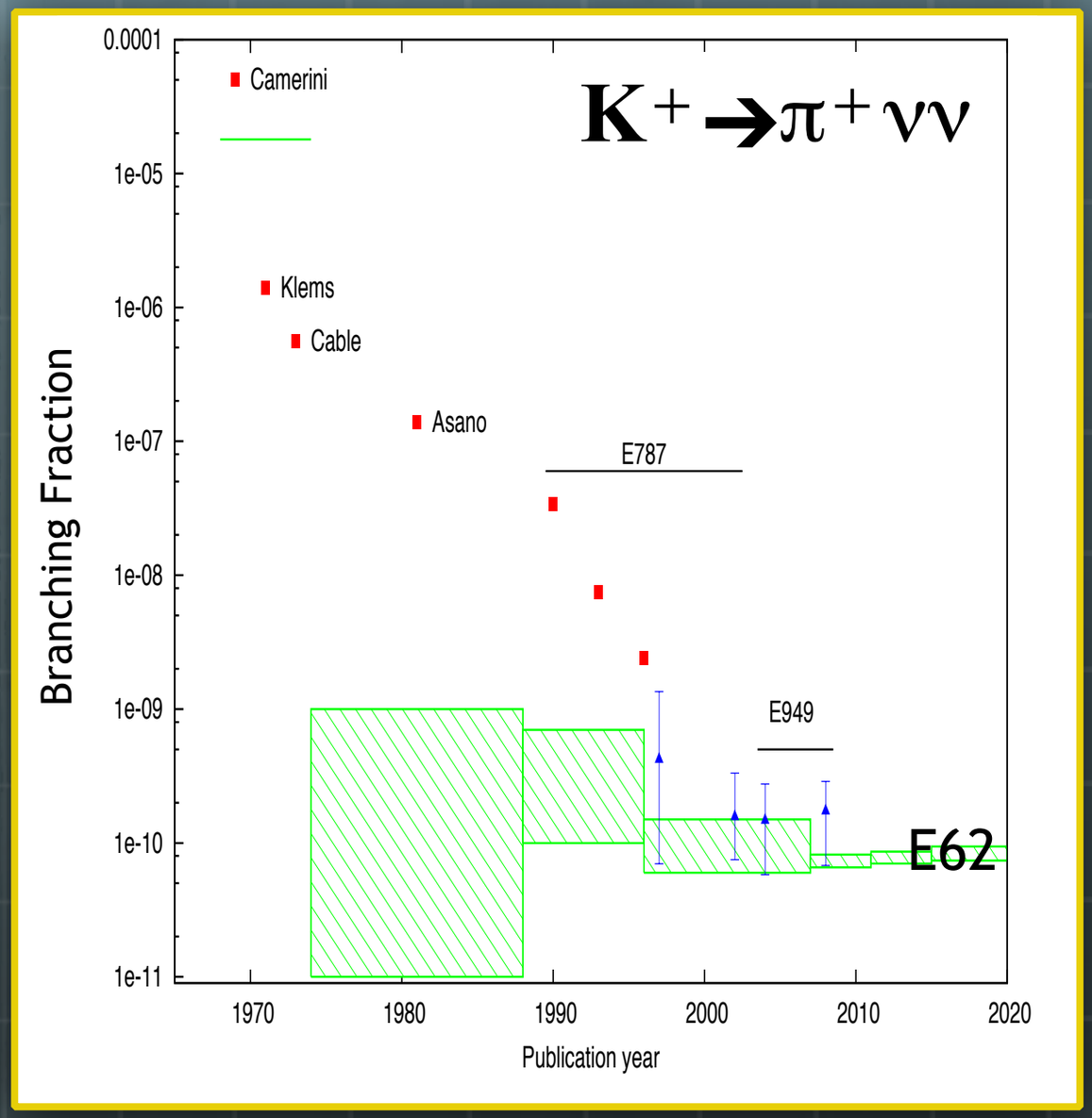

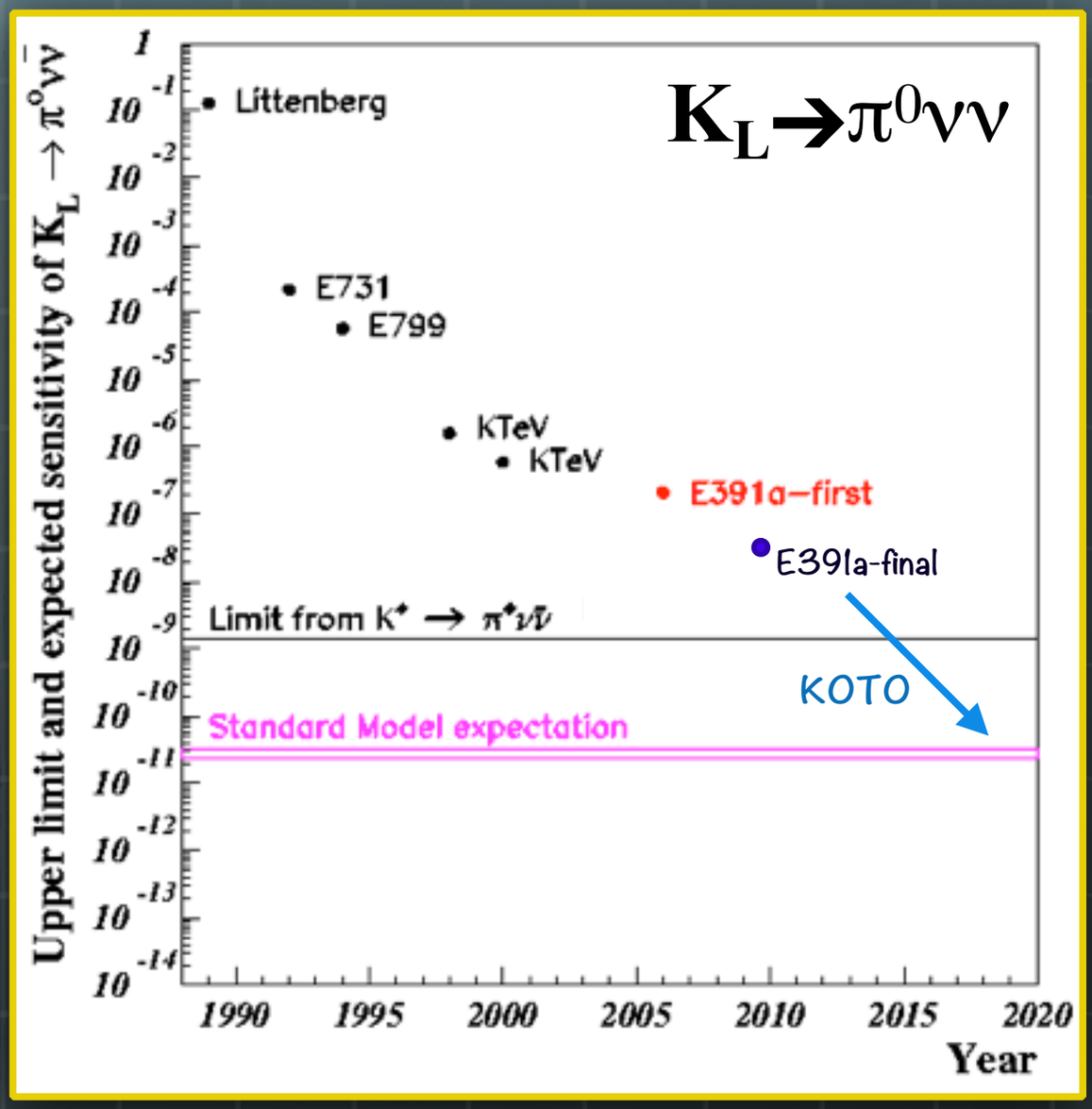

Still far from the goal …

Decay

Transition from a (unstable) state to other (stable) state

Conservation : Energy-momentum, charge, CPT

Key observation : decay probability

Observable

$$\Gamma_{i\to f} = \frac{2\pi}{\hbar}\cdot\int d\rho_f \cdot \mid M_{i\to f} \mid^2$$

Kinematics

How many momentum state for given energy

$K_S \to \pi^0\pi^0$ **v.s.** $K_L \to \pi^0\pi^0\pi^0$

Dynamics

For given process to consider
Nature of (mixed) interaction
Coupling constants, mixing etc.

Unitarily Triangles and New physics beyond SM

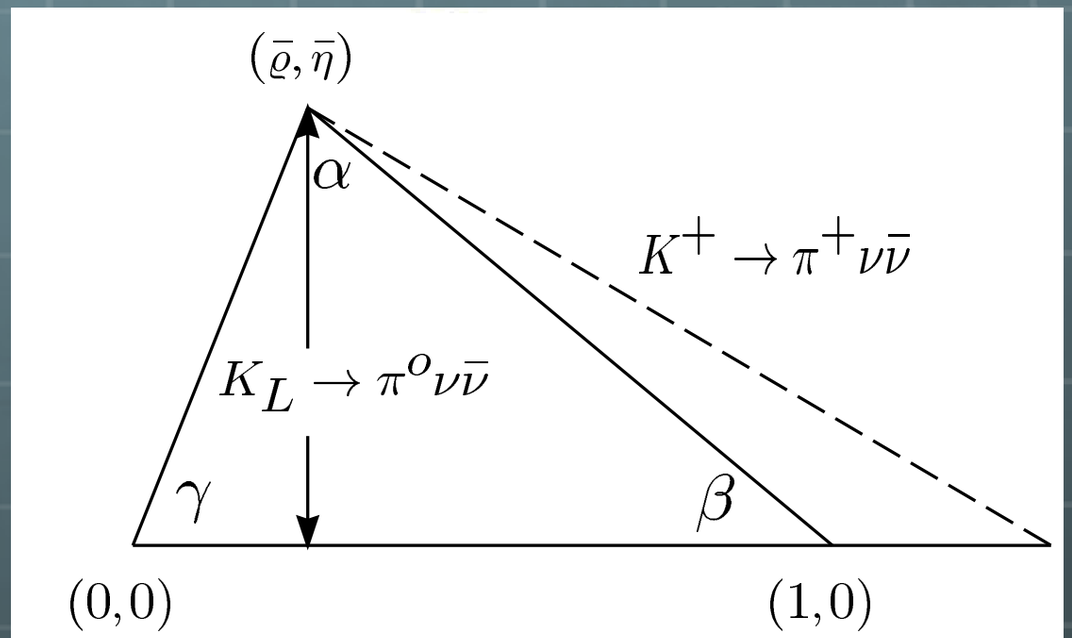

$$B(K_L^0 \to \pi^0 \nu\bar{\nu}) = 1.94 \cdot 10^{-10} \eta^2 A^4 X^2(x_t)$$

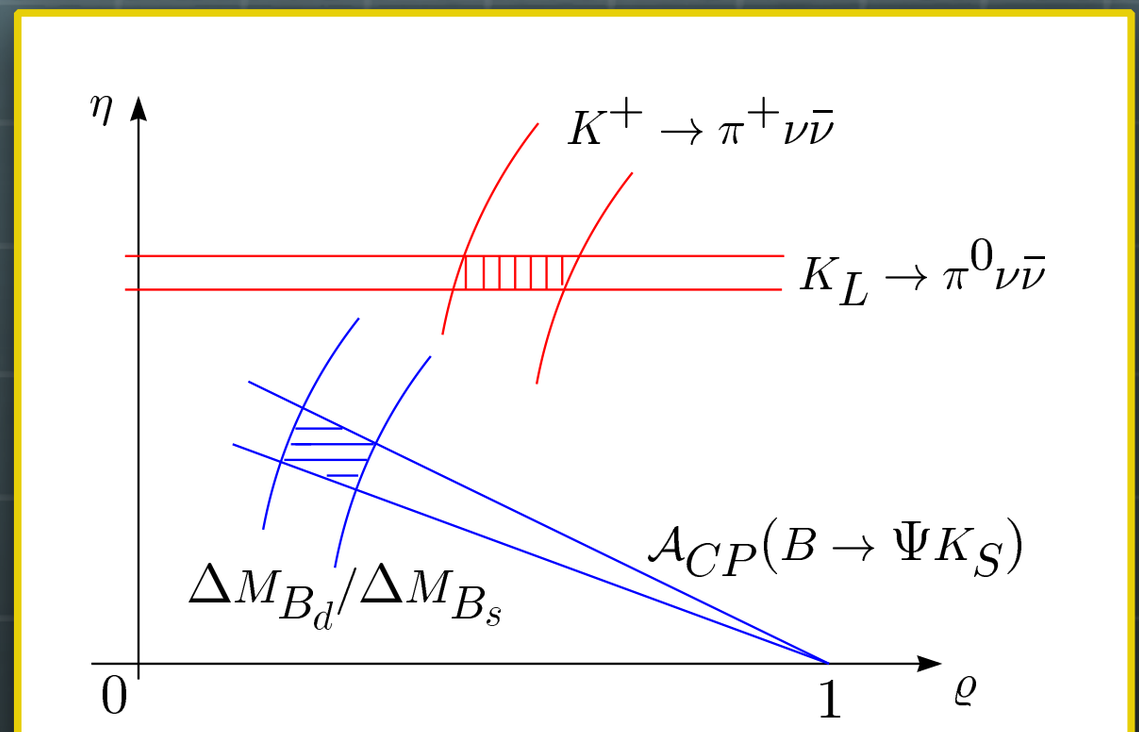

G. Buchalla arXiv:0110313

Highly suppressed process (in SM)

$$K^+ \to \pi^+ \nu\overline{\nu}$$

$$K_1 \to \pi^0 \nu\overline{\nu} \qquad\qquad K_2 \to \pi^0 \nu\overline{\nu}$$

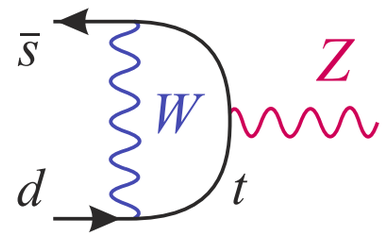

$$\frac{m_t^2}{M_W^2}(\mathrm{Re}\, V_{ts}^\dagger V_{td} \sim \lambda^5) \qquad \frac{m_t^2}{M_W^2}(\mathrm{Im}\, V_{ts}^\dagger V_{td} \sim \lambda^5)$$

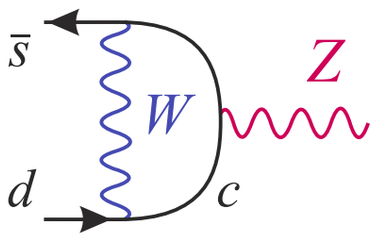

$$\frac{m_c^2}{M_W^2}(\mathrm{Re}\, V_{cs}^\dagger V_{cd} \sim \lambda) \qquad \frac{m_c^2}{M_W^2}(\mathrm{Im}\, V_{cs}^\dagger V_{cd} \sim \lambda^5)$$

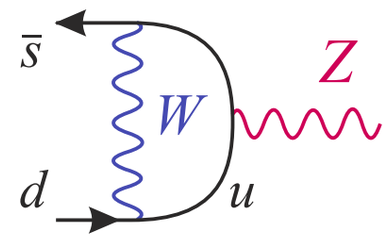

$$\frac{m_u^2}{M_W^2}(\mathrm{Re}\, V_{us}^\dagger V_{ud} \sim \lambda) \qquad \frac{m_u^2}{M_W^2}(\mathrm{Im}\, V_{us}^\dagger V_{ud} = 0)$$

C. Smith, arXiv:1409.6162

Hadronic matrix elements

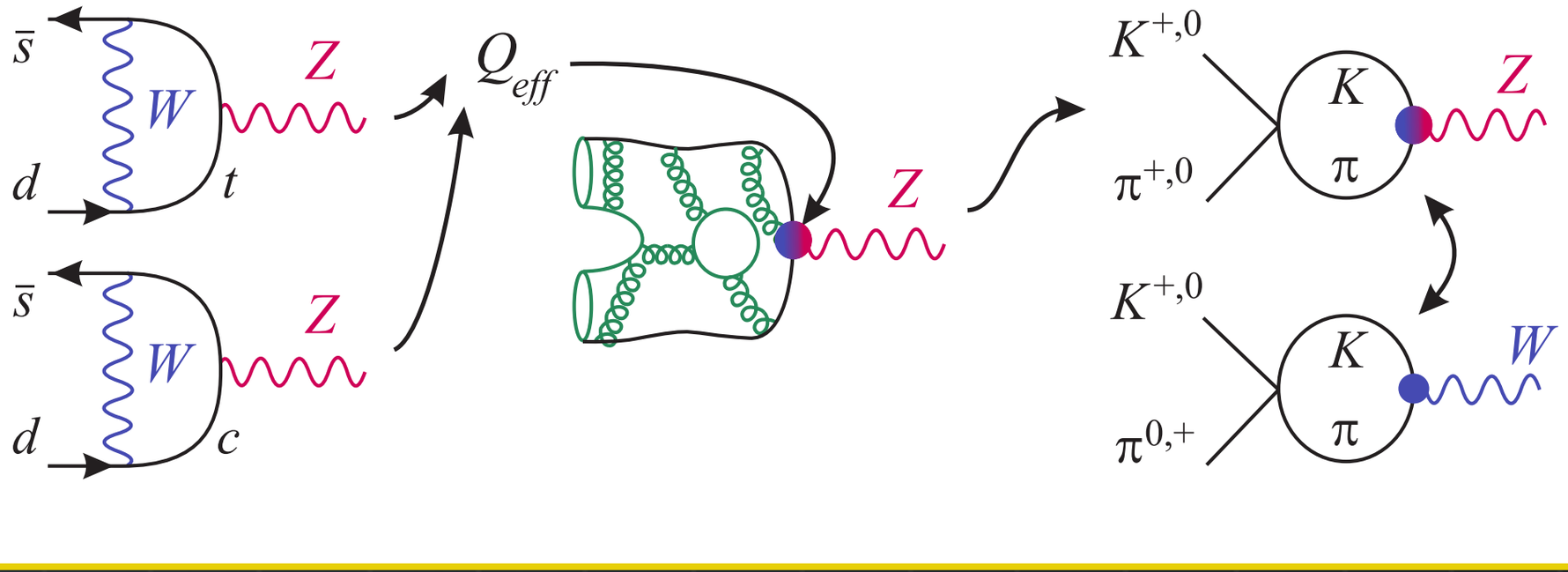

K→πνν

K→πlν

C. Smith, arXiv:1409.6162

Standard Model

- Materials are made of fermions (Quarks and Leptons).
- We need three generation of fermions (flavor).
- Interactions are mediated by gauge bosons.
- Mass of particles are realized as a result of interaction with Higgs boson.

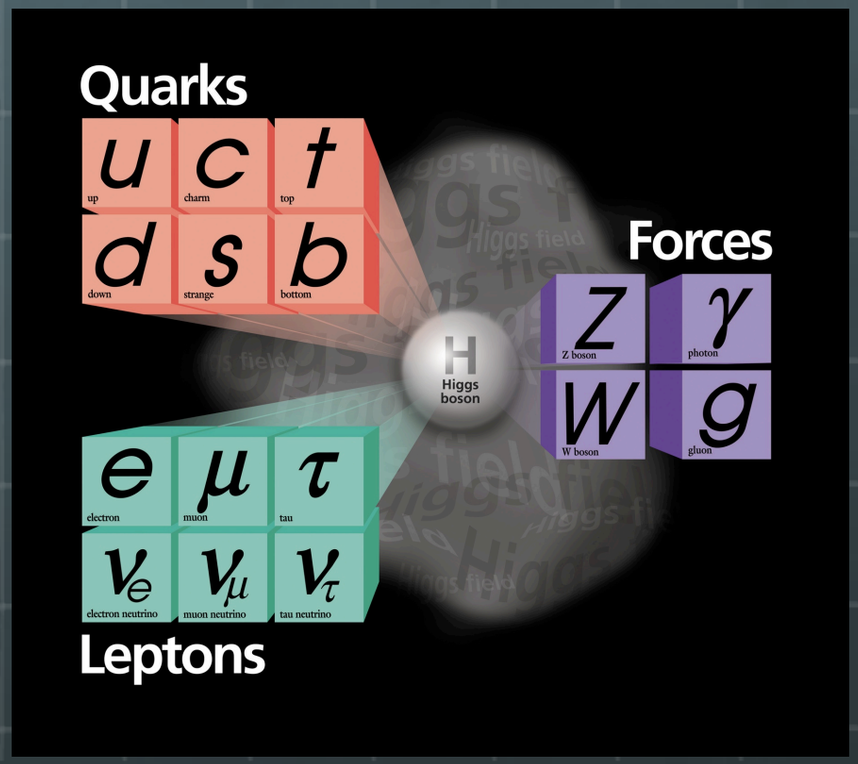

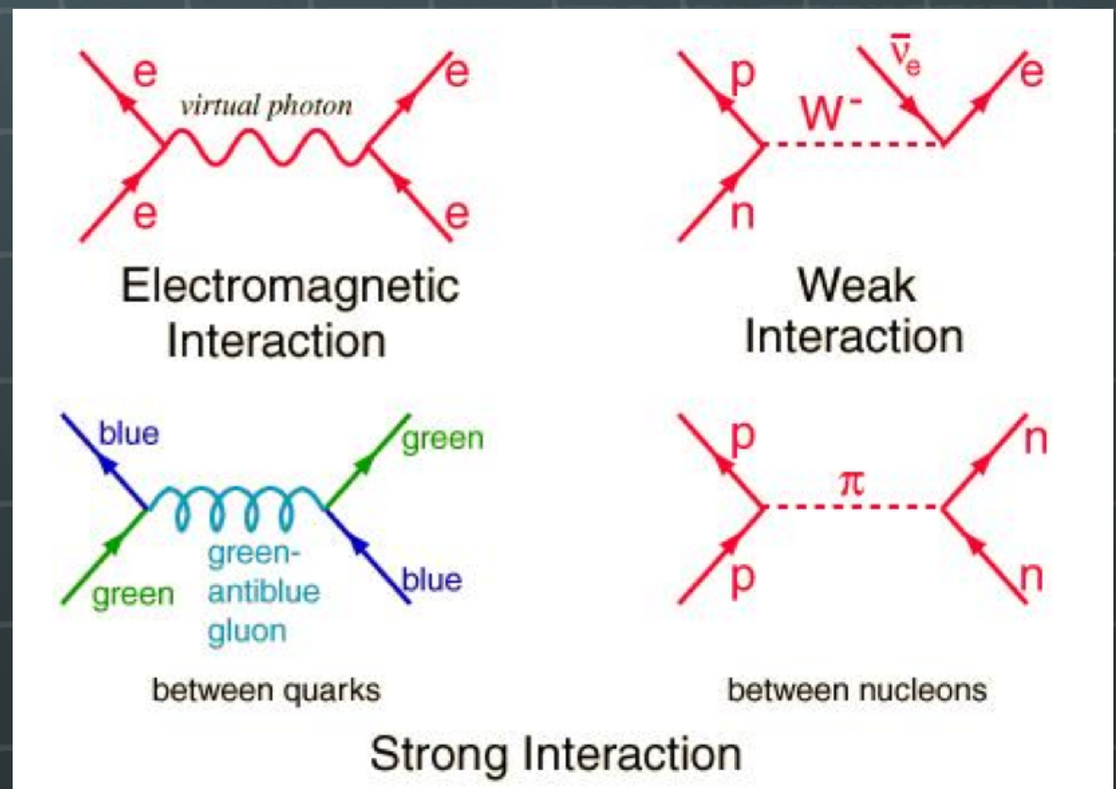

$K_L \to \pi^0 \nu\bar{\nu}$ versus $K^+ \to \pi^+ \nu\bar{\nu}$

AJB, Buttazzo, Knegjens, 1507.08672

$K_L \to \pi^0 \nu\bar{\nu}$

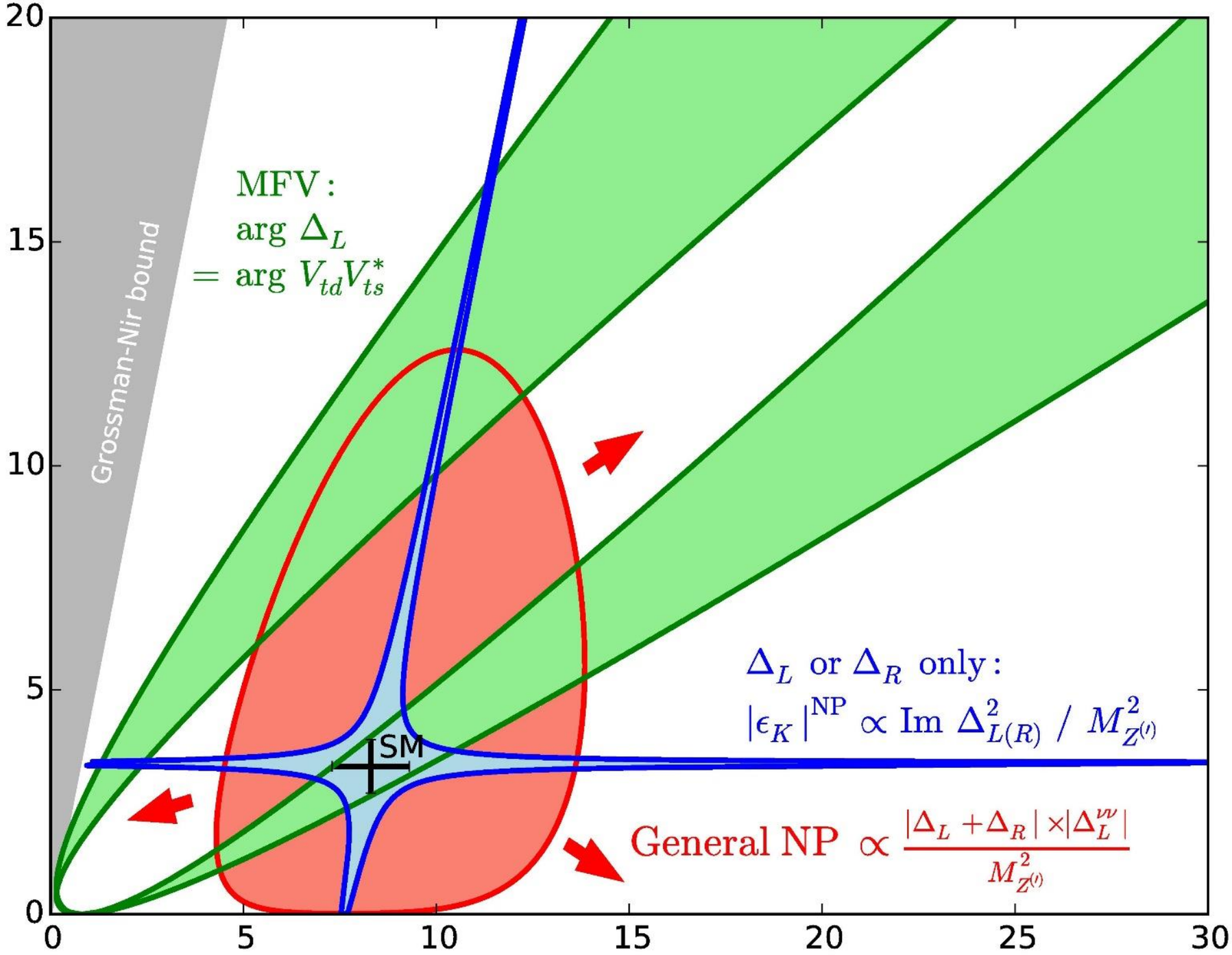

$K^+ \to \pi^+ \nu\bar{\nu}$

LHT

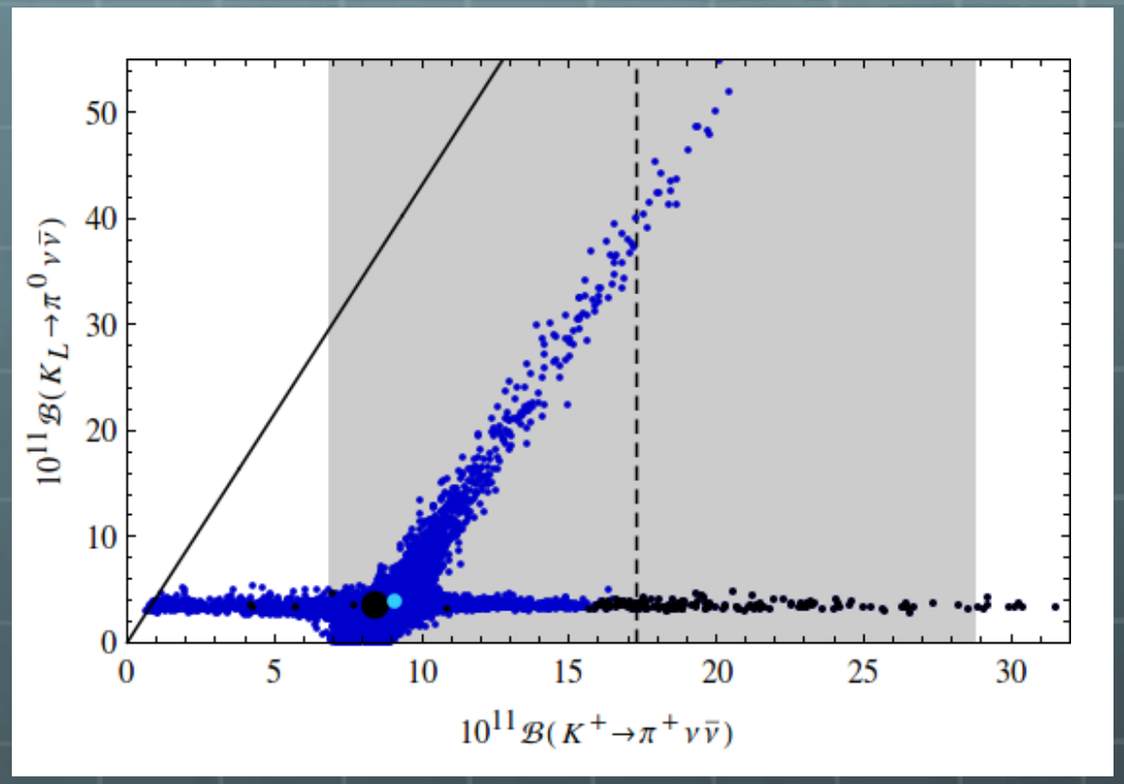

M. Blanke et. al., arXiv:1507.06316v2

RSc

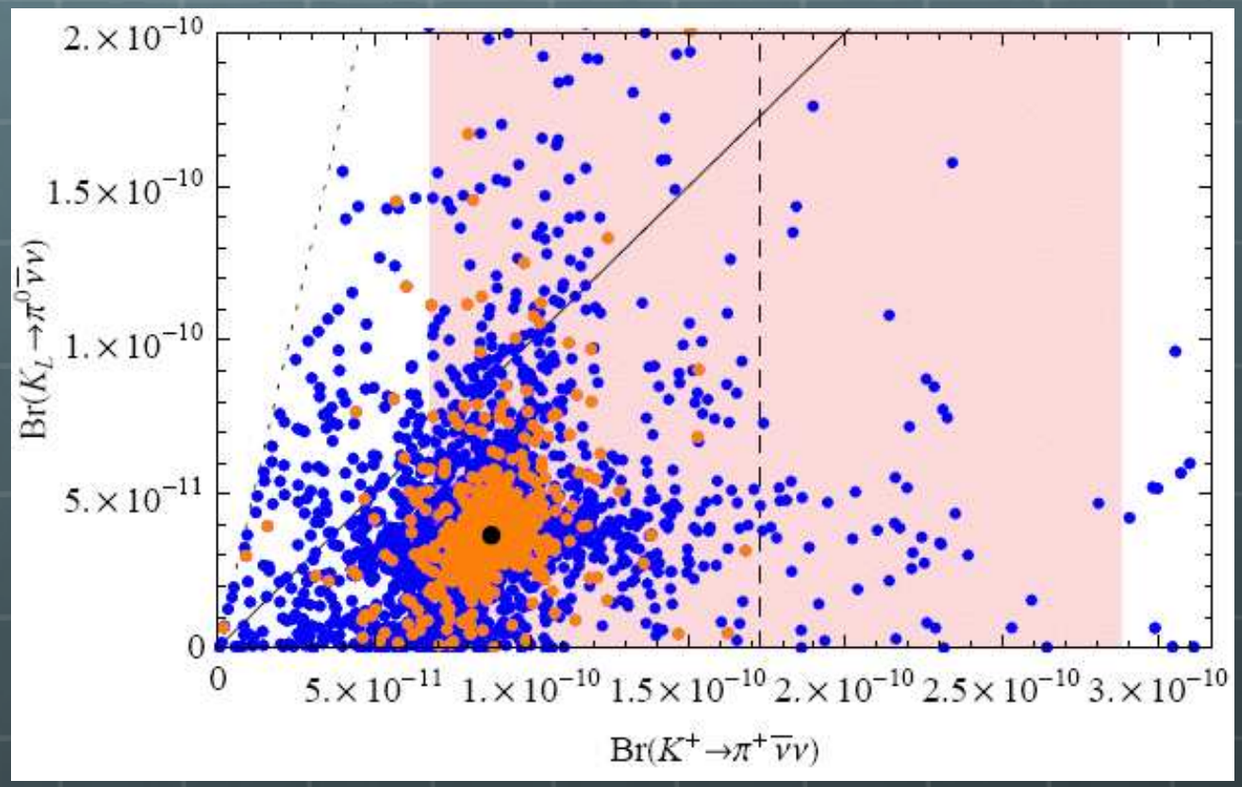

M. Blanke et. al., arXiv:0812.3803

K. Axixi et. al., arXiv:1508.03980v2

In the MFV

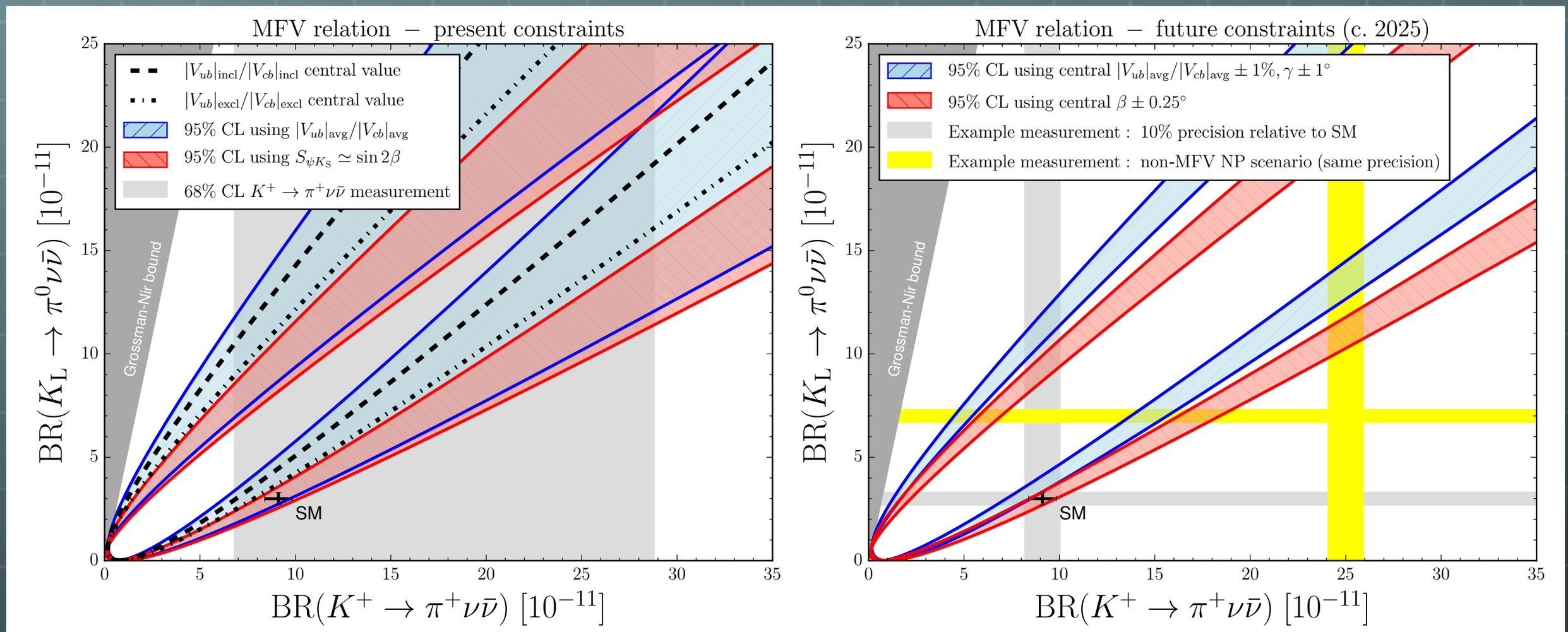

A. Buras et. al., arXiv:1503.02693v2

Higher energy SUSY

$$M_2 = 1\ (6)\ \text{TeV}, \qquad \mu = 1.5 \sim 2.5\ (6.3 \sim 7.8)\ \text{TeV},$$

$$m_{\tilde{t}_1} = 10\ \text{TeV}, \qquad m_{\tilde{t}_2} = 11\ \text{TeV}. \quad m_{\tilde{u}_L} = 2\ (15)\ \text{TeV}.$$

$$\theta^t_{LR} = 0.3 \qquad s^{uL}_{13} = s^{uL}_{23} = 0.1 \sim 0.3$$

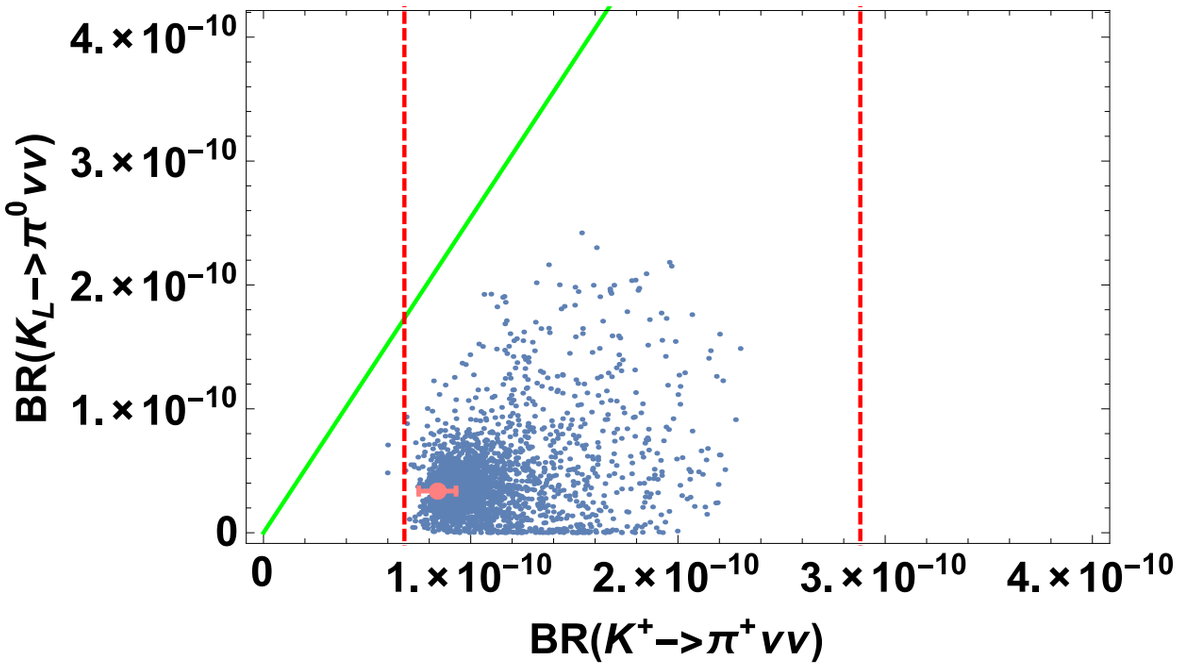

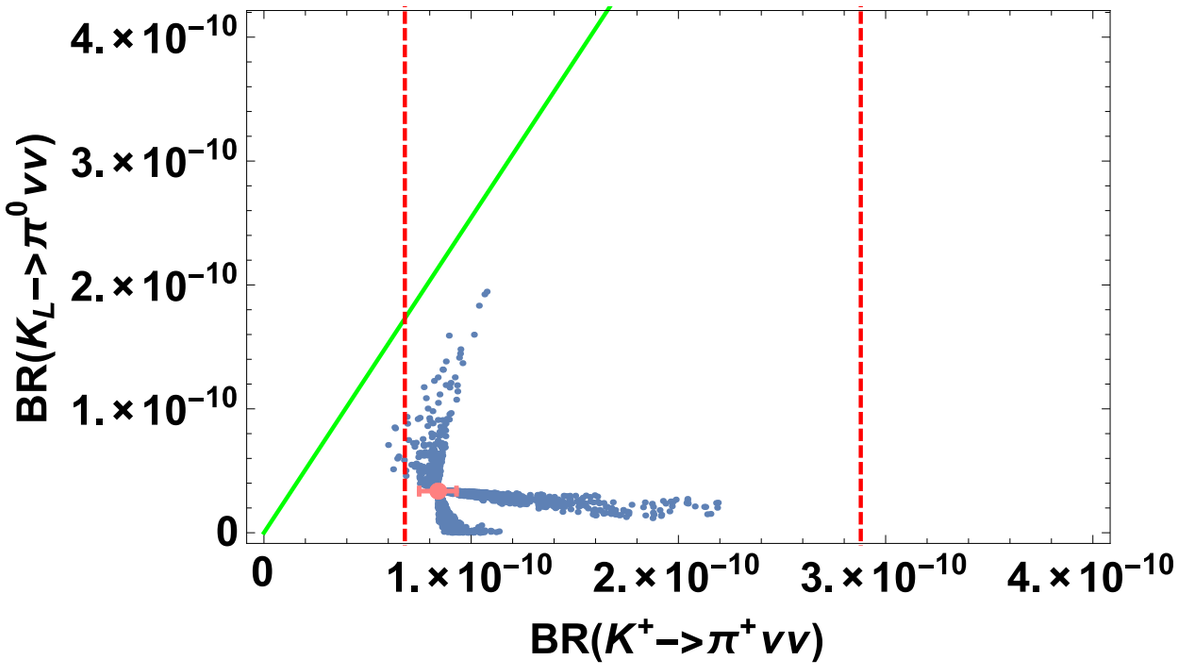

M. Tanimoto and K. Yamamoto, arXiv:1603.07960V2

Energy Resolution of CsI Calorimeter

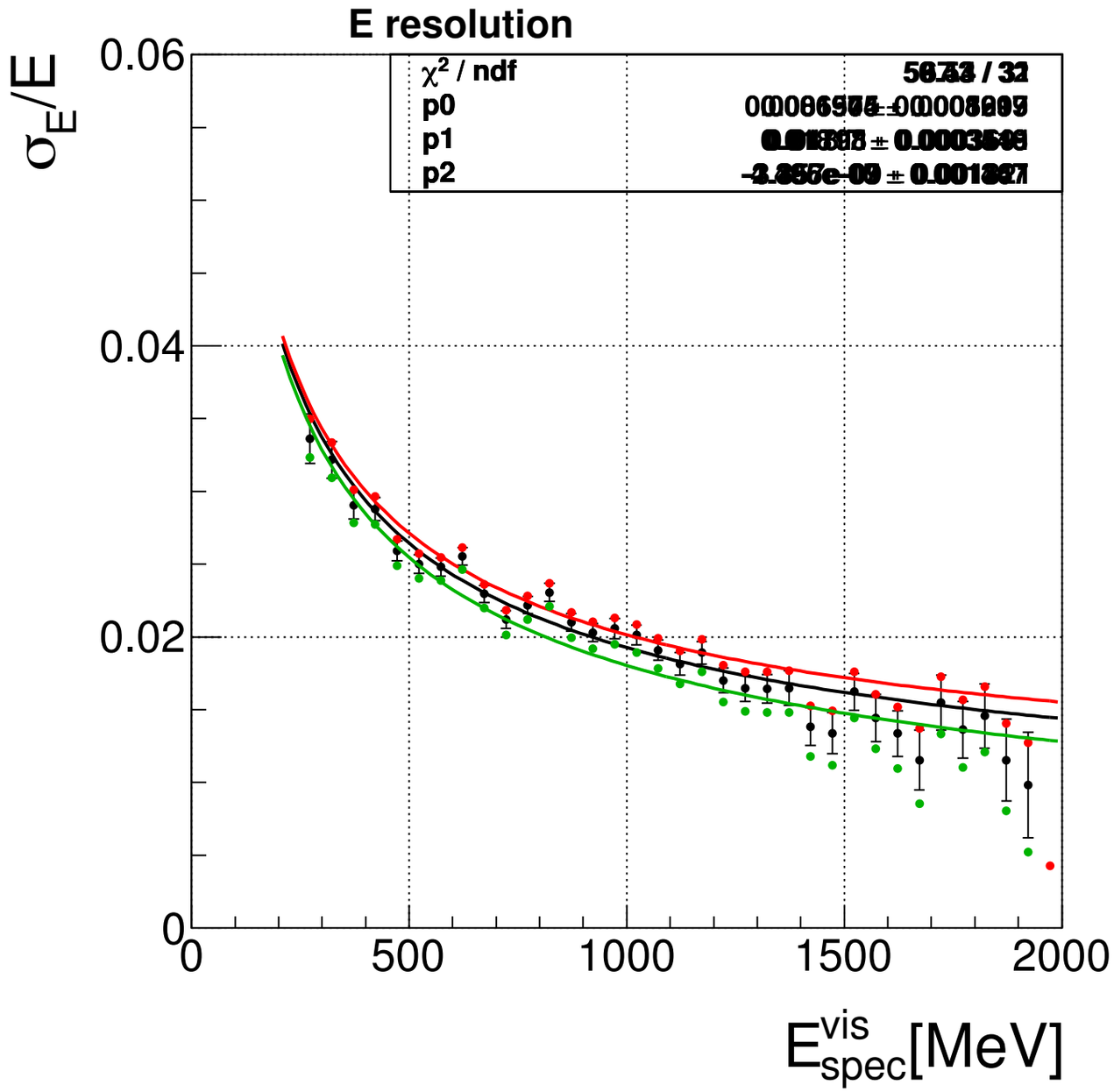

$$\frac{\sigma_E}{E} = p_1 \oplus \frac{p_2}{\sqrt{E[\mathrm{GeV}]}}$$

$$p_1 = (0.66 \pm 0.12 \pm 0.51)\%$$
$$p_2 = (1.81 \pm 0.04 \pm 0.02)\%$$

$$p_1 = (1.71 \pm 0.11 \pm 0.13)\%$$
$$p_2 = (1.31 \pm 0.10 \pm 0.01)\%$$

Search for new physics

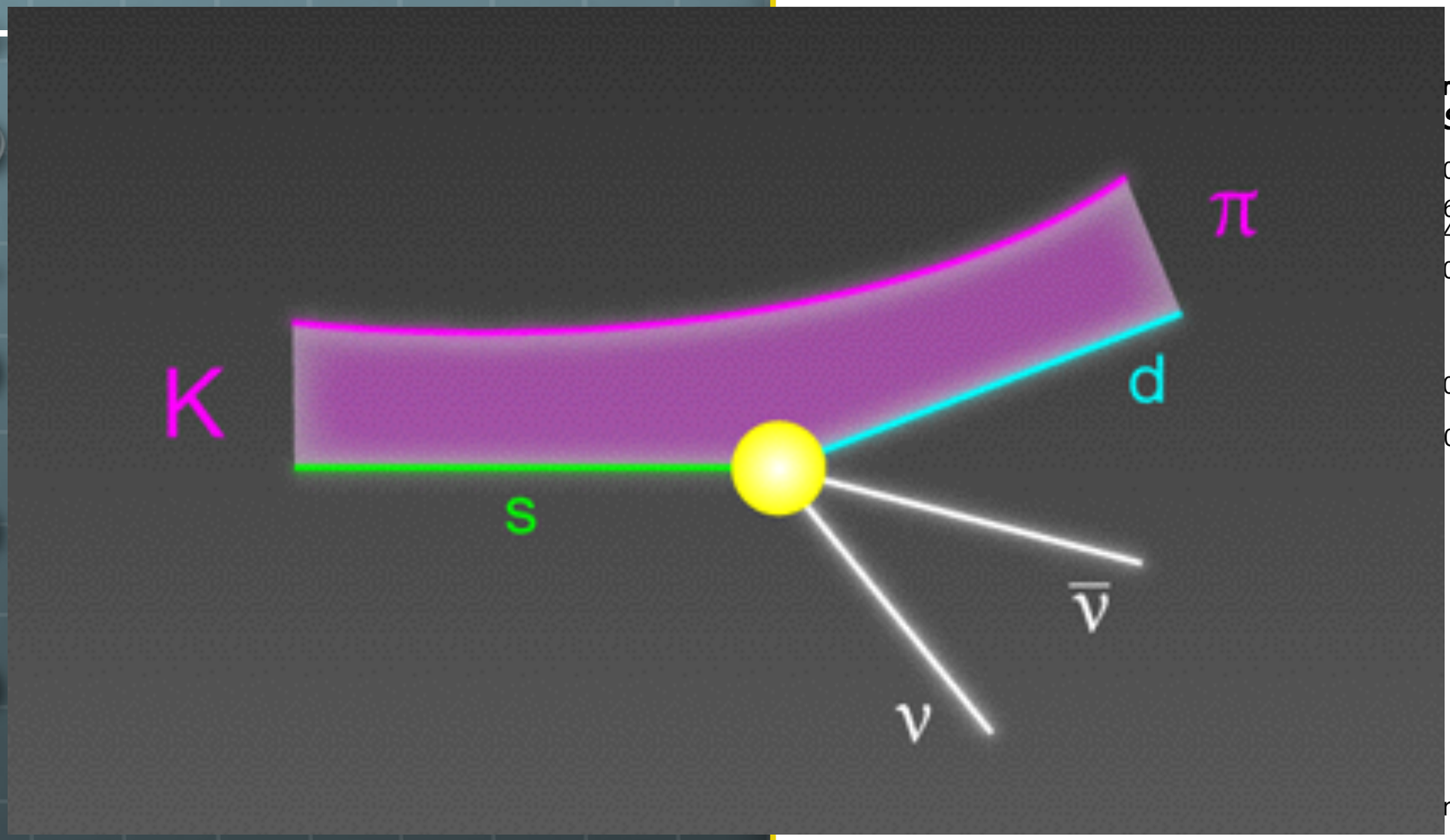

number (*LF*)
S1) modes

0.11) $\times 10^{-9}$

$^{6}_{4}$) $\times 10^{-12}$

0.19) $\times 10^{-7}$

$\times 10^{-9}$

$\times 10^{-11}$

0.27) $\times 10^{-9}$

0.21) $\times 10^{-8}$

$\times 10^{-10}$

$\times 10^{-10}$

$\times 10^{-8}$

$\times 10^{-7}$

$\times 10^{-12}$

$\times 10^{-11}$

$\times 10^{-11}$

$\times 10^{-10}$

range.pdf

Rare precess : $\Delta t \cdot \Delta E \sim \hbar$

Stopping Power S

$$S = -\frac{dT}{dx} = k\,\frac{z^2}{A\beta^2}\,ZB$$

$$B = \ln\,\frac{2mc^2\beta^2\gamma^2}{I} - \beta^2 \equiv f(\beta) - \ln I,$$

$$B(z) = B_0 + zL_1 + L_2(z) + [G(z,\beta) - \delta(\beta)]/2$$

with

$$B_0(\beta) = f(\beta) - \ln I - \frac{C(\beta)}{Z},$$

$$B_x(\beta) = S_x(\beta)\frac{A\beta^2}{kz^2Z}$$

and an "experimental I value" I_x defined by

$$\ln I_x \equiv f(\beta) - B_x(\beta) - \frac{C(\beta)}{Z} + zL_1 + L_2(z) + [G(z,\beta) - \delta(\beta)]/2.$$

STOPPING POWER VALUES OF C, Al, Si, Ni, Ag AND Au FOR ^{3}He IONS

D.C. SANTRY and R.D. WERNER

Atomic Energy of Canada Limited Research Company, Chalk River Nuclear Laboratories, Chalk River, Ontario, Canada, KOJ IJO

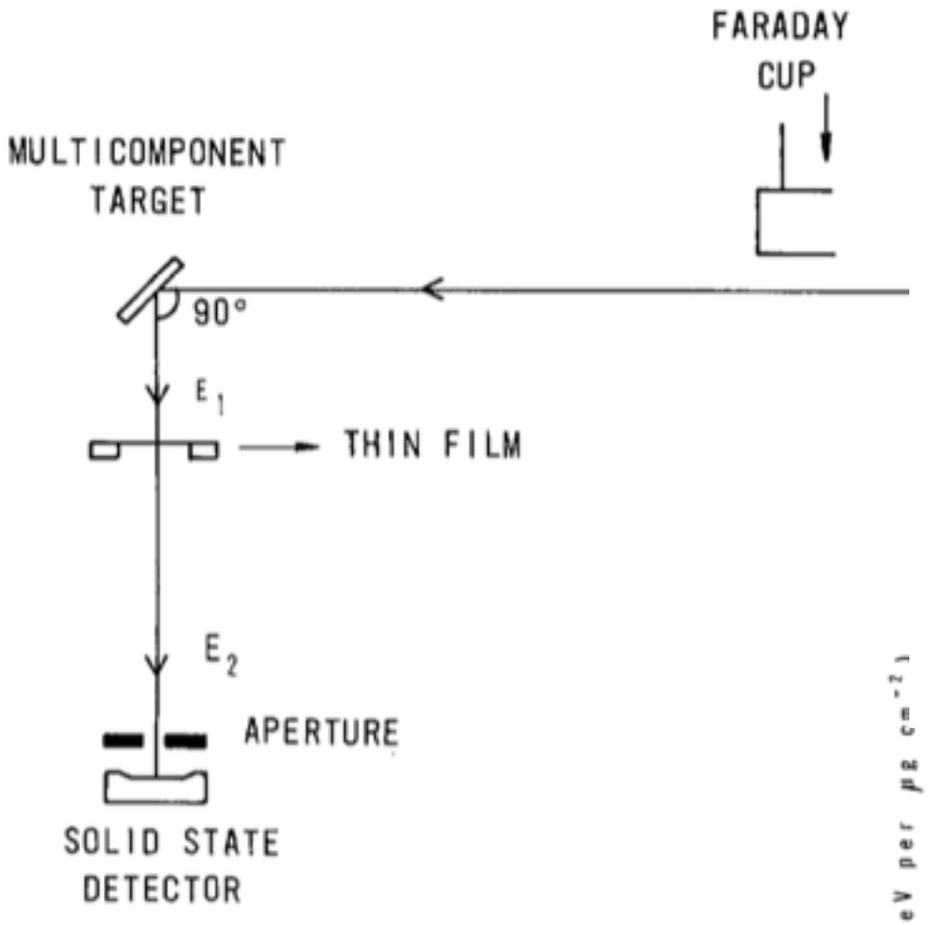

Fig 1. The experimental arrangement for measuring the e

plotting data in Figs. 3–8.

	Symbol
	×
Bader *et al.* [51], Borders [52]	◇
Luomajärvi [44], Langley and Blewer [53]	□
Green, Cooper, and Harris [54]; Knudsen, Andersen, and Martini [55]; Chumanov [56]	✦
Ishiwari and co-workers [48, 49, 57, 58]	⌑
MacKenzie and co-workers [59–62], Lin and co-workers [63, 64]	✠
Andersen and co-workers [45, 50, 65, 66], Fontell and Luomajärvi [67]	✕
Semrad [40], Chu *et al.* [68]	✲
Sirotinin *et al.* [69], Kuldeep and Jain [70]	○

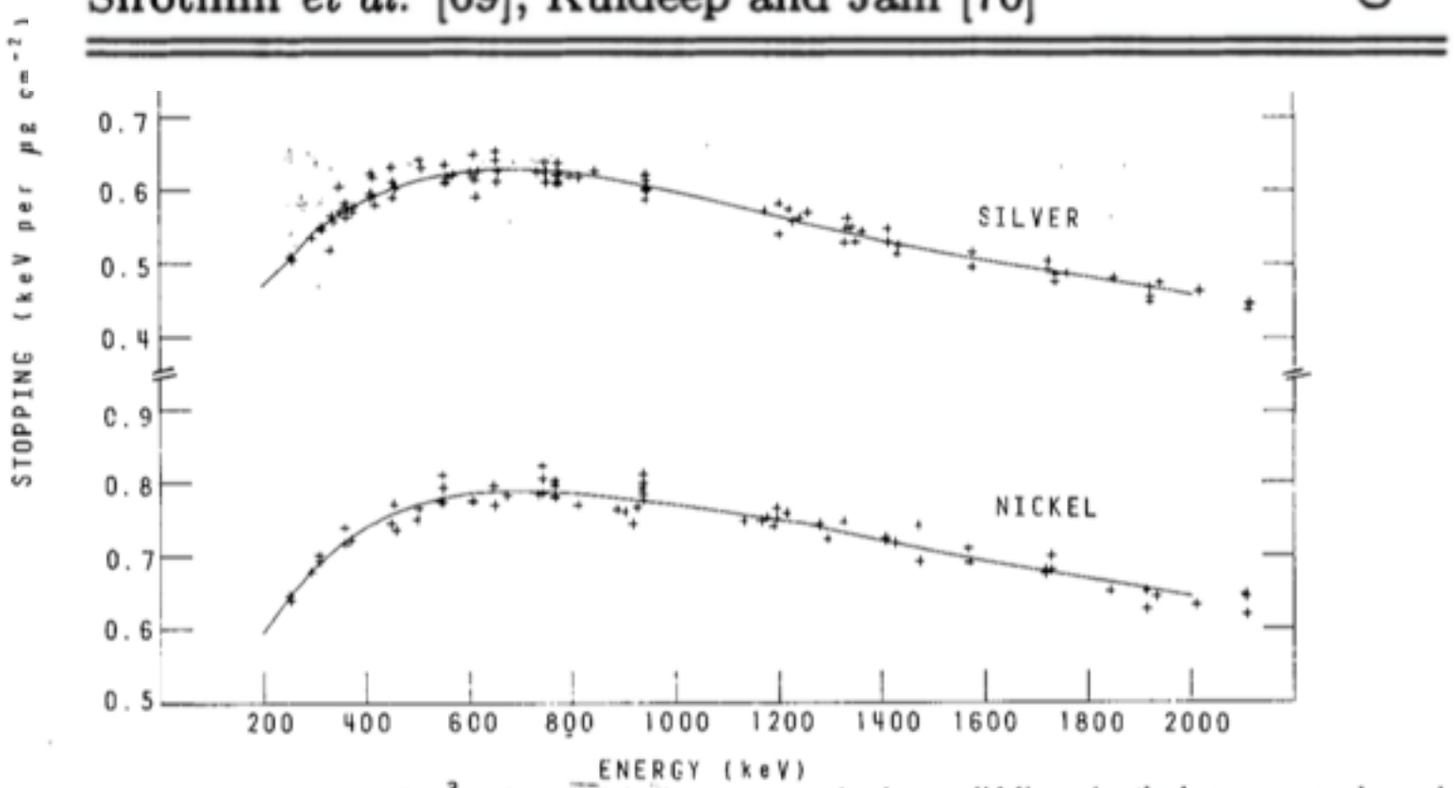

Fig. 3. Stopping values of Ni, Ag and Au for ^{3}He ions: (+) indicate measured values; solid lines give the last-squares polynomial fits.

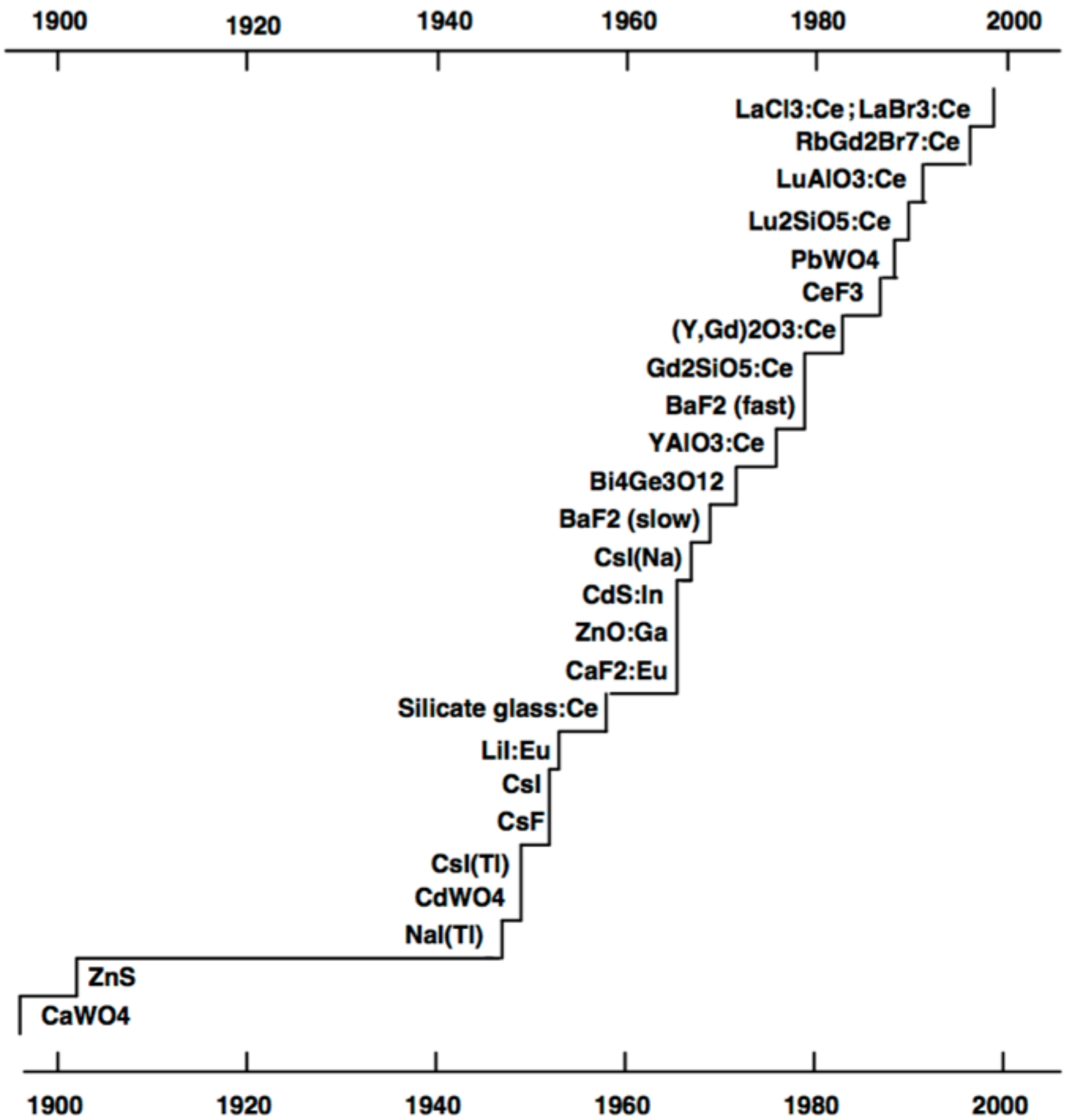

Fig. 1. History of the discovery of major inorganic scintillator materials.